Development and validation of novel fluorescent probes to advance research into glucose-dependent insulinotropic polypeptide (GIP) and glucagon-like peptide 1 (GLP1) receptor localisation and activity

Dr Anne Yingchol de Bray

Green Templeton College

Oxford Centre for Diabetes, Endocrinology and Metabolism

Supervisors: Professor David J. Hodson, Professor Jeremy W. Tomlinson

A thesis submitted for the degree of

Doctor of Philosophy

August 2025

Declaration of authenticity and copyright

I, Anne Yingchol de Bray, declare that the work presented in this thesis is my own, and that no part of the dissertation has been submitted for any other degree. Any work carried out by others has been acknowledged, appropriately referenced below and interpreted by myself.

Chapter 3:

sGIP probes were synthesised by our collaborator Dr Johannes Broichhagen at Leibniz-Forschungsinstitut für Molekulare Pharmakologie, Berlin, Germany.
In vitro pharmacological assays and associated figures were completed by our collaborator Dr Ben Jones at Imperial College London.

Chapter 4:

daLUXendin probes were synthesised by our collaborator Dr Johannes Broichhagen at Leibniz-Forschungsinstitut für Molekulare Pharmakologie, Berlin, Germany
In vitro pharmacological assays and associated figures were completed by our collaborator Dr Ben Jones at Imperial College London.
Labelling and imaging of MIN6-CB4 cells was performed by a former DJH lab colleague, Dr Julia Ast. Subsequent analysis was performed by myself and Prof David J Hodson.

Chapter 5:

dSTORM imaging, part of sample preparation, data analysis and figure creation were performed by a colleague in the DJH lab, Mr Jason Tong and Professor David J Hodson.

TIRF and STED imaging, sample preparation, data analysis and associated figures were performed by our collaborators in Leibniz-Forschungsinstitut für Molekulare Pharmakologie, Berlin; Christiane Huhn, Blaise Gatin-Fraudet, Kilian Roßmann and Dr Johannes Broichhagen.

Chapter 6:

Food intake studies were performed by our collaborators at University College London; Dr Alice Adriaenssens and Dr Anna Roberts.

Intraperitoneal glucose tolerance tests were performed by a colleague in the DJH lab, Dr Sarah Armour.

In vivo peripheral administration of daLUXendin into GLP1R and GIPR reporter mice and isolation of pancreata was performed by Dr Alice Adriaenssens and Dr Anna Roberts. Subsequent processing, sectioning, imaging and analysis was performed by myself.

In vivo peripheral and central administration of daLUXendin into WT and GLP1R and GIPR reporter mice, brain isolation, RNAscope, vimentin staining, imaging and associated figures were completed by Dr Alice Adriaenssens and Dr Anna Roberts.

Acknowledgements

I would like to begin by thanking my funding body, the Medical Research Council, who awarded me a Clinical Research Training Fellowship and without whom this research would not have been possible. Thank you also to the University of Birmingham (Medical School and MSS) and the University of Oxford (RDM, OCDEM and Green Templeton College) for supporting and providing opportunities for me. Additionally, I am very grateful for my incredible support networks, both professional and personal, that have enabled me to complete this DPhil.

To David, I'm so grateful for your support and hard work investing in me. You are an inspiring and driven scientist without whose vision and guidance I would have not been able to complete this DPhil, thank you.

To Jeremy, thank you for your kind and honest support. I have appreciated your approachability, encouragement and advice.

To Julia, I will never forget the patience and guidance (and baby scales!) you gave me in navigating my first steps into both PhD life and motherhood. I have you (and Fede and Kat) to thank for how I approached designing and recording experiments and am grateful for the good habits that I picked up from you.

To the Birmingham HodSquad: Fede, Nick, Fiona, Annie, Lewis. Thank you for all the troubleshooting, supervision and socialising from ACF to PhD. Your generous welcoming of an inexperienced clinician will never be forgotten.

To the Oxford HodSquad: Daniela, Kat, Kaja, Jason, Charlotte, Ali, Sarah, Claire, Lottie and Christopher. Thank you for all your support, guidance, humour and understanding as I came back from maternity leave and had to navigate working with a long commute and a sleep-deprived brain. I'm so grateful for you keeping me involved, doing mouse work for me and helping me with tasks while I was remote working. I couldn't have asked for a nicer and more supportive lab group and will always remember your kindness.

To my many clinical and clinical-academic colleagues, friends and mentors who have encouraged, helped and advised me; thank you. This includes, but is not limited to, Prof Kristien Boelaert, Prof M. Ali Karamat, Dr Jon Hazlehurst, Ms Lisa Shepherd, Dr Agata Juszczak, Dr Zainab Akram, Dr Rochelle Velho, Dr Becky Sagar, Dr Petra Hanson, Dr Annie Tung, Dr Liz Baranowski.

Finally, thank you to the human donors who were so kind to consent to donation, I'm so grateful for your decision.

To my parents, I would not have achieved all I have without your encouragement, support and sacrifice and I will always be grateful for that, thank you.

To my brother, Theo, thank you for the long chats on my drives back from Oxford, for grounding me and for (most of) your humour.

To my lovely extended family; the Ross', Beckers, Browns and Amadi-Browns. Thank you for your love, encouragement and for listening to me vent. There are several people that I wish were still here to give my thanks to, not least Auntie Bunny, Grandma Victoria and Khun Yai. Incredible women that have influenced me throughout my life.

To my fantastic and inspiring friends; the Core, school friends, university friends, the Crew, maternity leave friends and work friends. I am so grateful for your encouragement at all

points during this DPhil, your help with applications, talking through career plans and co-parenting.

To my wonderful husband and life teammate, Seb. I would not be able to achieve anything without your patience, encouragement, help and humour. I'm so happy to be married to you and so very grateful for your support and love.

My brilliant son, Thomas. Truthfully, it probably would have been easier to complete this DPhil without you, but it would have been a lot less special.

Abstract

Diabetes and obesity are chronic conditions which cause significant impact upon the individual, healthcare services and society. Medications agonising glucagon-like peptide-1 receptor (GLP1R) and dual agonists targeting GLP1R and glucose-dependent insulinotropic polypeptide receptor (GIPR) are revolutionising treatment for type 2 diabetes and obesity and showing promise in other conditions such as MASLD and IIH. Dual agonists demonstrate superior efficacy compared to GLP1R agonists for glycaemic control and weight loss. However, the mechanisms of their superiority remain unclear as confirmation of GIPR presence and dual agonist cellular targets remains challenging.

In this thesis, we present the development and validation of novel GIPR (sGIPs) and dual GLP1R/GIPR (daLUXendins) fluorescent agonist probes and apply them to relevant models to visualise cellular targets.

The sGIP probes demonstrate specificity in over- and endogenously expressed systems and suggest that GLP1R may be upregulated in GIPRKO models.

With the daLUXendin probes, we have generated non-lipidated (daLUXendin) and lipidated (daLUXendin+) forms. We show that the non-lipidated probes advantageously show greater selectivity for mouse GIPR over mouse GLP1R and label all major endocrine cell types in mouse islets and human stem-cell derived islet-like structures. Such labelling shows greatest intensity with ß cells > α cells = δ cells. Peripheral administration of daLUXendins labels circumventricular organs in a similar manner to single GLP1R agonists and antagonists, suggesting that depth of brain penetration is not a contributor to superior dual agonist efficacy. Central daLUXendin administration shows labelling of

tanycytes. daLUXendins are also suitable for single-molecule imaging and enhance nanodomain formation compared to single agonist/antagonist binding.

Together, this thesis presents the novel sGIP and daLUXendin probes which are specific for their cognate receptors and versatile for use in a range of super-resolution imaging modalities. We have used them to confirm dual agonist targets in the pancreas and brain and presented interrogable avenues to investigate the superior efficacy of dual agonists compared to single agonists.

Table of contents

List of figures

List of tables

List of abbreviations

AP	Area postrema
ARH	Arcuate nucleus of the hypothalamus
AUC	Area under the curve
BAT	Brown adipose tissue
BBB	Blood-brain barrier
BCB	Blood-cerebrospinal fluid barrier
BSA	Bovine serum albumin
cAMP	Cyclic adenosine monophosphate
CHO	Chinese hamster ovary cell
CNS	Central nervous system
CMRL	Connaught medical research laboratories
CSF	Cerebrospinal fluid
CTCF	Corrected Total Cell Fluorescence
CVO	Circumventricular organ
DAPI	4',6-diamidino-2-phenylindole
DMEM	Dulbecco's modified Eagle's media
DMSO	Dimethylsulfoxide
DNA	Deoxyribonucleic acid
DPP4	Dipeptidyl peptidase-4
DPP4i	Dipeptidyl peptidase-4 inhibitor

dSTORM	Direct stochastic optical reconstruction microscopy
DVC	Dorsal vagal complex
EC_{50}	Half maximal effective concentration
ELISA	Enzyme-linked immunosorbent assay
FACS	Fluorescence-Activated Cell Sorting
FBS	Fetal Bovine Serum
FFA	Free fatty acid
FRET	Förster Resonance Energy Transfer
GABA	Gamma-aminobutyric acid
GDF15	Growth/differentiation factor 15
GCG	Glucagon
GCGR	Glucagon receptor
GIP	Glucose-dependent insulinotropic polypeptide
(m/h) GIPR	(mouse/human) glucose-dependent insulinotropic polypeptide receptor
GIPRA	Glucose-dependent insulinotropic polypeptide receptor agonist
GIPRAb	Glucose-dependent insulinotropic polypeptide receptor antibody
GLP1	Glucagon-like peptide 1
(m/h) GLP1R	(mouse/human) glucagon-like peptide 1 receptor
GLP1RA	Glucagon-like peptide 1 receptor agonist
GLP2	Glucagon-like peptide 2
GLP2R	Glucagon-like peptide 2 receptor
GPCR	G-protein coupled receptor
GPR40	G-protein coupled receptor 40

HbA1c	Glycated haemoglobin
HFD	High fat diet
HILO	Highly inclined and laminated optical sheet
HPLC	High-performance liquid chromatography
HRMS	High-resolution mass spectrometry
IIH	Idiopathic intracranial hypertension
INS	Insulin
IPGTT	Intraperitoneal glucose tolerance test
K_d	Dissociation constant
KO	Knock out
LCMS	Liquid chromatography-mass spectrometry
MASLD	Metabolic dysfunction-associated steatotic liver disease
ME	Median eminence
mRNA	Messenger ribonucleic acid
NHS	National health service
NICE	National institute for health and care excellence
Nluc	Nanoluciferase (tagged)
NTS	Nucleus of the tractus solitarius
OVLT	Organum vasculosum of the lamina terminalis
PBS	Phosphate buffered saline
PFA	Paraformaldehyde
PKA	Protein kinase A
PVN	Paraventricular nucleus of the hypothalamus
RNA	Ribonucleic acid

RPMI	Roswell Park Memorial Institute
RT-PCR	Real time polymerase chain reaction
scRNAseq	Single-cell ribonucleic acid sequencing
SC-islets	Stem cell derived islets
S.E.M.	Standard error of the mean
SiR	Silicone rhodamine
SFO	Subfornical organ
SNP	Single nucleotide polymorphism
snRNAseq	Single-nuclei RNA sequencing
SST	Somatostatin
STED	Stimulated emission depletion microscopy
STR profiling	Short tandem repeat profiling
TIRF	Total internal reflection fluorescence
TMR	Tetramethylrhodamine
WAT	White adipose tissue
WT	Wild-type

Chapter 1: Introduction

The impact of diabetes and obesity

Diabetes and obesity are highly prevalent, chronic conditions which cause significant morbidity and mortality. Worldwide, in 2024 an estimated 589 million people live with diabetes and the number is predicted to rise to 853 million by 2050 (1). In England in 2024, there were 3.7-3.9 million people living with diabetes (2,3). Most people living with diabetes have been diagnosed with type 2 diabetes (1,2). In 2022, globally, 878 million people lived with obesity (4) and in England 29% of people live with obesity (5,6).

Both diabetes and obesity impact on people's day-to-day lives as well as putting them at risk of serious long-term complications and death.

In 2022, in England type 2 diabetes led to 7,565 lower limb amputations and 500,000 people were living with chronic kidney disease due to type 2 diabetes (7). The risk of admission to hospital due to a heart attack if a person has type 2 diabetes is 3.8-6x higher than the non-diabetic population and 3.2-4.5x higher for a stroke (7). Diabetes was responsible for 3.4 million deaths worldwide in 2024 (1).

Obesity is associated with an increased risk of hypertension, type 2 diabetes, cardiovascular disease and increased incidence and mortality from certain types of cancer (8–12). A raised BMI (overweight and obesity i.e. BMI >25kg/m^2) accounts for 1.6 million premature deaths from non-communicable diseases each year (13). The global burden of high BMI has doubled since 1990 and is predicted to continue to rise (14,15).

Additionally, the economic cost of these conditions is high. The global cost of diabetes has been estimated as over 1 trillion US dollars (1). In the UK, the NHS spent £10.7 billion in 2021/22 on diabetes, with almost 60% of costs treating complications (16). An estimated £3.2 billion was spent on indirect costs of diabetes due to absenteeism and early mortality (16).

Worldwide, the global cost of obesity has been estimated as almost US$2 trillion, with indirect costs almost double the value of direct costs (17). Annual direct and indirect costs of obesity in the UK in 2022 were found to be £58 million, with NHS spend on obesity-related conditions £6.5 billion (18). However, the biggest contributor to obesity-related costs was the reduction in Quality Adjusted Life Years (18), a well-established measure of longevity and quality of life, estimated to be worth £38.9 billion.

The underlying pathophysiology of both diseases are interlinked, with obesity increasing the risk of the development of type 2 diabetes by seven-fold (19) through inducing insulin resistance and attenuating ß cell function (20). Both type 2 diabetes and obesity form part of the metabolic syndrome. The metabolic syndrome is a cluster of conditions which increase the risk of type 2 diabetes and atherosclerotic cardiovascular disease (21–23). Such conditions include obesity, hypertension and dyslipidaemia (21–23). Therefore, therapeutic interventions which target several aspects of the metabolic syndrome are advantageous.

The definitions of diabetes and obesity

Type 2 diabetes is defined as a chronic, metabolic condition characterised by hyperglycaemia (24–26). Type 2 diabetes is diagnosed if a person has a HbA1c ≥48mmol/mol (6.5%), a fasting plasma glucose of ≥7mmol/l or random blood glucose ≥11.1mmol/l in the presence of symptoms (25,26).

Obesity is defined as a BMI ≥30kg/m^2, adjusted to >27.5kg/m^2 if the person is of an ethnicity at higher risk of complications, such as Black African or Caribbean and Asian background (27,28). Obesity can then be further assessed or staged by measuring waist circumference, waist:height ratio (28,29) or using the Edmonton Obesity Staging System (29,30).

Physiological control of blood glucose

The pancreas is both an endocrine and exocrine organ. It contributes to digestion of food by secreting digestive enzymes into the duodenum and aims to limit blood glucose levels to between 4-6mM through the secretion of several hormones (31,32).

There are five main endocrine cells, α, ß, δ, ε, γ cells (33–37), which are arranged in clusters called islets (32,36–39). The main cells which regulate blood glucose are glucagon-secreting α cells, insulin-secreting ß cells, somatostatin-secreting δ cells (32,40). The abundance of each cell type and the structure of the islet varies between species, summarised in Table 1 and Table 2, and even within species (41).

Mouse islets	Brissova 2005 (33)	Cabrera 2006 (42)	Kilimnik 2012 (43)	Kim 2009 (41)
α cells	9-31%	18%	15%	
ß cells	61-88%	77%	85%	85% +/- 14%
δ cells	1-13%			

Table 1: Summary of abundance of α, ß and δ cells in mouse pancreatic islets. Described as % total islet volume.

Human islets	Brissova 2005 (33)	Cabrera 2006 (42)	Ionescu-Tirgoviste 2015 (44)	Kilimnik 2012 (43)	Kim 2009 (41)
α cells	10-65%	38%	32.6%	30%	
ß cells	28-75%	55%	57.1%	70%	64% +/- 21%
δ cells	1.2-22%		10.2%	Approx. 17%	

Table 2: Summary of abundance of α, ß and δ cells in human pancreatic islets. Described as % total islet volume.

Blood glucose levels are lowered by insulin and raised by glucagon (32,45). Insulin is released during hyperglycaemia and binds to its cognate receptors in muscle, liver and adipose tissue which triggers insulin-dependent glucose uptake, storage and use (32,46). Insulin also mediates protein and lipid metabolism by inducing lipogenesis, hepatic glycogenesis and protein synthesis (32,47).

In contrast to insulin, glucagon release from α cells is suppressed by hyperglycaemia and triggered by hypoglycaemia (37) and is further amplified by circulating amino acids and adrenergic stimulation (48). Glucagon triggers hepatic gluconeogenesis and glycogenolysis to raise blood glucose (47,49,50).

Hyperglycaemia also triggers somatostatin release but effects of somatostatin upon glucose control is via paracrine action rather than direct effects (40,48,51). The paracrine effects of glucagon, insulin and somatostatin all help to regulate insulin secretion and therefore contribute to glucose homeostasis (Figure 1). Glucagon stimulates both insulin (52,53) and somatostatin (54,55) release. Insulin inhibits glucagon secretion (56–59) and somatostatin inhibits both insulin and glucagon secretion (32,40,60,61). Therefore, although ß cells are the sole secretors of insulin, failure in any one of these axes can dysregulate insulin secretion and lead to hyperglycaemia. Furthermore, paracrine signalling with the islet is complex with other molecules proposed to play a part (such as

glutamate and GABA) and optimised islet function and cell survival is also dependent upon preserved cell-cell connections (such as via e-cadherin and gap junctions) (62,63).

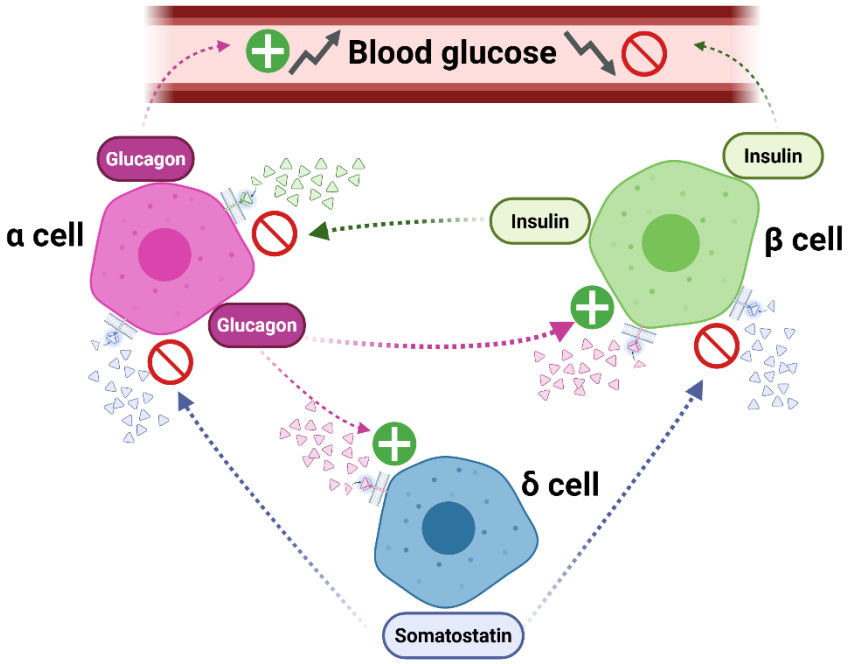

Figure 1: Schematic of α and ß cell effects on blood glucose and paracrine signalling between α, ß and δ cells in the pancreatic islet.
This simplified diagram of paracrine singalling between α, ß an δ cells has been traditionally taught but in recent years understanding of the interdepedence of each cell type upon each other for their function and survival has come to light. Created with biorender.com.

Pathophysiology of type 2 diabetes and obesity

The underlying pathology of type 2 diabetes begins many years before the dysglycaemia reaches diagnostic levels (64–67). Consensus view of the pathogenesis of type 2 diabetes is that there are elements of pancreatic ß-cell failure (68–71) and insulin resistance (46,68,72–76) which leads to failure to suppress hepatic gluconeogenesis (76) and subsequent perpetuation of these pathological mechanisms from gluco/lipotoxicity (76–78).

Insulin resistance can be defined as a reduction in the ability of insulin to lower blood glucose, induce glucose disposal in skeletal muscle and suppress hepatic

gluconeogenesis (79). It can be caused by genetic and environmental factors, with a significant epigenetic influence (80). Insulin resistance occurs early in the pathogenesis of type 2 diabetes with insulin resistance resulting in reduced muscle glycogen formation and consequently excess glucose undergoing hepatic lipogenesis (76,77,81). Hepatic lipid accumulation worsens insulin resistance which further reduces the ability of insulin to suppress hepatic gluconeogenesis and over years, rising blood glucose leads to increased circulating insulin. Increased insulin leads to worsening of hepatic lipid accumulation as insulin promotes this deposition. This cyclical interaction and intensification of insulin resistance and hepatic gluconeogenesis is known as the Twin Cycle hypothesis (76).

Initially, ß cells compensate for increased insulin resistance through increasing ß cell mass (mainly through hypertrophy rather than proliferation (82)) and insulin production (69,83–85). After some time, ß cell dysfunction and failure occurs which leads to the onset of type 2 diabetes. Initially, it was thought that ß cell failure was due to exhaustion from the prolonged increase in insulin production and ß cell death from gluco-/lipotoxicity-induced metabolic and oxidative stress (86–89) . However, it has since been postulated that changes to ß cell identity, such as de-differentiation and transdifferentiation, and alterations to cell metabolism and intracellular signalling, due to oxidative stress and ER stress, also contribute to ß cell failure in the setting of type 2 diabetes (reviewed in (90)). It is likely that the underlying factors vary between individuals but that both changes to ß cell identity and ß cell signalling play a role in the decline of ß cell function and survival in type 2 diabetes.

Obesity develops due to both genetic and environmental factors, in addition to the impact of epigenetics (91). Adipose tissue is highly active with numerous metabolic, hormonal

and immunological roles (92). Excess adipose tissue results in complications through chronic, low-grade inflammation and significant alteration to the gut microbiome (93). Activation of the inflammatory response of immune cells results in further potentiation of inflammation and a dysregulated immune system (92,94,95). The gut microbiome influences adipose tissue deposition, insulin resistance and inflammation (96) with weight loss induced in people with obesity after faecal microbiota transplant (97). However, obesity has been shown to rapidly alter microbial composition and function (96,98), suggesting a bidirectional relationship between obesity and the gut microbiome.

Obesity leads to type 2 diabetes by both attenuating insulin action (91,99) and inducing hyperglycaemia via increasing circulating free fatty acids (FFAs). A rise in circulating FFAs provides an alternative fuel source for skeletal muscle leading to reduced glucose uptake and FFAs oxidation in the liver triggers hepatic gluconeogenesis (91). Excess adiposity also contributes to the development of diabetes-associated complications, such as heart failure and chronic kidney disease, for some time before type 2 diabetes is diagnosed (100).

Current treatments for diabetes and obesity

It has long been established that for diabetes, controlling blood glucose leads to a reduction in costly complications (101,102). Blood glucose levels correlate with a U-shaped curve for risk of complications – with higher morbidity and mortality associated with either very high or very blood glucose (103). However, all glucose-lowering medications have risks and side effects which can limit their use. Therefore, treatment choices and targets are tailored to an individual to bring blood glucose into a safe range. Currently, in England and Wales only around 65% of patients with type 2 diabetes are

achieving their target blood glucose (2) and in addition, type 2 diabetes progression occurs in most patients regardless of medication choice (104). This drives innovation to develop more efficacious medications with fewer side effects and compatibility with other existing medication.

Glucagon-like peptide 1 receptor (GLP1R) agonists have been of particular interest in the world of diabetes and obesity not only because they significantly improve blood glucose control and drive weight loss, but also because they allow dose escalation without the risk of hypoglycaemia.

For type 1 diabetes, the only treatment option is insulin. For type 2 diabetes, oral medications are first line in the UK (105) and the current options are summarised in Table 3.

Medication class and examples	Mechanism of action	Significant benefits	Adverse effects
Biguanides *Metformin*	Improves insulin resistance Reduces hepatic gluconeogenesis	No risk of hypoglycaemia Safe in pregnancy	GI upset Vitamin B12 deficiency Lactic acidosis
Sulfonylureas *Gliclazide*	Simulate insulin release from ß cells, suppresses glucagon secretion from α cells	Rapid glucose lowering	Hypoglycaemia Weight gain
PPAR-γ agonists *Pioglitazone*	Improve insulin resistance; hepatic gluconeogenesis suppression, enhanced skeletal muscle insulin-dependent glucose uptake	Significant improvement in insulin resistance, low risk of hypoglycaemia	Fluid retention Bladder cancer
SGLT2-inhibitors *Canagliflozin, dapaglifozin, empagliflozin*	Inhibits SGLT2 transporter in renal tubules, permitting glycosuria	Mild weight loss, some have proven cardiovascular benefit	Urinary tract infection Euglycaemic ketoacidosis
DPP4-inhibitors *alogliptin,*	Inhibit DPP4 enzyme to prolong half-life of	Low risk of hypoglycaemia, can	Pancreatitis

linagliptin, sitagliptin	endogenous GLP1 and GIP	be used in renal failure	
GLP1R agonists *exenatide, liraglutide, semaglutide (Ozempic)*	Improve glucose-dependent insulin secretion Reduce hepatic gluconeogenesis	Weight loss, some have proven cardiovascular benefit	GI upset Pancreatitis Gallbladder disease
GLP1R and GIPR dual agonist *Tirzepatide (Zepbound)*	Improve glucose-dependent insulin secretion Reduce hepatic gluconeogenesis	Weight loss	GI upset Pancreatitis Gallbladder disease
Insulin	Binds to insulin receptor	Rapid glucose lowering	Hypoglycaemia Weight gain

Table 3: Summary of NICE approved medications for type 2 diabetes.
(105,106). Medication names listed are generic, with trade name licensed for type 2 diabetes in brackets. DPP4 = dipeptidyl peptidase 4, GIPR = glucose-dependent insulinotropic polypeptide receptor, GLP1 = glucagon-like peptide 1, GLP1R = glucagon-like peptide 1 receptor, PPAR = peroxisome proliferator-activated receptor , SGLT2 = sodium-like glucose transporter 2.

For obesity, four medications are currently licenced in the UK, summarised in Table 4.

Medication	Medication class	Year of NICE approval	Notes
Orlistat	Lipase inhibitor	1998 2009 – available without prescription	Significant gastrointestinal side effects
Liraglutide (Saxenda)	GLP1R agonist	2020	Only available in Tier 3 weight management services
Semaglutide (Wegovy)	GLP1R agonist	2023	Only available in specialist weight management services
Tirzepatide (Mounjaro)	GLP1R and GIPR dual agonist	2024	Available in primary care within restrictions of funding variation (107) as well as specialist weight management services

Table 4: Summary of NICE-approved medications for obesity.
(28,108). Medication names listed are generic, with trade name licensed for obesity and overweight in brackets. GIPR = glucose-dependent insulinotropic polypeptide receptor, GLP1R = glucagon-like peptide 1 receptor.

One of the earliest medications available to the NHS to treat obesity in England was orlistat. Orlistat is a lipase inhibitor which prevents the digestion and subsequent

absorption of fat in ingested food (109,110). Orlistat induces an average weight loss of 2.9% more than placebo over a year (111) but can cause significant gastrointestinal side effects including diarrhoea and bloating (109,110). Sibutramine and rimonabant were also available for use but were withdrawn within the European Union due to safety concerns (112,113).

In people with obesity, liraglutide drives an average weight loss of -5.4% total body weight more than placebo after 56 weeks (114) but requires once-daily injection, unlike once-weekly semaglutide and tirzepatide. In the STEP-8 head-to-head trial, over 68 weeks semaglutide induced a weight loss of 13.9% more than placebo and 9.4% greater than liraglutide in people with obesity or overweight (115). Tirzepatide combines GLP1R agonism with glucose-dependent insulinotropic polypeptide (GIP) receptor agonism. Compared with placebo, tirzepatide induces an average weight loss of 17.8% in people with obesity (116). Furthermore, in a head-to-head cohort study of people with obesity and/or type 2 diabetes, tirzepatide was found to induce an additional 6.9% average weight loss compared to semaglutide (117). Weight loss to this degree was only previously attainable at a large scale through bariatric and metabolic surgery (118,119).

On the horizon, are further dual and triple incretin agonists and antagonists; the trials for obesity are summarised in Table 5.

Medication name	Mechanism of action	Route/ frequency	Manufacturer	Clinical trials.gov ID	Expected completion date
Phase 3 obesity trials					
CagriSema	GLP1RA + Amylin RA	SC OW	Novo Nordisk	NCT05567796	Completed June 2025
Maritide	GLP1RA + GIPR antagonist	SC Monthly	Amgen	NCT06858839	Apr 2027
Mazdutide (4-6mg)	GLP1RA + Glucagon RA	SC OW	Innovent Biologics	NCT05607680	Completed Apr 2024
Mazdutide (9mg)	GLP1RA + Glucagon RA	SC OW	Innovent Biologics	NCT06164873	Sept 2025
Orforglipron	GLP1RA	PO OD	Eli Lilly	NCT05869903	July 2025
Retatrutide	GLP1RA + GIPRA + Glucagon RA	SC OW	Eli Lilly	NCT05929066	May 2026
Survodutide	GLP1RA + Glucagon RA	SC OW	Boehringer Ingelheim	NCT04667377	Completed Oct 2022
Phase 2 obesity trials					
Bimagrumab + Semaglutide	Activin receptor II inhibitor + GLP1RA	(B) IV/ monthly; (S) SC OW	Versanis Bio	NCT05616013	June 2025 (120)
Cagrilintide	Amylin RA	SC OW	Novo Nordisk	NCT03856047	Completed Mar 2021
Danuglipron	GLP1RA (small molecule)	PO BD	Pfizer	NCT04707313	Completed Oct 2023 but discontinued (121)
Dapiglutide	GLP1RA + GLP2RA	SC OW	Zealand Pharma	NCT05788601	Aug 2025
Efinopegdutide	GLP1RA + Glucagon RA	SC OW	Hanmi Pharmaceut-icals	NCT03486392	Completed March 2019 now solely for MASLD
Maritide	GLP1RA + GIPR antagonist	SC Monthly	Amgen	NCT05669599	Completed Jan 2025
NNC0165-1875 + Semaglutide	PYYRA + GLP1RA	SC twice-weekly	Novo Nordisk	NCT04969939	Completed Jan 2023 but discontinued (122)
Pemvidutide	GLP1RA + Glucagon RA	SC OW	Altimmune	NCT05295875	Completed Sept 2023
S-309309	MGAT2 inhibitor	PO OD	Shionogi	NCT05925114	Completed May 2024

Table 5: Summary of novel dual- and multi-incretin-based therapies current under Phase 2 or Phase 3 investigation for obesity.
Adapted and amended from Melson et al (123). BD = bis die (twice daily); GIPR = glucose-dependent insulinotropic polypeptide receptor, GIPRA = glucose-dependent insulinotropic polypeptide receptor agonist; GLP1RA = glucagon-like peptide 1 receptor agonist; GLP2RA = glucagon-like peptide 2 receptor agonist; MASLD = metabolic-dysfunction associated steatotic liver disease; MGAT2 = monoacylglycerol O-acyltransferase 2; OD = omni die (once daily); OW = once weekly; PYYRA = peptide YY receptor agonist; RA = receptor agonist, SC = subcutaneous.

Medications of particular interest are maridebart cafraglutide (MariTide), a GLP1R agonist/GIPR antagonist; orforglipron, a small molecule GLP1R agonist and retatrutide, a triple GLP1R/GIPR/GCGR agonist.

MariTide is a monoclonal GIPR antagonist antibody with two identical GLP1R agonist peptides conjugated to the heavy chains, developed by Amgen for type 2 diabetes and obesity (124). Phase 1 and 2 trials have demonstrated dose-dependent weight loss in people with obesity and an acceptable safety profile (124,125). Phase 2 trials also reported 6.7%-10.6% total body weight loss compared to placebo and a 1.1%-1.5% percentage point reduction in HbA1c compared to placebo (125). One key advantage of MariTide is its long-half life (14-21 days) which allows for the less frequent monthly dosing in addition to sustained weight loss (150 days in phase 1 trial) after discontinuation (124) – neither of which have been features of currently licensed GLP1R agonists or tirzepatide. However, MariTide requires a higher dose and higher volume of injection compared to such currently licensed medications – 6ml for maximum dosing of MariTide (420mg at 70mg/ml) compared to 0.6 ml (15mg at 25mg/ml) for tirzepatide (126). This significant difference in injection volume may have negative implications for patient acceptability and manufacturing and would need to be considered when interpreting any head-to-head trials between MariTide and GLP1R agonists or tirzepatide.

Orforglipron is a non-peptide small molecule GLP1R agonist suitable for once-daily oral administration developed by Eli Lilly (127). It is a partial GLP1R agonist and biases signalling towards Gs rather than ß arrestin recruitment (127). Top line results for the phase 3 trial of orforglipron for the treatment of obesity were recently published and reported 11.5% total body weight loss compared to placebo (128). Orforglipron has also shown promise in phase 3 trials for diabetes, with reductions in HbA1c of up to 1.1-1.4%

(129). Discontinuation rates due to side effects, primarily gastrointestinal, were 2.2%-5.7% (130), which is similar to the discontinuation rates reported in a recent head-to-head trial comparing tirzepatide (2.7% discontinuation rate) and semaglutide (5.6%) (131). Oral administration is generally viewed as a more acceptable route of administration than injectable routes but so far, the success of oral incretin-based medications has been limited to semaglutide. Although there have been no head-to-head trials comparing oral and subcutaneous (SC) semaglutide, a network meta-analysis reported that maximally dosed SC semaglutide was more efficacious than oral semaglutide for both reductions in HbA1c and weight, although oral semaglutide was more efficacious than the other SC GLP1R agonists, dulaglutide and liraglutide (132). Therefore, the oral route of administration for orforglipron is a distinct advantage and may aid in its success should dedicated cardiovascular outcome trials report positive results.

Retatrutide is a triple GLP1R/GIPR/GCG receptor agonist developed by Eli Lilly and currently undergoing phase 3 trials (133). In pharmacological assessment linked to a phase 1 trial, retatrutide has demonstrated reduced cAMP potency at the hGLP1R and hGCGR but enhanced potency at hGIPR (134). The phase 2 trial in people living with diabetes had the advantage of comparing retatrutide with, and showing benefit over, the widely used GLP1R agonist, dulaglutide. For the highest dose of retatrutide, the reported a mean reduction in HbA1c was -2.02% more than placebo and -0.61% more than dulaglutide at 24 weeks (135). The same study also reported mean total body weight loss of -13.94% more than placebo and -14.92% more than dulaglutide. The phase 2 trial for people living with obesity reported an impressive mean total body weight reduction of -22.1% with their maximum dose compared to placebo (136). Phase 3 trial results are expected in 2026, and it will be interesting to see outcomes for the secondary end points concerning lipids and other cardiovascular parameters.

There are many other medications undergoing Phase 1 trials, mostly receptor agonists similar to those currently under investigation (123). Additionally, agents with novel targets were investigated at a Phase 1 level such as GDF15 analogues (137–139) and a dual amylin receptor and calcitonin receptor agonist (140,141) although only one new class (full agonists of the free fatty acid receptor GPR40 (142)) has had sufficiently positive results to warrant Phase 2 trials.

Incretin physiology

At the turn of the 20th century, hormones were discovered (143) and a link was made between the gastrointestinal tract and the pancreas. Extracts from the gut were shown to stimulate release of pancreatic exocrine secretions (144) and lower urinary glucose (145). In 1929, Jean La Barre purified glucose-lowering extracts from the gut and coined the name incretin (INtestine seCRETion INsulin) (146,147).

However, it wasn't until the discovery of insulin (148) and development of radioimmunoassays (RIA) (149), that more accurate measurement of low-level circulating molecules such as peptide hormones could be achieved, which permitted incretins to be further explored (146). Using RIA to measure insulin, it was discovered that oral glucose load produces a much greater insulin response than an intravenous infusion of glucose (150,151). This suggested the presence of a gut-pancreas axis to control blood glucose and was termed the "incretin effect".

GIP was the first incretin to be discovered in the 1970s (146), initially noted to inhibit gastric secretion and named gastric inhibitory peptide, it was later renamed to glucose-

dependent insulinotropic polypeptide after the observation that it lowered blood glucose in an insulin-dependent manner (152).

GLP1 was discovered in the 1980s after immunoreactivity was detected in the intestinal mucosa that was similar to glucagon but different to the well-characterised form of pancreatic glucagon (153,154). This led to cloning and sequencing of preproglucagon and discovery of two novel glucagon-like peptides within its structure; GLP1 and GLP2 (155,156).

GLP1 was found to be synthesised in its full structure but also as N-terminally truncated forms, which demonstrated substantial insulin release and glucagon inhibition (157,158) and counteracted the hyperglycaemia in diabetes (159,160).

GLP2 does not mediate glucose metabolism but instead modulates intestinal nutrient absorption and epithelial biology (161) and a GLP2 receptor agonist has been licensed for short bowel syndrome (162–164). It is worth noting that several other gut-derived hormones also stimulate insulin secretion (such as gastrin, cholecystokinin) which would fit the definition of an incretin hormone, but their study and development into therapeutical agents has been overtaken by that of GLP1 and GIP (146).

Both GIP and GLP1 are peptide hormones produced by enteroendocrine cells in the gastrointestinal tract; GIP is secreted from K cells in the duodenum and upper jejunum (165) and GLP1 is secreted from L cells in all parts of the intestine but more so distally (166). GLP1 production was also identified in the brain, and its structure was confirmed to be the same as GLP1 produced in the intestines (157,158,167).

GIP and GLP1 are released from their respective gastrointestinal enteroendocrine cells in response to the presence of intraluminal (168) and bile acid (169) to regulate metabolism

in many tissues (Figure 2). However, their action is short-lived as they undergo rapid proteolytic degradation by dipeptidyl peptidase-4 (DPP4)(170).

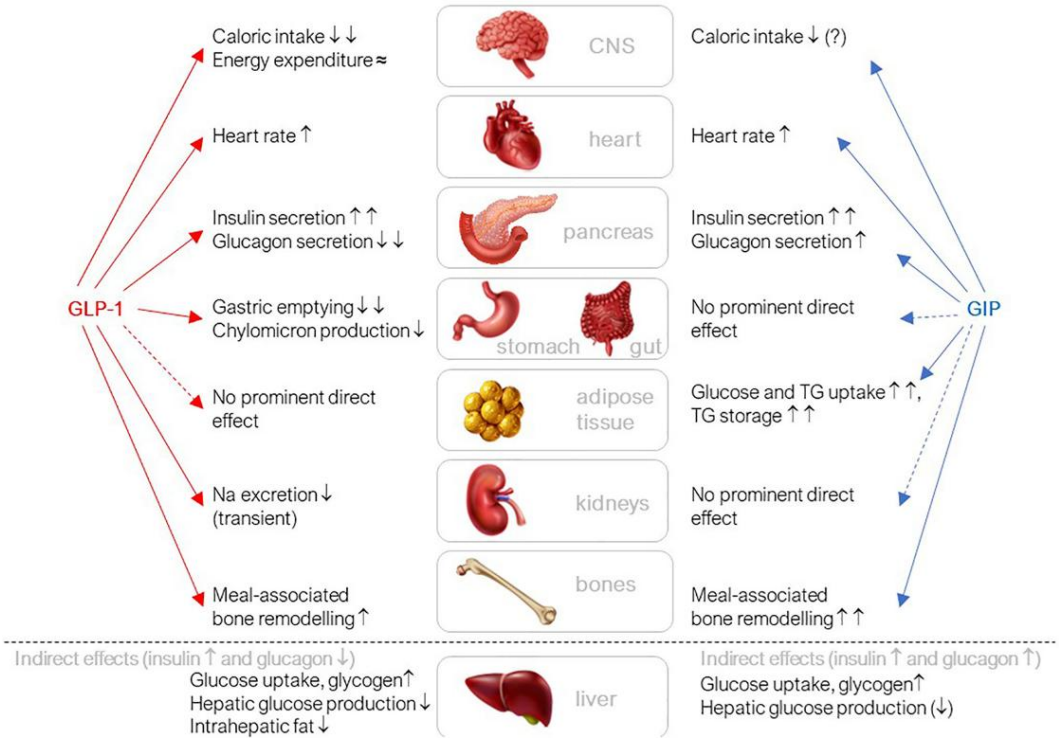

Figure 2: Summary of GLP1 and GIP action in different tissues. Reproduced from Nauck et al 2021 (174).

GLP1 and GIP action on tissue occurs via their cognate receptors, GLP1R and GIPR respectively. *Glp1r* mRNA or GLP1R expression has been found in the pancreas, lung, brain, kidney, stomach, intestines, heart and vasculature (171–174).

Gipr mRNA has been found in the pancreas, heart, adipose tissue, brain, lung, bone and vasculature (174). However, identifying or locating protein expression has been limited, with only a small number of studies reporting receptor expression (174).

Of relevance to this thesis, GLP1 and GIP action upon the pancreas and brain improves blood glucose control and facilitates weight loss. Incretin action in the brain will be explored in Chapter 6.

Incretin action in the pancreas

Upon GLP1 binding to its cognate receptor on β cells, it engages $G_{\alpha s}$ to activate adenylate cyclase which induces cAMP release and insulin secretion via PKA-dependent and PKA-independent pathways (175). This occurs in the setting of hyperglycaemia; the mechanisms which mediate this are unclear but theorised to be related to K_{ATP} and K_v channels (175). Additionally, there is evidence that GLP1R activates other pathways, such as the MEK-ERK pathway, via recruiting ß arrestins, and also engages other Gα subunits, such as $G_{\alpha i}$ and $G_{\alpha q}$ (176).

Similarly to GLP1, GIP potentiates insulin release via cAMP-mediated PKA-dependent and PKA-independent pathways. (177,178) as well as via phospholipase A2 and specific protein kinase signalling pathways (179–181). GIP stimulates insulin release in a glucose-dependent manner (54,61–66) and in hypoglycaemia, GIP-mediated insulin release is attenuated (62).

GLP1 and GIP have opposing actions upon glucagon secretion. GLP1 is known to suppress glucagon release in a glucose-dependent manner (182) although whether this occurs directly through GLP1R on α cells (183,184) or via paracrine signalling of somatostatin release (185–187) remains debated since GLP1R/GIPR protein detection has been a challenge.

Gipr expression has been found in α cells (188–190) and upon GIP binding to GIPR, glucagon is released in a dose-dependent manner, including in a hyperglycaemic state in rodent islets (61,62,67). In hyperglycaemia, this GIP-mediated glucagon release partially attenuates glucagon suppression by glucose (62,67).

Both *Glp1r* (188,191) and *Gipr* (192) expression has been detected in δ cells, though to a lesser extent than in α and ß cells. In the rodent pancreas, both GLP1 and GIP stimulate somatostatin release (54). However, for GLP1 this only occurs in euglycaemia and not in hyperglycaemia whereas higher concentrations of GIP are able to stimulate somatostatin release in a moderately hyperglycaemic state (54).

Additionally, both GLP1 (193,194) and GIP (195,196) have been shown to improve ß cell survival through protection against apoptosis and enhanced proliferation.

Incretin impairment in diabetes and obesity

The incretin effect is attenuated in the setting of type 2 diabetes (197). There is conflicting evidence about whether GLP1 secretion changes in type 2 diabetes (198,199). It is thought that perhaps changes to GLP1 secretion are a consequence rather than cause of type 2 diabetes (198,199) and that the reduced GLP1 effect is due to reduced ß cell responsiveness (200–204) or reduced GLP1R expression (205).

GIP secretion appears to be unaltered in people with type 2 diabetes (197,202) but its insulinotropic effects are lost (206–208). It has been suggested that this is due to GIPR downregulation (205,209–211) or a defect in post-receptor GIPR signalling (202,208).

Suggesting that GIP is beneficial for glucose control, genetic mouse models have demonstrated that interference with GIP/GIPR signalling results in impaired glucose tolerance (212–214). However, these results have not been borne out in pharmacological studies with antagonists (215) until recently when combined with GLP1R agonism (124). Human studies have demonstrated that GIPR antagonism results in increased plasma glucose and reduced insulin secretion, showing the importance of GIPR-stimulated

insulin secretion in both participants with and without diabetes (reviewed in Rosenkilde 2024). Furthermore, while GLP1 infusion can stimulate insulin release (216) and improve glucose tolerance in people with type 2 diabetes (200,201,217,218), this is not the case for GIP (200,217,218), which has led to a lack of interest in GIP as a therapeutic option until recently.

In the setting of obesity, the incretin effect is also attenuated even without impaired glucose tolerance or diabetes (219–221). This blunted effect has been shown to be a marker of early ß cell dysfunction (222) and a predictor of future weight and insulin insensitivity (223) in young people with obesity. It is unclear if this attenuated incretin effect is due to changes in post-prandial GLP1 secretion as evidence differs regarding whether levels are reduced (224), enhanced (225) or unchanged in obesity (226).

The role of GIP in the development or treatment of obesity remains controversial. GIP has long been considered an obesogenic hormone since global GIPR KO (227) and antagonism (228–231) afforded GIPR-/- and *ob/ob* mice protection against diet induced obesity. Conversely, several reduced or loss of function GIPR variants in humans have been associated with reduced BMI (232–235) but impaired glucose tolerance (236), compared with an equivalent non-carrier. Furthermore, several other studies have demonstrated that GIPR agonism induces weight loss in humans (215,237) and in mice (215,237) or at least does not induce weight gain in humans (238–240) and rodents (238–240). However, it is likely that GIPR agonist effects on glycaemia and weight loss depend upon the treatment duration as functional GIPR desensitisation can occur with chronic GIPR agonist administration (241,242).

The picture of whether GIPR agonism or antagonism is beneficial for glucose control and weight has become even more perplexing since superior weight loss and glucose control

have been demonstrated when GLP1R agonism is combined with either GIPR agonism (116,237,243) or GIPR antagonism (125,244).

To resolve this conflict, it has been suggested that the comparable weight loss induced from both GIPR agonism and antagonism could be due to chronic pharmacological GIPR activation inducing functional antagonism in a subgroup of neurones. Desensitisation has been reported for GPCRs (245) and has been observed for GIPR in adipocytes, pancreatic islets cell lines and mouse neuroblastoma Neuro2a cells (241,246–249). However, GIPR antagonism and agonism have been found to have opposing effect upon gene expression in neurones of the dorsal vagal complex, a hindbrain centre for regulating energy homeostasis, suggesting that agonism and antagonism of GIPR in this brain region exert different effects (250). However, it is important to note that the tissue samples in this study were collected after one dose of the ligands and more chronic administration may be required to induce functional antagonism.

A potential explanation for improved glucose control induced by impaired GIP/GIPR signalling is that there is increased receptor sensitivity of GLP1R. This was suggested when GLP1 resulted in greater insulin secretion in GIPR-/- mice compared to controls (212). This was also found in islets from GIPRßcell-/- mice, suggesting that any increased GLP1 sensitivity is mediated at the ß cell level (196). This increased GLP1 sensitivity is unlikely to be due to increased GLP1 levels or increased GLP1R expression as these parameters were comparable with control mice for both the GIPR-/- and GIPRßcell-/- mice (196,212). Resistance to weight gain from HFD has also been observed in GIPR-/- mice (251). However, any increased GLP1 sensitivity which might account for this is likely via a non-ß cell mechanism, as enhanced weight loss was not seen in GIPRßcell-/- mice administered a GLP1RA (252).

A further possible explanation is that the different structures and pharmacology of GIPR agonists and antagonists results in differences in target cells engaged with or post-receptor GLP1R signalling. In the brain, GIPR peptide agonists combined with GLP1RAs act upon GABAergic neurons to reduce food intake and weight (253,254). However, the loss of GABA-ergic neurones does not impede the effect of GIPR antagonism in conjunction with GLP1R agonism upon weight loss and reduced food intake (250). Tirzepatide is a dual GLP1R/GIPR agonist but has been shown to be a biased and imbalanced agonist (255). The imbalanced agonism refers to the observation that tirzepatide preferentially binds to GIPR>GLP1R in humans and the biased agonism refers to the difference in downstream signalling compared with GLP1 (cAMP over ß-arrestin at GLP1R) (255). Furthermore, changes to the structure of tirzepatide alter its binding affinity with GLP1R and GIPR (256), confirming that inherent differences in ligand structure could underlie differences in efficacy.

Identifying GLP1R and GIPR

To further investigate incretin and dual agonist biology, the ability to identify the presence and location of GLP1R and GIPR is key and the importance of having well-validated, specific reagents to detect mRNA or protein has long been highlighted (257,258).

As reviewed in (259), many reagents and methods for mRNA or protein expression have been developed for *Glp1r*/GLP1R but very few have been developed for *Gipr*/GIPR. Additionally, there are varying degrees of validation for each reagent (259).

Transcriptomic studies using RNA sequencing have identified the presence of *Glp1r* and *Gipr* in several relevant cells such as pancreatic islet cells and neurones

(188,190,191,260). However, for Class B GPCRs like GLP1R and GIPR there is discordance between the degree of gene or RNA expression and final protein expression (261). This could be due to many factors including rates of translation, stability and half-life of mRNA and protein (262,263) as well as differences in sensitivities of detecting reagents. Therefore, transcriptomic studies should be interpreted with a degree of caution.

Genetic modification of mice has yielded some helpful models with which to investigate incretin physiology. Global or cell-specific GLP1R-/- and GIPR-/- knockout mice have revealed novel aspects of incretin physiology (212,264) and identified cellular substrates of dual agonists (253). However, on their own they cannot be used to explore GLP1R/GIPR interactions.

Reporter mice have been generated, where a reporter gene is put under the control of a promoter gene, which is transcribed when the gene for the protein of interest is expressed. In the field of incretins, fluorescent proteins have been incorporated into the genes for GLP1R (265,266) or GIPR (267), which allows the visual identification of cells which are expressing *Glp1r* or *Gipr*. This has revealed novel cell types which express *Glp1r* but, as for transcriptomic studies, it is important to recognise that it may not be reflective of true protein expression.

The *Glp1r* and *Gipr* genes have been modified to incorporate self-label protein tags. This fusion gene is then transfected into cells of interest (268) or genome-edited into transgenic mice (269). The cell or tissue is incubated with an organic fluorophore which fluoresces once it binds to the protein tag (270). Such self-label protein tags include the SNAP-tag (271–273), HaloTag and CLIP-tag (274). SNAP_GLP1R and SNAP_GIPR have been generated and well characterised in cell lines (241,275–277). Halo-GLP1R has also been developed and reported on (278–280). Mice with SNAP-tagged GLP1R (GLP1RSNAP/SNAP)

have been generated using CRISPR/Cas9 genome editing and validated to ensure intact GLP1R function and ability to bind to validated fluorescent probes and antibodies (269). A mouse model with Halo-Tag GIPR was generated (GIPRHalo/Halo) but responses to GIP were impaired (281). This was postulated to be due to decreased cell surface GIPR expression and impaired downstream signalling (281) and serves as a reminder of the importance of robust validation of novel models and reagents to explore incretin biology. Advantages of self-label proteins include labelling of the protein of interest without interfering with orthosteric binding and that substrates can be modified to alter their properties without affecting their binding to the SNAP-tag, for example to become cell permeable/impermeable to suit the target localisation (282).

However, inherently these transgenic mouse models and self-label protein tags are unable to connect the binding of a drug with its function within a cell. Furthermore, they are limited to exploring non-human incretin physiology; an important consideration in light of the contrasting affinity and action of tirzepatide in mice compared to humans (264).

Antibodies are commonly used to confirm protein presence and location, although they are limited to use in fixed tissue. Several GLP1R antibodies (agonist, antagonist and neutral) have been developed and suitably validated – for example, demonstrating lack of labelling in knockout models or cells not expressing GLP1R (reviewed in (259)). However, only a few GIPR antibodies have been generated and insufficient data showing their specificity has been published (252,283) or they are not commercially available, despite our requests (284).

Fluorescent probes are capable of addressing some of the challenges of identifying GLP1R and GIPR. Probes are peptides conjugated to a fluorophore which bind to the orthosteric binding site and can be modified to be agonists or antagonists. Not only are they suited for

live imaging and imaging post-fixation, but they can also be administered in vivo to assess which cells exogenously applied ligands can access. They can also be applied alongside markers for other receptors, genes or hormones of interest, such as antibodies and in reporter mice. Prior to commencement of this work, no fluorescent probes for GIPR or dual GLP1R/GIPR had been published. During the course of this work, two relevant probes were published: GIP-TMR (281,285) and Alexa647-conjugated tirzepatide (256).

GIP-TMR did not label islets from *Gipr*-/- mice and demonstrated similar intracellular labelling compared with SNAP-labelled GIPR (285). However, the doses administered were somewhat higher than pharmacological dosing; 1μM compared to nanomolar pharmacological range (286,287). Furthermore, detailed pharmacological characterisation was not published (such as binding affinity) which can be altered when a ligand is conjugated to a fluorophore. Alexa647-conjugated tirzepatide was reported (256) but evidence of its validation was not. Pharmacological data such as binding affinity or potency was not reported, which should lead to the probe being considered as non-specific until such data is presented. Additionally, it did not label *Glp1r*$^{-/-}$ mice, when it would be expected to see some residual GIPR labelling, suggesting that the probe may not be able to bind to GIPR or has a low sensitivity in the setting of endogenously expressed GIPR.

Table 6 summarises the current methods of identifying GLP1R and GIPR.

Model/reagent	GLP1R	GIPR	GLP1R/GIPR
Knockout mice	GLP1R-/- (288) GLP1R-/-ßcell (289)	*Gipr*-/- *Gipr*-/-ßcell (196) *Gipr*-/-Ap2 (adipose)(290) *Gipr* Tie2-/- (haemopoetic)	Double GIPR/GLP1R knockout (291)
Reporter mice	Three, reasonable validation (259)	*Gipr*EYFP (267) *Gipr*GFP knock in (213)	None
Self-label enzymes	SNAP-GLP1R Halo-GLP1R	SNAP-GIPR	-
Antibodies	Many validated options (259)	Very few, not well-validated (259)	-
Fluorescent probes	Several, well validated options (259)	GIP-TMR (281,285)	Alexa647-tirzepatide (not validated) (256)

Table 6: Summary of current reagents available to identify GLP1R and GIPR Adapted from Ast et al (259).

Thesis aim

A greater understanding of GIP biology is required to reconcile the paradox of beneficial results of GIPR agonism and antagonism and to interrogate the cellular substrates and mechanism of action of dual GLP1R/GIPR agonists.

Visualising GLP1R and GIPR and quantifying their number and location in the setting of chronic agonism would help shed light on whether a functional antagonism through downregulation of GIPR occurs. Identifying GIP cell targets, for example in adipose tissue or the brain, would further our understanding of how GIP modulates weight and identify pathways to target to further optimise treatments.

Evidence reported so far points to a deep intertwining of GIPR and GLP1R dynamics. There have been no recent human studies which assess the effect of GIPR agonism or antagonism without GLP1RA activity. However, in the context of many further dual and triple incretin medications being licensed, interrogating the interplay between GIPR and GLP1R activation and signalling would be a step towards determining whether GLP1R agonism is the key factor for resolving this paradox.

Furthermore, determining the impact of GIP/GIPR interactions upon GLP1R agonism will enable greater understanding of how dual agonists or antagonists work and will contribute to the development and optimisation of novel agents. For example, it is not known if the synergism between GLP1R and GIPR activation from dual GLP1R/GIPR agonism is a result of action upon the same cell expressing both receptors, or each receptor on different cell types. In the pancreas, GIPR was not needed for weight loss from GIPR antagonism/GLP1R agonism in GIPR-/-ßcell mice, suggesting that at least in the ß cell, the synergism may not be from same-cell mechanisms such as receptor dimerization or internalisation kinetics (215,252).

As explored in subsequent chapters, there are challenges in detecting GIPR and visualising dual GIPR/GLP1R targets and activation. This thesis aims to present the development of high quality, novel probes that address some of these challenges. We provide fresh insight into GIPR and dual GIPR/GLP1R biology and begin to bridge the gap in knowledge of what happens to dual agonists after in vivo administration and physiological impact.

Firstly, novel fluorescent GIPR agonist probes, sGIP549 and sGIP646, will be presented. We describe their pharmacological profile and the validation of their specificity in relevant settings, such as GIPR-/- and GIPR-/-ßcell mice.

Next, our novel fluorescent GLP1R/GIPR dual agonist probes, daLUXendin544 and daLUXendin660 will be presented. Following the assessment of their pharmacological profiles, probes were validated in relevant settings, such as GLP1R-/- mice and in the presence of excess GIP agonist. We then demonstrate that the probes are suitable for several super-resolution and single molecule imaging techniques (such as dSTORM, TIRF and STED microscopy) and show that dual agonism likely increases GIPR and GLP1R interaction. Finally, we also undertook in vivo work to confirm that the pharmacological profile is reflective of in vivo efficacy and then demonstrated the cell targets of the probes in islets and the brain, providing insight into dual agonist access.

Chapter 2: Materials and methods

General chemicals and solvents

General chemicals and solvents were acquired from Sigma, Thermo Fisher Scientific or Cambridge Bioscience.

Ethics

Animal studies were completed in accordance with the Animals (Scientific Procedures) Act 1986 of the United Kingdom (Project Licences P2ABC3A83, PP1778740 and PP6526002). Ethical approval was granted by the University of Birmingham, University of Oxford and University College London Animal Welfare and Ethical Review Bodies (AWERB).

Fluorescent peptide synthesis

The novel sGIP and daLUXendin probes were synthesised on solid phase support prior to global deprotection and purification by reverse-phase HPLC and HRMS characterisation. Maleimide "click chemistry" was used to conjugate the Cy3 and Cy5 fluorophores to the peptides before HPLC purification and characterisation using LCMS and HRMS.

HTRF cAMP assay

AD293 cells (RRID:CVCL_9804) were transiently transfected for 24h before the assay using Lipofectamine 2000 in six-well plates with plasmids encoding wild-type hGLP1R, mGLP1R, hGIPR or mGIPR. AD293 cells were authenticated at source using STR profiling. Cells were detached and treated with a range of agonist concentrations in serum-free

DMEM + 0.1% BSA for 30min, 37°C in 96-well plates, followed by the addition of lysis buffer 2 (Cisbio/Revvity, cat no 62CL2FDF) at a 1:2 ratio. Lysates were further diluted 1:10 to avoid spectral interference from the higher concentrations of fluorescent ligands in the HTRF assay, and the concentration of cAMP was determined after the addition of cAMP Dynamic detection reagents (Cisbio/Revvity, cat no 62AM4PEB). Three-parameter logistic fitting was used to determine signalling potencies for each ligand, with EC50 ratios relative to the cognate ligand for each receptor used to establish test agonist selectivity for GLP1R versus GIPR.

NanoBRET binding assays

HEK293T cells (RRID:CVCL_0063) were cultured in Dulbecco's Modified Eagle Medium (DMEM)/F12 GlutaMAX (ThermoFisher, cat no 10565018), supplemented with 10% FBS and 1% antibiotic-antimycotic solution and cultured at 37°C, 5% CO2. HEK293T cells were authenticated at source using STR profiling. Cells transiently expressing Nluc–GLP1R or Nluc–GIPR were seeded onto white 96-well plates and cultured for 24h. Media was then removed, and cells were incubated in PBS supplemented with 0.1% BSA and 0.01% NanoGlo (Promega, cat no N1110). For saturation binding assays, daLUXendins were added across the concentration range 0.1–31.6nM, in the absence or presence of 1μM GIP and 1μM Exendin-9 to determine specific binding. For competition binding assays, cells were co-treated with 10nM daLUXendin and GLP1 or GIP across the range 1μM to 1pM. Plates were read using a PheraSTAR microplate reader, using the NanoBRET filter module. BRET ratios (λacceptor/λdonor) were calculated, and saturation data fit using the 'One Site – Specific Binding' equation of GraphPad Prism 10. Competition binding was fit using the 'One Site – Fit Ki' equation.

AD293 cells culture and transfection with SNAP_hGIPR/hGLP1R and HALO_GLP1R

AD293 cells (RRID:CVCL_9804) are derived from Human Embryonic Kidney 293 cells and favoured for their ease of transfection and improved adherence (292). Cells were acquired from Agilent Technologies LDA UK Limited (cat no 240085). To identify target receptors without interfering the ligand binding site, cells were transfected with plasmids for two receptors harbouring enzyme self-labels, SNAP_GIPR (Alejandra Tomas lab) and/or HALO_GLP1R (generated in-house).

AD293 cells were grown in 10ml AD293 culture medium in a T75 flask and incubated at 37°C, 5% CO2 and passaged at 80-90% confluency. AD293 culture medium consisted of DMEM High Glucose (Merck Life Science UK Limited, cat no D6546-500ML) supplemented with 10% fetal bovine serum (FBS), 1% penicillin/streptomycin (pen/strep), 1% glutamine. For seeding, at 80-90% confluency in a T75 flask, one third of the cell volume was seeded, 100µL per well, on a glass-bottomed 96-well imaging plate (Miltenyi Biotec Ltd, cat no 130-098-265) previously coated with poly-l-lysine 0.01% (SLS, cat no P4707-50ML). Cells were incubated overnight in AD293 media at 37°C, 5% CO2 until they reached 90-100% confluency.

Next, culture media was removed, and cells were transfected with 0.3µL Lipofectamine 2000 (Invitrogen, cat no 11668027) per well and 50ng DNA (SNAP_GIPR or SNAP_GLP1R plasmid) per well in 110µL OptiMEM/well and incubated overnight 37°C, 5% CO2. Cells co-transfected with both plasmids received 50ng of each DNA. Control, non-transfected cells were cultured overnight in 50µL OptiMEM without the addition of Lipofectamine 2000 or DNA.

The next day, culture media was removed and 50-100µL of labelling solution or AD293 media (for unlabelled control) added to each well, as detailed below.

Probe and SNAP_GIPR/HALO_GLP1R AD293 cell labelling

For validation of the novel GIPR probes, a day after transfection the transfection media was removed, and cells were incubated in 50-100µL of the following solutions:

1. 100nM sGIP549, 500nM BG-Sulfo646
2. 100nM sGIP648, 500nM BG-Sulfo549
3. 100nM sGIP549
4. 100nM sGIP648
5. 500nM BG-Sulfo646
6. 500nM BG-Sulfo549
7. AD293 media (unlabelled control)

Additionally, two wells of non-transfected cells were incubated in dual probe solutions (solutions 1 and 2).

For validation of the fluorescent daLUXendin probes, a day after transfection the transfection media was removed before cells were incubated in 50-100µL of the following solutions:

1. 500nM daLUXendin544, 500nM SBG-OG, 500nM CA-Sulfo646
2. 500nM daLUXendin660, 500nM SBG-OG, 500nM CA-Sulfo549
3. 500nM daLUXendin544
4. 500nM daLUXendin660
5. 500nM SBG-OG
6. 500nM CA-Sulfo549
7. 500nM CA-Sulfo646

8. AD293 media (unlabelled control)

Additionally, two wells of non-transfected cells were incubated in triple probe solutions (solutions 1 and 2).

The probes were diluted in AD293 media and cells were incubated in the solutions for 55 minutes at 37°C, 5% CO2. After 55 minutes, 0.5µL 1:100 Hoechst 33342 (Merck, cat no 14533) was applied to each well and the cells were further incubated for 5 minutes at 37°C, 5% CO2 and then washed once with 100µL AD293 media. Cells were then imaged in 100µL AD293 media.

MIN6-CB4 cell culture and labelling

MIN6-CB4 cells were generated and phenotyped in line with previously published protocols (293). Cells were grown to 70% confluency in MIN6 media: DMEM High Glucose (Merck Life Science UK Limited, cat no D6546-500ML) supplemented with 15% FBS, 71µM 2-mercaptoethanol, 2mM glutamine, 100u/ml penicillin, 100mg/L streptomycin. Cells were then seeded in 100µL MIN6 media per well, on a glass-bottomed 96-well imaging plate (Miltenyi Biotec Ltd, cat no 130-098-265) previously coated with poly-l-lysine 0.01% (SLS, cat no P4707-50ML).

The day after seeding, cells were incubated with either 500nM daLUXendin660, 100nM sGIP549 or 100nM LUXendin551, a combination of two or MIN6 media for 1h at 37°C, 5% CO2. One repeat was incubated for 55 minutes and Hoechst 33342 (Merck, cat no 14533) added for the last 5 minutes of incubation (final concentration of Hoechst 33342 1:10,000). Cells were then washed 2-3 times with MIN6 media and then imaged in 100µL MIN6 media.

EndoC-βH5 cell model and culturing

EndoC-βH5 cells are an immortalised human beta cell line which retain appropriate insulin secretion in response to glucose and incretin stimulation (294). EndoC-βH5 cells were obtained from Human Cell Design and cultured in EndoC-βH5 media at 37°C, 5% CO2 for 7 days prior to experimentation. 12-15 islets were picked per condition and were labelled with probes and washed as per the islet probe labelling protocol described above.

Gipr-/- mouse model

Islets from global *Gipr*-/- mice were kindly provided by collaborators (Frank Reimann and Fiona M. Gribble, Institute of Metabolic Science & MRC Metabolic Diseases Unit, University of Cambridge, Cambridge, UK). Methods for generation of this global knock-out model using CRISPR-Cas9 genome-editing technology are detailed in (295) and summarised below.

Firstly, Red/ET recombination technology was used to replace the *Gipr*-coding sequence (from the start codon in exon2 to the stop codon in exon 14) in the bacterial artificial chromosome RP23-384-I23 with an *iCre*-sequence.

A sequence containing the *iCre* sequence flanked by 816bp and 879bp from the *Gipr* locus was amplified and cloned into a vector (pCR-BluntII-TOPO). The circular donor plasmid was injected into one-cell stage fertilized C57Bl6/CBA-F1 embryos along with Cas9-protein, guide RNAs targeting the wild-type *Gipr* gene and SCR7 inhibitor. Embryos with positive recombination were identified using PCR analysis specific for the recombined allele and Sanger sequencing confirmed correct recombination. Off target genetic modifications were minimised through sequencing and excluding likely off-target genetic alterations and crossing offspring with C57Bl6/JN for >8 generations. Heterozygous mice were then back-crossed into C57Bl6 >8 generations before then generating homozygous

Gipr-Cre mice (*Gipr* knock-out). The pancreata of resulting homozygous *Gipr*-/- mice were then used for primary islet isolation before shipment to our laboratory.

Upon receipt of shipment, islets were centrifuged (1500RPM, 2 minutes, room temperature), supernatant discarded, and islets resuspended in 5mL complete RPMI media: RPMI 1640 media (Life Technologies Ltd, cat no 21875034) supplemented with 10% fetal bovine serum, 1% penicillin/streptomycin, 1% glutamine. The islet resuspension was filtered through a 40µm cut-off filter (Greiner Bio One, cat no 542040) and captured islets were washed from the filter using complete RPMI media. Islets were then picked into a fresh dish of complete RPMI media and incubated at 37°C, 5% CO2 for at least 24h before experimentation.

Gipr-/-βcell mouse model

Islets from mice with β-cells devoid of GIPR were kindly provided by a collaborator (Jonathan Campbell, Department of Medicine, Duke University Hospital, Durham, NC, USA). This *Gipr*-/-βcell line was generated using tamoxifen-inducible Cre recombinase, detailed in (296) and summarised below.

MIPcreERT mice are a transgenic line on a C57BL/6J background which express tamoxifen-inducible Cre driven by the mouse insulin promoter (297). MIPcreERT mice were bred with floxed *Gipr* mice (*Gipr*flfl), backcrossed 8 times to C57BL/6J background to generate *Mip-Cre*+/-;*Gipr*fl/fl mice (ß cell *Gipr* knockout; *Gipr*-/-βcell) and Mip-Cre+/-;*Gipr*+/+ (littermate control; Mip-Cre) mice.

Once mice reached 6 weeks of age, they underwent 5 consecutive daily intraperitoneal injections of tamoxifen to cause Cre-induced inactivation of the *Gipr* gene. Four weeks later, *Gipr*-/-βcell mice and WT littermates underwent Schedule 1 procedure and pancreata were then used for primary islet isolation before shipment to our laboratory.

Upon receipt of shipment, islets were centrifuged (1500RPM, 2 minutes, room temperature), supernatant discarded, and islets resuspended in 5mL complete RPMI media (as detailed above). The islet resuspension was filtered through a 40µm cut-off filter and captured islets were washed from the filter using complete RPMI media. Islets were then picked into a fresh dish of RPMI media and incubated at 37°C, 5% CO2 for at least 24 hours before experimentation.

*Glp1r*KO/KO / *Glp1r-/-* mouse model

An in-house line of global GLP1R knock-out mice was used, with details of model generation published in (298) and summarised below.

A single base pair deletion into exon 1 of the *Glp1r* locus was introduced using CRISP-Cas9 genome-editing technology. Fertilized eggs of female Cas9-overexpressing mice were harvested following super-ovulation and modified single-guide RNA targeting exon 1 of *Glp1r* and a single-stranded repair-template were injected into the pronucleus of embryos at the one-cell stage. Embryos that reached the two-cell stage were implanted into surrogate mice. Genotyping PCR identified *Glp1r-/- / Glp1r KO/KO* mice, in which the repair-template was not integrated but instead harboured a single-nucleotide deletion which resulted in a frame-shift mutation and global loss of GLP1R protein.

The top 10 loci of off-target sites in the targeted locus of *Glp1rKO/KO* offspring were predicted using the CRISPR Guide Design Tool (crispr.mit.edu), amplified by PCR and analysed with Sanger sequencing. Subsequent founder animals harbouring alleles with small deletions were backcrossed to C57BL/6J WT mice for 1–3 generations to outbreed impacted off-targets before generating homozygous *Glp1rKO/KO*. Detail of primer used in

the genotyping PCRs are available in (299). To ensure the availability of *Glp1r*WT/WT or *Glp1rWT/KO* littermates, animals were bred in heterozygous pairs.

*Glp1r*SNAP/SNAP mouse model

An in-house line of SNAP-labelled GLP1R mice was used with details of model generation detailed in (300) and summarised below.

CRISPR-Cas9 genome-editing was used to knock-in the SNAPf-tag after the N-terminal signal sequence of the *Glp1r*. In vitro testing of the construct showed signalling to be identical to human GLP1R-GFP and other SNAP-GLP1R constructs. Two offspring integrated repair template and one founder to C57BL6/J mice were backcrossed until no off-target mutations were detected in predicted loci after 1-2 generations. The pancreata of resulting homozygous *Glp1r*SNAP/SNAP mice were then used for primary islet isolation.

Glp1r-tdRFP, *Gipr*-GFP and *Gipr*-GCaMP3 mouse model

Islets from this fluorescent GLP1R mouse line were kindly provided by a collaborator (Stefan Trapp, Division of Biosciences, University College London, London, UK). This line has been published and validated, with details of its generation in (301) and summarised below.

First, Cre-recombinase was expressed under the control of the *Glp1r* or *Gipr* promoter by using Red/ET recombination technology to insert an optimised Cre (*iCre*) sequence in *Glp1r*/*Gipr* in the murine based bacterial artificial chromosome (BAC) RP23-408N20. Direct sequencing using oligonucleotides was used to confirm the identity and correct positioning of the *iCre* sequence.

BAC-DNA was purified and the plasmid injected into the pronuclei of ova derived from C57B6/CBA F1 parents and the embryos reimplanted into pseudopregnant females. DNA from pups was obtained from ear clips and screened for the transgene using PCR. The founder strain was backcrossed with C57B6 mice for >8 generations and then two founder strains crossed with a ROSA26-tdRFP (302), ROSA26-EYFP (266) or ROSA26-GCaMP3 (303) reporter strains. Generated strains were assessed for fluorescence in islets and taken forward for experimentation.

Primary islet isolation and culture

7–12-week-old male and female mice were used as tissue donors. Animals were euthanised in accordance with a schedule-1 procedure and bile ducts injected with Serva NB8 1mg/ml collagenase. The pancreata were dissected, islets isolated using a histopaque gradient (Merck, cat no 10831 and 11191) and cultured at 37°C, 5% CO2 in RPMI 1640 media (Life Technologies Ltd, cat no 21875034) supplemented with 10% FBS, 1% pen/strep, 1% glutamine (complete RPMI). Islets were used up to four days after isolation.

iPSC model and culture

ALSTEM #iPS11 human-induced pluripotent stem cells (iPSC) were obtained from Novo Nordisk. Two differentiations were used for experimentation, both from the iPSC-11 cell line; Diff-1 and WT CAS9.

iPSCs were cultured on iPSC qualified Matrigel in mTeSR+ media (STEMCELL Technologies #05826). Differentiation to islet-like structures (SC-islets) was carried out in a suspension-

based, magneticCELLSPIN bioreactor system (PFEIFFER). Differentiation media was changed daily by letting spheres settle by gravity for 3–10 minutes. Upon maturation, SC-islet clusters were cultured in 2ml of maturation media in a 6-well suspension plate upon a shaker at 100RPM at 37°C, 5% CO2. Maturation media was changed every 2 days. SC-islet differentiation was based on published protocols (189,304).

Human islet isolation and culturing

Human islets were received from the Diabetes Research and Wellness Foundation (Churchill Hospital, Oxford, UK), European Islet Transplantation Consortium (Milan, Italy) and the Alberta Diabetes Institute Islet Core (Alberta, Canada).

Upon receipt of shipment, islets were centrifuged (1300RPM, 2 minutes, room temperature), supernatant discarded, and islets resuspended in 10mL human islet media: Connaught Medical Research Laboratories media (CMRL; Thermo Fisher Scientific, cat no 11530037), 10% FBS, 1% pen/strep, 0.1% Amphotericin B (Sigma Aldrich, cat no A2942). The islet resuspension was filtered through a 40µm cut-off filter (Greiner Bio One, cat no 542040) and captured islets were washed from the filter using human islet media. Islets were then picked into a fresh dish of human islet media and incubated at 37°C, 5% CO2 for at least 24h before experimentation. Media changes were performed daily for the first 3 days.

Human islet labelling and fixation

For both live and fixed imaging, islets (15-20 islets for live, 40-50 islets for fixed) were incubated in 100µL 500nM daLUXendin544 or 500nM daLUXendin660 for 1 hour at 37°C, 5% CO2. Islets were then washed three times in 1x PBS or human islet media.
For live imaging, islets were then transferred to 100µL human islet media for imaging in a glass-bottomed 96-well plate (Miltenyi Biotec Ltd, cat no 130-098-265).
For fixed sample imaging, islets then were fixed in 4% PFA for 15 minutes at room temperature before three more washes in 1x PBS. Islets were then mounted on a microscope slide with 20µL Everbrite Hardset Mounting Medium with DAPI (Biotium, cat no 23004) and a coverslip applied. Islets treated with lipofuscin autofluorescence quencher were incubated in 50µL TrueBlackPlus (Cambridge Bioscience, cat no 23014-T-BT) for 10 minutes at room temperature then washed three times in 1x PBS immediately prior to mounting. Slides were dried overnight at 4°C before imaging at least 24h hours later.

Mouse islet and EndoC-ßHC cell labelling and live imaging

LUXendins are fluorescent, antagonistic GLP1R peptide probes which produce intense and specific membrane labelling in both live and fixed tissue (305) which we have used to identify GLP1R+ cells.
For mouse islets, 24-72h after isolation islets were picked into a plastic, round-bottomed 96-well plate into wells containing 100µL complete RPMI with:

1. 100nM sGIP549 and 100nM LUXendin645 or
2. 100nM sGIP648 and 100nM LUXendin551 or
3. 500nM daLUXendin544 and 100nM sGIP648 or

4. 500nM daLUXendin544 and 100nM LUXendin645 or
5. 500nM daLUXendin660 and 100nM sGIP549 or
6. 500nM daLUXendin660 and 100nM LUXendin551

Islets were incubated in these solutions for 1h, 37°C, 5% CO2.

For WT islets, 12-15 islets of medium to large islets pooled from 2-3 mice (n=1 for each condition). For GIPR KO mice, 12-15 non-pooled islets were picked from each mouse. For EndoC-ßHC cells, 12-15 cell clusters were picked from each batch.

For SNAP labelling, 24-48h after isolation GLP1RSNAP/SNAP islets were picked from individual mice or pooled from 2-3 mice. For each condition, 12-15 islets of medium to large size were picked into a round-bottomed 96-well plate (Sarstedt, cat no 83.3926.500) into wells containing 100µL complete RPMI. Islets were treated with 500nM SNAP-label and/or another fluorescent label with orthogonal excitation then incubated for 1h, 37°C, 5% CO2.

For probe or SNAP labelling, islets were then washed two to three times with 100µL complete RPMI or PBS prior to transfer to a glass, flat-bottomed 96-well imaging plate (Miltenyi Biotec Ltd, cat no 130-098-265) where they were imaged in 100µL complete RPMI.

GIPAib2 incubation

15-20 WT and *Glp1r*KO/KO islets were incubated in 100µl 1µM GIPAib2 or complete RPMI for 30 minutes, 37°C, 5% CO2. Islets were then incubated in 500nM daLUXendin544 or 500nM daLUXendin660 or vehicle (ddH2O/DMSO in complete RPMI) for 1h, 37°C, 5% CO2. Islets were then washed three times with 1x PBS prior to transfer to a glass, flat-bottomed

96-well imaging plate (Miltenyi Biotec Ltd, cat no 130-098-265) where they were imaged in 100µL complete RPMI.

Islet labelling, fixation, IHC and imaging

For each condition, 20-30 islets were incubated in 500nm daLUXendin544 or daLUXendin660 for 1h at 37°C, 5% CO2.

Islets were washed three times with 1x PBS then incubated in 100uL 4% PFA for 15 minutes at room temperature.

Islets were then washed three times with 1x PBS or stored in 200uL 1x NaAzide at 4°C then washed three times with 1x PBS when ready for antibody application. Prior to antibody incubation, islets were incubated in permeabilising blocking buffer (1x PBS, 0.1% Triton X, 2% BSA) for 1 hour at room temperature. Islets were then incubated in primary antibody (Table 7) overnight at 4°C. Primary antibodies were diluted in permeabilising blocking buffer.

The following day, islets were washed twice with PBS-Tween (1x PBS, 0.2% Tween, 2% BSA) before incubation with secondary antibody with excitation orthogonal to the daLUXendin used (Table 7) for 2h at room temperature. Islets were washed twice with PBS-Tween and mounted on a microscope slide with 20µL Everbrite Hardset Mounting Medium with DAPI (Biotium, cat no 23004) and a coverslip applied. Slides were dried overnight at 4°C before imaging at least 24h hours later.

	Target	Origin	Working concentration	Supplier	Ex/em wavelengths
Primary antibody	Insulin	Rabbit	1:500	Cell Signalling, cat no 3014S	N/A
	Glucagon	Mouse	1:2000	Sigma, cat no G2654	N/A
	GLP1R	Mouse	1:30	Developmental Studies Hybridoma Bank, cat no Mab7F38	N/A
	Somatostatin	Mouse	1:5000	Invitrogen eBioscience, cat no 14-9751-80	N/A
Secondary antibody	Mouse Alexa488 (Used for GLP1R)	Goat	1:1000	Life Technologies, cat no A11001	ex λ 499nm em λ max 520nm
	Rabbit DyLight488 (Used for insulin)	Donkey	1:1000	Thermo Fisher Scientific, cat no SA5-10038	ex λ 492nm em λ max 519nm
	Mouse Alexa568	Goat	1:1000	Thermo Fisher Scientific, cat no A11004	ex λ 579nm em λ max 603nm
	Mouse DyLight633	Goat	1:1000	Thermo Fisher Scientific, cat no 35513	ex λ 620nm, em λ max 649nm

Table 7: Details of primary and secondary antibodies

Glucose tolerance testing

Male and female 8–12-week-old *Glp1rWT/WT*, *Glp1rWT/KO* and *Glp1rKO/KO* (298) littermates (on a C57BL/6J background) were fasted for 4–6h, with free access to water. Wild-type and heterozygous mice were used as controls, as loss of a single *Glp1r* allele was found to exert minimal influence on phenotype (289). Tirzepatide and daLUXendin were administered at 10nmol/kg before intraperitoneal injection of 2g/kg glucose 60 minutes later. Glucose was measured in blood from the tail vein at 0, 15-, 30-, 60-, 90- and 120-minutes post glucose challenge. Mice were socially housed in specific-pathogen-free conditions under a 12h light–dark cycle with ad libitum access to food and water, relative humidity 55 ± 10% and temperature 21 ± 2°C.

Food intake study

Male and female 12–14-week-old C57BL/N mice were singly housed in a 12h dark–light cycle (14:00–02:00h) and habituated to FED3 feeding devices (306) for 7 days before commencing the study. Food intake was monitored during the habituation phase to ensure that it was stable prior to the end of habituation, There was no significant difference noted in food intake during habituation for mice in any condition. All mice were kept on a 12h light–dark cycle at 20–24°C and 45–65% relative humidity (typically 21°C and 55%). On test days, mice were fasted for 3h before onset of the dark phase by removal of the FED3 devices. At dark onset, mice were injected subcutaneously with either vehicle, daLUXendin660 (10 nmol/kg) or tirzepatide (10nmol/kg), the FED3 devices were returned and food intake was recorded over a 24h period. The study was performed using a three-

way crossover design. A 1 week washout period was observed between experimental days. FED3 devices were checked, serviced and food was topped up daily.

Glp1r-tdRFP and *Gipr*-GFP mice daLUXendin660 labelling, sectioning and imaging

To investigate probe efficacy in vivo, two *Glp1r*-tdRFP and one *Gipr*-GFP mice underwent tail vein intravenous injection of 100nmol/kg daLUXendin660 or vehicle control (ddH2O). After 40 minutes, mice were terminally anaesthetised with pentobarbital and perfused with ice-cold 10X PBS followed by 4% formalin solution. Pancreata were excised and submerged at room temperature in 15% sucrose overnight then 30% sucrose for 24-48h before shipment to our laboratory.

Pancreata were removed from 30% sucrose and incubated in 50:50 30% sucrose: Optimal Cutting Temperature compound (OCT) (Cell Path, cat no KMA-0100-00A) for 15 minutes at room temperature. Pancreata were then embedded in OCT and frozen using dry ice. 10-micrometer sections were obtained using a Leica CM1900 cryostat at between -15°C to -20°C and transferred onto Superfrost Plus microscope slides (Thermo Fisher Scientific, cat no J1800AMNZ). Three non-sequential sections were applied to each microscope slide.

Selected samples were then mounted, or washed in 1 x PBS for one minute then mounted, using 8-20µL Everbrite Hardset Mounting Medium with DAPI (Biotium, cat no 23004) and 0.13-0.17mm thick rectangular cover glass. Mounting media was set overnight at room temperature and stored long term in 4°C. Unmounted samples were stored at -80°C. Samples were imaged with an Olympus FV3000 or Olympus FV4000, as detailed below.

Brain and pancreas labelling

For brain tissue analysis, GLP1R-tdRFP mice and GIPR-Cre:GCaMP6 (GIPR-GCaMP6) mice were terminally anaesthetized using ketamine hydrochloride (Ketavet, Zoetis; 75mg/kg, intraperitoneally) and medetomidine hydrochloride (Domitor, OrionPharma; 1mg/kg, intraperitoneally). Meloxicam (Metacam, Boehringer Ingelheim; 5mg/kg, subcutaneously) was given for peri-surgery analgesia. Mice were placed in a stereotaxic frame, and daLUXendin was injected unilaterally into the lateral ventricle at doses of 5nmol/kg body weight at a rate of 1µl/min. Coordinates relative to bregma were A/P −0.5mm; D/V −2.5mm; M/L 1mm. At 1h post injection, mice were perfused with ice-cold 0.1M PBS followed by 4% formalin solution. All brains were cryo-sectioned coronally at 30µm and mounted onto microscope slides with VECTASHIELD antifade mounting medium (Vector Laboratories, cat no H-1000).

Immunofluorescence labelling in brain tissue

Brains were cryo-sectioned coronally at 30µm and sections processed for amplification of fluorescent reporter signals by immunofluorescence labelling of vimentin (a marker for ependymal cells and tanycytes). Antigen retrieval of free-floating sections was performed using sodium citrate buffer at 80°C for 20 minutes. Sections were next blocked in 5% normal donkey serum, 0.2% Triton X-100 for 1h and then incubated overnight in primary antibody (diluted in blocking buffer) at room temperature (primary antibody: chicken anti-vimentin, 1:750; Abcam, cat no Ab24525). Sections were next incubated for 2h in secondary antibody (in 1% normal donkey serum, 0.2% Triton X-100) at room temperature (secondary antibody: donkey anti-chicken IgY (H+L) highly cross-adsorbed secondary antibody, Alexa Fluor 488, 1:500; Thermo Fisher Scientific, cat no A78948). Sections were

stained with DAPI to mark nuclei, then mounted on Superfrost Plus slides using a Prolong Antifade medium. Sections were imaged on an inverted Leica SP8 confocal microscope using either a ×25 or ×63 oil immersion objective. Three-dimensional reconstructions of daLUXendin660-labelled tissue or antibody-stained cells were rendered using the Surfaces function in Imaris (v.10.1.1) (Oxford Instruments). Opaque surfaces are three-dimensional reconstructions of overlapping areas of daLUXendin660 labelling and antibody staining created using the Coloc function in Imaris.

RNAscope in situ hybridization

Midbrain sections (30µm) containing the ARH from a GIPR-Cre:GCaMP6 (GIPR-GCaMP6) mouse intracerebroventricularly administered daLUXendin660 (3.3nmol/kg body weight) were collected on Superfrost Plus slides and allowed to air-dry at room temperature for 1h. Slides were then dipped in molecular-grade ethanol and further air-dried overnight at room temperature. RNAscope in situ hybridization was performed on these sections using the RNAscope Multiplex Fluorescent Kit (v.2) (Advanced Cell Diagnostics, cat no 323100) as per the manufacturer's instructions, with a modification to the pre-treatment procedure (Protease IV incubation conducted for 20minutes at room temperature). Sections were processed for in situ hybridization of *Glp1r* mRNA (Advanced Cell Diagnostics, cat no 418851-C2). Following hybridization, slides were cover-slipped using a Prolong Antifade medium.

Confocal microscopy

Imaging of live of fixed cells/tissue was performed with either:

1. A Zeiss LSM780/LSM880 meta-confocal microscopes equipped with sensitive GaAsP spectral detectors and 40x and 63x/1.2 W Korr FCS M27 objectives
2. An Olympus FV3000 confocal microscope equipped with GaAsP spectral detectors and UPLSAPO 60x / 1.30 NA silicone and 60x / 1.41 NA oil objectives
3. An Olympus FV4000 confocal microscope equipped with SilVIR spectral detectors and a UPLSAPO 60x / 1.41 NA oil objective

Excitation (ex) and emission (em) wavelengths are shown in Table 8.

Probe	ex λ (nm)	em λ (nm)
sGIP549	561	568-621
sGIP648	633	639-692
LUXendin 551	561	568-621
LUXendin 645	633	639-692
daLUXendin544	561	569-623
daLUXendin660	633	640-694
SBG-OG	488	496-542
BG-JF549	561	569-614
BG-JF646	633	641-694
BG-Sulfo549	561	569-623
BG-Sulfo646	633	640-694
CA-Sulfo549	561	568-613
CA-Sulfo646	633	640-694
Hoechst 33342	405	410-488

Table 8: Excitation and emission wavelengths for probes used in live cell and islet imaging

dSTORM nanoscopy

Islets were labelled with LUXendin645 (500nM), sGIP648 (1µM) or daLUXendin (1µM), before fixation in 2–4% formalin for 15–30 minutes. Islets were mounted on cavity slides, submerged in STORM buffer (Abbelight) and sealed using a 170µm coverslip and dental resin. Samples were imaged in HILO mode on an Evident/Abbelight SAFe 180 system,

using a ×100/1.5 NA Olympus UPLAPO100XOHR objective. LUXendin645, sGIP648 or daLUXendin660 (all Cy5) were pumped to the dark state using an Oxxius laser combiner and 600mW 640nm Coherent Obis diode laser before initiation of photoblinking. Single-molecule events were recorded using an LP650 filter with an integration time of 50ms on a Hamamatsu ORCA-Fusion sCMOS for 20,000–40,000 frames. Localizations were extracted and images reconstructed using Abbelight NEO software. Density-based spatial clustering of applications with noise (DBSCAN) was used to determine localization clustering, implemented in Abbelight NEO software (v.39), with ε = 25 nm (the average precision of the data) and minPts = 8. Results were confirmed using a custom RNA segmentation and DBSCAN routine implemented in R Project (v.4.4.3) (https://cran.r-project.org/web/packages/dbscan/index.html) (307).

Live confocal and STED imaging

Live confocal and STED imaging of CHO-K1:SNAP-GLP1R:Halo-GIPR cells (CHO-K1, RRID:CVCL_0214) was performed on a STEDYCON system (Abberior Instruments), mounted on a Nikon Eclipse TI research microscope equipped with a Plan APO Lambda ×100/1.45 NA oil objective (Nikon) and controlled by NIS Elements (Nikon). CHO-K1 cells were authenticated at source using DNA barcoding and DNA profiling. An incubation chamber surrounding the microscope setup was set to 37°C 24h before live-cell imaging. To provide stable focus during imaging, the Perfect Focus System (Nikon) was used. Imaging was performed in FluoroBrite Medium (Gibco, cat no A1896701) at 37°C. Excitation was delivered with a 405, 488, 568 or 640nm diode laser, and emission was detected with avalanche photodiodes at 461, 520, 566 or 671nm, respectively. Live STED images were acquired with a 640nm excitation laser, 775nm depletion laser (at 20%

intensity) and 671nm detector (gate, 1–7ns). Pixel size was set to 30nm × 30nm, with 10µs pixel dwell time, and a line accumulation of 1 was used during acquisition. STEDYCON 9.0.799-g22f03ed2 software was used for image acquisition and analysis.

Single particle tracking

MIN6-CB4 cells were labelled with 500pM daLUXendin660 in complete media for 20 minutes at 37°C and washed three times in HEPES-bicarbonate buffer, ensuring sparse labelling of GLP1R/GIPR. Cells were mounted on cavity slides and imaged in HEPES-bicarbonate buffer supplemented with 11mM D-glucose before TIRF imaging at 40Hz using an Evident/Abbelight SAFe 180 system and a ×100/1.5 NA Olympus UPLAPO100XOHR objective. Single particles were recorded using an LP650 filter with an integration time of 25ms on a Hamamatsu ORCA-Fusion sCMOS for 1,750 frames. Single particle analysis was performed using the Trackmate plugin for ImageJ51, with trajectories shown as maximum displacement.

Image analysis

For figures throughout this thesis, brightness and contrast were linearly adjusted across the entire image and applied equally between all states under examination.
Labelling of probes, antibodies and enzyme self-labels was analysed using Corrected Total Cell Fluorescence (CTCF). First, fluorescence of cells and islets in images was measured using ImageJ (NIH); regions of interest (ROI) were drawn around cells or islets in addition to three background ROI. Area, integrated density and mean grey value were

measured for each ROI in each channel of the image. CTCF for each cell/islet was calculated using the formula:

(CTCF) = Integrated Density – (Area of Selected Cell x Mean Fluorescence of Background readings)

Colocalization was determined using Manders' coefficient, which calculates the proportion of pixels in one channel that also show intensity from both channels (308). Percentage of total islet area labelled by sGIP549 or LUXendin645 in *Gipr-/-ßcell* islets was determined using the rolling ball background subtraction method (pixel ball sizes: sGIP549 = 12; LUXendin645 = 10) then applying a threshold algorithm (sGIP549 Moments; LUXendin645 IJ_Isodata). Full width at half maximum was used to analyse labelling patterns at the membrane versus cytoplasm.

Statistical analysis

Graphical depiction of CTCF values and statistical analysis for significance were performed using GraphPad Prism 9 (9.4.1) or 10 (10.3.1). For parametric data, comparisons were made using unpaired t test, ANOVA or repeated-measures ANOVA. For non-parametric data, the Mann-Whitney test was used for pairwise comparisons and multiple comparisons were made using the Kruskal-Wallis test. Error bars represent mean and S.E.M. and a p-value of <0.05 was considered significant.

Chapter 3: Development, generation and validation of a novel GIPR probe

Introduction

As described in Chapter 1, significant interest in modulating GIPR to lower blood glucose and body weight has emerged. Treatments which interact with GIPR have shown to enhance the beneficial effect of GLP1 in diabetes and obesity (117,125) and many more agents are under development (123,309).

Many medications are licensed and in use for a long time before all targets or confirmation of the beneficial mechanisms of actions are discovered (310). However, given the debate about whether GIP agonism or antagonism is beneficial for glucose control and weight loss, and with incretin medication being investigated for a wide range of other conditions (311–316), there is pressing need to confirm where GIPR is expressed.

Gipr/GIPR identification

Reporter mice

*Gipr*GCaMP3 mice have been generated through crossing *Gipr*-Cre mice (267) with a ROSA26-GCaMP3 reporter strain (303). In *Gipr*-Cre mice, the gene for the Cre recombinase enzyme is inserted next to the *Gipr* (267) and in GCaMP3 mice, the gene for GCaMP3 is inserted into the genome next to two loxP sites flanking a stop codon (303). In *Gipr*GCaMP3mice, when *Gipr* is expressed Cre recombinase is also expressed, which recognises the loxP sites and removes the stop codon between them to permit GCaMP3 to

be expressed. Therefore, the *Gipr*GCaMP3 mouse enables fluorescent identification of cells which have expressed *Gipr*.

However, it is worth noting that GCaMP3 and other fluorescent reporters label the cell indelibly so many not be suitable for identifying cells that change phenotype over time. Additionally, reporter approaches only identify cells which have expressed the transcript rather than protein, and discordance has been reported between GPCR (GLP1R) RNA and protein expression (261).

Self-label enzymes

As described in Chapter 1, well-validated self-label enzymes have been developed for GLP1R, allowing for visualisation of GLP1R without interference with the orthosteric binding site. These include SNAP_GLP1R and Halo_GLP1R plasmids which can be transfected into suitable cells or is present in SNAP_GLP1R transgenic mice (269). SNAP_GIPR and Halo_GIPR (281) plasmids have been developed and their use in cell lines has been informative with regard to GIPR dynamics, demonstrating that GIPR agonism can desensitise GIPR and functionally act as antagonism (241) and that formation of GIPR nanodomains are constitutive and not agonist-dependent (275).

GIPR antibodies

An antagonistic anti-murine GIPR antibody was developed, named muGIPR-Ab (252). It successfully antagonised GIP-induced cAMP generation in cells and pre-treatment of mice with muGIPR-Ab abolished the insulinotropic effect of a GIP analogue (252). Following this, the same group also created a human (h)GIPR-Ab. It was used to demonstrate that antagonising GIPR augments GLP1-mediated weight loss and that the effects on weight loss are likely occurring at a site other than ß cells (252). However, neither antibody was modified or worked up for visualisation or localisation of GIPR so serve purely as antagonists.

In the same and a subsequent paper (283), the authors used a commercially available hGIPR antibody (RnD Systems MAB8210) and demonstrated specificity by showing labelling of SNAP_hGIPR-U2OS cells which overlapped with SNAP label fluorescence (283). The manufacturers report that the antibody detected GIPR in direct ELISAs and prevented recombinant human GIP binding to GIPR as detected by flow cytometry (317). However, in our experience and following discussions with other labs, we have found that this antibody lacks sensitivity when used in non-overexpression systems, which are important settings for exploring the outstanding questions related to incretin biology. More recently, Yu et al used a fluorescent GIPR antibody to assess GIPR expression in white adipose tissue of transgenic mice which harbour doxycycline-inducible overexpression of GIPR in adipose tissue (318). However, the antibody is not commercially available, and no data was presented regarding its specificity.

As mentioned previously, antibodies require fixation and permeabilization of cell membranes to bind to their targets so are unsuited to assessing live receptor dynamics or confirming substrates for peripherally injected ligands.

Fluorescent GIPR probes

Fluorescent probes are suitable for imaging tissue either live or post-fixation (alongside other protein or cell markers) and can be administered in vivo. They can be modified to have agonist or antagonist properties, and harbour epitopes or fluorophores of different excitation wavelengths so they can be applied alongside reagents detecting other substrates. Therefore, they can bridge the gap between pharmacological, gene expression and antibody-localisation studies with receptor knockout studies by confirming which tissues peripherally administered ligands can access.

Since our work began on developing our novel fluorescent probes, one fluorescent agonist GIPR probe has been reported in the literature: GIP-TMR (281,285). Demonstrating specificity, it did not label islets from *Gipr*-/- mice and levels of intracellular labelling was comparable with SNAP-labelled GIPR (285). However, moderately high concentrations of GIP-TMR were required to label WT islets; 1μM compared to the circulating picomolar concentrations of native GIP (319) or nanomolar range for pharmacological effect (320,321). As a result, GIP-TMR may be less suitable as a proxy for native GIP when assessing function. Additionally, no detailed pharmacological data was provided, for example binding affinity, which can be altered with the conjugation of a fluorophore (discussed below). Furthermore, some features of TMR render it less suitable for labelling complex tissue – it can be cleaved intracellularly (298) and rhodamine-based dyes have been observed to be taken up non-specifically into cells, including astrocytes (322,323). Aside from GIP-TMR, no other fluorescent probes have been reported.

Considerations for GIPR probe generation

Generating modified synthetic peptides can be challenging, as even small changes to amino acid sequences can disrupt the structure and potency of the peptide (324). Furthermore, different fluorophores, and any required linker molecules, can alter the pharmacological and photophysical properties of the resulting ligand (325–327), so robust characterisation of novel probes is required.

Firstly, consideration must be given to whether an agonist or antagonist probe is desired. Antagonist probes allow for localisation of cognate receptors on the cell surface. Agonist probes have the advantage of activating the cognate receptor, permitting the visualisation of activated receptor internalisation and trafficking.

GIPR, unlike many GCPRs, is constitutively internalised and recycled back independent of ligand activation and do not basally reside at the cell membrane (328). Peptides have poor membrane permeability and are unable to enter the cell to target intracellular substrates (329) so for GIP it is advantageous to have an agonist peptide to visualise the internal compartment of GIPR.

Furthermore, and specific to GIP, it has been shown that antagonistic GIP-based peptides demonstrate significant species difference in pharmacology and are also deemed unsuitable for fluorophore conjugation (259). As an example of species difference with GIPR antagonists, one such antagonist displayed reasonable potency at the human GIPR (IC50 = 64.1 nM) but severely limited potency at the mouse GIPR (IC50>6000nM) (330).

When considering where to incorporate the fluorophore within the GIP peptide, current literature suggests that GIP possesses multiple contact residues that contribute to high-affinity receptor binding, divided between GIP1-14 and GIP19-30 (331–333). However, several studies utilising cryogenic electron microscopy (334), crystallography (335) and interrogating structure-activity relationships (331,336,337) have demonstrated that the N-terminus of GIP is key for engaging and activating the GIPR and determines the binding affinity and efficacy.

Hinke et al (338) measured cAMP responses from different GIP fragments in CHO cells transfected with rat GIPR. The C-terminally truncated GIP (1-14) and N-terminally truncated GIP (19-30) induced the greatest cAMP responses. However, several other N-terminally truncated fragments were found to be weak affinity antagonists of GIPR; these included GIP (15-42), GIP (15-30), GIP (16-30) and GIP (17-30).

In GIPR transfected CHL cells, the C-terminally truncated GIP fragment GIP (1-16) was only able to induce 35% of native GIP cAMP response but N-terminally truncated fragments GIP (4–42) and GIP (17–30) were unable to stimulate any cAMP responses (339).

Echoing this, in the pancreatic ß cell line BRIN-BD11, GIP (1-16) attained only 50-90% maximal native GIP-induced insulin secretion. Whereas GIP (4–42) and GIP (17–30) failed to induce any significant insulin response and antagonised native GIP-induced insulin secretion (339).

Furthermore, substitution of one of the first 14 amino acids in the GIP sequence resulted in significantly reduced or complete loss of binding affinity for the GIPR, particularly when amino acids were substituted for alanine in positions 1, 3, 4 or 5 (324). Finally, further supporting the importance of preserving the N-terminus, DPP4 truncates the N-terminus of GIP to terminate its function (340).

Chapter aim

In the context of our inability to reliably label GIPR in live cells or tissue, in this chapter I present the generation of two novel, fluorescent GIPR agonist probes. I describe their structure and pharmacology and show our validation of the specificity of the probes for GIPR but not GLP1R. This was achieved through co-localisation studies in both the overexpression setting (SNAP_hGIPR and SNAP_hGLP1R AD293 cells) and the endogenously expressed setting in highly relevant mouse models.

Results

sGIP549/sGIP648 structure and pharmacology

Given the importance of the N-terminus to retain GIP potency as described above, we hypothesised that modification to the C-terminus to incorporate a fluorophore would still permit effective binding and activation of GIPR.

To create our sGIP (synthetic GIP) probes, firstly a linker of three amino acids was inserted at the C-terminal of GIP to create sGIP_GGC. The linker was comprised of three amino acids; glycine, glycine, and cysteine, immediately before the free carboxyl group of the GIP molecule (Figure 3b). This linker was required because GIP does not harbour any reactive C terminal amino acids (such as lysine or cysteine (341,342)), or amino acids that can easily be switched to a reactive substitute, to facilitate conjugation. Glycine is a favoured amino acid for linker formation as it is small, and its polarity lends itself to improving stability of the linker (343).

Then a Cy3 or Cy5 fluorophore was conjugated onto the Cys residue using maleimide "click chemistry" to create sGIP549 (Cy3) and sGIP648 (Cy5) (Figure 3c,d).

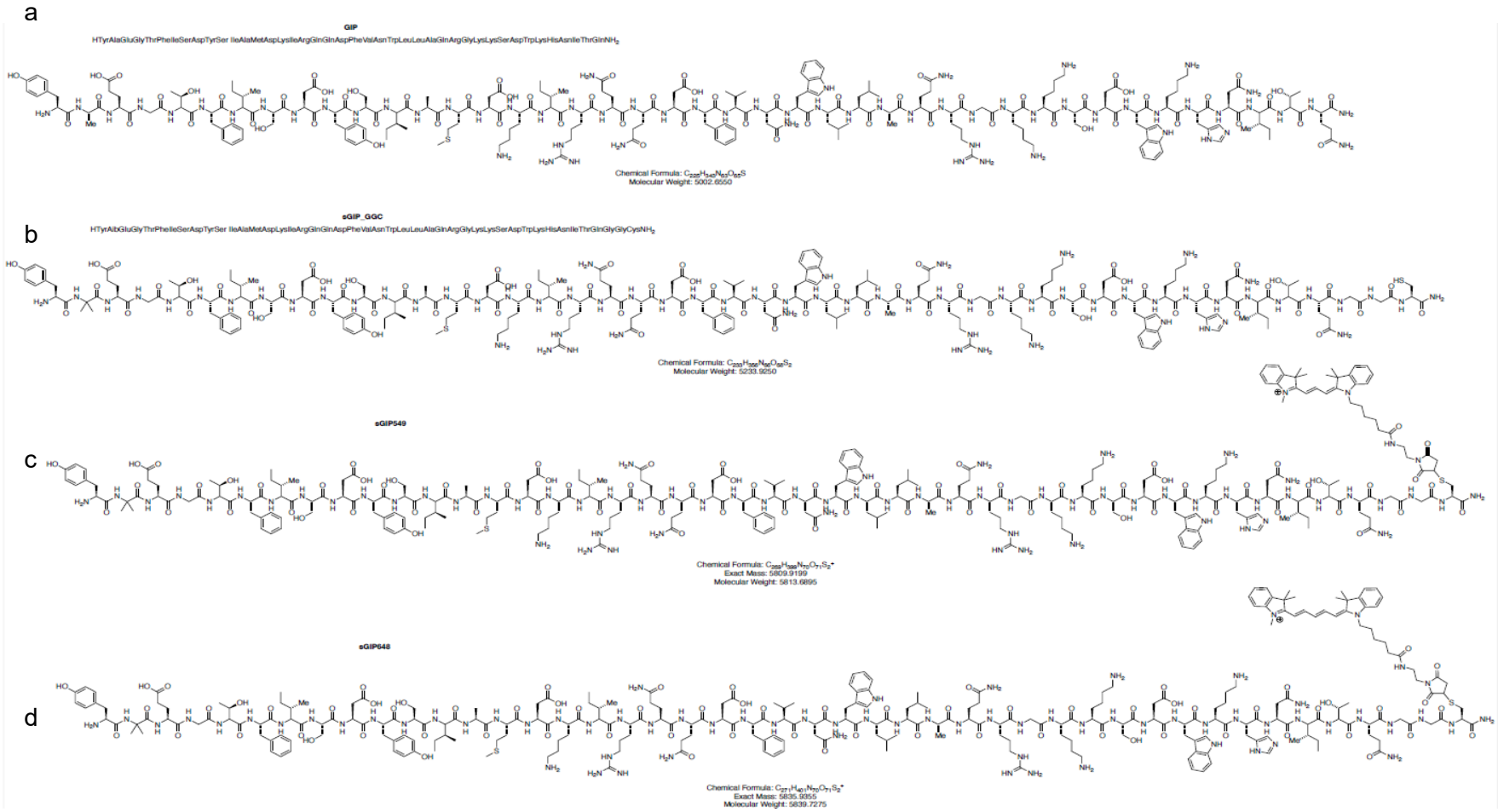

Figure 3: Chemical structure of native GIP (a), sGIP (b), sGIP549 (c) and sGIP648 (d).
sGIP (b) has the addition of GlyGlyCys prior to the C-terminus, upon which Cy3 and Cy5 fluorophores are attached in sGIP549 (c) and sGIP648 (d) respectively.

Activation of the adenylyl cyclase/cAMP cascade by the GIPR is thought to be the primary mode of insulinotropic action of GIP (344–346) so we used cAMP response as a proxy of GIPR activation and potency of ligands binding to GIPR. To determine if our C-terminus modification had altered the potency of sGIP, cAMP assays were undertaken, comparing the novel probes to native GIP in T-REx-SNAP_hGIPR cells (Figure 4).

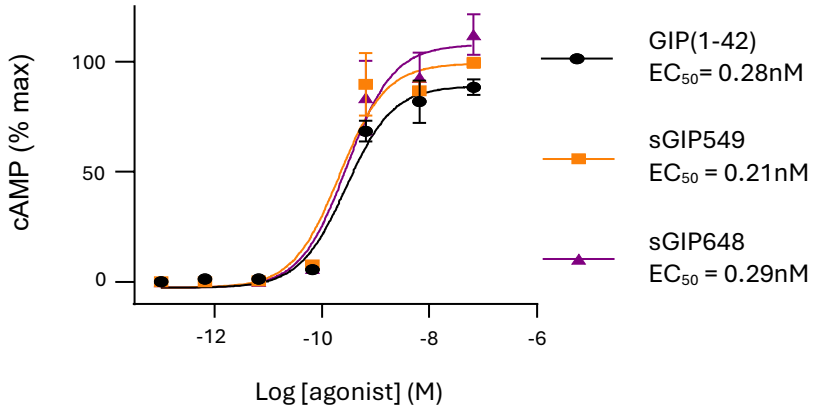

Figure 4: sGIP cAMP responses
cAMP signalling responses of GIP(1-42), sGIP549 and sGIP648 in T-REx-SNAP_hGIPR cells. (n=3).

T-REx-SNAP_hGIPR cells were induced to express SNAP_hGIPR then incubated with different concentrations of the agonists (as indicated in Figure 4), lysed and then cAMP was assayed using homogeneous time-resolved fluorescence technology (HTRF). EC_{50} values were then calculated for each agonist. EC_{50} values are derived from the Hill equation and are a more commonly used unit for assessing ligand efficacy, which in turn is used to infer ligand potency, EC_{50} values were found to be comparable between both sGIP549, sGIP648 and native GIP (Figure 4). Therefore, the modifications do not adversely impact the potency of the sGIP probes for cAMP, making them suitable for experimentation in more relevant settings e.g. cell lines, islets.

sGIP probes are specific for hGIPR in an overexpression system

To demonstrate the specificity of sGIP549 and sGIP648 for hGIPR, AD293 cells were transfected with SNAP-tagged hGIPR or hGLP1R. Use of SNAP-tagged receptors allowed for identification of the receptor without interference with the orthosteric binding site. Cells were incubated with either sGIP549 or sGIP648 plus a cell-permeable SNAP label of orthogonal excitation (BG-JF646 or BG-JF549 respectively) and imaged.

Expression of SNAP_hGIPR and SNAP_GLP1R was confirmed through the fluorescence of SNAP labels (Figure 5 and Figure 6). In cells expressing SNAP_hGIPR, there was co-localisation of fluorescence between the SNAP label and of both sGIP probes (Figure 5a and Figure 6a). For cells expressing SNAP_hGLP1R, there was no fluorescence of either sGIP probe (Figure 5b and Figure 6b).

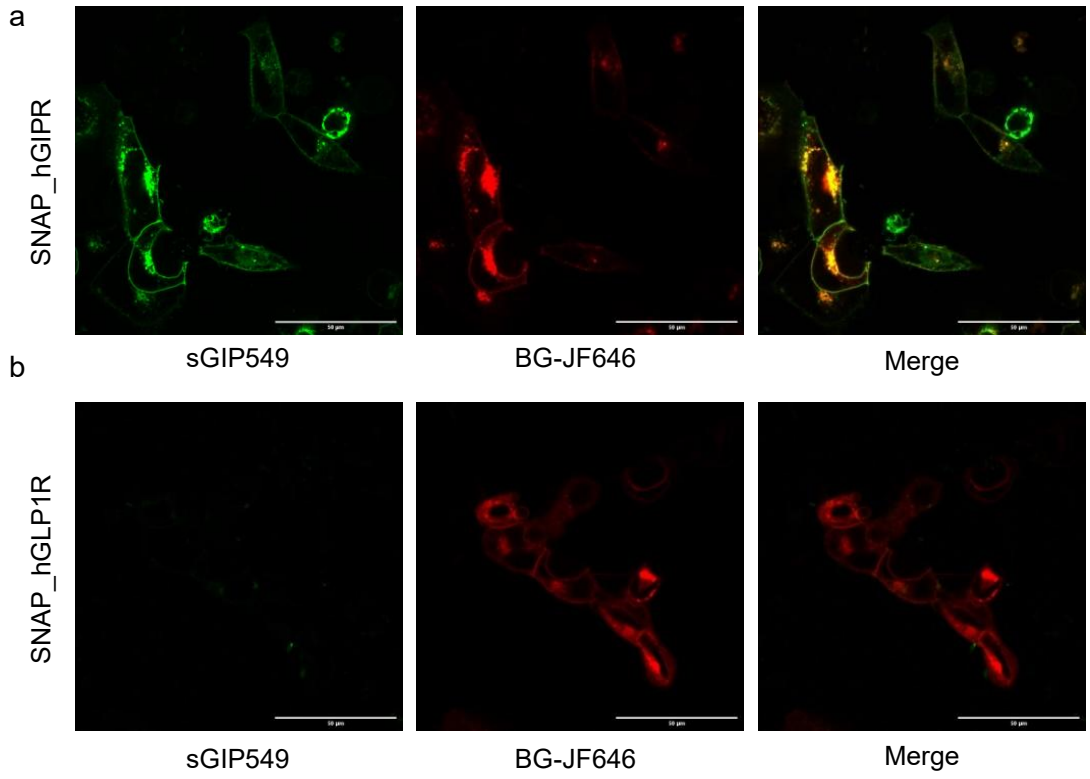

Figure 5: sGIP549 in SNAP_hGIPR and SNAP_hGLP1R AD293 cells.
Representative images of AD293 cells transfected with a) SNAP_hGIPR or b) SNAP_hGLP1R and incubated with sGIP549 and SNAP label BG-JF-646(n=42 cells, 3 repeats). Scale bar = 50µm.

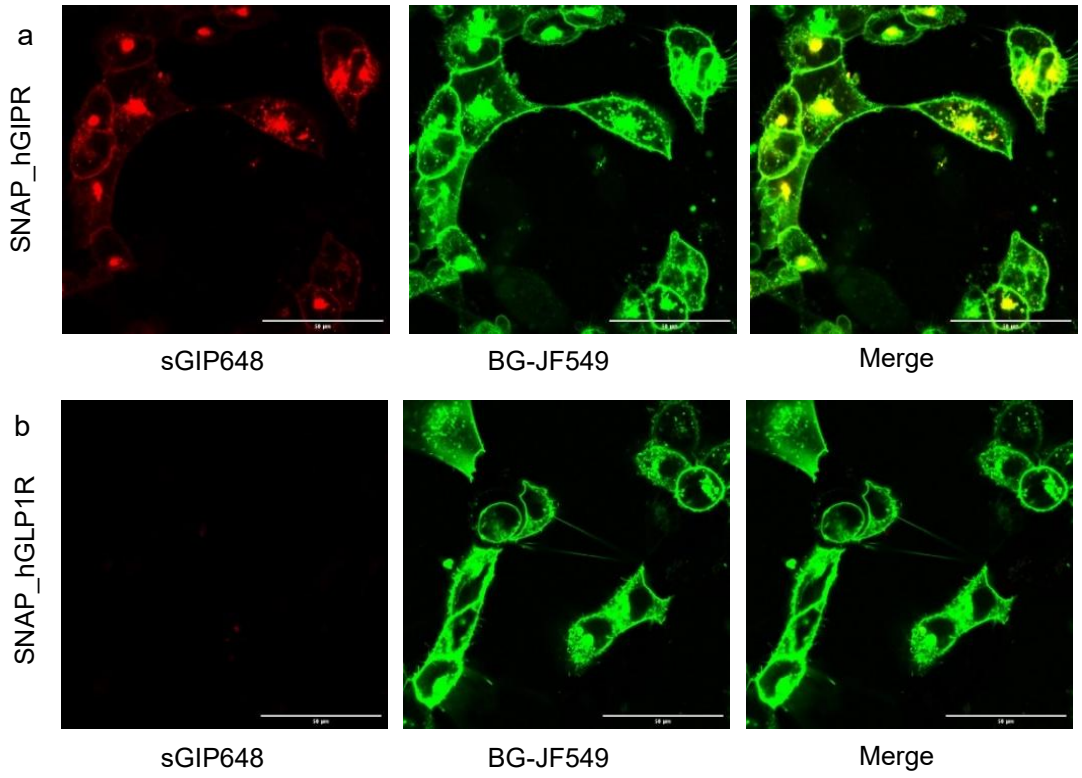

Figure 6: sGIP648 in SNAP_hGIPR and SNAP_hGLP1R AD293 cells.
Representative images of AD293 cells transfected with SNAP_hGIPR (a) or SNAP_hGLP1R (b) and incubated with sGIP648 and SNAP label BG-JF549.Scale = 50µm.

The co-localisation, or not, of fluorescence between the SNAP label and probes was further quantified through analysis of fluorescence levels (Corrected Total Cell Fluorescence, CTCF) of whole cells, to capture both membrane and cytosolic labelling. There was a large, statistically significant reduced level of sGIP probe labelling in SNAP_GLP1R cells compared with SNAP_GIPR cells (Figure 7). This suggests that the probes specifically label GIPR.

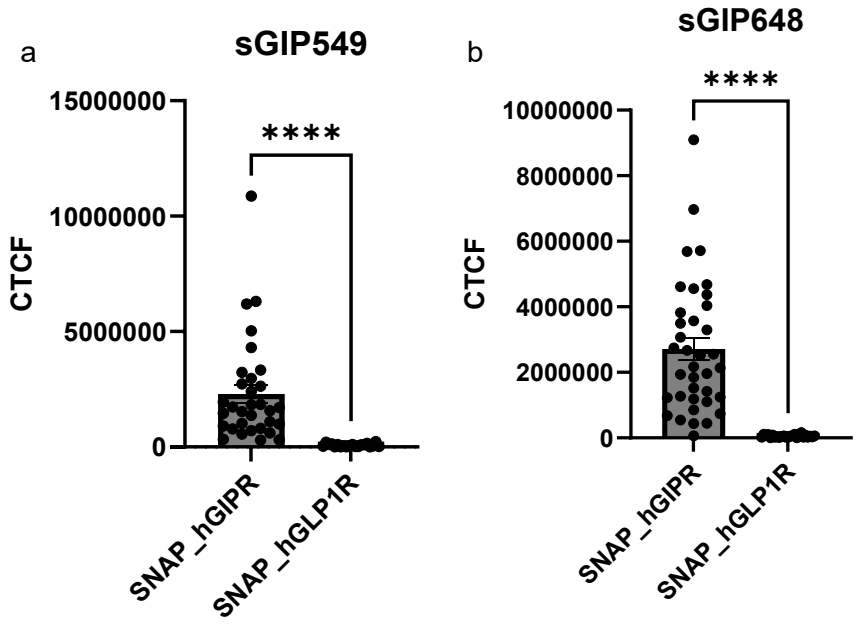

*Figure 7: Quantified fluorescence of sGIP in SNAP_hGIPR and SNAP_hGLP1R AD293 cells. Corrected Total Cell Fluorescence (CTCF) of sGIP549 (a) and sGIP648 (b) in SNAP_hGIPR vs SNAP_hGLP1R AD293 cells. Bar graphs show mean CTCF and SEM. Statistical analysis performed using unpaired t-test. ****p<0.001. CTCF calculated from 1-2 randomly selected cells from every image taken for each condition, with 3 independent repeats per condition. (Total number of cells analysed: sGIP549/SNAP_hGIPR n=32 cells, sGIP648/SNAP_hGIPR n=37 cells, sGIP549/SNAP_hGLP1R n=21 cells and sGIP648/SNAP_hGLP1R, n=25 cells)*

sGIP probes co-localise with *Gipr*+ cells in islets

To examine the probes' ability to label GIPR in a non-overexpression system, and to demonstrate their utility in a widely used setting for diabetes research, we next tested the sGIP probes in mouse islets.

To initially examine the specificity of sGIP549 and sGIP648 to cells expressing *Gipr* in islets, the probes were applied to islets from fluorescent *Gipr* reporter mice; *Gipr*GCaMP3. Although GCaMP3 is used to visualise and quantify changes in intracellular calcium, we used it simply as a *Gipr* reporter. The overlap of GCaMP3 and sGIP fluorescence was compared.

Representative images in Figure 8 demonstrate co-localisation of sGIP549 and sGIP648 with GCaMP3+ cells with the islet. Fluorescence intensity of GCaMP3 generally corresponded with intensity of sGIP probe fluorescence, suggesting concordance between *Gipr* transcript and GIPR protein.

There are cells which have been labelled with the sGIP probe but are GCaMP3-; these tend to be peripheral cells with high intensity staining which is in keeping with non-specific uptake by dead or unhealthy cells with damaged cell membranes allowing intracellular diffusion of hydrophilic peptides (347,348).

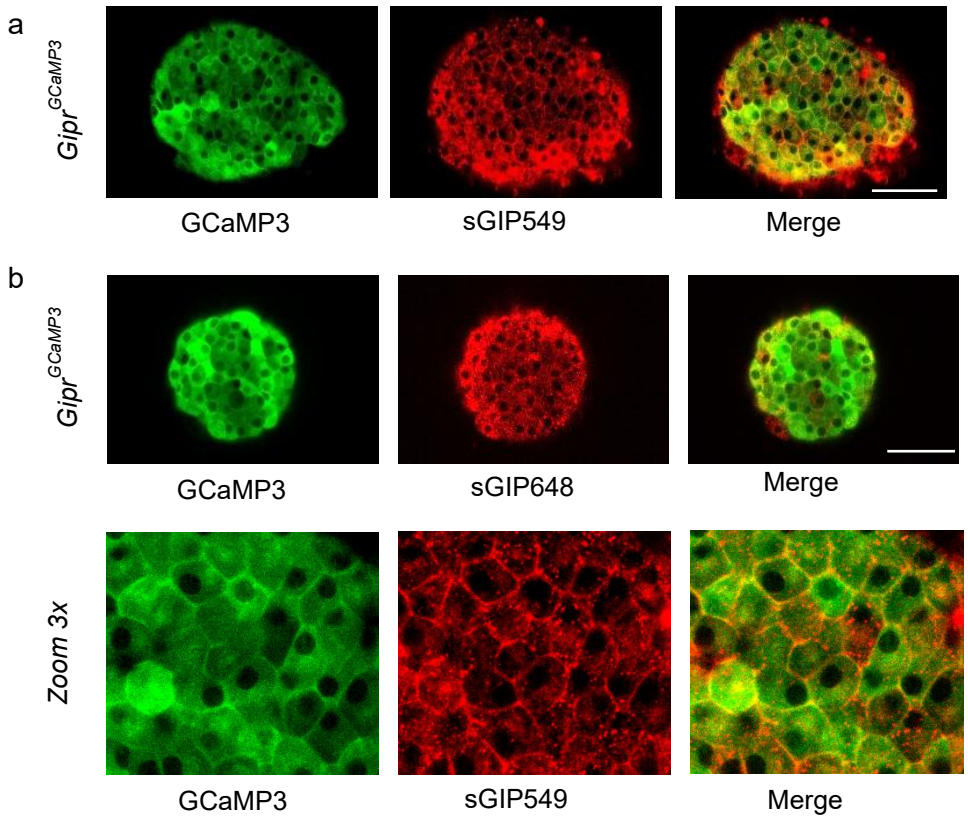

Figure 8: sGIP549 (a) and sGIP648 (b) in GiprGCaMP3 reporter mice islets. Zoom panels highlighting the membrane and cytosolic staining of sGIP549 and the concordance of fluorescence intensity between sGIP549 and GCaMP3 (n=11-12 islets, 2 animals). Scale bar 53µm.

To further demonstrate specificity of the probe only binding to GIPR+ cells (bearing in mind that GCaMP3 is a proxy for *Gipr* transcription rather than receptor presence), we then

applied the sGIP probes to wild-type (WT) islets along with a GLP1R antagonistic probe of orthogonal fluorescence, a LUXendin.

In the pancreatic islet, ß cells are known to express both GLP1R and GIPR whereas α cells are only considered to express GIPR (147,349). Therefore, the sGIP probes should label all the LUXendin+ cells (i.e. GLP1R+/GIPR+ ß cells) and some LUXendin- cells (i.e. GLP1R-/GIPR+ α cells) (Figure 9). Additionally, there should be no GLP1R+/GIPR- cells, as GLP1R is only expressed in high abundance in ß cells and ß cells should also express GIPR (Figure 9). However, this should be caveated with considering that LUXendin sensitivity may not be able to detect GLP1R expressed at low abundance and there is evidence to suggest that GLP1R and GIPR are expressed in α and δ cells at the RNA level(188,191,192) , as discussed in Chapters 1 and 7.. Additionally, it is worth noting that given the close proximity of cells in an islet, it is challenging to definitively confirm if a fluorescent probe is labelling the membrane of one cell, or its neighbour.

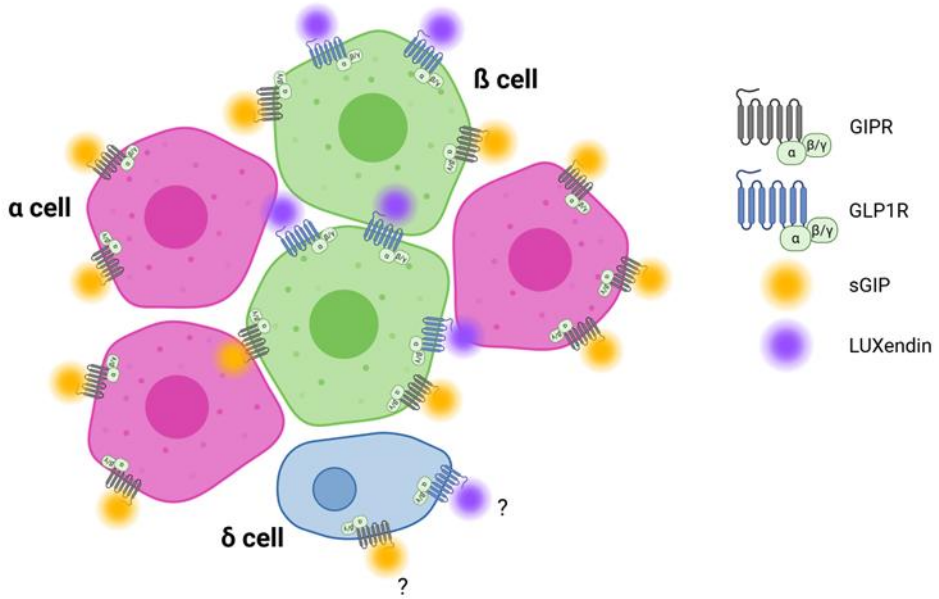

Figure 9: Schematic demonstrating the expected labelling of sGIP and LUXendin probes of main endocrine cells within a pancreatic islet.
GLP1R is only present on ß cells, which should also express GIPR so there will be some cells co-labelled by sGIP and LUXendin. GIPR is also present on α cells where there should be no GLP1R, resulting in some cells with only sGIP labelling. However, there are no cell types with only GLP1R (if RNA data is correct about δ cells expressing both receptors) so there should not be any LUXendin cells without sGIP labelling. Created in Biorender.

Representative images in Figure 10 show the predicted co-localisation of the sGIP probe with LUXendin labelled (GLP1R+) cells, with the majority of other cells only labelled with sGIP (GIPR+), with the zoomed images highlight such GLP1R-/GIPR+ cells. To quantify this, I examined every cell within each imaged islet to determine if it was labelled with LUXendin (GLP1R+) or sGIP (GIPR+), or both.

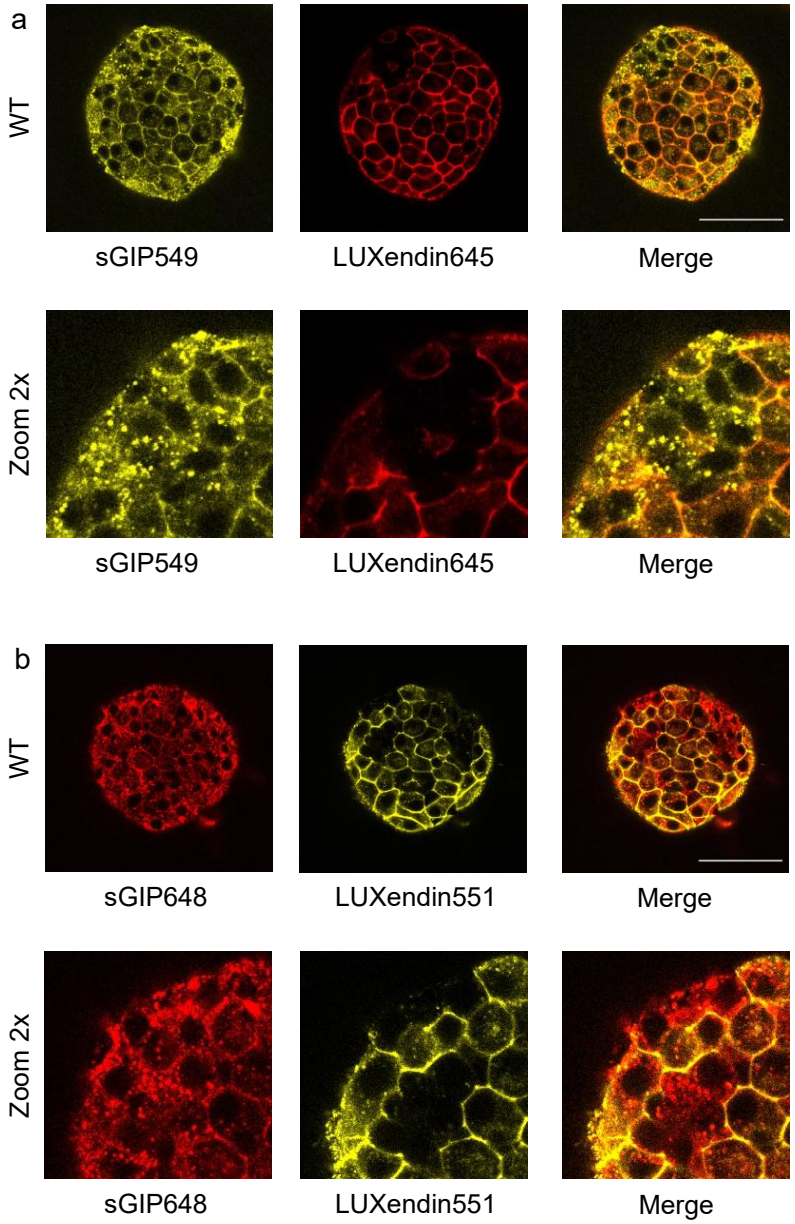

Figure 10: sGIP and GLP1R probe labelling in WT islets.
WT islets labelled with sGIP549 with LUXendin645 (a) and sGIP648 with LUXendin551 (b).Co-localisation is demonstrated on most cells with all other cells only labelled with sGIP probes. Scale bar 53µm.

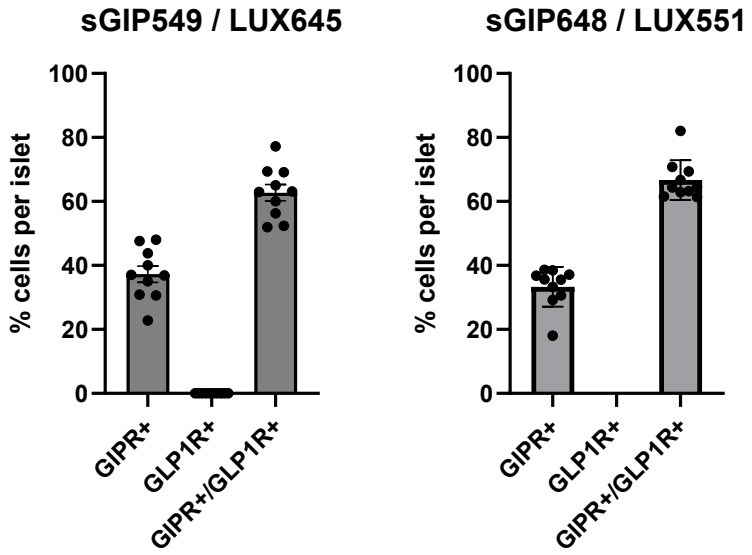

Figure 11: sGIP and GLP1R probe co-localisation in WT islets.
Analysis of presence of sGIP (GIPR+) or LUXendin (GLP1R+) on each cell within each WT islet. sGIP presence is found on all LUXendin⁺ (GLP1R+) cells, further GLP1R- cells but no GLP1R-/GIPR+ cells were identified. (n=10 islets from 3 mice for both sGIP probes)

Upon quantification (Figure 11), for sGIP549/LUXendin645 treated islets, 37% of cells were solely GIPR+ (presumed α cells) and 63% were GLP1R+/GIPR+ (presumed ß +/- δ cells). For sGIP648/LUXendin551, 33% of cells were solely GIPR+ (presumed α +/- δ cells) and 66% were GLP1R+/GIPR+ (presumed ß +/- δ cells). This is in keeping with known composition of cell types within mouse islets as described in Chapter 1. For both combinations of probes, no cells were GLP1R-/GIPR+.

sGIP probe labelling is reduced in *Gipr*-/- islets

Following on from the above, we elected to further demonstrate specificity of the sGIP probes to GIPR by comparing labelling between WT mouse islets and mouse islets with GIPR knocked out. Confirming such specificity in *Gipr*-/- mice has been highlighted has an important facet of novel probe development (259).

We were fortunate to be able to obtain different GIPR knock-out models from two different collaborators.

Firstly, we obtained islets from mice with the GIPR globally knocked out; *Gipr*-/-. As detailed in Chapter 2, this model was developed from GIPR-Cre knock-in mice bred to homozygosity for Cre (267). These *Gipr*-/- mice were protected against HFD-induced weight gain when heterozygous and WT counterparts were not (267), in keeping with previously published results from another *Gipr*-/- model (350).

We hypothesised that the sGIP probes would not label cells in the *Gipr*-/- but would label the majority cells in the WT islets used as a control. Furthermore, we also expected that GLP1R labelling would remain the same in *Gipr*-/- islets, compared with WT islets. Therefore, *Gipr*-/- and non-littermate WT islets were treated with sGIP probes and a LUXendin (GLP1R) probe of orthogonal fluorescence.

The representative images shown in Figure 12 and Figure 13 demonstrate a reduction but not complete absence of sGIP probe labelling in *Gipr*-/- islets compared with WT islets and an increase in LUXendin labelling, more marked with LUXendin 645, in *Gipr*-/- islets compared with WT islets. I quantified these differences in fluorescence by measuring CTCF of the islets, shown below in Figure 14.

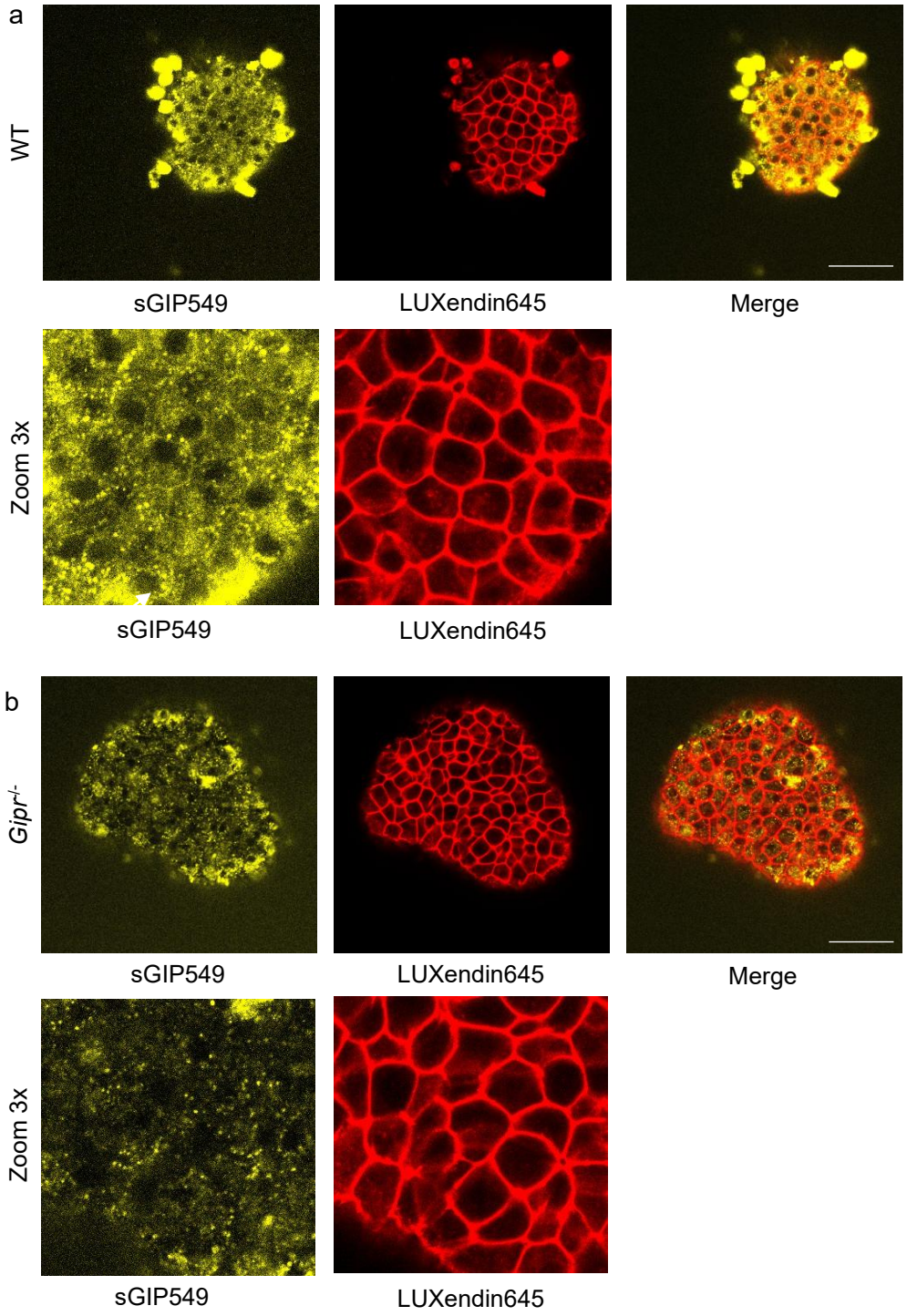

Figure 12: sGIP549 labelling in WT and Gipr-/- islets.
Representative images of WT (a) and Gipr-/- islets labelled with sGIP549 (GIPR) and LUXendin645 (GLP1R).
In (a) white arrow points to sGIP549 membrane labelling (n=3) Scale bar = 53µm.

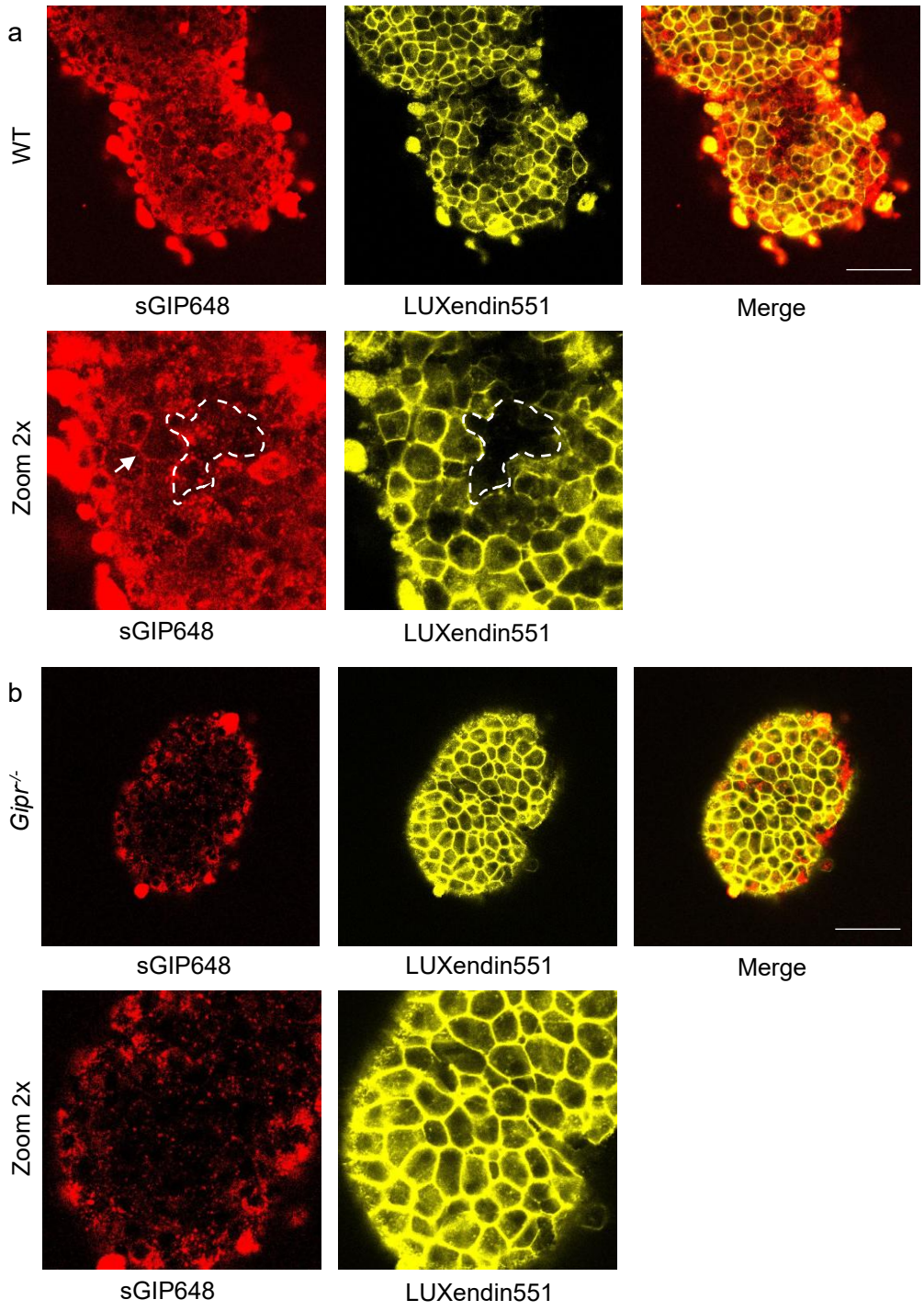

Figure 13: sGIP648 labelling in WT and Gipr-/- islets.
Representative images of WT (a) and Gipr-/- islets labelled with sGIP648 (GIPR) and LUXendin551 (GLP1R). In (a) white arrow highlights membrane labelling of sGIP648, dotted line outlines cells not labelled by LUXendin (i.e. α or δ cells) where sGIP labelling is predominantly cytoplasmic (n=3). Scale bar = 53μm.

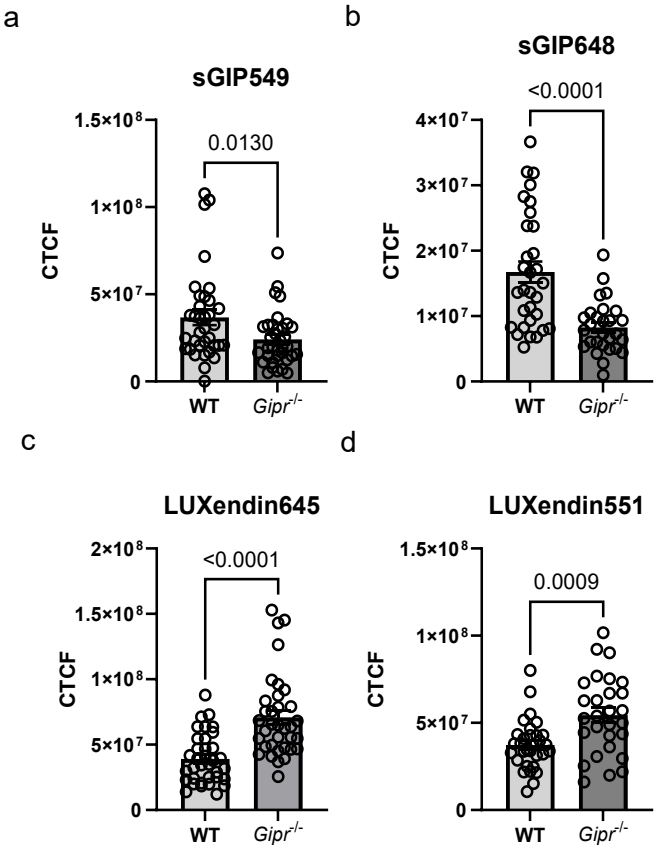

Figure 14: Quantification of sGIP and GLP1R probe fluorescence in WT and Gipr-/- islets. Fluorescence (CTCF) of sGIP probes (a,b) and LUXendin probes (c,d) in WT and Gipr-/- islets. Statistical analysis performed using Mann-Whitney U test. (n=35 islets from 3 mice for each condition)

CTCF values were reduced in *Gipr-/-* islets for both sGIP probes to a statistical significance. However, the residual labelling in *Gipr-/-* islets is unexpected. One cause could be that the quality of islets was reduced due to the impact of overnight shipping. High quality transportation of islets allows purity, viability and function, e.g. glucose stimulated insulin secretion, to be preserved (351,352). However, transportation of islets is also associated with upregulation of certain genes and downregulation of others, as well as upregulation of inflammatory and stress signalling pathways in ß cells (353). Additionally, a variety of factors can affect islet viability during transportation (354) which can lead to uncontrolled uptake of substrates, including fluorescent peptide probes,

through damaged cell membranes (355). Nonetheless, the reduction in labelling demonstrates target specificity.

LUXendin labelling (as CTCF) was higher in the *Gipr*-/- islets compared with WT islets. This might suggest upregulation of the GLP1R in a state of GIPR absence, fitting with increased islet sensitivity of mouse islets to GLP1 when GIPR is knocked out (212) although data regarding upregulated GLP1R protein expression is limited, which I will explore further below.

Additionally, the WT islets were not littermate controls, so direct comparison should be reviewed cautiously. Littermate controls were not available for this experiment but would have had the benefit of providing a more reliable control setting due to consistency of genetic background and minimising the impact of differences in environment upon the animal e.g. pathogen status, microbiome (356). Furthermore, it can be hard to determine the extent of knockout as the efficiency of Cre-mediated recombination is unpredictable, with a risk of mosaicism, where the desired genetic alteration is not achieved uniformly throughout a tissue (357,358). Additionally, Cre itself could be having an effect on islet viability as Cre toxicity has been demonstrated in many cell types (359–361), including ß cells, where Cre toxicity has attenuated insulin secretion (362–365).

Therefore, we next obtained islets from a different mouse line from another collaborator, along with WT littermates. These islets were from tamoxifen-driven, beta-cell specific GIPR knock-out model, *Gipr*-/-βcell.

We hypothesised that, compared to WT islets, sGIP probe labelling would be reduced in the *Gipr*-/-βcell islets but still present, as alpha cells would retain GIPR. To confirm that any reduction in labelling was beta-cell specific, I again co-labelled the islets with a LUXendin (GLP1R) probe of orthogonal fluorescence. Following this, I measured the

percentage of total islet area labelled by sGIP549/LUXendin645 to determine the degree of difference between WT and *Gipr-/-ßcell* mice.

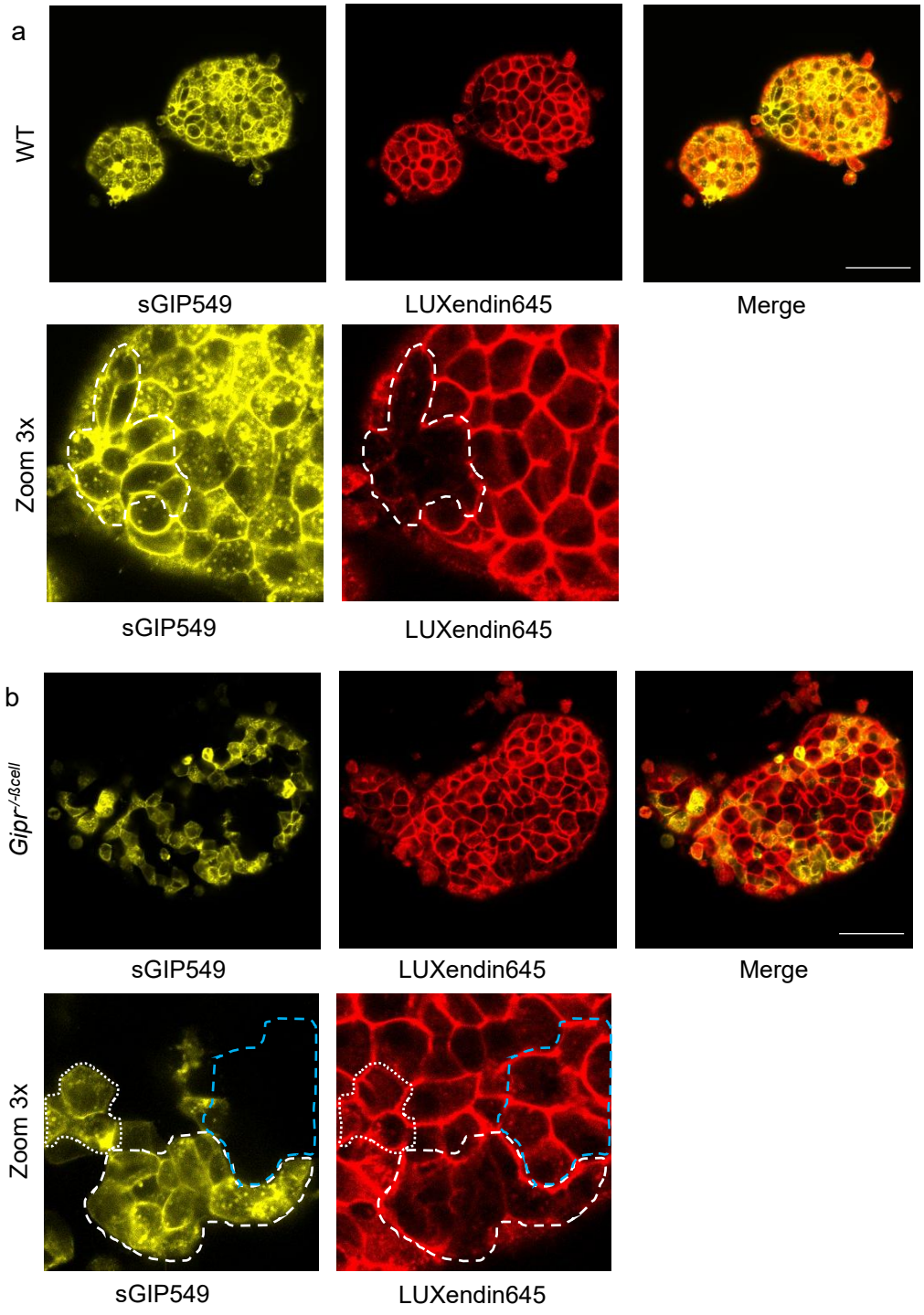

Figure 15: sGIP549 in WT and GIPR-/-ßcell islets.
Representative images of WT (a) and beta cell GIPR knock out (b) islets treated with sGIP549 and LUXendin645. In (a and b) white dashed lines show cells labelled with sGIP but not LUXendin, suggesting α or δ cells. In (b) blue dashed line demarcate cells labelled with LUXendin but not sGIP, suggesting Gipr-/- ß cells; white dotted lines outline cells with both LUXendin and sGIP labelling, suggesting ß cells with retained GIPR or perhaps δ cells. Scale bar = 50µm.

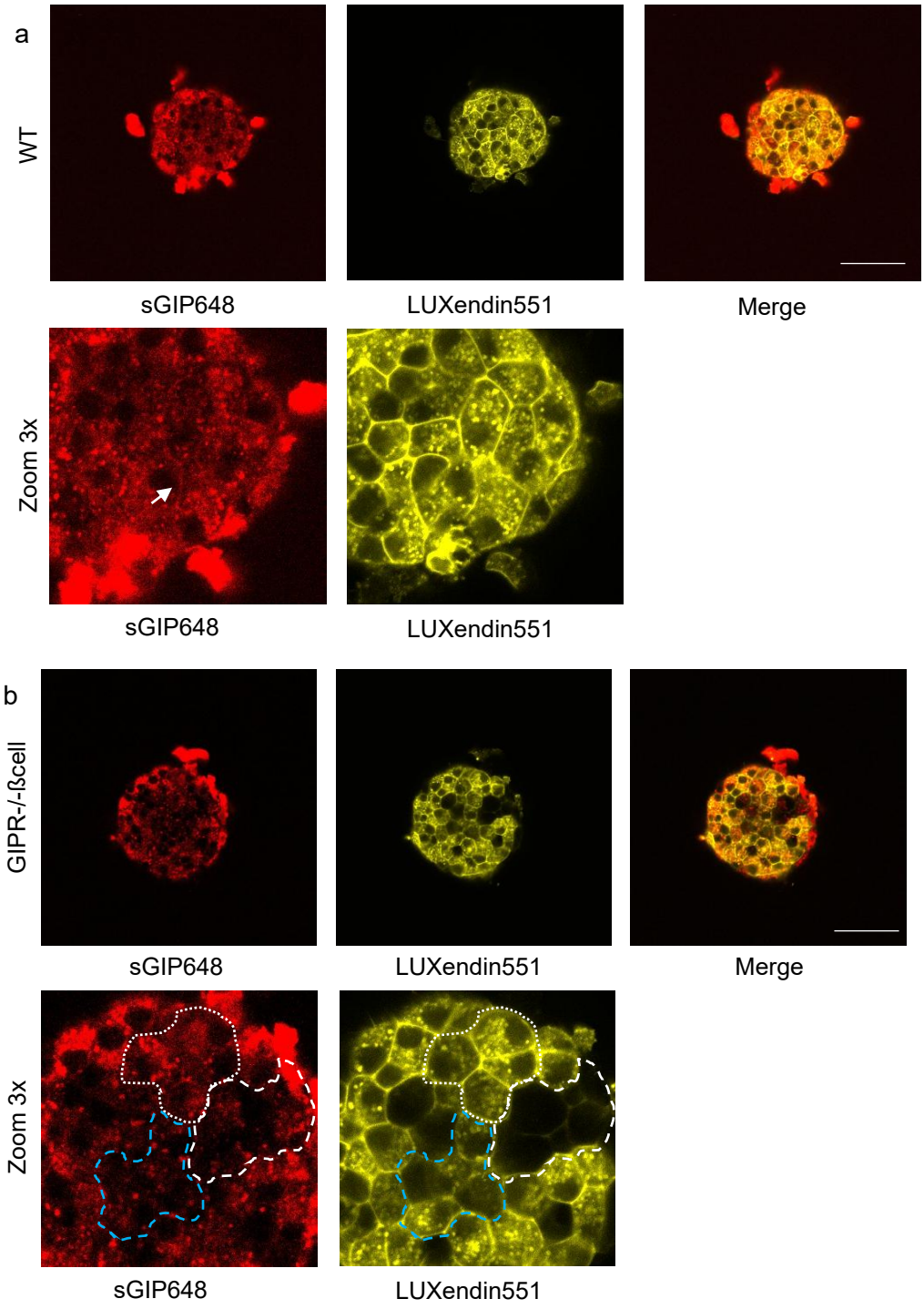

Figure 16: sGIP648 in WT and GIPR-/-ßcell islets.
Representative images of WT (a) and Gipr-/-ßcell (b) islets treated with sGIP648 and LUXendin551.
In (a) arrow highlights sGIP membrane labelling. In (b) white dashed lines outline cells with (minimal) sGIP labelling but not LUXendin labelling, suggestive of α or δ cells; blue dashed line marking cells labelled with LUXendin but not sGIP, suggesting Gipr-/- ß cells; white dotted lines outline cells with both LUXendin and sGIP labelling, suggesting ß cells with retained GIPR or perhaps δ cells. Scale bar = 50μm.

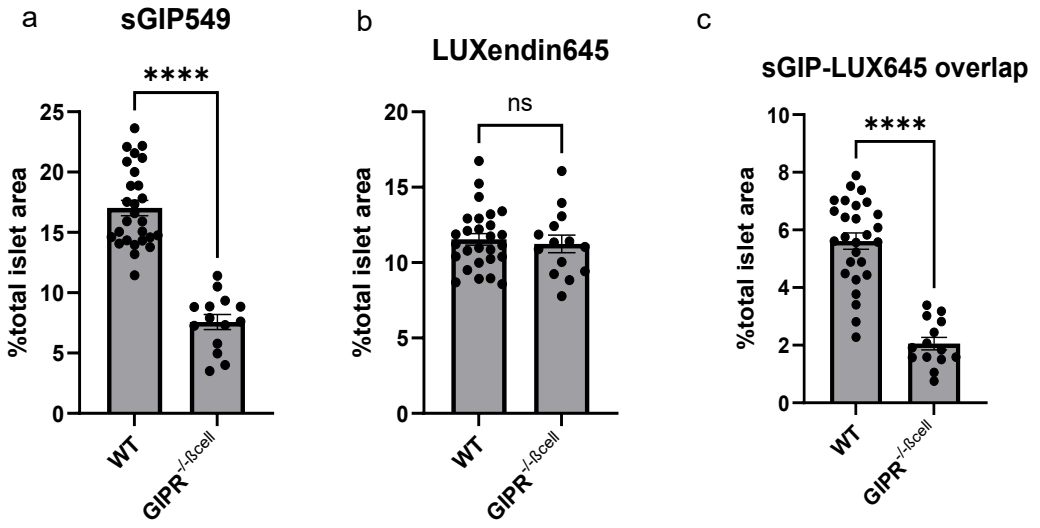

Figure 17: Total islet area labelled by sGIP in WT and Gipr-/-ßcell islets.
Percentage of total islet area labelled by sGIP549 (a), LUXendin645 (b) and both sGIP549 and LUXendin645 in Gipr-/-ßcell islets. Statistical analysis performed using unpaired t-test with p<0.0001 as significant (n=27 islets from 4WT and 14 islets from 3 GIPR$^{-/-ßcell}$ mice).

Representative images (Figure 15, Figure 16) demonstrate several things. Firstly, the sGIP648 probe was not as effective at labelling these islets. Binding to a peptide or protein and the tissue environment itself can affect fluorophore properties and signal (366–368), which could explain why the Cy5 probe was not as effective, despite cAMP responses comparable to native GIP and sGIP549.

Secondly, the architecture of the islet is not as expected; with mouse islets α cells are predominantly peripheral but sGIP549 labelling in *Gipr-/-ßcell* islets occurs throughout the islet (Figure 15). The difference in expected architecture could be due to the plane at which the image was taken, with central cells in a more peripheral plane actually being on the periphery of the islet rather than the core. This could be confirmed with a z-stack imaging. Additionally, in *Gipr-/-ßcell* islets a small amount of sGIP549 labelling co-localises with LUXendin labelling, as demarcated by white dotted lines in Figure 15b and Figure 16b and as quantified in Figure 17. There is variation in the extent of this between islets and although still present, quantification of percentage of islet mass labelled by each probe shows a significant reduction in sGIP labelling of LUXendin positive area in the

knockout model (Figure 17c). This could suggest that either the sGIP549 probe is labelling ß cells with retained GIPR expression, or the sGIP probe labels GLP1R or another ß cell protein/receptor. The latter is unlikely given the specificity shown in the cell work described earlier in this chapter and the lack GIP promiscuity (239,369).

The case that some ß cells retain GIPR is possible and could be due to the use of tamoxifen induction. The extent of tamoxifen induction can be variable and be influenced by many factors such as cell type, pharmacodynamics and age of the mouse (370,371). The *Gipr*-/-βcell mice showed an expected phenotype compared to controls (attenuated glucose tolerance and no insulin response to GIP in perifused islets) and residual *Gipr* mRNA transcripts across the islet were low (a 90% reduction compared to control islets) (196).

A further possibility is the both the sGIP and LUXendin probes are labelling GIPR and GLP1R, respectively, on δ cells. However, as discussed earlier in Chapter 1, δ cells are much less abundant in the islet (certainly not to the degree of residual sGIP-labelled cells in the *Gipr*-/-βcell islets) and the consensus is not yet been reached about whether δ cells express GIPR and GLP1R.

One method to determine the cell type of the residual sGIP labelling, is to co-stain them with proxy markers for different cell types e.g. antibodies against insulin for beta cells, glucagon for alpha cells. However, the various techniques for this require cell fixation and membrane permeabilization for antibody application and so far, the sGIP probes have been applied to tissue and imaged live. Therefore, we next elected to test the probes in fixed islets.

sGIP in fixed islets

Establishing that the sGIP probes work after fixation would allow further demonstration of the specificity of the sGIP probes to GIPR, through co-localisation with antibodies for different islet hormones, in addition to demonstrating the versality of these probes for use in imaging tissue after fixation as well as live imaging. sGIP549 labelling has proven to be more dependable, so we applied sGIP549 to islets prior to fixing.

Application of peptide probes is required before formaldehyde fixation as formaldehyde can result in changes to protein shape and configuration, through cross-linking and disruption of hydrogen bonds (372), which could affect orthosteric site ligand binding. Application of fluorescent probe prior to fixation and immunohistochemistry has been successful with the similarly engineered LUXendin probes (298).

Unfortunately, the sGIP probe did not produce a substantial signal in the fixed islets. Initially the standard concentration as used for live imaging of islets was applied, but there was minimal signal (Figure 18).

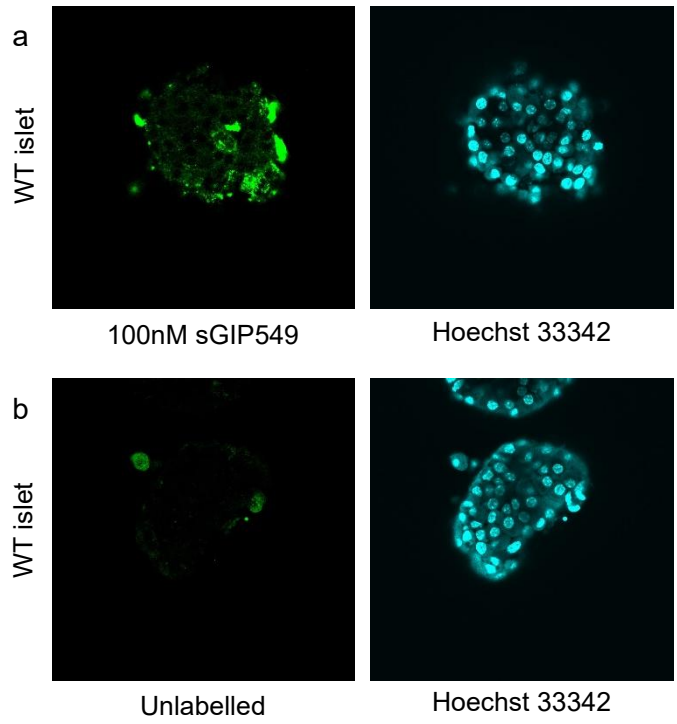

Figure 18: sGIP in fixed islets.
WT islets labelled with either 100nM sGIP549 (a) or unlabelled (b). Islets were then fixed and labelled with Hoechst 33342.

Fixation can reduce probe and fluorescent protein brightness and lifetime (373–375) and multiple washing steps, as occurs in fixation protocols, can promote ligand dissociation (376). Additionally, use of detergent to permeabilise membranes after fixation can generate intracellular fluorescent artifacts which can mask probe signals or act as false-positive signals (373,374,377).

Therefore, I repeated labelling prior to fixation but used increasing concentrations of sGIP549. Although there was increased fluorescence with 500nM and 1µM, the labelling was diffuse, punctate and predominantly cytoplasmic (Figure 19) without any membrane labelling as previously seen (Figure 10). Work is ongoing to optimise this, including Quality Control checks, labelling comparison with a more recently synthesised probe and using fresh DMSO, as DMSO can degrade into molecules with reducing properties, which can unconjugate disulfide bonds related to cysteine residues (378).

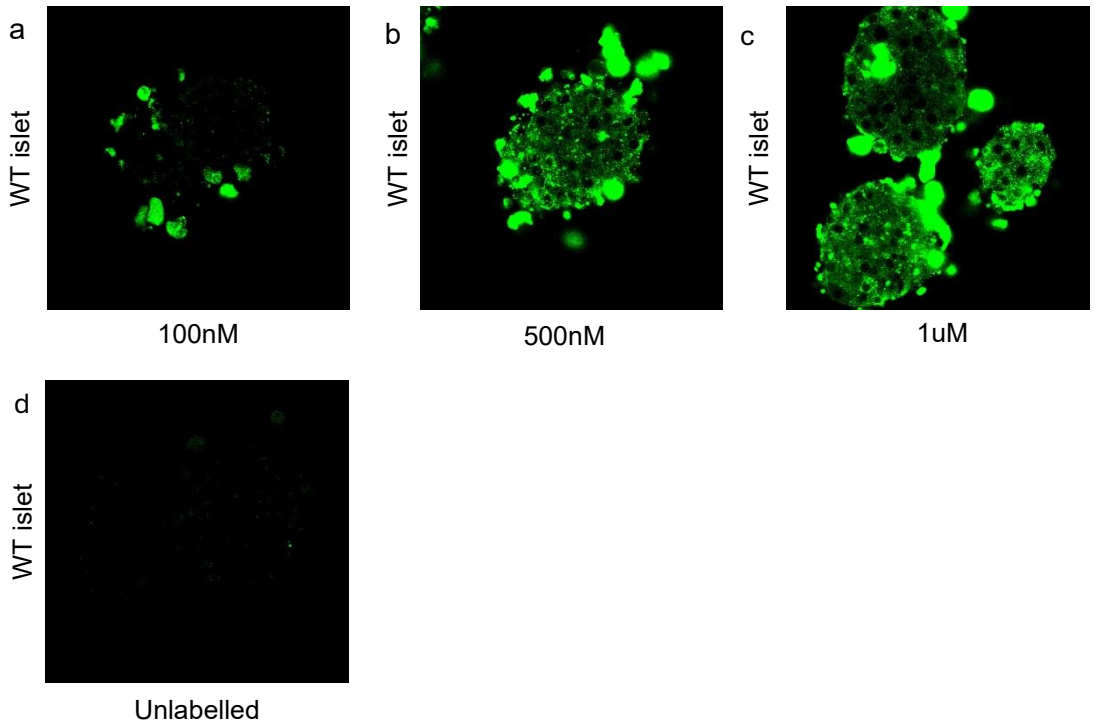

Figure 19: Increasing concentrations of sGIP in fixed WT islets
WT islets labelled with 100nM (a), 500nM (b) or 1μM (c) sGIP549 or unlabelled (d).

Discussion

In this chapter, the development of novel fluorescent GIPR agonist peptides is discussed. As detailed in Chapter 1, techniques for identifying and tracking GIPR in vitro and in vivo are limited. There is only one other available fluorescent peptide for the GIPR, which does show reduced labelling in *Gipr*-/- islets but lacks the detailed reporting of pharmacology and validation in various settings that we have shown for the sGIP probes (285). Currently antibodies for GIPR have either only been used for functional studies (252), have been tested in limited settings (283,317) or are not commercially available (318).

The importance of studying GIPR continues to grow as the field of incretin-based therapeutics advances with the advent of further dual and triple-incretin agonists, as summarised in (379).

However, with the interplay between GIP/GLP1 and mechanisms of biased agonism of dual GLP1R/GIPR agonism unclear (380), there is a pressing need for tools to identify GIPR in live and fixed tissue (259). To this aim we created a synthetic form of GIP with two fluorophore options. Previous studies have shown that the N-terminus is integral to the ability and efficacy of GIP binding to GIPR (331,334–337,381). Therefore, native GIP was modified to GIP_GGC through the addition of GlyGlyCys prior to the C-terminus and then conjugated a Cy3 or Cy5 fluorophore to the Cys residue to generate two novel fluorescent probes; sGIP549 (sGIP conjugated to Cy3) and sGIP648 (sGIP conjugated to Cy5).

We demonstrated that these modifications had not resulted in any disruption to the probes' cAMP potencies for the GIPR through showing comparable EC50 between sGIP549, sGIP648 and native GIP. EC50 is the effective concentration for 50% of the maximal response and is commonly used as a method for comparing the potency of drugs (382) and these results demonstrate that sGIP549 and sGIP648 can be used as suitable

proxies for GIP where the receptor needs to be visualised and agonised. However, it is worth noting that although cAMP is the major pathway for GIPR signalling (346), we cannot definitively say that the modifications have not altered signalling potency via other important pathways e.g. ß arrestin.

In vitro, in SNAP_GIPR AD293 cells, specificity of the probes was shown through binding to hGIPR but not hGLP1R (Figure 7). This is to be expected as although GLP1R permits promiscuous binding of several non-GLP1 ligands, such as glucagon (383–386) and GLP2 (387,388), GIP or its truncated fragments have not been shown to bind to GLP1R (239,369). Confirming specificity of the probes to GIPR is important to establish as these probes are currently the first validated fluorescent GIPR agonist peptides and have the potential to expand experimentation capabilities in the incretin field. The literature has already been complicated regarding GLP1R expression as several studies have used GLP1R antibodies which have been later found to be non-specific (257) or of questionable reliability (172).

In the crucial setting of islets, where GIPR is endogenously expressed, the sGIP probes appropriately label ß cells and non-ß cells, presumed to be predominantly α cells but potentially δ cells (Figure 10). However, it was not possible to determine the degree of sGIP probe δ cell labelling as the failure to label islets after fixation rendered other techniques of δ cell identification, e.g. co-staining with somatostatin antibody, unviable. sGIP labelling in live islets is both at the membrane and cytoplasmic, with less membrane labelling than the LUXendin probe. This limited membrane labelling is likely a reflection of both the fact that sGIP probes are agonists labelling internalised receptors but also that in WT islets, there is less GIPR at the cell surface compared with GLP1R (285).

We note that the intracellular labelling of sGIP probes is punctate which may reflect localisation of the activated GIPR to the endosomal compartment, as seen with

fluorescent GLP1R agonist labelling (285). In that study, GIPR was observed to be predominantly membrane-bound with minimal endosomal localisation. However, the incubations times were much shorter than in these experiments (5-15 minutes c.f. 1 hour) and, with their conclusion that the GIPR is slowly internalised after agonism (285), it could be that our longer incubation allowed for more GIPR internalisation and accumulation in the endosomal compartment.

It has been shown that both knock out and antagonism of GIPR increases sensitivity to GLP1 (389–391). Understanding this apparent compensatory response to loss of GIPR function has been challenging and the mechanism remains unclear. This increased sensitivity is unlikely to be explained by increased GLP1 release as previous studies reducing GIP secretion or antagonism of GIPR have not shown any increase in circulating GLP1 concentration (213,214,228). The interesting increase in GLP1R labelling in the *Gipr-/-* islets found in our work may suggest that the observed increased sensitivity to GLP1 in *Gipr-/-* islets could be due to upregulation of the GLP1R. However, this has not been studied extensively, with just two studies measuring levels of *Glp1r* mRNA in *Gipr-/-* islets but without information regarding protein expression. The first study of global *Gipr-/-* mice found that *Glp1r* mRNA was comparable between *Gipr-/-* and *Gipr+/+* islets (212) whereas a second study of *Gipr-/-ßcell* mouse islets found a slight increase in *Glp1r* mRNA compared with control MIP-Cre islets (196). Enhanced GLP1R synthesis in *Gipr-/-* islets could explain the increased sensitivity to GLP1 observed in literature. To make this fit with the similar, or only slightly increased, *Glp1r* mRNA found in *Gipr-/-* mice, there are several possible theories.

Firstly, there may be cross-regulation between the two receptors which is altered when GIPR is knocked out. In pancreatic cancer cell lines, GLP1R expression (as measured by flow cytometry of myc-tagged GLP1R and anti-myc antibody) was reduced when GIPR was

co-expressed (392). Therefore, knocking out the GIPR could lead to enhanced GLP1R expression. However, in HEK293 cells increasing concentrations of GIPR have been found to decrease GLP1R internalisation, via a reduction in ß-arrestin-2 recruitment, in a dose-dependent manner (277). This fits with the findings that the agonism of tirzepatide (dual GLP1R/GIPR agonist) is biased towards cAMP over ß-arrestin recruitment (255) and doesn't support the notion of increased GLP1R cell surface expression/labelling when GIPR is knocked out.

A second theory could be related to ß cell dedifferentiation. TCF1 is a transcription factor expressed in mature ß cells which is driven by GIP to improve ß cell survival (196) and contributes to maintaining the differentiated state of a ß cell (393). TCF1 is downregulated in ß cells from donors with diabetes and *Gipr-/-ßcell* mice (196), suggesting dedifferentiation of the ß cells in these states. Dedifferentiation of the ß cell due to glucotoxicity has been shown to amplify the *Glp1r* gene (393) so it could be possible that knocking out GIPR could lead to increased GLP1R expression through a degree of ß cell dedifferentiation. However, mRNA levels of *Glp1r* were found to be slightly reduced in TCF1 knockout mice (196). Furthermore, glucotoxicity (394) and age (395) are known drivers of ß cell dedifferentiation, and levels of the transcription factor and marker of ß cell maturation, Pdx-1, are lowered in dedifferentiated ß cells (396–398). Pdx-1 promotes GLP1R expression and is central to GLP1R mediated insulin secretion (399,400) so it might be expected that ageing and metabolic stress would reduce Pdx-1 and therefore GLP1R expression. However, we have found that HFD-induced metabolic stress and ageing leads to increased GLP1R expression (401). Take together, this suggests that although ß cell dedifferentiation could play a role in changes to GLP1R expression in GIPR knockout mice, the transcription factor networks that could influence GLP1R expression are not yet fully understood.

Alternatively, it is worth bearing in mind that wide-scale analysis of a range of mRNA and corresponding protein expression has shown a weak correlation between expression levels (402). This dissonance has been reported for *Glp1r*/GLP1R where a review of single cell RNAseq data suggested that approximately 80% mouse ß cells express *Glp1r* mRNA, in contrast to nearly all ß cells expressing GLP1R protein using reporter mice and a validated antibody (261). However, it is important to recognise that for relatively low expression genes like *Glp1r*, there can be significant drop out with RNA sequencing (403,404) so mRNA levels may be underestimated.

Additionally, it has been shown that while mRNA levels play a central role in fold changes of protein expression in a dynamic system, post-transcriptional regulation contributes significantly to the total level of protein expressed (405). Therefore, there could conceivably be differences in post-transcriptional activities which increase GLP1R in the setting of unchanged mRNA levels, but this has yet to be studied.

In summary, we have developed, and disseminated through publication (406), two thoroughly validated, novel fluorescent probes for GIPR, which demonstrate comparable receptor activation to native GIP and specificity for hGIPR. The probes have already contributed to advancing the field of incretin research by demonstrating suitability for peripheral administration and identifying that access to brain regions is restricted to areas without a blood-brain barrier (407).

Chapter 4: Validation of novel dual GIPR/GLP1R probes

Introduction

Tirzepatide is a dual GIPR/GLP1R agonist which has demonstrated superior effects upon glycaemic control and weight loss compared to the leading GLP1R agonist (243). As described in Chapter 1, consensus has not been reached about how both GIP agonism and antagonism confer weight loss and glycaemic benefit. In the context of GLP1R agonism demonstrating clear benefit and being developed into a class of medications for diabetes and obesity (408), it is therefore surprising that tirzepatide has such pronounced clinical effects when it demonstrates preferential binding and increased potency at the GIPR > GLP1R in humans (255).

Furthermore, GLP1R agonism itself is altered with signalling bias away from ß-arrestin and towards cAMP generation (255). ß-arrestins are key GPCR regulators and both inhibit signalling from the GPCR and traffic the receptor away from the cell surface (409,410). The limited ability of tirzepatide to recruit ß-arrestin at GLP1R was consistent with its reduced efficacy to internalise GLP1R (maximal effect being 40% of GLP1-mediated internalisation) (255). Maintaining GLP1R presence at the ß cell surface and permitting its ongoing signalling via cAMP to release insulin, may underlie tirzepatide's enhanced glucose-lowering effects.

While there is pharmacological data detailing the differences between single and dual agonism (e.g. differences in binding affinity, receptor potency and effect upon secondary messengers (255,411,412) as detailed in Chapter 1), pharmacological studies are

generally performed in stable, controlled, over-expression systems. However, in the pancreatic islet it is known that cell-cell interactions and paracrine signalling are key in modulating cell activity in response to GLP1R and GIPR expression and activity (reviewed in (349)). For example, GIP-stimulated release of glucagon from α cells potentiates insulin secretion from ß cells and the action of likely both GIP and GLP1 upon their cognate receptors on δ cells induces somatostatin release, which inhibits insulin and glucagon release, helping to regulate α and ß cell activity.

However, at present, it is challenging to determine which cell interactions may be targeted to enhance glucose control or weight loss because the cell substrates to which dual GLP1R/GIPR agonist can access and bind to is poorly defined. For example, to understand how dual GLP1RA/GIPRA-induced glucagon secretion is regulated, it is important to confirm which cells within the islet that dual agonists bind to.

Therefore, exploring dual agonist targets in the setting of endogenously expressed GLP1R/GIPR is the next step in interrogating dual agonism, particularly when administered peripherally. However, currently there are no tools to visualise dual GIPR/GLP1R agonist binding in live tissue after peripheral administration or at the single molecule level.

Transgenic rodent models harbouring conditional knockout of GLP1R or GIPR have served as useful settings to explore incretin physiology (212,412) and infer the tissue targets of dual agonists (253). However, they are unable to provide information on the cell populations targeted by dual agonists or upon recruitment of different receptor subpopulations.

Reporter approaches permit the identification of cells which express *Glp1r/Gipr* transcripts (265–267). However, it is not possible to infer detail about protein expression levels, localisation of receptors or confirm which cells are targeted by dual agonists.

Furthermore, caution should be applied when using transcription as a proxy for incretin

receptor expression as discordance has been found between *Glp1r* and GLP1R expression in mouse islets (261). Determining the degree of discordance was precluded with the methodology of this paper, through the use of a dichotomous measurement of GLP1R protein presence or absence. However, functional work found that a reduction in Glp1r expression of approximately one third, induced by multiparity, did not affect GLP1-induced insulin secretion (261),

Antibodies have been developed for GLP1R (summarised and reviewed in (259)) but they are only suitable for use in fixed tissue and cannot interrogate dual agonist orthosteric binding sites. A handful of GIPR antibodies have been synthesised, including antagonistic antibodies. However, they are more suited as modulators of GIPR signalling, as little (283) to no (252,413) information regarding specificity, such as lack of labelling in knockout models, has been provided and are very human-specific so not suited for use in mice. Additionally, with the brain being an important site of action for the weight loss effects of GLP1 and GIP there is anecdotal evidence that fluorescent GLP1R antibody immunostaining is less effective in the brain, limiting the ability to co-localise signal with neuronal or cell type markers (259). So, at present, while antibodies may be suited to identifying GIPR and GLP1R separately, they are not suited for interrogating dual agonist binding sites.

Therefore, we turned to developing a fluorescent agonist peptide probe based on the structure of the dual GLP1R/GIPR agonist, tirzepatide. As described in Chapter 3, the advantages of fluorescent probes are that they can be applied to cells or tissue and imaged either live or fixed alongside other makers. Additionally, peptide probes can be dosed to enable in vivo labelling and could be modified for single molecule imaging. These are important features for determining binding targets of a peptide and tracking activated receptor dynamics, which are poorly delineated for dual GIPR/GLP1R agonists.

The tirzepatide molecule is 39 amino acids long and based on a GIP backbone with prolongation of the C-terminal with a C-terminal sequence of the GLP1R agonist exenatide, a synthetic form of Exendin-4 (414) (415).

As well as the addition of the exenatide C-terminal to the GIP backbone, there are two further modifications to confer additional therapeutic properties to tirzepatide. Firstly, two α-amino isobutyric acid (Aib amino acids) at positions 2 and 13 and secondly, the conjugation of a fatty diacid chain acylated to the molecule C20 position (414,416). These two modifications impart resistance against degradation by the native enzyme dipeptidyl-peptidase 4 (DPP4) and provides high affinity albumin binding, respectively (414).

Chapter aim

In this chapter, I present the development of novel fluorescent dual GLP1R/GIPR agonist probes. We characterise their pharmacology, demonstrate their ability to label endogenous receptor and showcase our validation in relevant settings such as knockout models.

Results

daLUXendin structure and pharmacology

As for the development of the sGIP probes, we carefully considered the modifications to the chemical structure of tirzepatide to install a fluorophore. As previously described in Chapter 3, the potency of GIP is dependent upon the sequence of amino acids residing at the N-terminus (324,338,339). As tirzepatide incorporates the structure Exendin-4 we also considered how the structure of Exendin-4 affects its potency. As recently reviewed by Thorens and Hodson (417), seminal studies found that N-terminus truncation of Exendin-4 results in potent antagonism. Therefore, we chose to limit modifications to the C-terminus of tirzepatide. However, the C-terminus does contain a reactive amino acid (such as cysteine of lysine (418)) upon which a fluorophore could be installed.

It has previously been shown that substituting a C-terminal serine with a cysteine to create a S39C mutant, to install a fluorophore, does not affect the potency of Exendin4 (298,419). Therefore, we leveraged this stable modification for tirzepatide, created a S39C mutant tirzepatide molecule and installed a Cy3 or Cy5 fluorophore to the cysteine to create daLUXendin544 (Cy3) and daLUXendin660 (Cy5) (Figure 20).

We synthesised two versions of daLUXendin544/660, without the diacid side chain (daLUXendin544/660, Figure 20) and with (daLUXendin544+/660+, Figure 21). Although retaining the acylation would allow the fluorescent version to be more structurally similar to the original tirzepatide molecule, there are several potential advantages to creating a non-acylated version.

The diacid side chain confers high affinity albumin binding which is not required and can be detrimental in certain settings. Albumin binding is not required for in vitro or in vivo labelling of binding sites and ligand access studies are likely to be performed in mouse

islets where the side chain reduces affinity to both receptors but does not induce the GIPR > GLP1R selectivity of tirzepatide found in humans (256,420). Furthermore, the binding of daLUXendin to albumin may interfere with relevant in vitro assays where albumin is used a non-specific blocking agent (e.g. insulin/glucagon secretion assays, Fluorescence-Activated Cell Sorting).

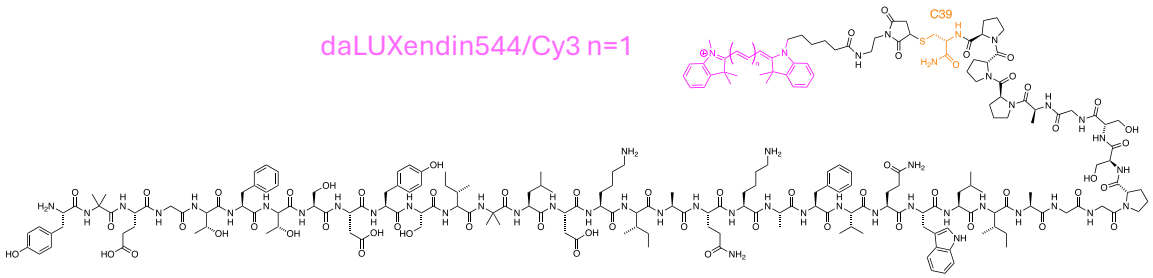

Figure 20: Chemical structure of non-acylated daLUXendin544/660.
The molecule is a mutant of tirzepatide, tirzepatide_S39C (H-YAibEGTFTSDYSIAibLDKIAQKAFVQWLIAGGPSSGAPPPC-NH2), without a diacid side chain and position 39 serine substituted for a cysteine (orange) and a Cy3 or Cy5 fluorophore conjugated onto the C-terminal cysteine (magenta).

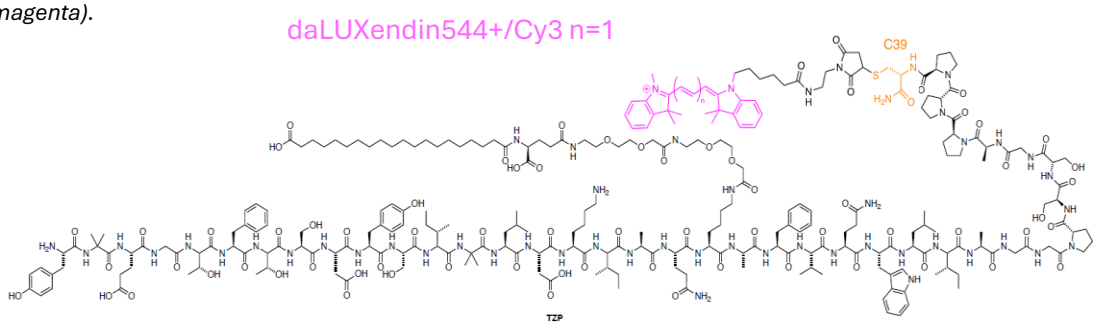

Figure 21: Chemical structure of acylated daLUXendin544+/660+.
The molecule is a mutant of tirzepatide, tirzepatide_S39C with preservation of the diacid side chain at position 20 (H-YAibEGTFTSDYSIAibLDKIAQK(lipid)AFVQWLIAGGPSSGAPPPS-NH2), and with position 39 serine substituted for a cysteine (orange) and a Cy3 or Cy5 fluorophore conjugated onto the C-terminal cysteine (magenta)

To determine if the removal of the diacid side chain, S39C substitution and the conjugation of a fluorophore affected the potency of the daLUXendin probes, cAMP production and binding affinity was measured and compared with relevant ligands (Figure 22). Human GLP1 and GIP were used as comparators as they generate similar cAMP responses or insulin secretion at mGLP1R and mGIPR compared with mGLP1 (421) and mGIP (422). At both hGLP1R and mGLP1R, tirzepatide and the daLUXendin probes showed

reduced cAMP production compared to GLP1, with the order of potency daLUXendin660 > tirzepatide > daLUXendin544.

At GIPR, both daLUXendin probes and tirzepatide showed reduced cAMP production compared to GIP, but more markedly at the mouse GIPR (Figure 22). This is in keeping with recent findings of tirzepatide having reduced potency at the mGIPR compared to the hGIPR (412). daLUXendin544 demonstrated reduced cAMP production compared to daLUXendin660 at all receptors. Both probes showed similar favouring of GIPR at the human receptors (EC50 ratio ~2:1 hGIPR:hGLP1R) and favoured GLP1R in mice (EC50 ratio ~1:2 mGIPR/mGLP1R). Tirzepatide demonstrated similar preferences but with higher degree of selectivity; hGIPR:hGLP1R EC50 ratio ~3:1, mGIPR:mGLP1R 1:8. Details of the cAMP values and selectivity calculations are available in Appendix 1.

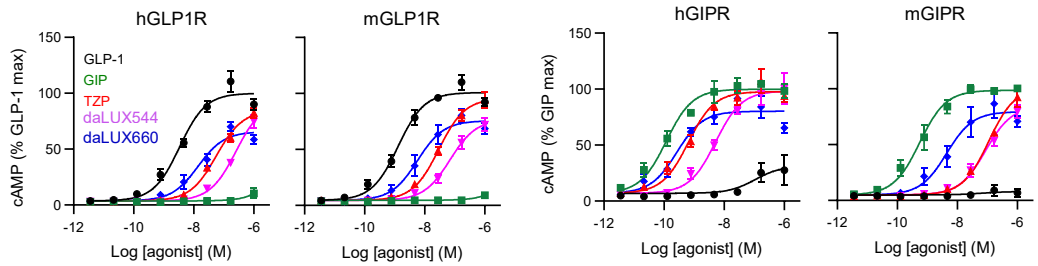

Figure 22: cAMP responses to hGLP-1, hGIP, Tirzepatide, daLUXendin554/660. Performed in AD293 cells transfected with either human/mouse GLP1R (hGLP1R/mGLP1R) or human/mouse GIPR (hGIPR/mGIPR).

To determine if the presence of the diacid side chain altered potency between the daLUXendin vs daLUXendin+ probes, we then compared the cAMP responses between them and found responses to be comparable (Figure 23).

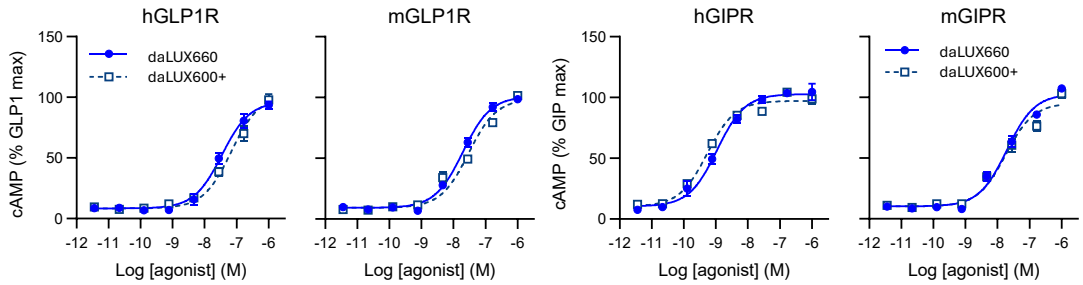

Figure 23: cAMP responses to daLUXendin660 and daLUXendin660+.
Performed in AD293 cells transfected with human or mouse GLP1R or GIPR.

We then assessed binding affinity using Bioluminescence Resonance Energy Transfer (BRET) to determine the Kd. There was interference with the BRET signal from the Cy3 probe so we were only able to interrogate binding affinity for daLUXendin660/660+. daLUXendin660 (Figure 24) and daLUXendin660+ (Figure 25) showed binding affinity in the nanomolar range for both the hGLP1R and hGIPR, with higher binding affinity for hGLP1R than hGIPR (Figure 24b and Figure 25b).

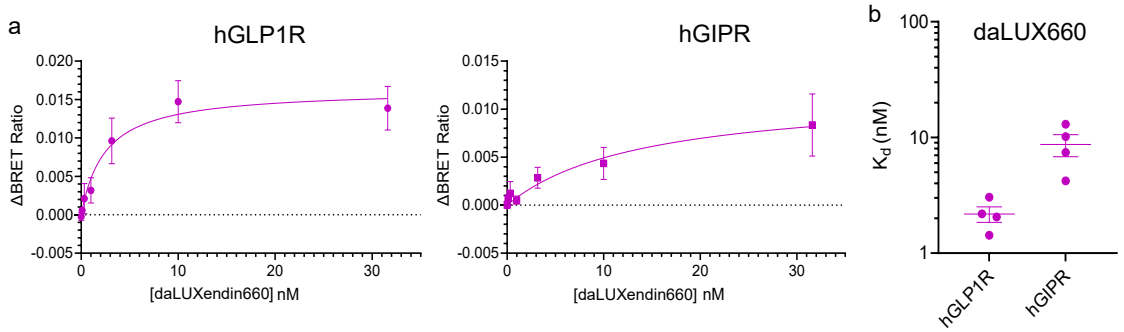

Figure 24: BRET ratios daLUXendin660 at the hGLP1R and hGIPR.
Performed in HEK293T cells transiently expressing Nluc-GLP1R or Nluc-GIPR showed nM binding affinity

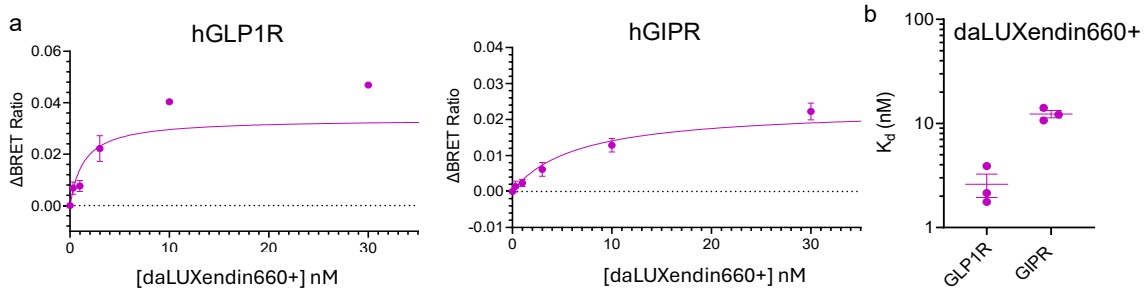

Figure 25: BRET ratios of daLUXendin660+ at the hGLP1R and hGIPR.
Performed in HEK293T cells transiently expressing Nluc-GLP1R or Nluc-GIPR showed nM binding affinity

To further assess the strength of receptor binding, competition assays were undertaken for daLUXendin660 (Figure 26a), Exendin-4-Cy5 and GIP-Cy5 (Figure 26b). The binding affinity (pKi) for hGLP1/hGLP1R and hGIP/hGIPR was similar between the three probes (Figure 26c), confirming the strength of daLUXendin660 binding compared to native, single agonists. pKi, the negative logarithm of the Ki value, was used as Ki values can span many orders of magnitude and make comparisons more challenging.

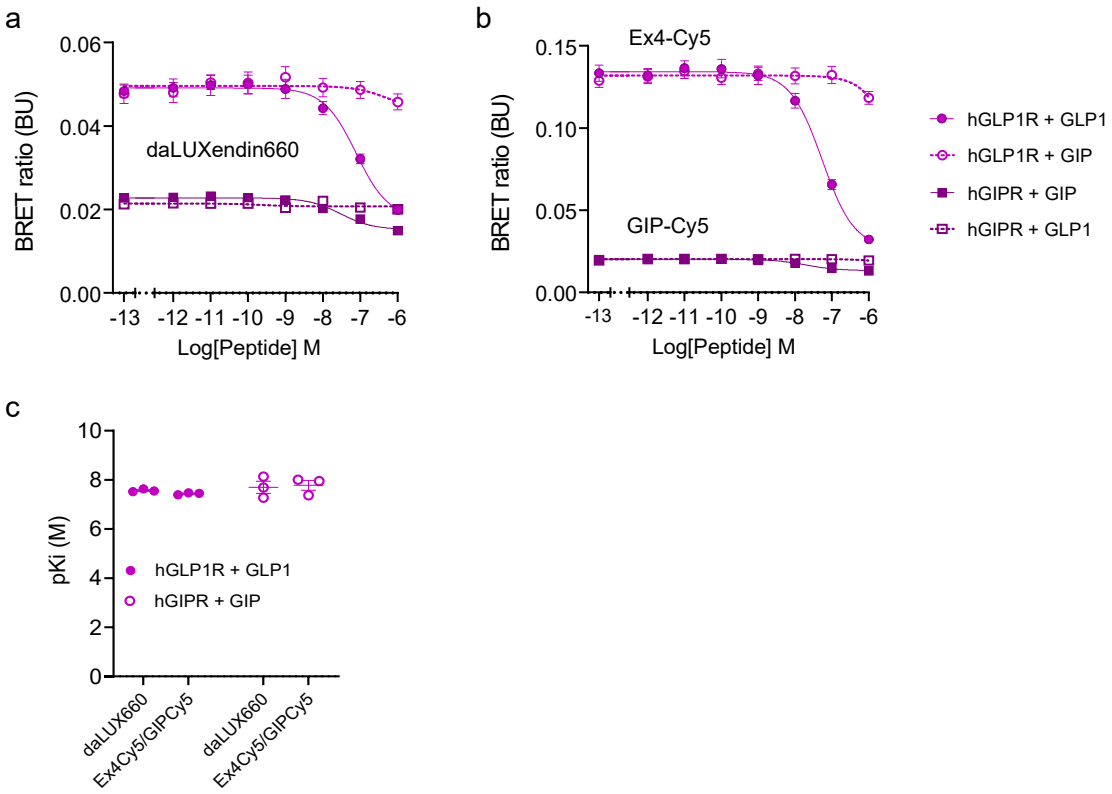

Figure 26: daLUXendin competition binding assays.
Competition binding for daLUXendin660 (a) and either Exendin-4-Cy5 or GIP-Cy5 (b) at hGLP1R and hGIPR versus GLP1 and GIP. (one-site fit Ki). pKi values for daLUXendin660, Ex4-Cy5 and GIP-Cy5 at hGLP1R and hGIPR versus GLP1 and GIP (c) (n = 3 independent repeats).

Together, these results demonstrate that our daLUXendin and daLUXendin+ probes have similar potency and strong receptor binding at both GLP1R and GIPR when compared to tirzepatide. However, we also show that daLUXendins have reduced selectivity for GLP1R in mice. Therefore, this suggests that our modifications, from a pharmacological

assessment, are not only a suitable substitution for tirzepatide but that they confer an advantageous imbalanced agonism i.e. selectivity closer to tirzepatide's selectivity at human GLP1R/GIPR. Due to the advantages mentioned above regarding absence of a diacid side chain, we began validation with the non-acylated daLUXendin544/660 probes.

daLUXendin544/660 demonstrate specificity for hGLP1R and hGIPR in an over expression system

To corroborate the pharmacokinetic results described above, we applied the probes to AD293 cells transiently transfected with tagged human GLP1R and GIPR; SNAP_hGLP1R and Halo_hGIPR.

As described in Chapter 1, self-labelling protein tags such as SNAP-tags and HaloTags can be incorporated into proteins of interest. Following incubation with an organic fluorophore which fluoresces upon binding to the tag, it permits the identification of the protein without interfering with the orthosteric binding site.

Specificity of the daLUXendin probes was therefore demonstrated via co-localisation of the probes with signal from the fluorescent labels binding to the SNAP-tagged GLP1R (BG-OG) and Halo-Tagged GIPR (CA-Sulfo549, CA-Sulfo646) (Figure 27). In non-transfected AD293 cells, there was no labelling from the daLUXendin probes (Figure 28) which demonstrates that the probes do not engage in off-target labelling and can be regarded as specific.

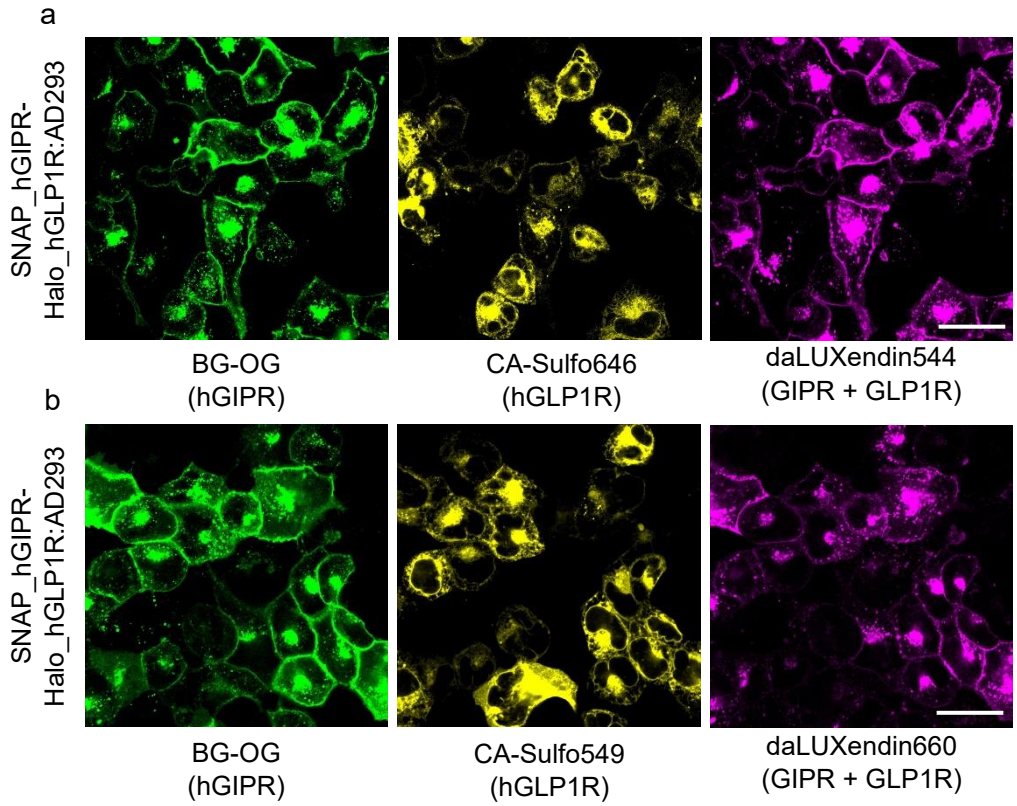

Figure 27: daLUXendin in SNAP_hGIPR-Halo_GLP1R AD293 cells.
Representative images of AD293 cells transfected with SNAP_hGIPR and Halo_hGLP1R and labelled with daLUXendin544/660.Cells co=labelled with orthogonal labels for hGIPR (SNAP label BG-OG) and hGLP1R (Halo label CA-Sulfo549/646). Scale bar = 33.7µm.

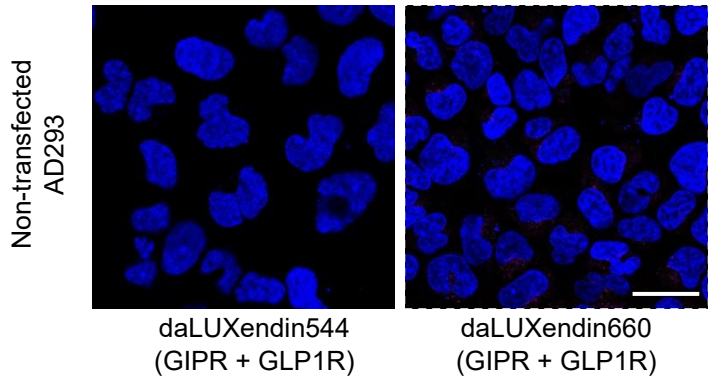

Figure 28: daLUXendin labelling in non-transfected AD293 cells.
Non-transfected AD293 cells incubated with DAPI and daLUXendin544/660.Scale bar = 33.7µm.

daLUXendin660 labels endogenous GLP1R and GIPR in cells

Using overexpressing systems is important for pharmacological studies and demonstrating receptor specificity. However, it is important to demonstrate that our probes can label GLP1R/GIPR at the much lower, endogenously expressed level to confirm that they are suitable for more translatable studies.

To determine if the daLUXendin probes were able to label GLP1R/GIPR at endogenously expressed levels daLUXendin660 was applied to MIN6-CB4 cells. MIN6 is an immortalised rodent beta cell line (423) which express GLP1R (293,424) and GIPR (424). The CB4 variant is an optimised line which retains GSIS in long-term culture (293) and anecdotally, our lab has seen enhanced GLP1R/GIPR insulinotropic responses compared to other cell lines.

daLUXendin660 was applied alongside either a GLP1R antagonist probe (LUXendin551 (298,419)) or a GIPR agonist probe (sGIP549) of orthogonal fluorescence. Although daLUXendin would be competing with LUXendin551 and sGIP549 for GLP1R and GIPR, respectively, there was still co-localisation with each receptor (Figure 29) likely due to labelling of different pools of receptors not discernible from each other at this resolution. We quantified this co-localisation with correlation coefficient analysis, which analyses the overlap of fluorescence in each pixel of an image. Demonstrating specificity for the GLP1R and GIPR, we found a high correlation of daLUXendin660 with both LUXendin551 and sGIP549 (Figure 30).

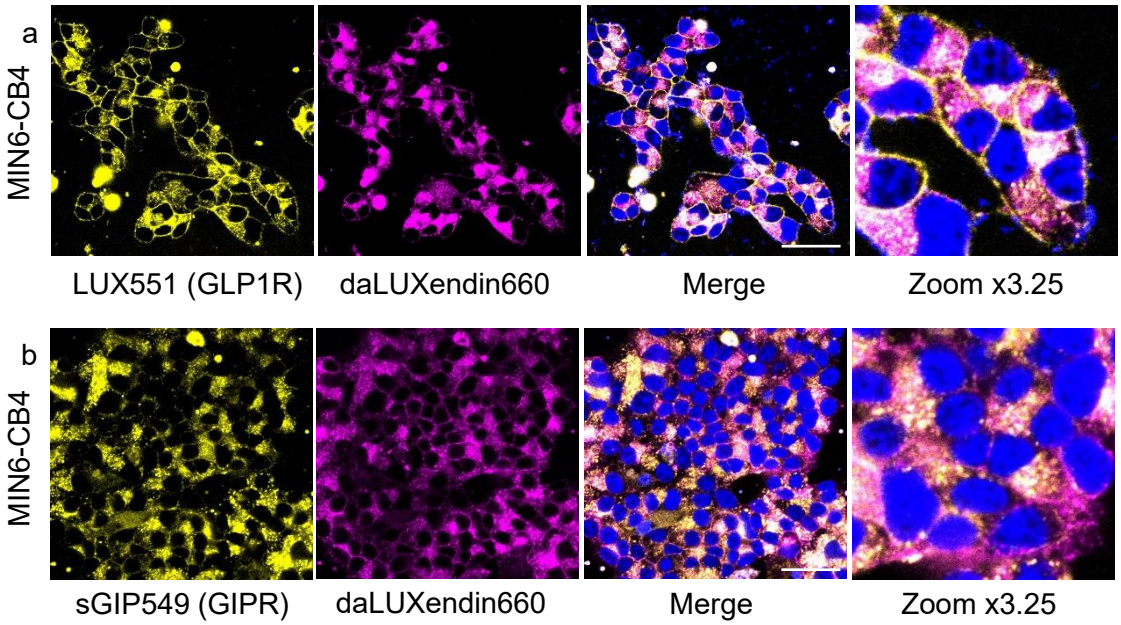

Figure 29: daLUXendin in MIN6-CB4 cells.
MIN6-CB4 cells labelled with daLUXendin660 and either GLP1R label LUXendin551 or GIPR label sGIP549. Scale bar 33.7µm.

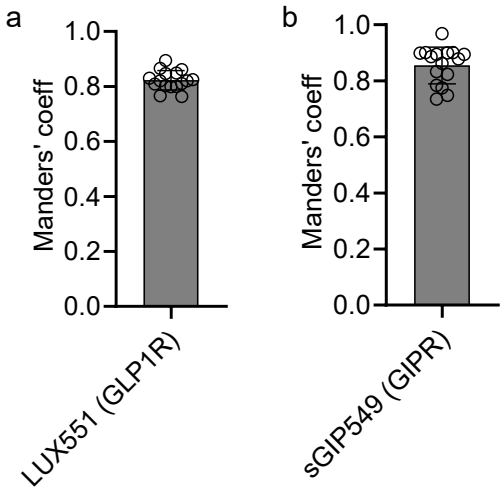

Figure 30: Correlation of daLUXendin with GLP1R and GIPR probes
Mander's coefficient of daLUXendin660 with (a) LUXendin551 (mean0.86) or sGIP549 (mean 0.82) (n = 16 images from 4 wells, 2 independent repeats)

Due to the species difference in tirzepatide potency and signalling at GLP1R and GIPR (412), it may be difficult to tease out translatable biological novelty using purely mouse models. Therefore, we next turned to EndoC-βH5 cells, aline of human ß cells with several pertinent properties. Firstly, they retain endogenous expression of both GLP1R and GIPR (425) – although this is transcriptomic data and hasn't been confirmed at a protein level. Secondly, they demonstrate appropriate insulin secretion in response not only to glucose, but also to GIP and GLP1 (425).

As for the MIN6-CB4 cells, clusters of EndoC-βH5 cells were labelled with daLUXendin660 and either LUXendin551 or sGIP549. daLUXendin660 co-localised with both probes but there were high levels of autofluorescence in the yellow-green spectrum in unlabelled cells (Figure 31). Further, the LUXendin551 labelling was not limited to the membrane, which would be expected with an antagonist probe (Figure 31). From this data, we could not be confident that EndoC-βH5 cells express GLP1R/GIPR at detectable levels or whether the level of autofluorescence is at a prohibitively high level that obscures probe signal.

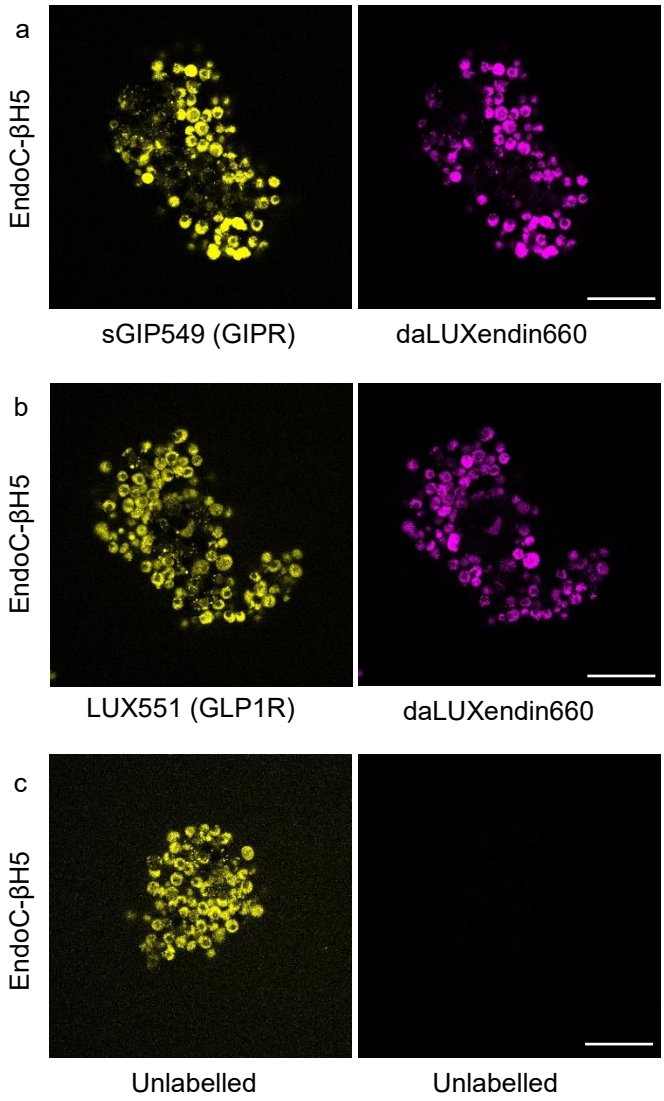

Figure 31: daLUXendin labelling in EndoC-βH5 cells
EndoC-βH5 cells labelled with sGIP549 and daLUXendin660 (a), LUXendin551 and daLUXendin660 (b) or unlabelled (c). (n=1). Scale bar 53µm.

daLUXendins label endogenous GLP1R and GIPR in mouse islets

daLUXendin544 labels membrane and cytosolic pools of GLP1R and GIPR, as shown through co-localisation with GLP1R (Figure 32) and GIPR (Figure 33) probes. Demonstrating specificity, correlation co-efficient analysis found high co-localisation of daLUXendin544 with both GLP1R and GIPR probes (Figure 34).

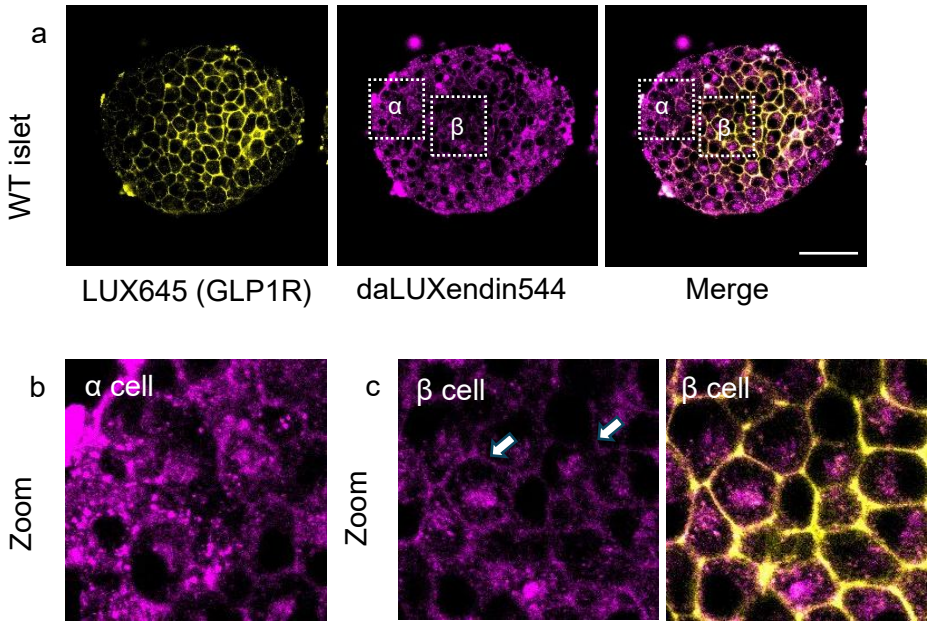

Figure 32: daLUXendin and LUXendin labelling in WT islets.
Representative images of WT islets labelled with LUXendin645 and daLUXendin544.
Zoom panels of α cells (GLP1R-) and β cells (GLP1R+). Arrows highlight the increased membrane labelling in β cells (c) compared with α cells (b) (n=37 islets from 3 mice). Scale bar = 53μm.

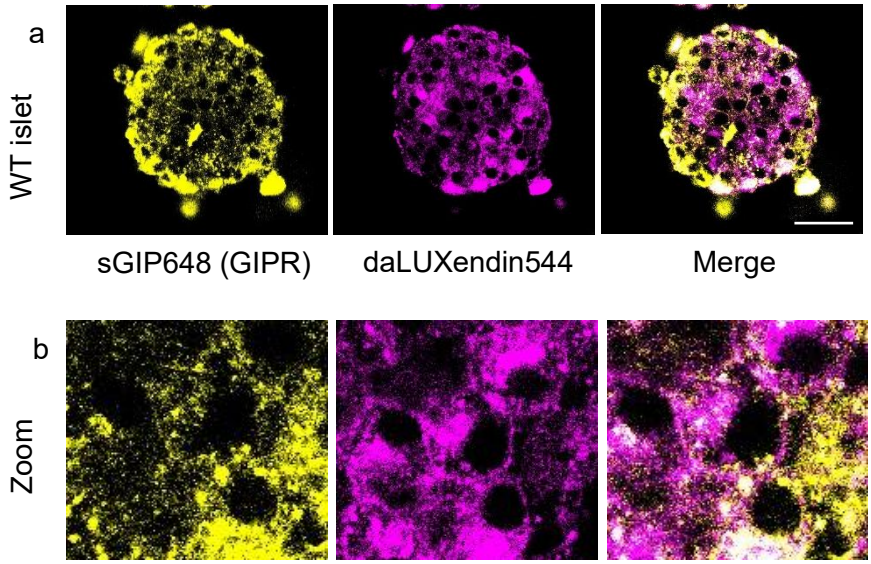

Figure 33: daLUXendin and sGIP probe labelling in WT islets.
Representative images of WT islets labelled with GIPR probe sGIP648 and daLUXendin544.
Zoom panel illustrating co-localisation (n=37 islets from 3 mice). Scale bar = 53µm.

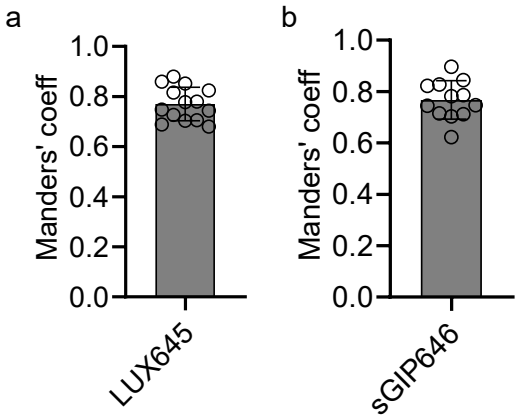

Figure 34: Correlation analysis between daLUXendin544 and LUXendin645 (a) and sGIP648 (b) in WT islets. (n=43 islets from 2 mice)

daLUXendin544 demonstrated more membrane labelling in β cells (identified by LUXendin645/GLP1R labelling) than in α cells (identified by lack of LUXendin645/GLP1R labelling). To explore this difference, daLUXendin probes were applied to GLP1RSNAP/SNAP islets (269) alongside a cell-impermeable SNAP labels (279). This would allow for daLUXendin labelling and co-localisation analysis without interference

with the orthosteric binding site from other probes but also to assess the degree of receptor internalisation for each probe.

There was increased internalisation of GLP1R when co-treated with each probe (Figure 35 and Figure 36). Using Full Width Half Maximum (FWHM) to quantify this, the degree of GLP1R internalisation was slightly greater with daLUXendin660, while daLUXendin544 retained more GLP1R at the cell surface (Figure 38).

FWHM involves measuring fluorescence intensity across a membrane (Figure 37) and measuring the width at half-maximum of the peak. Increased internalisation of the labelled receptor will lead to a greater spread of high fluorescence either side of the membrane, leading to an increased width at half-maximum. Retention of labelled receptor at the membrane will lead to rapid drop off of fluorescence either side of the peak fluorescence of the membrane, leading to a narrower/decreased width at half-maximum.

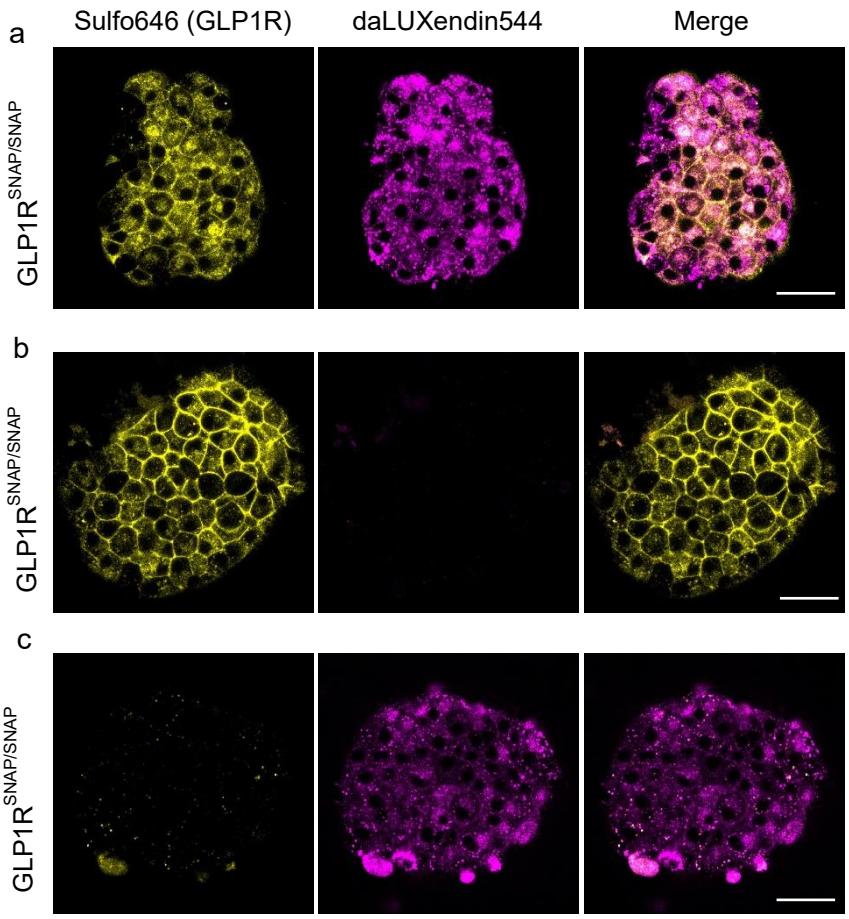

Figure 35: daLUXendin660 and SNAP labelling in GLP1R$^{SNAP/SNAP}$ islets.
Representative images of GLP1R$^{SNAP/SNAP}$ islets labelled with SNAP label Sulfo646 and/or daLUXendin544, SNAP label Sulfo646 and/or daLUXendin544 (a), just Sulfo646 (b) or just daLUXendin544 (c). Scale bar = 53µm.

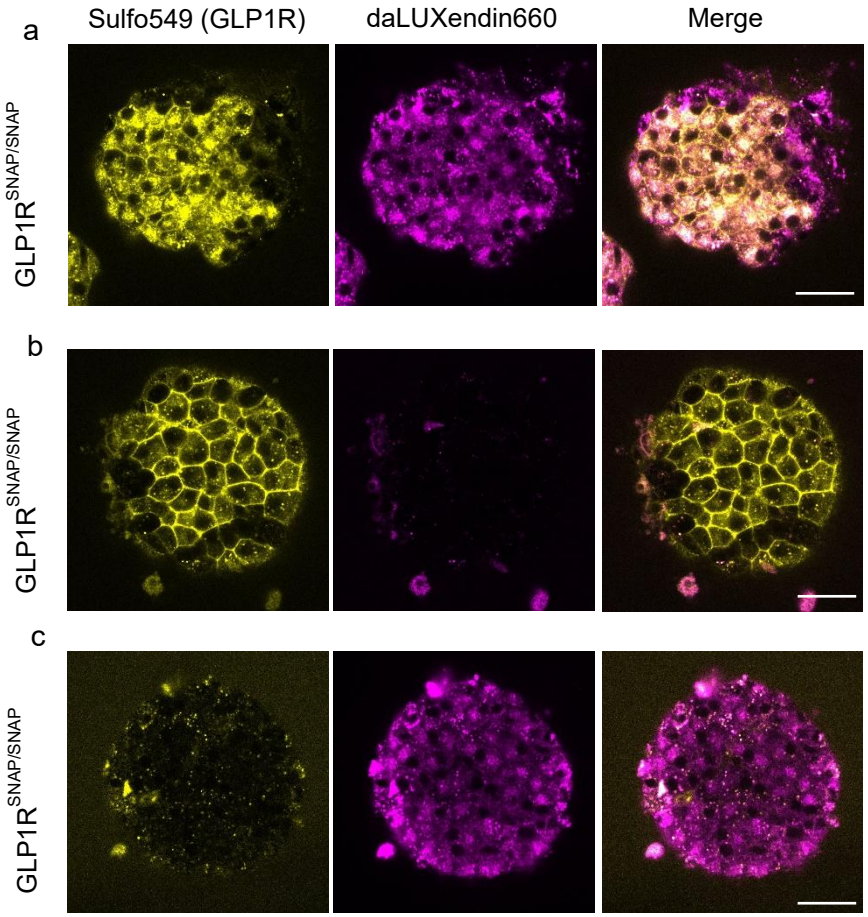

Figure 36: daLUXendin660 and SNAP labelling in GLP1R$^{SNAP/SNAP}$ islets.
Representative images of GLP1R$^{SNAP/SNAP}$ islets labelled with SNAP label Sulfo549 and/or daLUXendin660 SNAP label Sulfo549 and daLUXendin660 (a), just Sulfo549 (b) or just daLUXendin660 (c). Scale bar = 53µm.

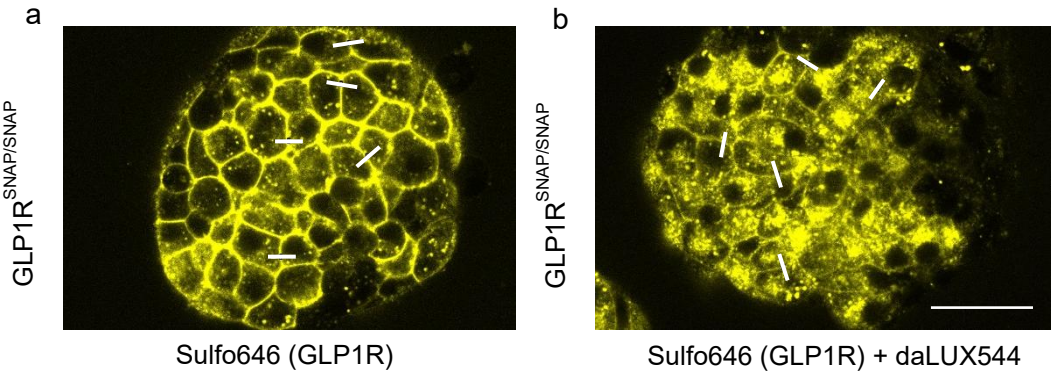

Figure 37: Line placement for FWHM measurement
Representative images of line placement used to measure full width at half maximum (FWHM) in GLP1R$^{SNAP/SNAP}$ islets.Islets labelled with either Sulfo646 (a) or Sulfo646 with daLUXendin544 (b) (n=18-24 islets from 5-7 mice). Scale bar 53µm.

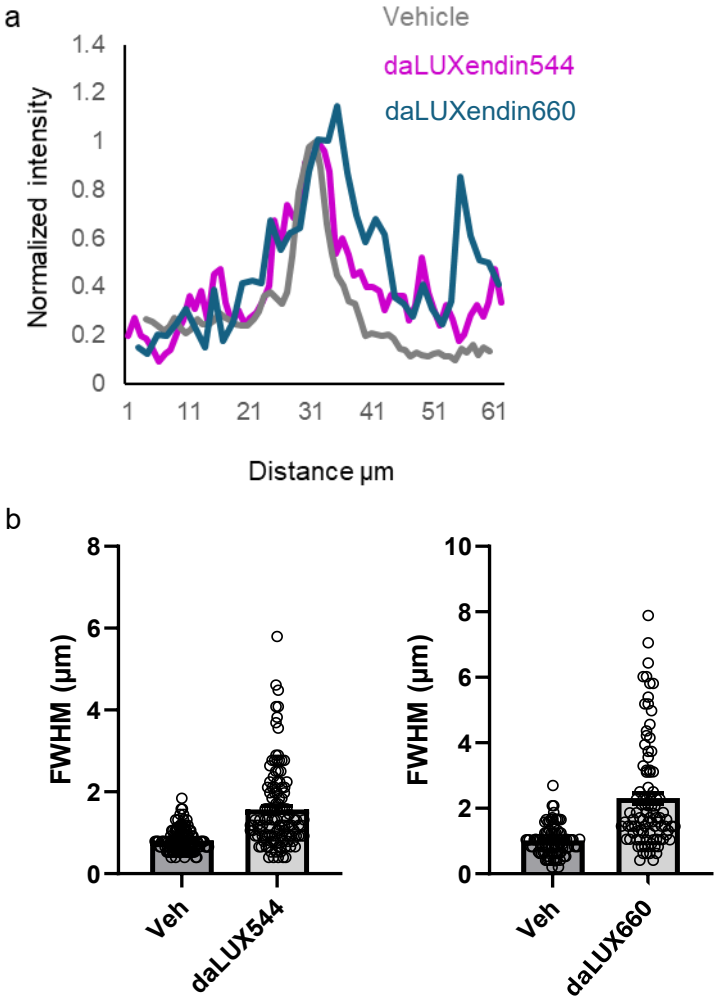

Figure 38: Width of SNAP labelling with and without daLUXendin co-administration. Average normalised intensity for Sulfo549/646 across cell membranes treated with either daLUXendin660/544 respectively or vehicle (a).FWHM values for Sulfo646 co-labelled with either vehicle or daLUXendin544 and Sulfo549 co-labelled with either vehicle or daLUXendin660 (b).

daLUXendin labelling is reduced in *Glp1r-/-* islets and excess GIP agonism

An important setting to confirm probe specificity is in knock-out models. In *Glp1r-/-* mice daLUXendin probe labelling was reduced compared to WT labelling, with further reduction in fluorescence following pre-incubation with excess GIP agonist (1uM GIPAib2) to compete for GIPR (Figure 39). Fluorescence was quantified and showed a statistically significant reduction in fluorescence for both probes in *Glp1r-/-* islets compared to WT islets (Figure 39c). Further reduction in fluorescence was found with pre-incubation with excess GIP agonist, but this did not reach statistical significance with daLUXendin660 (Figure 39c).

The similar labelling of *Glp1r-/-* islets with and without pre-incubation with excess GIP agonist is unlikely due to residual GLP1R expression as the line has been well validated (298). The *Glp1r-/-* model was CRISPR-Cas9 genome edited to introduce a deletion into exon 1 which resulted in a frameshift mutation and subsequent non-transcription (426). This technique avoids the risk of variability in knock-out effectiveness, as found with e.g. tamoxifen-inducible knock-out models. Effective non-transcription was confirmed in this model in several ways. Firstly, islets isolated from this line retained glucose-stimulated insulin secretion but did not secrete insulin in response to GLP1R agonist Exendin4(1-39) (426). Secondly, *Glp1r-/-* islets did not generate cAMP in response to the GLP1R agonist Liraglutide and thirdly, there was no immunostaining with monoclonal GLP1R antibody (426). Therefore, it is unlikely that any residual GLP1R expression was the reason for ongoing daLUXendin660 labelling in islets pre-incubated with GIP agonist.

Another hypothesis might be that there was upregulation of GIPR in *Glp1r-/-* mice as has been suggested occurs for GLP1R in *Gipr-/-* mice (196,212,412). This would have to be a

significant increase in expression to overcome the excess agonist concentration. However, going against this is a recent study demonstrating no increased sensitivity to GIP (measured as GIP-stimulated insulin secretion) in *Glp1r*-/- vs *Glp1r*WT/WT mice (427). Therefore, it is more likely that as daLUXendin and GIP are in competitive equilibrium, the residual staining is a result of a GIPR pool that GIP is unable to block.

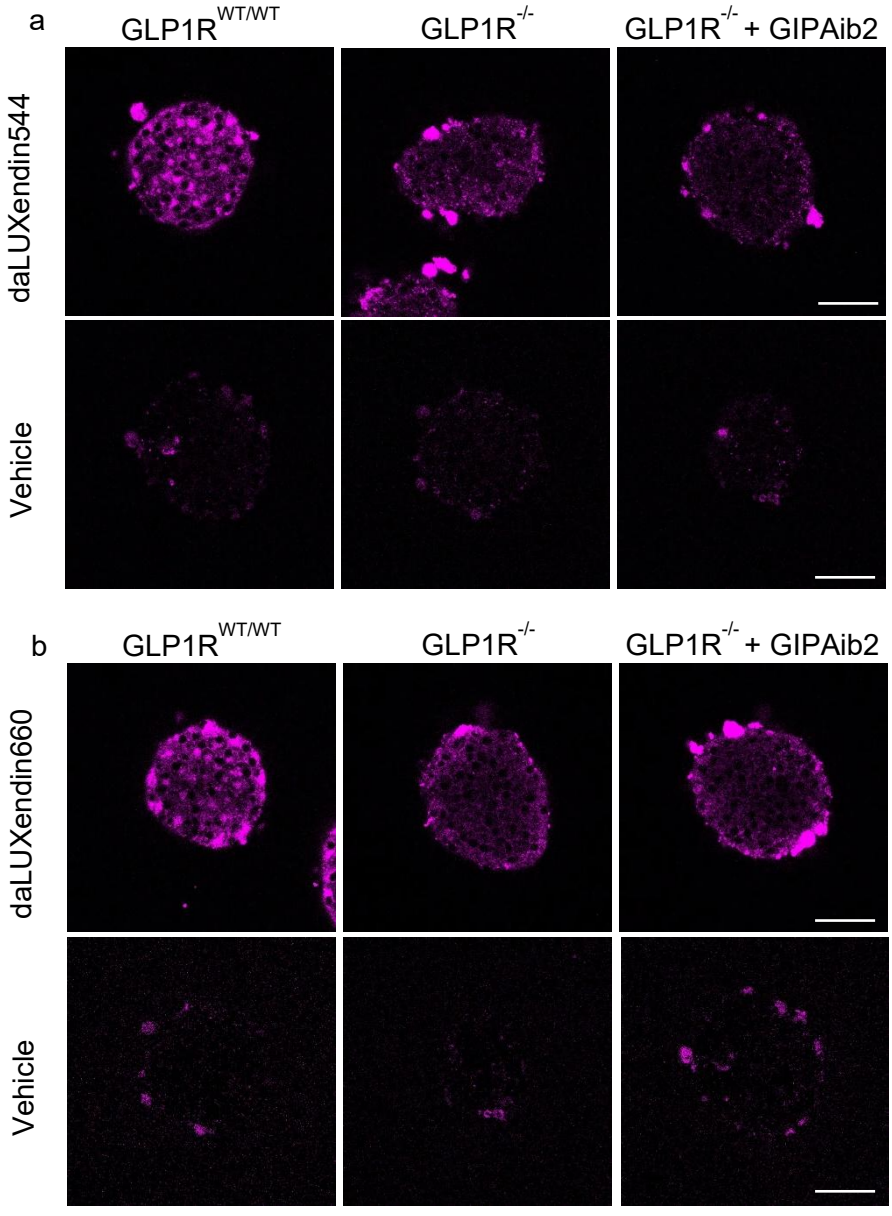

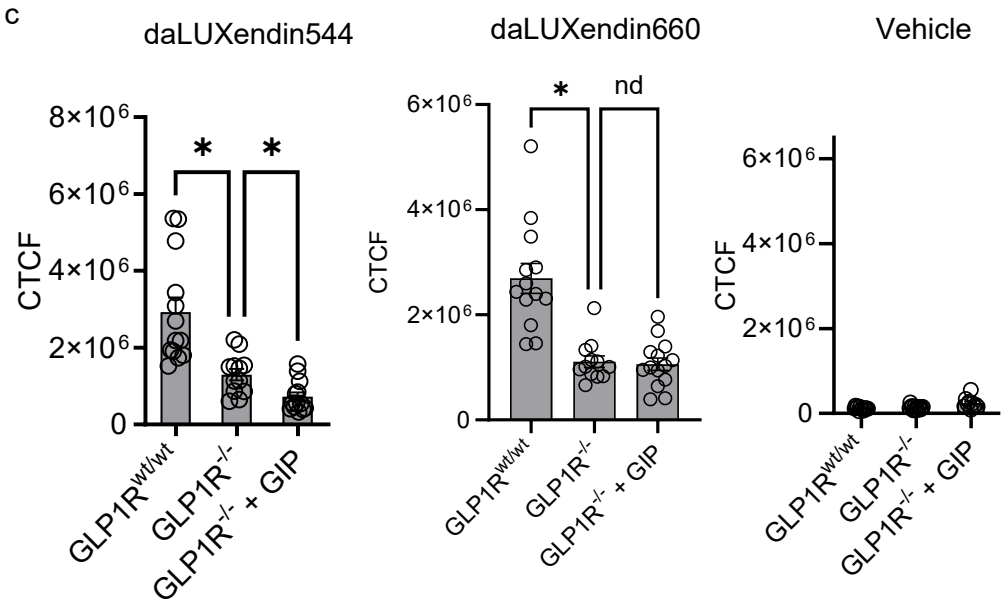

Figure 39: daLUXendin in GLP1RKO islets and excess GIP agonist.
Representative images of daLUXendin544 (a) and daLUXendin660 (b) labelling in WT islets, Glp1r-/- islets without and with pre-incubation with GIPR agonist GIPAIb2.Differences in fluorescence were quantified by measuring whole islet CTCF (c). (n = 37 islets from 2 mice) (Kruskal-Wallis test with two-stage linear step-up procedure of Benjamini, Krieger and Yekutieli). Scale bar = 53µm.

Discussion

In this chapter, we present the synthesis and validation of novel dual GLP1R/GIPR agonist probes daLUXendin544 and daLUXendin 660. These probes are specific for GLP1R and GIPR and provide a novel and straightforward method of identifying dual agonist targets and interrogation of binding sites.

We show that the probes have a similar pharmacological profile as tirzepatide but with greater mGIPR>mGLP1R selectivity.

By generating probes with (daLUXendin544/660+) and without (daLUXendin544/660) the C20 diacid side chain, but with similar potencies and binding affinities, we facilitate their use in a range of experiments where albumin-binding is either critical or a hinderance.

As discussed in the introduction, other current modalities to assess dual GLP1R/GIPR agonism are limited in their ability to visualise receptor location or identify target sites of dual agonists in live tissue. Although mouse genetics, reporter approaches and antibodies have their limitations, their utility can be maximised through use alongside the fluorescent daLUXendin probes to label live and fixed tissues. For example, lack of labelling by daLUXendin probes with cells which report *Glp1r*/*Gipr* expression may suggest cells in which protein expression is very low (below daLUXendin detection limit) or cells where the phenotype has changed.

During the course of this work, another fluorescent dual GLP1R/GIPR agonist probe was recently developed; Alexa647-conjugated tirzepatide (256). Labelling of mouse islets was retained after fixation and appropriately it did not label cells in *Glp1r*-null mice islets or WT mice islets pre-incubated with GLP1R antagonist, Exendin-4(9-39)(256). However, complete loss of labelling demonstrates that the probe does not have the advantageous mGIPR selectivity of the daLUXendins. Furthermore, full validation of the probe by with pharmacological data regarding binding affinity or potency was not provided. It is known

that fluorophore choice, conjugation, and any modification to permit conjugation, can alter these parameters at the GLP1R/GIPR (298,407,419). Alexa647 is a highly sulfonated fluorophore, which can limit its use in live tissue due to repulsion from the sulfonated charges (269,428).

Further supporting the notion that fluorophore conjugation affects binding affinity and potency, the same group reported that removal of the diacid side chain increases hGIPR binding affinity by four-fold compared with tirzepatide, without affecting hGLP1R binding affinity but increased GLP1R cAMP accumulation (256). However, this contrasts with our findings that cAMP responses from GLP1R and GIPR binding were similar between daLUXendin660 and daLUXendin660+. Of note, pharmacology assays in HEK293 cells are dependent upon receptor expression levels, particularly when assessing imbalance and bias. For our studies, we used moderate levels of expression, which may have masked this difference. Further detail regarding conjugation strategy of tirzepatide-Alexa647 was not provided but would be informative to compare with daLUXendin probes.

Following on from this, determining the degree of GLP1R vs GIPR selectivity is crucial when developing probes used to replicate tirzepatide action. In the human setting, tirzepatide shows greater affinity for and potency at GIPR than GLP1R (255,256,412). However, in the mouse, tirzepatide shows greater affinity for GLP1R and shows similar efficacy to GLP1R agonist semaglutide (255,412). This limits the use of mouse models to fully elucidate dual agonist effects translatable to the human setting, although mice remain an important model to investigate likely tissue and cell substrates following peripheral administration.

While daLUXendins show similar cAMP responses to tirzepatide, daLUXendin544/660 showed much less GIPR selectivity (1:2 mGIPR:mGLP1R) than tirzepatide (1:8 mGIPR:mGLP1R) in mice. This dependence upon mGIPR of daLUXendin was confirmed in

in vivo IPGTTs where mGLP1R:mGIPR selectivity was reduced for daLUXendin compared to tirzepatide (presented in Chapter 6). As explored in Chapter 3, human donor islets are a challenging setting for fluorescent labelling due to autofluorescence (82) and low expression of GLP1R/GIPR in most ß cells (429). Therefore, this difference in receptor selectivity has the translational benefit of giving daLUXendin labelling in a mouse setting a closer profile to tirzepatide in humans – with the caveat that the in vivo impact of daLUXendin, for example upon food intake, also needs to be evaluated in comparison to tirzepatide and/or single GLP1R agonists.

It is unclear exactly what mechanism(s) give rise to the differences between daLUXendin and tirzepatide pharmacology. However, given that our previous studies have shown that Cy5 increases efficacy (298), it is possible that the Cy3/5 moieties alter orthosteric interactions. Therefore, further engineering of the daLUXendin structure could reduce the receptor selectivity further or align it even closer to that of tirzepatide at human GLP1R/GIPR and transform the interrogation of dual agonist action in the mouse model.

In summary, I have presented our synthesis of fluorescent dual GLP1R/GIPR probes, daLUXendins. We describe the pharmacological profile of these probes compared to tirzepatide, which matches potency at relevant receptors but differs in receptor selectivity. We have robustly assessed the specificity of the probes for GLP1R/GIPR in over-expression and endogenously expressed settings.

Chapter 5: Interrogating the cell targets of daLUXendin probes in vitro

Introduction

GLP1 and GIP impact upon glucose and weight

GLP1 and GIP are important mediators of post-prandial glucose control, where insulin secretion is greater after oral glucose ingestion than intravenous glucose administration; this is termed the incretin effect (430). Both GLP1 and GIP are known to potently potentiate glucose-stimulated insulin release (175).

In diabetes, the incretin effect is reduced and contributes to dysglycaemia (197,208,431) and there is suggestion that a reduced incretin effect is an early marker of the condition (432). The reduced incretin effect in diabetes has been attributed to reduced sensitivity of β cells to GIP (197,208,431) and reduced secretion of GIP, but especially GLP1 (433,434).

In people with diabetes, early studies of GLP1 infusions first showed improvement in glucose excursions (217,435) and later, reduction in weight (436). GLP1-based therapies have been pursued and licensed for many years after demonstrating impressive glucose- and weight-lowering effects (summarised in (408)).

Despite evidence suggesting that GIP contributes to the majority of the incretin effect (437–439), the therapeutic benefit of GIP upon glucose metabolism have been less clear cut. In contrast to GLP1, early studies found reduced insulin secretion in response to GIP infusion in people with diabetes (206,217). A recent study of genetic variants of human GIPR have found that variants which impair GIPR function (impaired cAMP production and ß arrestin recruitment) are associated with a lower adiposity (234). Furthermore, results

from animal studies have found conflicting results. Both loss (213,350,440–442) and gain (237,443,444) of GIP function have been shown to confer protection against diet induced obesity. However, several other studies have found equivocal impacts of loss (231) or gain (238–240) of GIP function upon weight. For glycaemic control, loss of GIP function has been shown to have deleterious effects upon insulin secretion (213,214) but most gain of function studies have not interrogated glucose control, focusing instead upon changes in food intake and body weight. These opposing results are summarised in (380).

Furthermore, cardioprotection is an important facet of novel diabetes and obesity treatments. GIP lowers blood pressure and increases heart rate when administered to individuals with and without diabetes and obesity but whether this is cardioprotective or not remains unclear (445,446).

However, interest in GIP was renewed when correction of hyperglycaemia was found to rescue GIP action in people living with diabetes (447) and has further come the fore with the dual GLP1R/GIPR agonist tirzepatide showing superior glycaemic control (243) and weight loss than single GLP1R agonists (117) in clinical trials.

Glp1r/GLP1R and *Gipr*/GIPR expression in the pancreatic islet

GPCRs are generally expressed in low abundance (448). This is the case for *Glp1r* and *Gipr* transcripts which are much lower than insulin and glucagon transcripts (188) and GLP1R and GIPR protein are expressed at low levels in pancreatic islet cells (188,191,349). Until recently there has been a lack of reliable, suitably validated techniques to detect GLP1R/GIPR protein (259).

Glp1r/GLP1R is known to be abundantly expressed on β cells in rodents (188,191,298) and humans (Huising lab meta-analysis dataset (190) including data from (192,449–452)) but there is uncertainty on whether *Glp1r*/GLP1R is expressed on α or δ cells.

Some evidence (mRNA RT-PCR, immunoreactive assays) suggests the presence of *Glp1r*/GLP1R on subpopulations of mouse α cells (187,453). This has been supported by a recently developed GLP1R fluorescent probe which labelled 12.3 ± 3.3% α cells (298). However, Western blots in rats (454) and mouse RNAseq data (188,191) have been unable to find GLP1R/*Glp1r* in α cells. Human islet transcriptome studies have also found negligible expression of *Glp1r* RNA in α cells (190,455) and fluorescent immunostaining of human islet sections found negligible co-localisation of GLP1R in glucagon-positive cells (456).

When insulin and somatostatin receptors are blocked, GLP1 is still able to suppress glucagon secretion (457). This could give weight to the theory that that GLP1 is directly binding to GLP1R on α cells, but with expression levels too low to visualise without super resolution techniques. Or, with further studies showing that GLP1 suppresses glucagon secretion in *Glp1r*-/- mice but not *GCG*-/- mice (458), it has been proposed that GLP1 degradation products are able to activate the GCG receptor (349). Alternatively, given that GLP1 stimulates somatostatin release (185–187,459) and somatostatin inhibits α cell excitation (460,461), it could be that GLP1 mediated glucagon suppression is via paracrine somatostatin release (462).

There is limited evidence surrounding the presence of GLP1R in δ cells. Early radioactive ligand studies in rodent cell lines found the presence of GLP1R on δ cells, suggesting that GLP1 directly interacts with δ cells to stimulate somatostatin release (185). Single cell RNA sequencing data of islets from reporter mice found moderate expression of *Glp1r* in δ cells (188,191). More recent non-fluorescent (463) and fluorescent immunostaining (456)

studies in human pancreata found strong co-localisation of GLP1R antibody staining with insulin-positive cells in addition to weaker, but still present, co-localisation with somatostatin-positive cells. However, human islet transcriptome studies found very minimal expression of *Glp1r* RNA in δ cells (190,455).

The expression of *Gipr*/GIPR has been less studied. In mice, GIPR is considered to be expressed extensively in the pancreatic islet with transcriptomic studies reporting *Gipr* expression in equal measure in α, β and δ cells (188). Human transcriptomic studies have found similar expression, with *GIPR* RNA found in α, β and δ cells (189,190,455).

The current evidence for *Glp1r*/GLP1R and *Gipr*/GIPR expression in rodent models and humans is summarised below in Table 9 and Table 10 respectively. However, it is important to bear in mind that for class B GPCRs like GLP1R and GIPR, there is discordance between gene expression and RNA levels and actual protein expression (261). Therefore, transcriptomic studies should be interpreted with caution and weight should be given to techniques that are able to identify receptor expression and localisation, such as well-validated, specific antibodies and probes.

Rodent islets	Evidence of presence	Evidence of absence
α cells		
GLP1R	Rat islets: radiolabelled GLP1 co-localised with α cells (187) Mouse islets: fluorescent GLP1R antibody labelled small population of α cells (261) Mouse islets: fluorescent GLP1R probe labelled α cells (298)	Hamster α cell line (RRID:CVCL_0353): radiolabelled GLP1 did not localise to α cells in (185) Rat islet: Western blot unable to detect GLP1R in α cells (454) Mouse islets: scRNAseq; no expression of *Glp1r* in α cells (188,191) Mouse islets: *Glp1r* promoter not active in α cells (261) Rat islets: GLP1R anti-serum did not co-localise with α cells (429) Mouse islets: lack of fluorescent GLP1R probe labelling mouse islet α cells (401)
GIPR	Mouse islets: scRNAseq; moderate *Gipr* expression in α cells (188)	
ß cells		
GLP1R	Rat ß cell line (RRID:CVCL_W951): radiolabelled GLP1 localised to ß cells (185) Rat islet: mRNA detected in ß cells (454) Mouse islets: scRNAseq; moderate expression of *Glp1r* in ß cells (188,191,464) Mouse islets: *Glp1r* promoter active in ß cells (261) Rat islets: Western blot able to detect GLP1R in ß cells (454)	

	Rat islets: GLP1R anti-serum co-localised with ß cells (429) Mouse islets: fluorescent GLP1R antibody labelled majority of ß cells (261) Mouse islets: fluorescent GLP1R probe extensively labelled mouse islet ß cells (298,401)	
GIPR	Rat islets: mRNA detected in ß cells (454) Mouse islets: scRNAseq; *Gipr* expressed in ß cells (188,464)	
δ cells		
GLP1R	rat δ cell line (RRID:CVCL_U434): radiolabelled GLP1 localised to δ cells in (185) Rat islets: radiolabelled GLP1 co-localised with δ cells (187) Mouse islets: scRNAseq; moderate expression of *Glp1r* in δ cells (188,191,464) Mouse islets: *Glp1r* promoter active in δ cells (261) Mouse islets: fluorescent GLP1R antibody labelled small population of δ cells (261)	Rat islets: GLP1R anti-serum did not co-localise with δ cells (429) Mouse islets: no robust labelling of fluorescent GLP1R probe in δ cells (401)
GIPR	Mouse islets: scRNAseq; moderate *Gipr* expression in δ cells (188)	

Table 9: Summary of current literature that has investigated the presence of Glp1r/GLP1R and Gipr/GIPR in α, ß and δ cells in rodents.

Human islets	Evidence of presence	Evidence of absence
α cells		
GLP1R	Human pancreas sections: weak immunofluorescent GLP1R antibody labelling in α cells (456)	Human islets: scRNAseq; lack of *GLP1R* in α cells (190,455) Stem cell derived ß cells: Lack of co-localisation between fluorescent GLP1R probe labelling and INS-positive cells (298)
GIPR	Human islets: scRNAseq; *GIPR* expression found in α cells, at similar levels to β and δ cells (189,190,455).	
ß cells		
GLP1R	Human islets: scRNAseq; *GLP1R* detected in ß cells (192,449–452) Human pancreas sections: extensive immunofluorescent GLP1R antibody labelling in ß cells (456)	
GIPR	Human islets: scRNAseq; *GIPR* detected in ß cells (192,449–452) at similar levels to α and δ cells (189,190,455).	
δ cells		
GLP1R	Human pancreas sections: moderate non-fluorescent (463) and immunofluorescent (456) GLP1R antibody labelling in δ cells	Human islets: scRNAseq; minimal *GLP1R* expression in δ cells (190,455)
GIPR	Human islets: scRNAseq; *GIPR* expression found in δ cells, at similar levels to α and β cells (189,190,455).	

*Table 10: Summary of current literature that has investigated the presence of GLP1R/*GLP1R *and GIPR/*GIPR *in α, ß and δ cells in humans*

Intercellular islet interactions

With tirzepatide showing markedly superior glycaemic control than single GLP1R agonists in humans (243) and with further therapeutic dual and multi-agonists of incretins on the horizon (309,465–467), it is now imperative to confirm the cellular substrates that dual agonists bind to.

Delineating the target cells of dual agonists and determining the impact of dual agonism upon GLP1R/GIPR interactions will allow us to not only develop a deeper understanding of the superior glucose-lowering properties (i.e. is it islet-centric? Related to enhanced hormone secretion? By what mechanisms? What does this mean for how therapeutic GIPR antagonists act upon the islets?) but also to advance the understanding of how dual and multi-agonists might be engineered to gain the most therapeutic benefit. For example, discovering that tirzepatide is an imbalanced dual agonist preferentially binding to GIPR in humans (255), has allowed us to appreciate how different structural modifications and the resulting imbalanced, biased agonism can impact on ligand binding and affinity (256). Regarding enhanced glucose-lowering effects, it has since been shown that tirzepatide requires GIPR to trigger insulin release from islets and interestingly, can overcome the glucagon-inhibitory effect of GLP1, despite tirzepatide agonising GLP1R (412). Identifying the cellular targets of tirzepatide would help confirm if this might be central to tirzepatide's enhanced efficacy.

Beyond the effects of paracrine signalling (40,385,456,468–471), there is evidence that interactions between different subpopulations of cell types within the islet affects their function. The importance of cell-cell interactions is hinted at with the finding that most GLP1R+ α cells are found next to β cells (298). Furthermore, ß cells adjacent to α cells are more secretory and have earlier insulin release in response to hyperglycaemia than ß cells next to ß cells, due to pre-internalisation of GLP1R (401). Suggesting the importance of α-

β cell crosstalk in the incretin effect, alanine is unable to potentiate GIP-mediated insulin release when GIPR is specifically delated from α cells (472). This implies that GIP-mediated insulin release from β cells is reliant upon engaging α cells.

Furthermore, GLP1R has been found to engage a subnetwork of β cells which induces highly co-ordinated cell activation (204). However, not all β cells are engaged equally, with 3 different subpopulations recruiting GLP1R at different speeds and different GLP1R agonists stimulating the subpopulations to different degrees (269). Being able to localise dual agonists to these different subpopulations of cells is vital to fully exploring their effects.

Chapter aim

Therefore, in this chapter we aim to provide the cellular substrates that could explain the increased glucose-lowering efficacy of tirzepatide to determine if the mechanisms of superior glycaemic control are islet-centric.

We utilised the daLUXendins to confirm which cells dual agonists bind to within the pancreatic islet and explore how they might affect GLP1R-GIPR interactions by optimising the probe for single molecule imaging techniques.

Results

daLUXendin and daLUXendin+ probes label all islet cell types

To determine dual agonist cell targets in pancreatic islets, isolated islets were labelled with daLUXendin probes and co-stained with antibodies for the hormones secreted by the major cell types; insulin (β cells), glucagon (α cells) and somatostatin (δ cells). As these antibodies require tissue fixation prior to application, we first confirmed that daLUXendin labelling remains intact after fixation with 2% or 4% formaldehyde (Figure 40).

`

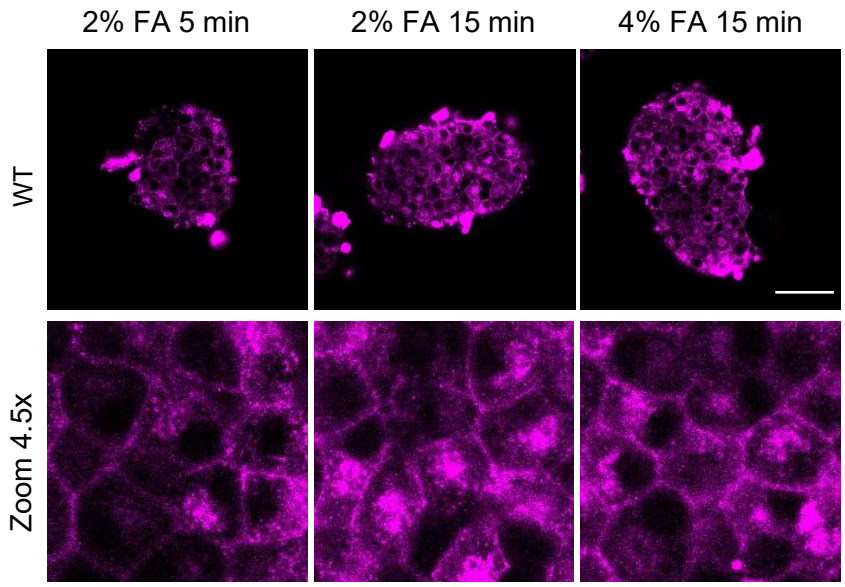

Figure 40: daLUXendin in fixed WT islets.
Representative images of WT islets labelled with daLUXendin544 prior to fixation in different concentrations and durations of paraformaldehyde. Zoom panels show retained membrane and intracellular labelling. Scale bar 53μm.

Following this, islets were co-stained with insulin (INS), glucagon (GCG) and somatostatin (SST) antibodies and secondary antibodies of orthogonal fluorescence. daLUXendin544/660 labeled all major cell types in the islet (Figure 41, Figure 42). The strongest labelling was in in INS+ cells, followed by GCG+ cells and then SST+ cells, as quantified in Figure 43.

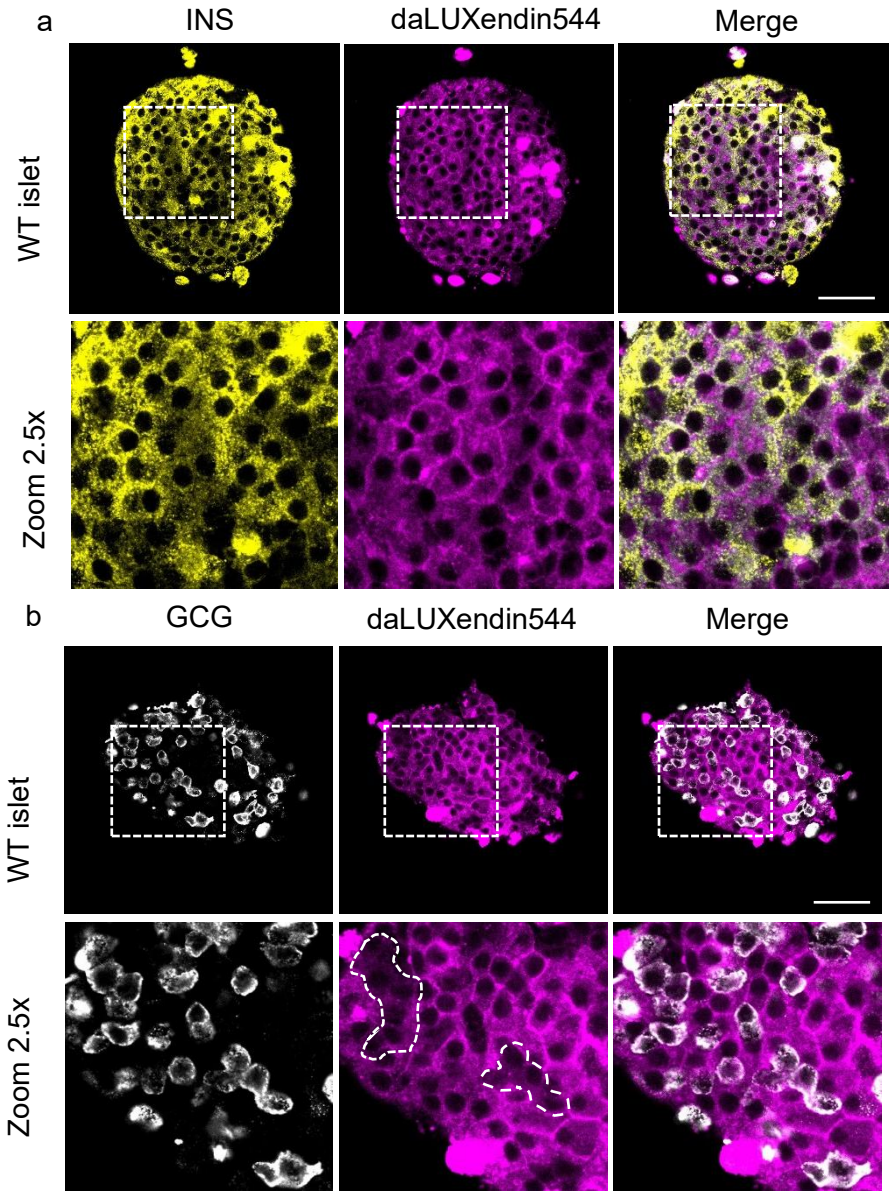
a
INS
daLUXendin544
Merge
WT islet
Zoom 2.5x
b
GCG
daLUXendin544
Merge
WT islet
Zoom 2.5x

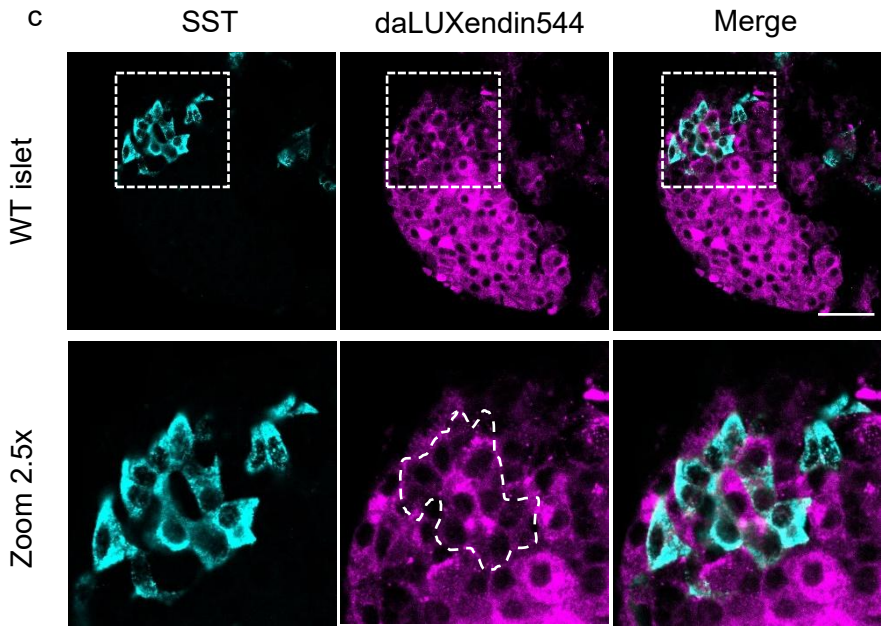

Figure 41: daLUXendin660 in fixed WT islets with immunohistochemistry for INS/GCG/SST
Representative images of WT islets labelled with daLUXendin544 prior to fixation and immunohistochemical staining of INS (a), GCG (b) and SST (c). 2.5x zoom panels highlight areas of high density for that cell type and demonstrate the daLUXendin544 labelling. Scale bar 53µm.

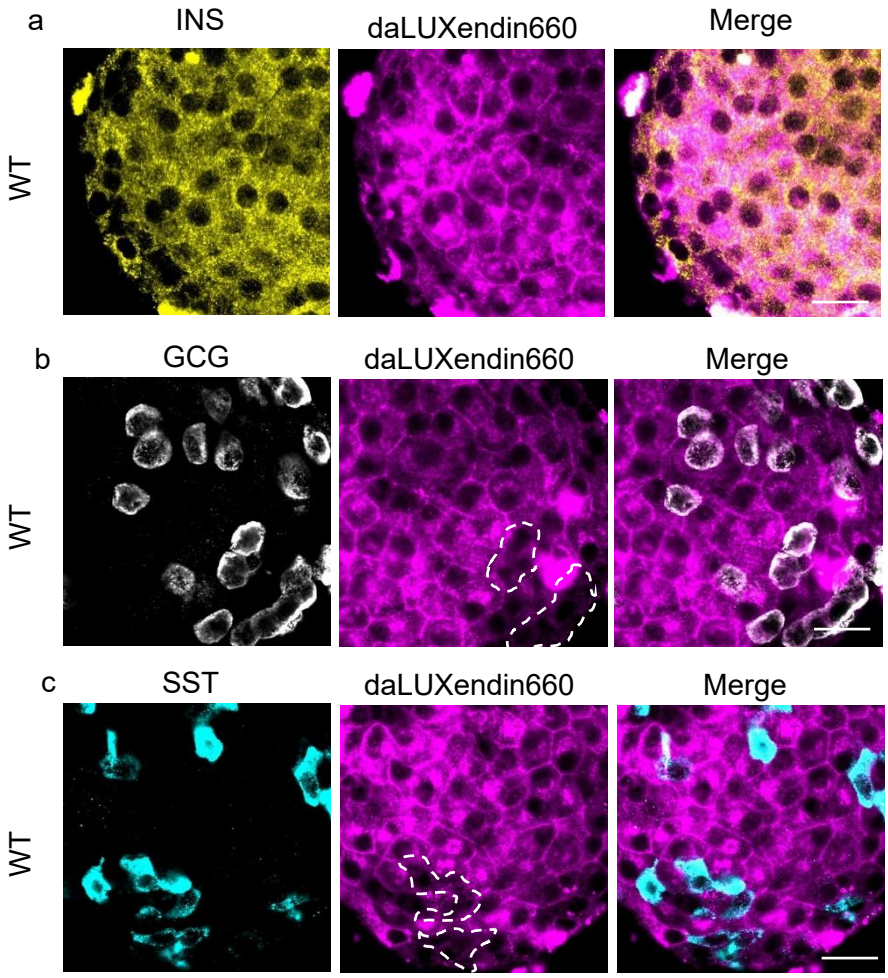

Figure 42: daLUXendin660 in fixed WT islets with immunohistochemistry for INS/GCG/SST. Representative images of WT islets labelled with daLUXendin660 prior to fixation and staining with primary antibodies for INS (a), GCG (b) and SST (c). Scale bar 21.2µm

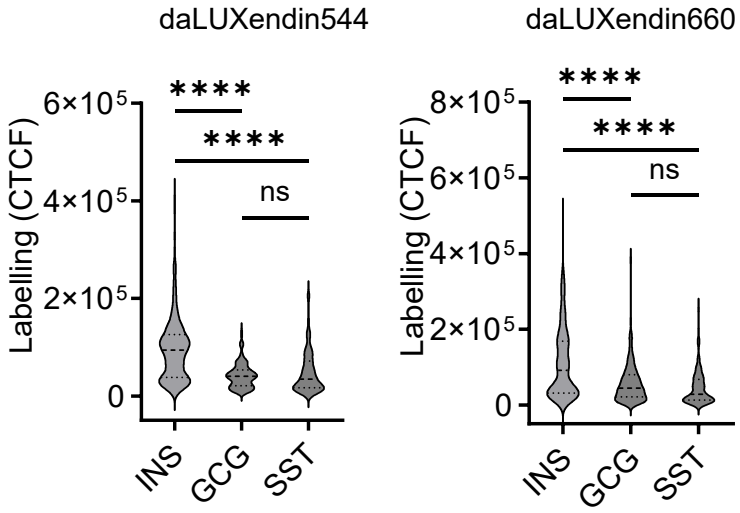

Figure 43: CTCF values of daLUXendin544 and daLUXendin660 in cells staining positive for INS/GCG/SST. Kruskal-Wallis comparative analysis of significance; α 0.05, daLUXendin544 INS vs GCG p <0.001, INS vs SST p<0.001, GCG vs SST p>0.9999; daLUXendin660 INS vs GCG p <0.001, INS vs SST p<0.001, GCG vs SST p0.0564. Violin plots show median and interquartile ranges. (INS = 44 islets from 5 mice; GCG = 25 islets, 7 mice; SST 29 islets, 7 mice)

Repeating the experiment with the acylated daLUXendin660+, there was a similar pattern of labelling. daLUXendin660+ labelled all major cell types within the islets, again with the brightest labelling of INS+ cells, followed by GCG+ then SST+ cells (Figure 44, Figure 45). This demonstrates that the inclusion of the diacid side chain does not alter cellular substrates targeted by daLUXendins.

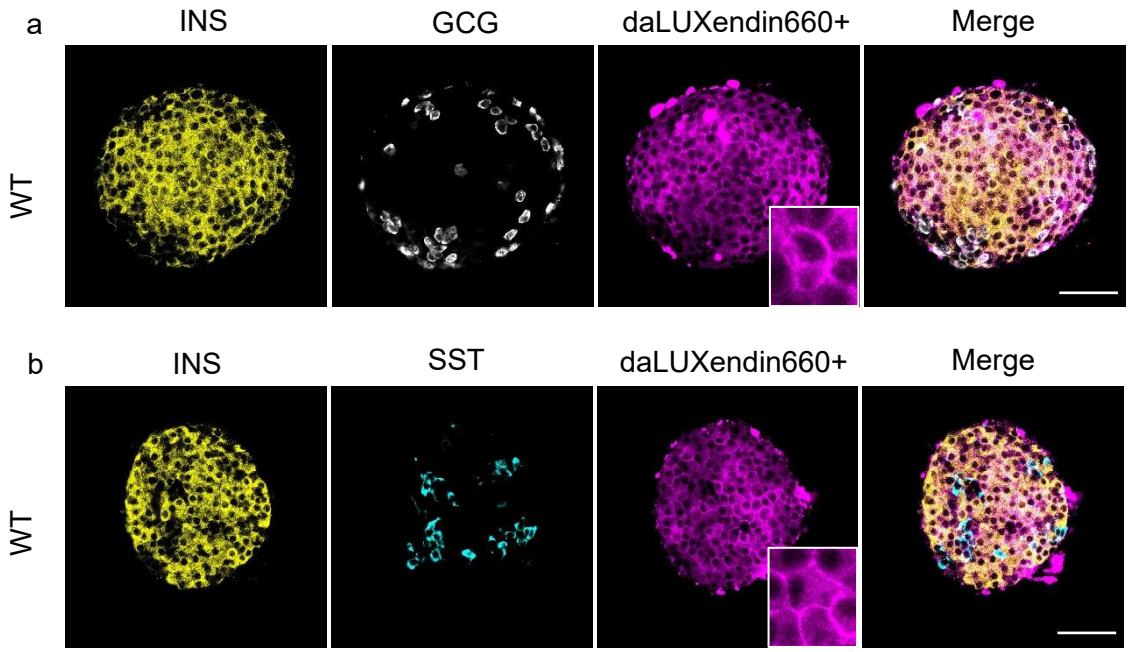

Figure 44: daLUXendin660+ in fixed WT islets with immunohistochemistry for INS/GCG/SST. Representative images of WT islets labelled with daLUXendin660+ prior to fixation and staining with primary antibodies for INS, GCG (a) and SST (b). Scale bar 53µm.

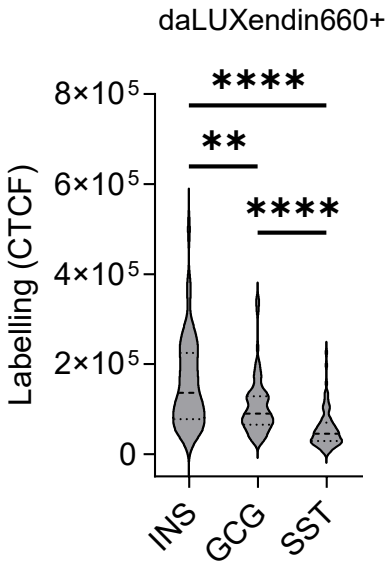

Figure 45: CTCF values of daLUXendin660+ in cells positively stained for insulin (INS), glucagon (GCG) and somatostatin (SST).
Kruskal-Wallis comparative analysis of significance; α 0.05, INS vs GCG p0.0020, INS vs SST p<0.0001, GCG vs SST p<0.0001. Violin plots show median and interquartile ranges. (INS = 34 islets from 4 mice; GCG = 17 islets from 3 mice; SST = 17 islets from 3 mice)

Mirroring these results, daLUXendin544/660 co-localised with GLP1R antibody with further, reduced labelling of GLP1R- cells, consistent with labelling α and δ cells (Figure 46).

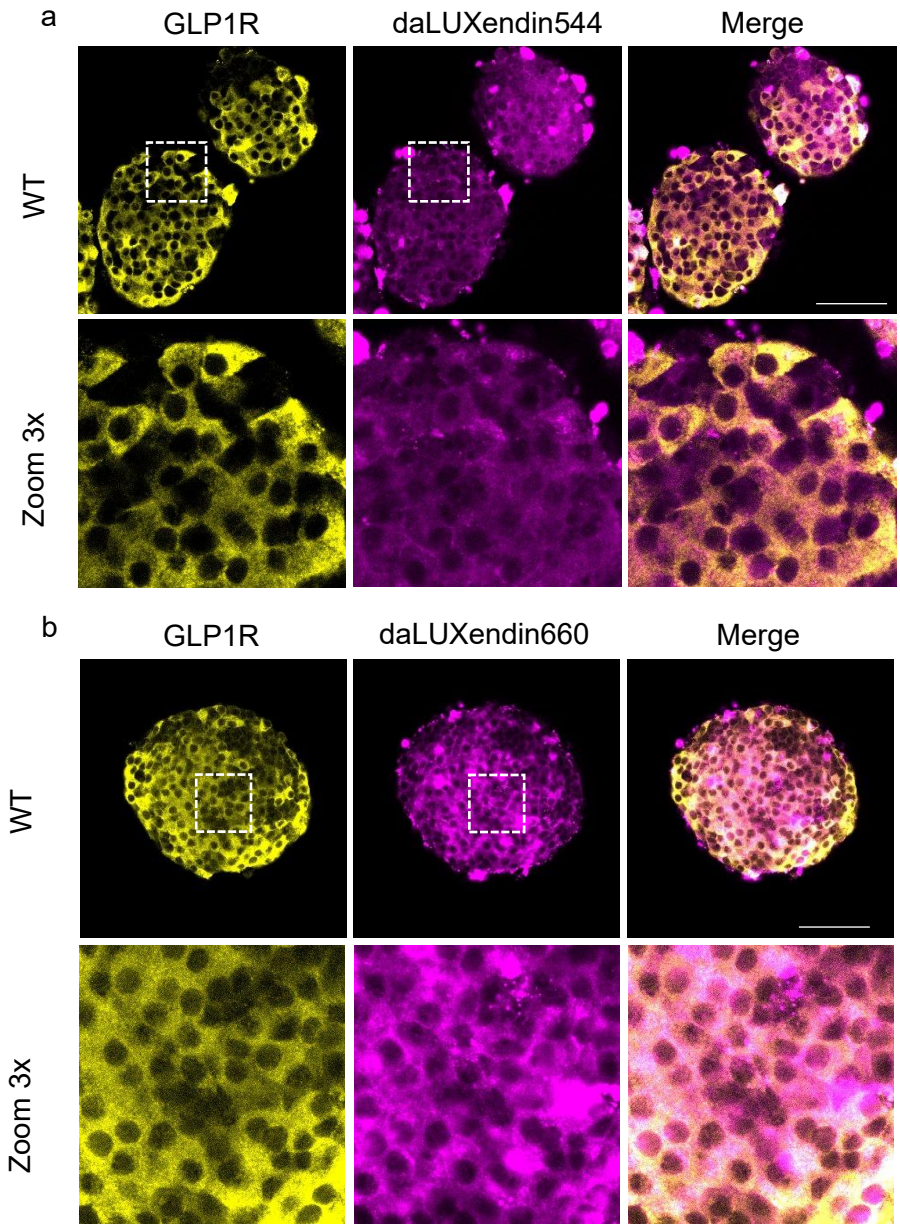

Figure 46: daLUXendin labelling in fixed WT islets and immunohistochemistry for GLP1R.
WT islets labelled with daLUXendin544 (a) or daLUXendin660 (b) prior to fixation and staining with primary GLP1R antibody. Scale bar = 53µm.

daLUXendin is unable to specifically label human islets

Being able to identify the cells that dual agonist target in human tissue would be the next piece of the puzzle to full leverage their benefits clinically. Thus, we next assessed daLUXendin labelling in human donor islets. Unfortunately, in both live and fixed human islets daLUXendin labelling was similar to vehicle due to significant autofluorescence (Figure 47).

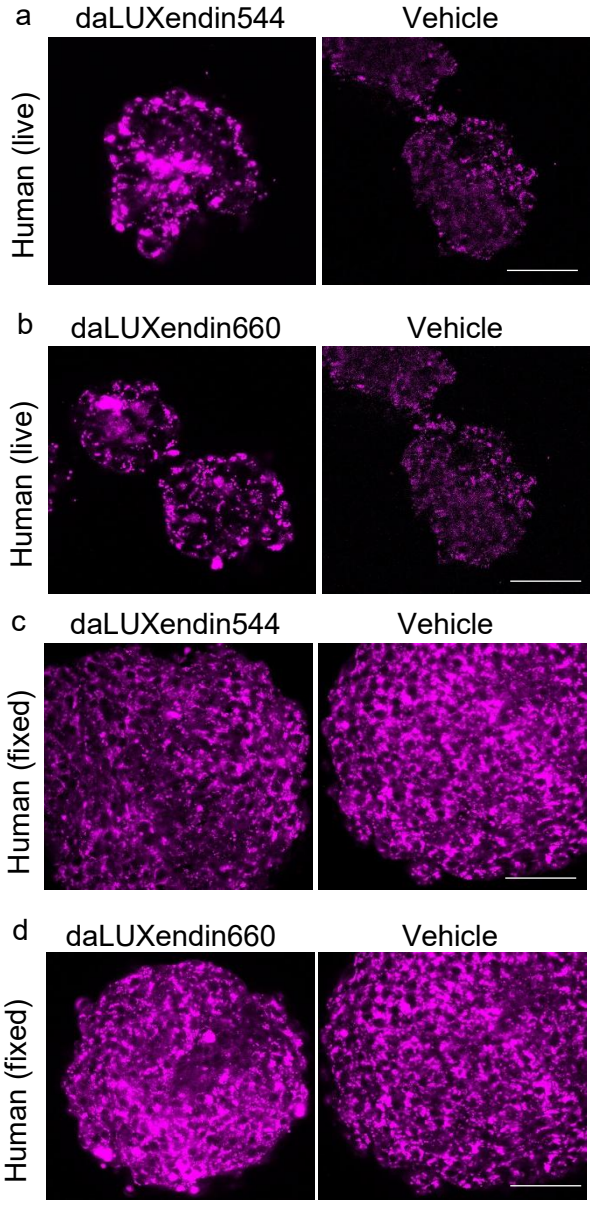

Figure 47: daLUXendin in fixed human islets
Representative images of live (a,b) and fixed (c,d) human islets labelled with daLUXendin542 (a,c) or daLUXendin660 (b,d) Significant autofluorescence is noted in corresponding vehicle-treated islets (live = 4 donors, fixed = 2 donors). Scale bar 53µm.

In case phenol red in the CMRL media could have contributed to the interfering fluorescence (473,474) and masked the signal from the daLUXendin probes, the live imaging was repeated with daLUXendin probes diluted in colourless 2.7mM glucose ATP buffer. There was no major difference between the fluorescence of each solvent (Figure 48).

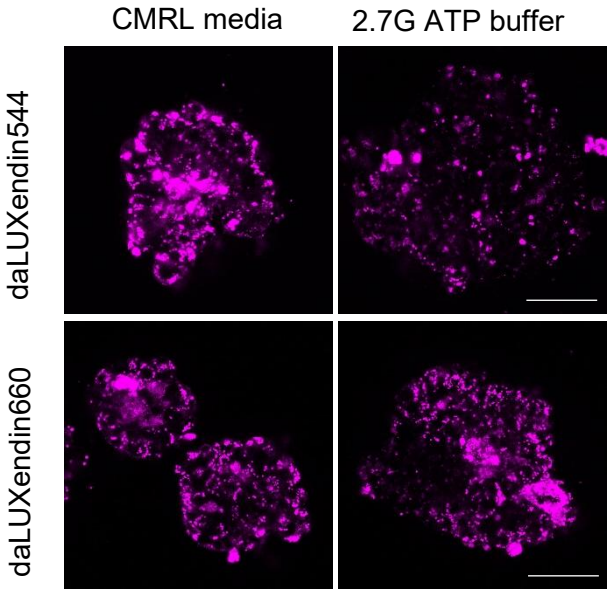

Figure 48: daLUXendin in fixed human islets in different diluents.
Representative images of human donor islets labelled with daLUXendin544/660 diiluted in either complete human islet media (CMRL) or 2.7mM glucose ATP buffer. (n = 1 donor). Scale bar = 53µm.

In an attempt to reduce the autofluorescence from the causative cellular substrates in human islets, such as lipofuscin (475), islets were labelled with daLUXendin544 then fixed and treated with TrueBlack®. TrueBlack® is a lipofuscin quencher which has been shown to reduce autofluorescence in a range of human and non-human tissues (476). There was no major improvement of daLUXendin544 fluorescence with TrueBlack® (Figure 49).

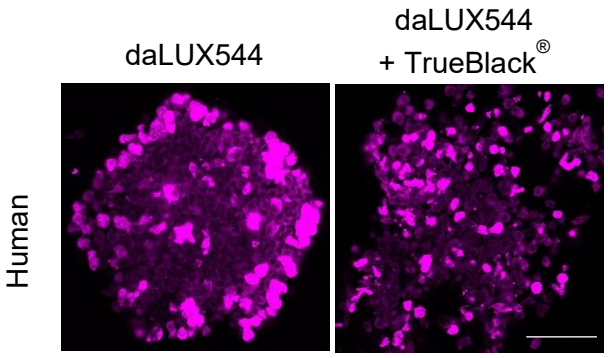

Figure 49: daLUXendin in fixed human islets with TrueBlack®
Representative images of human donor islets labelled with daLUXendin544 prior to fixation with and without incubation with TrueBlack® (n=1 donor). Scale bar = 53µm.

Aldehyde fixation can also contribute to increase autofluorescence of cells (477,478) as excessive aldehyde reacts with amines in proteins to generate fluorescent products. However, this is more marked with glutaraldehyde rather than the PFA (479) used in my protocol and given the high degree of autofluorescence in live vehicle-treated islets, fixation was unlikely to be the cause.

Whilst we recognised the translational importance of interrogating dual GLP1R/GIPR agonist targets in human tissue, particularly in the incretin-relevant setting of islets, human islets preparations were not a viable option for daLUXendin labelling. Our lab has found significant variability in GLP1R/GIPR protein expression in a human islets and pancreatic sections, with weaker and sometimes completely absent GLP1R expression using both antibodies and GLP1R-specific probes (LUXendins) (401). We attributed this to heterogeneity in GLP1R expression levels, heterogeneity in donors, as well as the impact of processing and islet isolation that can lead to a decline in GLP1R expression, as noted by others (480). Furthermore, there is heterogeneity of incretin- and glucose-stimulated insulin release between human islet preparations (481,482) which is further compounded with variation in viability arising from preparation (483) and different HbA1c in different donors (484). Given the many variables that can lead to heterogeneity of islet function

between donors, we felt that human islet preparations a less reliable setting to explore fluorescent dual agonist action.

daLUXendin labels human iPSC-derived islet structures

To circumvent the issues with autofluorescence and other potential issues with human islets, we turned to human induced pluripotent stem cell (iPSC)-derived islet-like structures (SC-islets). SC-islets are being developed as a potentially curative therapy for type 1 diabetes, with Time in Target Range 98% at one year post-transplantation (485), as well as a robust diabetes model for research (486–488). The benefit of transplanting stem-cell derived islets include the ability to reduce their immunogenicity (487) and removing the reliance upon the unpredictability of donor availability.

We reviewed scRNA-seq data of SC-islets (189) and, similar to the expression of *Glp1r/GLP1R* and *Gipr/GIPR* in mice and humans, found *GLP1R* and *GIPR* in early and late β- and δ-like cells and additionally *GIPR* in late α cells (Figure 50). This has been supported with protein labelling using GLP1R-specific fluorescent antagonist probe, LUXendin645, in mature SC-islets which found extensive GLP1R labelling of insulin-positive cells and little co-localisation with glucagon-positive cells (Figure 51) (298).

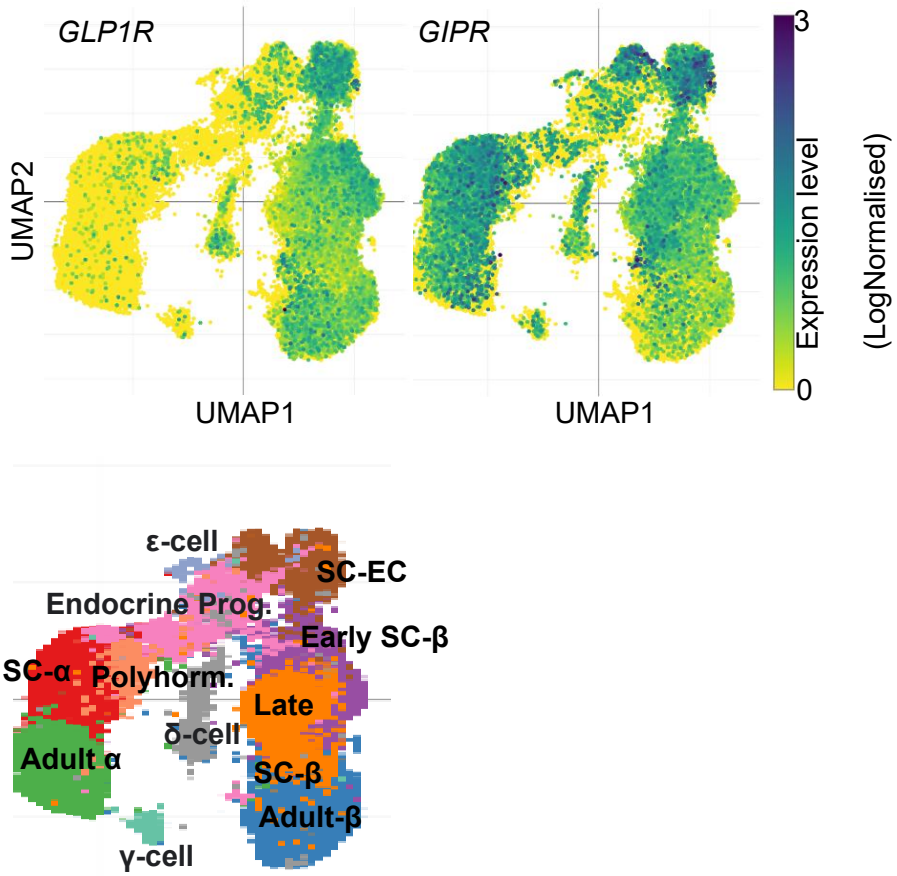

Figure 50: Uniform manifold approximation and projection (UMAP) plots showing GLP1R and GIPR expression in early and late SC-islet endocrine cell populations.
Reproduced from (189), and plotted using Single Cell Portal (707), study SCP1526).

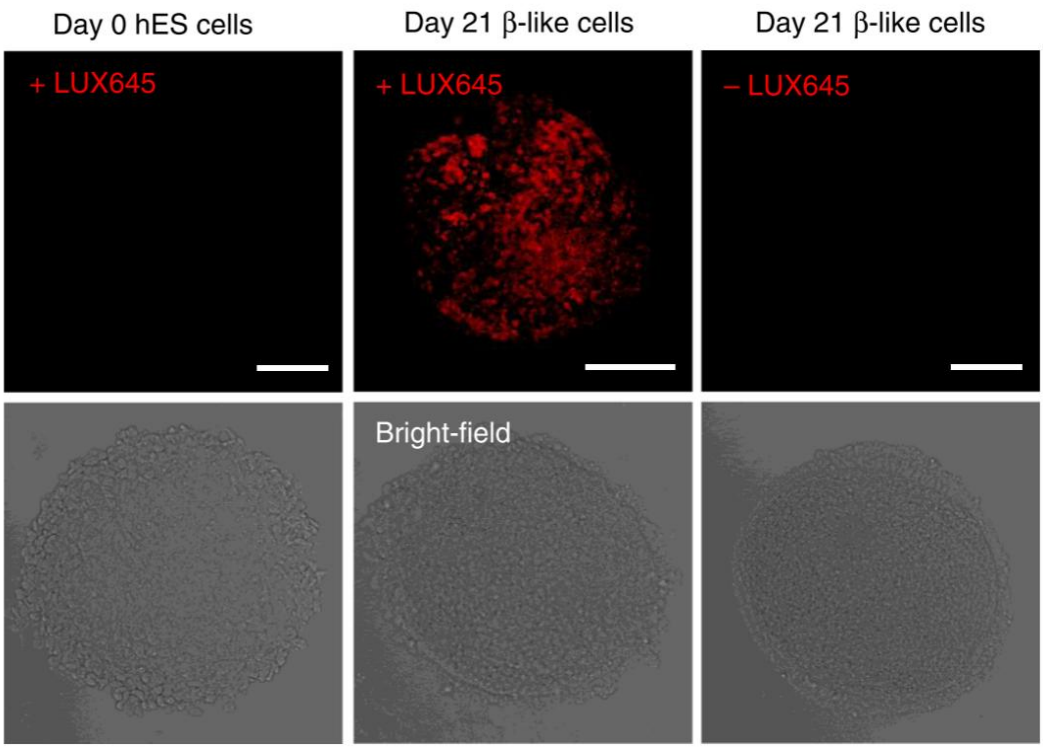

Figure 51: Embryonic stem cell-derived ß-like cells labelled with LUXendin645.
Extensive labelling found with LUXendin645 (GLP1R antagonist probe) in Day 21 differentiated mature ß-like cells but no labelling in Day 0 undifferentiated cells. No fluorescence was observed in unlabelled Day 21 differentiated cells. Scale bar = 100µm.

Both daLUXendin544 and daLUXendin660 labelled membrane and cytoplasm and cells in SC-islets (Figure 52). For vehicle-treated SC-islets, more autofluorescence was visible following excitation with the 561nm laser (used for daLUXendin544) (Figure 52). Following co-staining with antibodies, daLUXendin660 labelled INS-, GCG- and SST-positive cell populations in SC-islets (Figure 53). Mirroring results in mouse islets, labelling intensity was greatest in INS-positive cells and similar, reduced labelling of GCG- and SST positive cells (Figure 54).

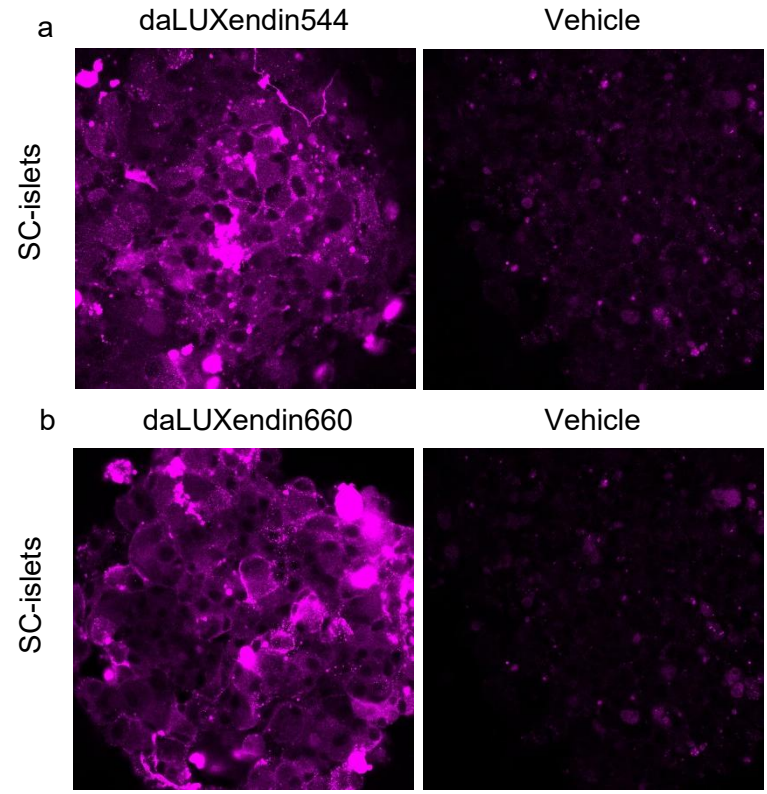

Figure 52: daLUXendin in fixed SC-islets.
Human induced pluripotent stem cell derived islet structures (SC-islets) labelled with daLUXendin544 (a), daLUXendin660 (b) or vehicle prior to paraformaldehyde fixation.
Vehicle images taken using same settings as respective daLUXendin probe.

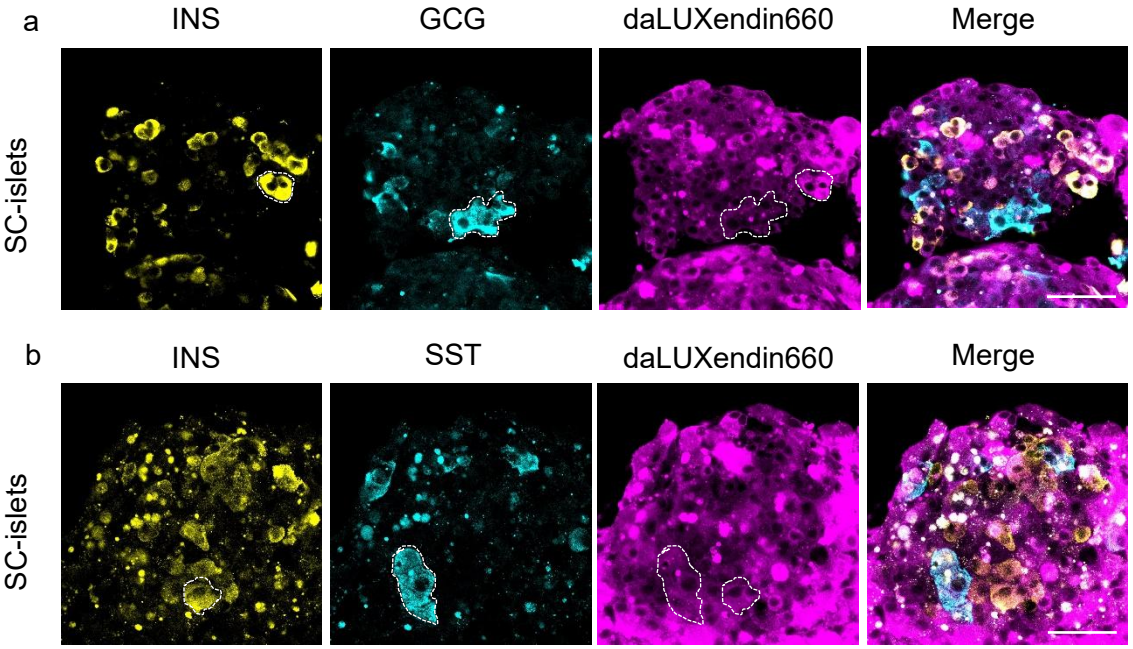

Figure 53: daLUXendin in fixed SC-islets with immunohistochemistry for INS/GCG/SST.
Representative images of SC-islets labelled with daLUXendin prior to fixation and labelling with primary antibodies for insulin (a,b), glucagon (a) and somatostatin (b).
Scale bar 53µm.

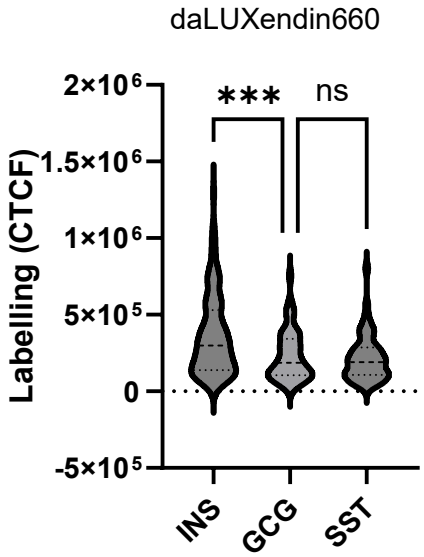

Figure 54: Violin plot of min/max/median CTCF values of daLUXendin660 in cells positive for INS, GCG and SST.
Violin plots show median and interquartile ranges. Significance calculated with Šídák's multiple comparisons test. (n = 2 differentiations; INS = 115 cells; GCG = 55 cells; SST = 60 cells).

daLUXendin660 is suitable for single-molecule, super-resolution imaging and engages GLP1R/GIPR nanodomains

GPCR signalling is rapid (489) and one of the mechanisms proposed to explain this speed is the formation of signalling clusters of GPCRs and effectors at the plasma membrane and intracellular compartments (275,490) via lipid rafts (491). Such clusters, or nanodomains, have been shown to play a role in the co-ordination of GPCR signalling and endocytosis (492). The formation of nanodomains has been confirmed for GLP1R (269,298) , with disruption of nanodomain recruitment (through lipid sequestration) leading to faster agonist dissociation, reduced GLP1R clustering andreduced cAMP generation (275). Clustering of GIPR has been less studied but has been shown to occur to a higher degree than GLP1R and is functionally important, as GIPR endocytosis is unable to occur when the formation of nanodomains is disrupted (275).

The impact of single agonism has been investigated, with agonism increasing GLP1R clustering (275,493) but not GIPR clustering (275). GLP1R agonism has also been shown to arrest GLP1R clusters at the membrane and suspend their diffusion across the plasma membrane (269). However, the impact of dual GLP1R/GIPR agonism upon clustering in primary tissue is yet to be interrogated.

We first applied LUXendin645 to bind to, but not activate, GLP1R in fixed mouse pancreatic islets. dSTORM imaging confirmed previous findings (269,298) of GLP1R clustering in discrete nanodomains, defined by the DBSCAN clustering algorithm (307), at the cell membrane in the unstimulated state (Figure 55, Figure 56).

The application of sGIP648, a GIPR agonist, also revealed nanodomains (Figure 55, Figure 56). There was a higher number of nanodomains with sGIP648 in comparison with LUX645 (Figure 57a) which could reflect both the increased number of GIPR across more cell types than GLP1R (α-, δ- and β cells vs β cells respectively) and the previous finding of GIPR forming more nanodomains than GLP1R (275).

daLUXendin660 demonstrated suitability for single-molecule, super resolution dSTORM imaging and was able to label receptors (Figure 55, Figure 56). Further, daLUXendin660 engaged the most nanodomains (Figure 57a), likely reflecting the increased number of receptors amenable to engagement by a dual agonist. To determine if dual agonism changes the configuration of the nanodomains, we assessed the number of receptors (localisations) per cluster and the density of clusters bound by each ligand. Whilst daLUXendin660 engaged a higher number of nanodomains than LUXendin645 and sGIP648, there was no difference in the number of localisations per cluster or the cluster density (Figure 57b and c). These data suggest that daLUXendin660 engages both GLP1R and GIPR into clustering and/or increases interactions between GLP1R and GIPR.

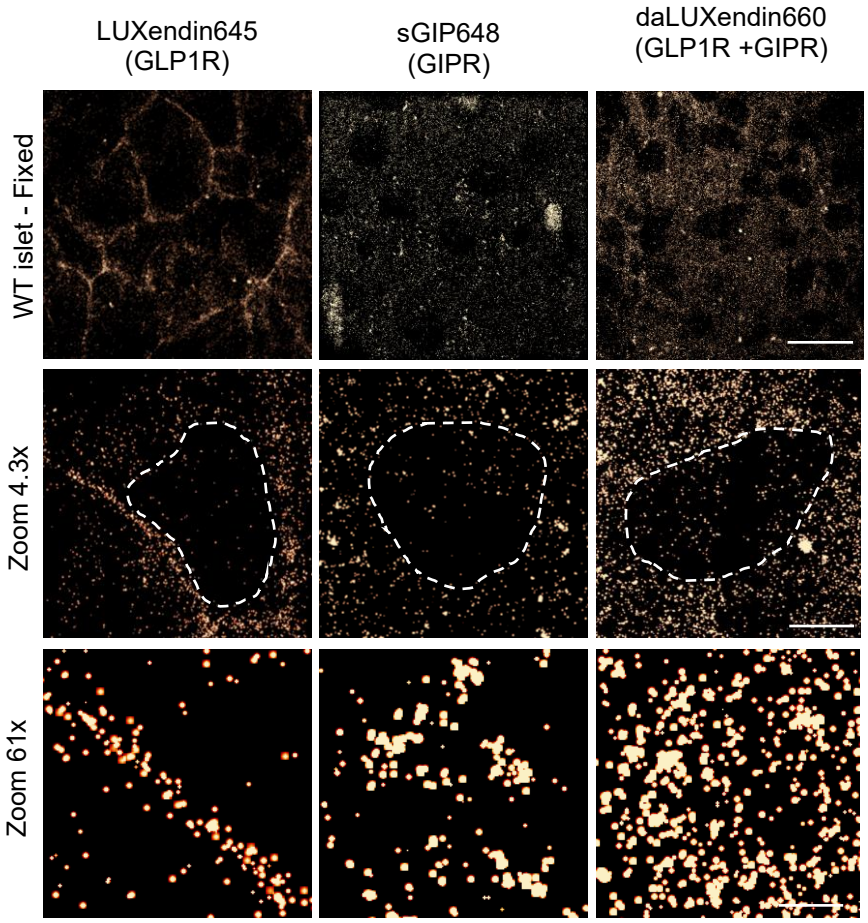

Figure 55: Representative dSTORM images of single molecule densities in fixed WT mouse islets labelled with GLP1R antagonist probe LUXendin645, GIPR agonist probe sGIP648 or daLUXendin660.
Dotted boundary delineates cell nucleus. Scale bars: top panel 11µm; zoom 4.3x 2.6µm; zoom 61x 180nm.

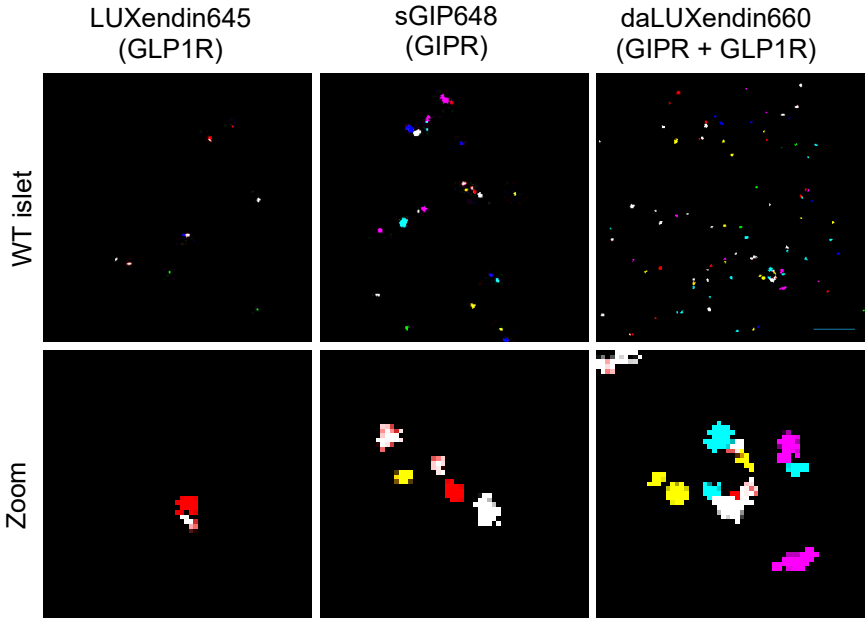

Figure 56: Representative DB scan images of clusters of receptors in fixed WT islets labelled with LUXendin645, sGIP648 or daLUXendin660.
Each coloured shape represents a distinct cluster of receptors. Zoom panels highlight increasing number of labelled clusters. Scale bar 360nm.

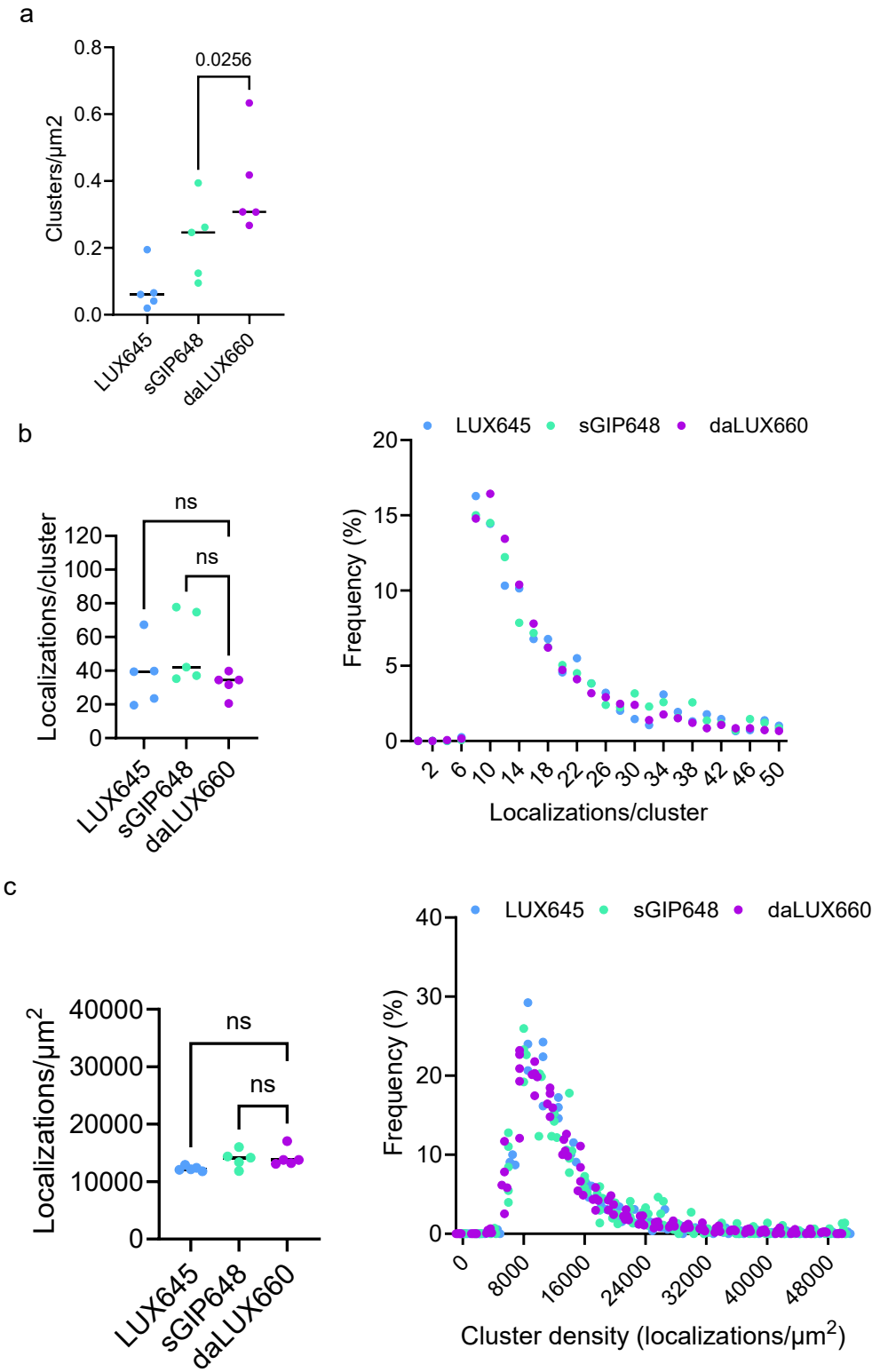

Figure 57: Quantification of dSTORM clusters labelled by LUXendin645, sGIP648 and daLUXendin660. (a) Number of clusters labelled by each probe (one-way ANOVA with two-stage linear step-up procedure of Benjamini, Krieger and Yekutieli); (b) mean and distribution of localisation per cluster for each probe (one-way ANOVA with Šídák's multiple comparisons test) and; (c) mean and distribution of cluster density for each probe(one-way ANOVA with Šídák's multiple comparisons test) (n = 5 islets pooled from 3 mice).

To further demonstrate the versatility of daLUXendin660, we next labelled MIN6-CB1 cells and undertook TIRF microscopy, a technique useful for single-particle tracking at the cell membrane (494,495). daLUXendin660 labelling was detected using TIRF microscopy and permitted visualisation of receptor movement (Figure 58).

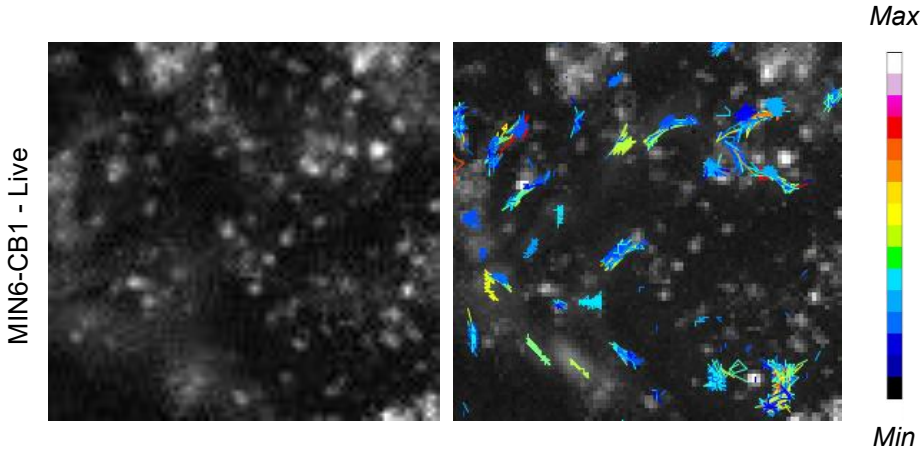

Figure 58: daLUXendin TIRF imaging.
Representative images of receptors labelled by daLUXendin660 in MIN6-CB1 cells and live imaged using TIRF microscopy. Trajectories are shown as minimum-maximum displacement.
(n = 5 cells, 2 independent repeats).

For super-resolution live imaging techniques such as stimulated emission depletion (STED) microscopy, fluorophores need to have a degree of stability and a compatible emission wavelength (496). Therefore, we created daLUXendin651-d12 by replacing the Cy5 fluorophore of daLUXendin660 with fluorogenic deuterated silicon rhodamine (SiR-d12) to improve brightness (497) (Figure 59).

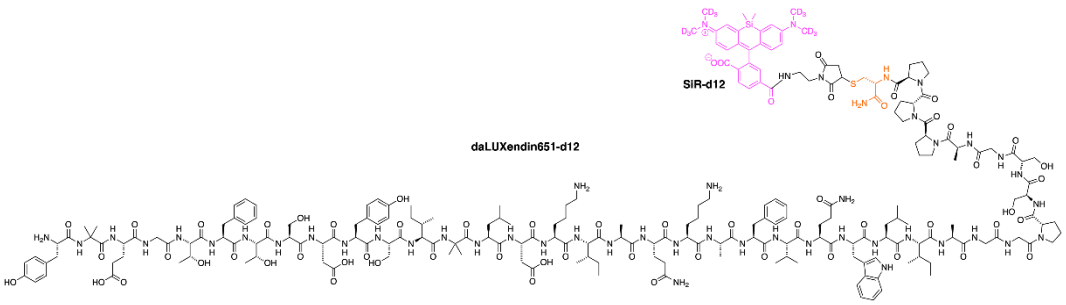

Figure 59: Structure of daLUXendin651-d12.
A variant of daLUXendin660 optimised for STED imaging by exchanging the Cy5 fluorophore for SiR-d12.

With STED microscopy, daLUXendin651-d12 labelling was too dim with endogenous receptor but was sufficient in an overexpression system - CHO-K1:SNAP-GLP1R:Halo-GIPR cells.

daLUXendin651-d12 was applied alongside a SNAP label (BG-Sulfo549) and Halo-label (CA-AF488) and was able to co-localise with GLP1R below the diffraction limit in widefield imaging (Figure 60a) and retained stable STED labelling across multiple frames (Figure 61). In CHO-K1:SNAP-GLP1R cells, daLUXendin651-d12 only co-localised with GLP1R and there was no further labelling from daLUXendin651-d12 or the Halo label in this absence of GIPR (Figure 60b).

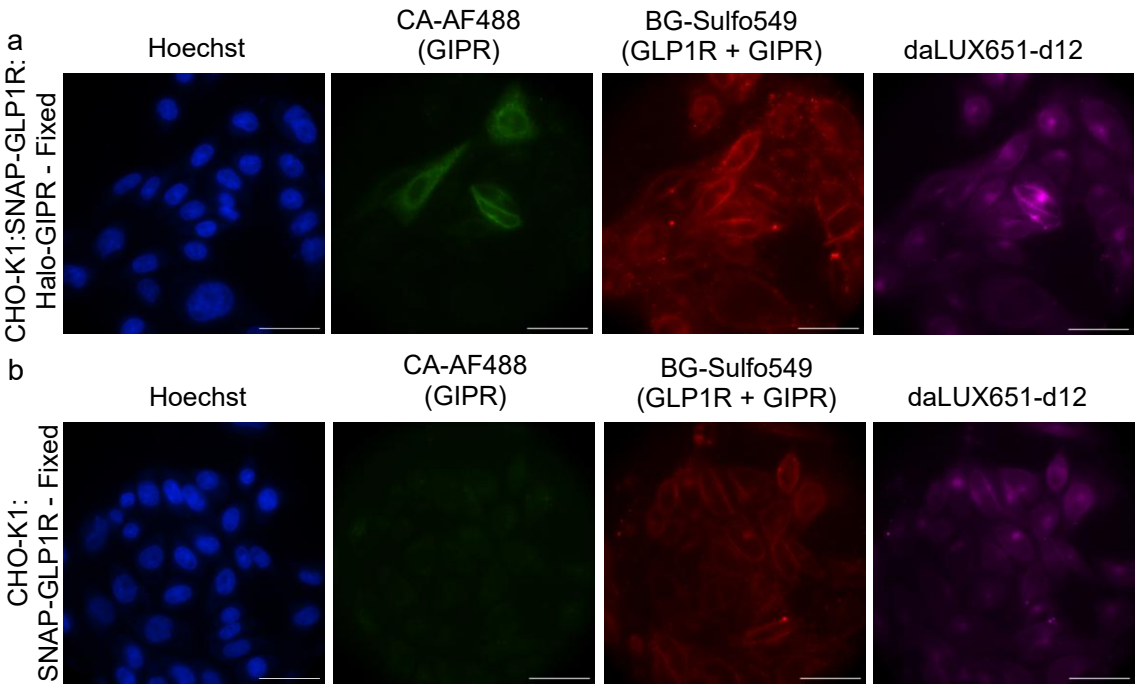

Figure 60: daLUXendin651-d12 widefield images
Representative widefield images of (a) fixed CHO-K1_SNAP-GLP1R:Halo-GIPR cells labelled with Hoechst, Halo-GIPR label (CA-AF488), SNAP-GLP1R label (BG-Sulfo549) and daLUXendin651-d12.
Images demonstrate co-localisation of daLUXendin651-d12 with GLPR and GIPR labels. (b) as for (a) but in CHO-K1:SNAP-GLP1R cells, showing no labeling with Halo label and co-localisation of daLUXendin651-d12 with GLP1R only. (n = 3) Scale bar 40μm.

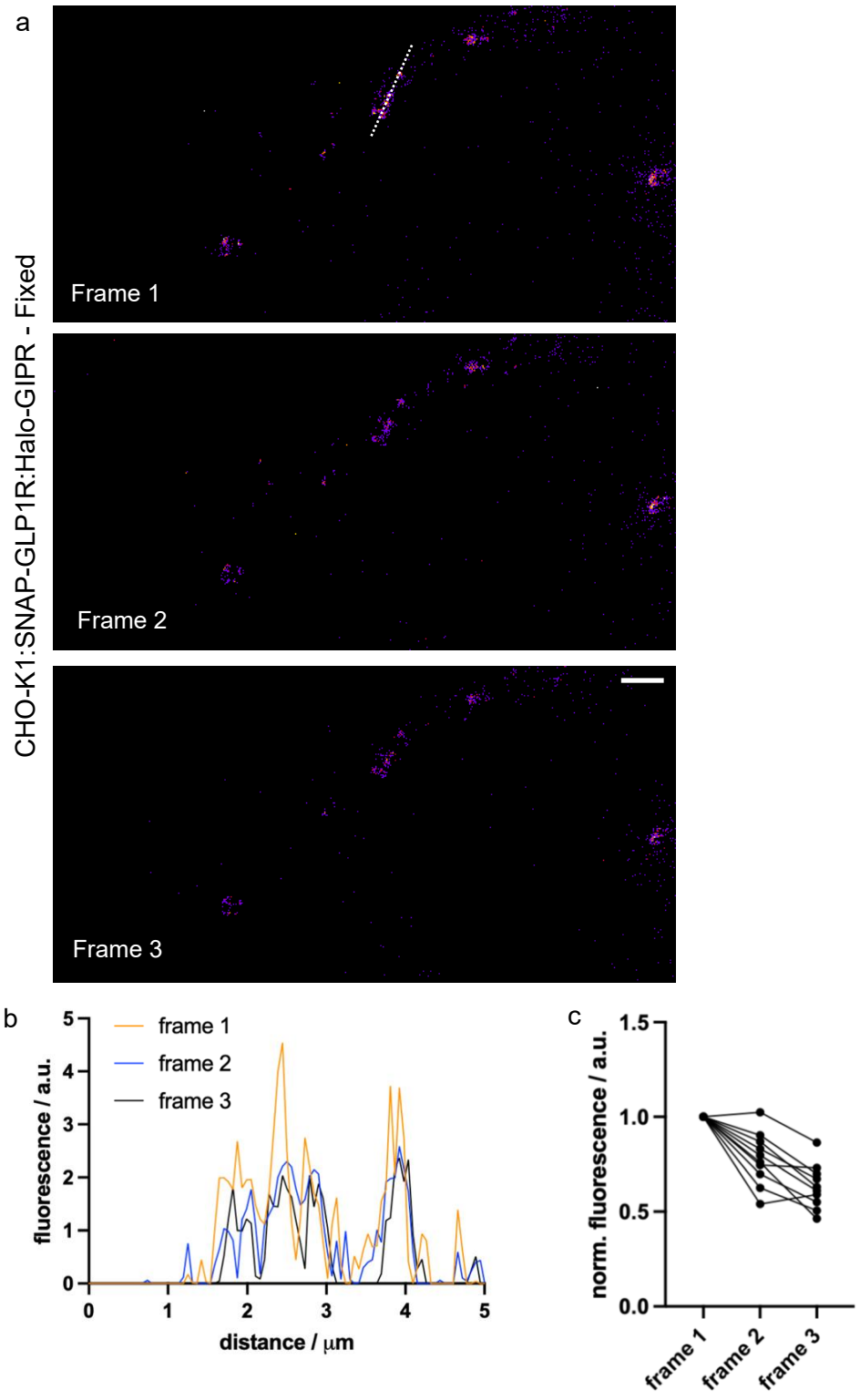

Figure 61: daLUXendin651-d12 STED imaging 1.
(a) representative images of stable daLUXendin651-d12 labelling in fixed CHO-K1:SNAP-GLP1R:Halo-GIPR cells across three STED frames with ROI for line scan. (b) average line scan of daLUXendin651-d12 fluorescence showing reduced but stable fluorescence in ROI across frames. (c) average fluorescence of ROIs normalised against average fluorescence in frame 1, showing reducing but ongoing signal of ROI across frames. (n = 3 repeats, n = 10 ROIs) Scale bar 2μm.

Direct application of daLUXendin651-d12 to CHO-K1:SNAP-GLP1R:Halo-GIPR cells resulted in rapid visualisation at the cell membrane (10 seconds), co-localising with SNAP-GLP1R and Halo-GIPR labels (Figure 62). Full width half-maximum of cell membrane fluorescence was reduced with STED compared to confocal imaging, demonstrating the improvement of resolution with STED (Figure 63).

These results demonstrate an effective choice in alternative fluorophore for STED imaging and following such optimisation, daLUXendin has visualised GLP1R and GIPR in live and fixed tissue in the super-resolution setting.

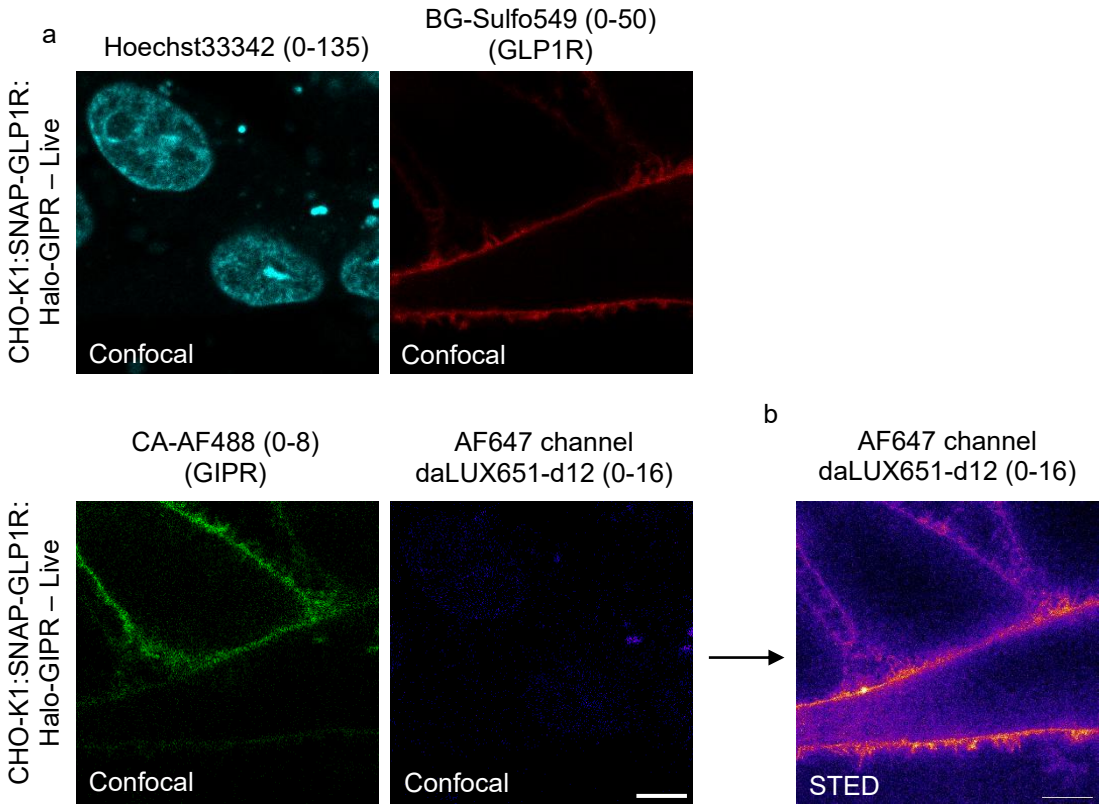

Figure 62: daLUXendin651-d12 STED imaging 2.
Representative images of (a) confocal images of GLP1R, GIPR and daLUXendin651-d12 labelling of CHO-K1:SNAP-GLP1R:Halo-GIPR cells followed by (b) application of 500nM daLUXendin651-d12 for 10 seconds and STED imaging. Scale bar 5μm.

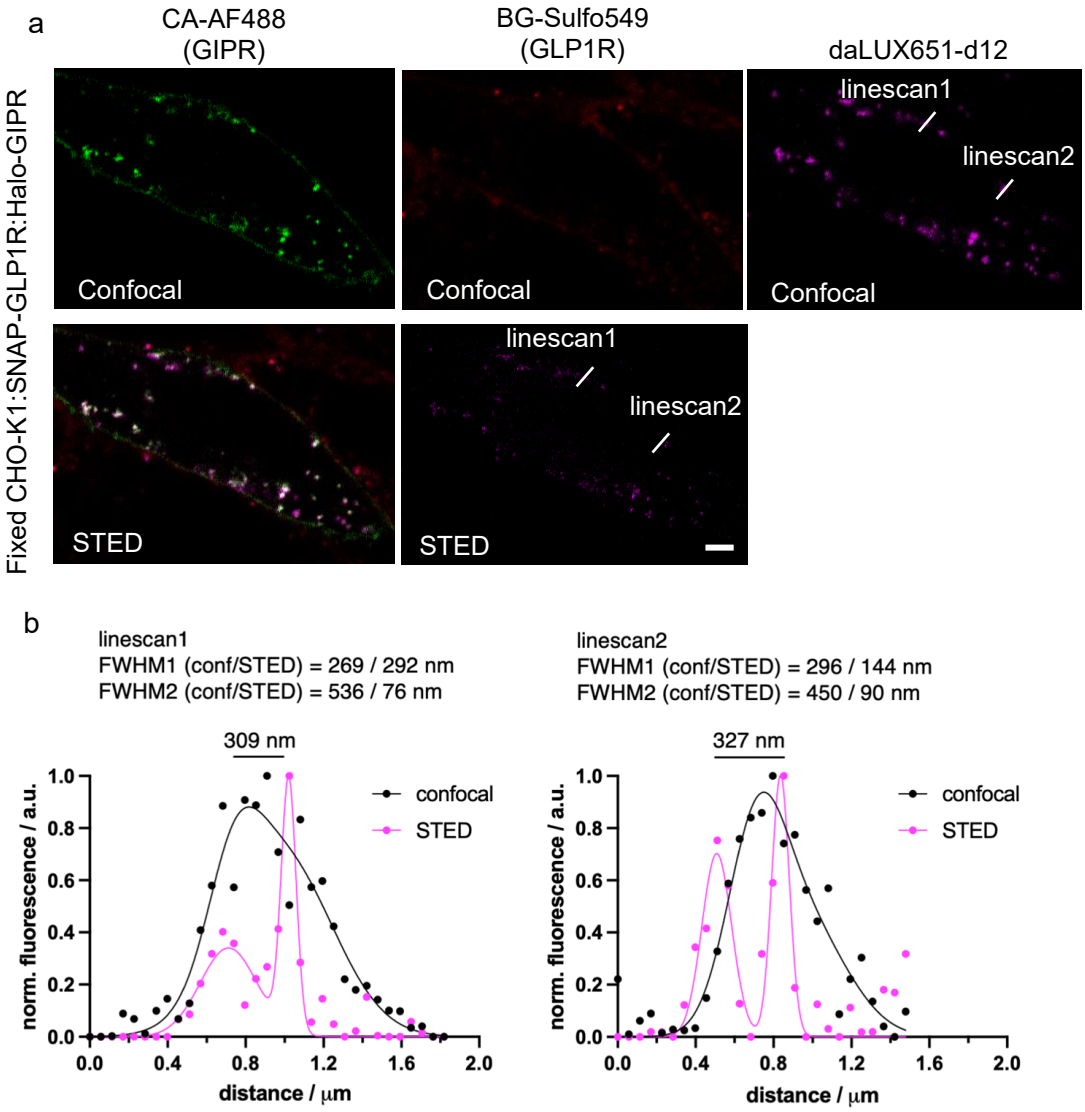

Figure 63: dalUXendin651-d12 STED imaging line scan.
(a) representative confocal and STED images of CHO-K1:SNAP-GLP1R:Halo-GIPR cells labelled with Halo label (CA-AF488), SNAP label (BG-Sulfo549) and daLUXendin651-d12 with ROI linescans. (b) fluorescence across linescans was measured and plotted and full width half-maximal was calculated for both peaks of STED fluorescence and then for confocal across the same distances along the linescan. (n = 8) Scale bar 2µm.

Discussion:

This chapter presents how daLUXendin probes have begun to delineate the cell targets of dual GLP1R/GIPR agonists and further showcased the versatility the probes for different super-resolution imaging techniques.

Although dual GLP1R/GIPR agonists have been shown to improve glycaemic control in people with diabetes (243,498) the target substrates and influence upon intra-cellular signalling at the pancreatic islet level is unclear (349). Determining the fate of dual agonists after peripheral administration helps bridge the gap between pharmacological knowledge and intracellular actions. The daLUXendin probes labelled all three major cell types in the pancreatic islet which is in keeping with transcriptomic (188,190,191,455) data. This engagement with all cell major types may explain the superior glucose-lowering effects of dual GLP1R/GIPR agonism versus single GLP1R agonism. Whilst there is evidence that tirzepatide stimulates the release of insulin, somatostatin and glucagon (349,412), whether this is directly or via paracrine pathways is unclear. This is perhaps unsurprising given that despite decades of research there remains uncertainty about whether GLP1 acts directly or indirectly on α cells to suppress glucagon (349). The strongest daLUXendin labelling was in β cells, with reduced labelling of α and δ cells. This lends weight to the notion that dual GLP1R/GIPR agonists exert their effects on all pancreatic cells both directly as well as in a paracrine manner.

The manner by which tirzepatide engages the different pancreatic cell types is likely to be related the expression pattern of the receptors as well as the imbalanced nature of the molecule. In β cells, *Glp1r* is expressed in a similar abundance to *Gipr* (188) but with tirzepatide having increased affinity for GIPR in human tissue (255), insulin secretion is likely to be predominantly mediated via GIPR. This correlates with previous work showing

a larger reduction in tirzepatide-induced insulin secretion when GIPR is antagonised than when GLP1R is antagonised in human islets (412).

In δ cells, although there remains uncertainty about exact expression levels of GIPR and GLP1R, there is slightly less difference between the expression of *Gipr* and *Glp1r* compared with ß cells, with slightly more *Gipr>Glp1r* reported in δ cells (188). Therefore, any direct action of tirzepatide on δ cells could be via GIPR with a smaller component of GLP1R engagement.

In α cells, the evidence suggests that GIPR is widely expressed with minimal, if any, GLP1R expression (188,190,349). Therefore, tirzepatide action on α cell glucagon release is likely stimulatory, via GIPR. While moderate glucagon release is beneficial due to its insulinotropic action (49,499) and protective effects upon ß cell survival via promiscuous GLP1R binding (383), unregulated glucagon secretion can cause problematic hyperglycaemia (49). Given that tirzepatide has an overall glucose-lowering effect, it is unlikely that the actions upon glucagon are purely stimulatory or lead to a net excess of glucagon secretion. With the known cross-talk and paracrine mediation of glucagon secretion via ß and δ cells (reviewed in (321,349)), it is likely that as well as directly stimulating glucagon release from α cells, tirzepatide also regulates its glucagon secretion through actions on ß and δ cells.

While both GLP1 and GIP potentiate glucose-stimulated insulin release, GIP is more potent (500) and may suggest that the imbalanced GIPR>GLP1R agonism of tirzepatide (412) plays a significant role in the enhancement of GSIS compared with single GLP1R agonism from semaglutide (243). However, glucagon stimulates insulin release in a paracrine manner in a hyperglycaemic state (385,471,501) and glucagon also promiscuously activates GLP1R (383–386). Therefore, tirzepatide potentiation of insulin secretion could also be due to α cell GIPR-mediated glucagon release.

Further work to delineate the importance of paracrine signalling or intercellular cross-talk behind dual or multi-receptor agonist superior glucose control could be achieved using daLUXendins in conditional knock out models. Applying daLUXendins to islets with GIPR or GLP1R knocked out from ß or δ cells and then comparing glucagon secretion might help to confirm any paracrine mediated glucagon suppression and visualise any compensatory binding to other cell types. Furthermore, knocking out GIPR or GLP1R in delta cells and then comparing daLUXendin labelling may help to confirm which receptor is predominantly used to modulate somatostatin release. However, such knock out experiments would first need to explore the potential of upregulation of the reciprocal receptor as GLP1R upregulation has been suggested to occur in global GIPR knock-out mice (196,212,412) and supported by our work with *Gipr-/-* islets. This could be achieved with single receptor probes such as sGIP or LUXendin in addition to comparing the labelling of daLUXendin in different cell types. Humanised GIPR mouse models would be the ideal setting to perform these experiments - only two models are commercially available (502,503). However, validation of protein expression was performed with antibodies which detected both mGIPR and hGIPR, they have yet to be validated or published by external authors and anecdotally, the mice have been found to be phenotypically abnormal.

Following on from this, it would be prudent to explore the importance different signalling pathways upon dual- or multi-agonist ligand efficacy. Recent work has investigated the impact of *GIPR* (234) and *GLP1R* (504) variants upon receptor signalling and phenotype by comparing in vitro functional characterisation with donor phenotypes. *GIPR* single nucleotide polymorphisms (SNPs) that resulted in loss of function of both GIPR cAMP signalling and GIPR ß arrestin 2 recruitment were associated with a lower adiposity phenotype (234). However, SNPs that resulted in loss of cAMP signalling but maintenance

of ß arrestin 2 recruitment did not have such a protective effect and GIP was unable to stimulate insulin release in ß arrestin knockout mouse islets (234). Taken together, this has suggested that ß arrestin is a key mediator of GIPR trafficking and signalling after activation. As would be expected given the clinical success of GLP1R agonists, *GLP1R* SNPs that led to loss of function were associated with increased BMI and impaired glucose tolerance (504). However, when loss of function variants for ß arrestin 2 were excluded, the correlation was even stronger (504). This suggests that ß arrestin recruitment is less important for GLP1R-mediated insulin secretion and may be the reason for the increased efficacy of tirzepatide which biases GLP1R signalling away from ß arrestin and towards cAMP production (255). However, this work was performed in HEK cells expressing the mutant genes and a more relevant model would be SC-islets engineered to bear the SNPs of interest.

The formation of nanodomains is important for GPCR signalling (269,275,493) and signalling between cAMP nanodomains related to GLP1R has been shown to facilitate amplification of specific signalling pathways (505). Disruption to the formation of GLP1R nanodomains has been shown to reduce Exendin-4 stimulated insulin release (275). As engagement of these nanodomains might be pertinent to tirzepatide's superior efficacy, we showed that daLUXendin probes can be used in super-resolution and single-particle tracking techniques. daLUXendin660 engaged more nanodomains than a GIPR-agonist alone, although the density and number of receptors per cluster were similar. Therefore, daLUXendin660 is likely engaging both GIPR and GLP1R to form nanodomains, although whether the increase in nanodomains compared with GIPR agonist alone are purely GLP1R clustering or joint clustering of GLP1R and GIPR remains unclear. However, given that tirzepatide influences GLP1R expression at the cell surface (255,506), we hypothesise that enhanced signalling via increased formation of these nanodomains could be a

mechanism for the enhanced efficacy of tirzepatide. More work is required to determine the degree (and importance) of GIPR:GLP1R, GLP1R:GLP1R and GIPR:GIPR interactions in these nanodomains. The techniques required for this (such as SiMPull and nanorulers) are currently limited for use in cell lines (279,507) and therefore would not be fully suited to explore receptor dynamics in a system under the influence of intracellular interactions, such as a pancreatic islet.

To demonstrate the suitability of daLUXendin for further optimisation for different uses, we engineered a daLUXendin probe suitable for super-resolution STED microscopy. Validation was limited to an overexpression system, likely because the SiR was fluorogenic and signal from fluorogenic compounds can vary depending on the microenvironment and efficiency of the reaction (508) so the signal may not have been strong enough when labelling at a low level of expression. Nevertheless, daLUXendin651-d12 was able to label GLP1R and GIPR with greater resolution with STED than confocal microscopy, demonstrating that the choice of fluorophore did not overtly affect receptor binding.

Many novel dual and triple agonists are currently in development (309,465–467). However, against the backdrop of single agonism mechanics not yet fully elucidated (173), daLUXendin probes are formidable tools to explore dual agonist targets and effect upon receptor synergism. We explore this further in the next chapter where we present functional data and targets accessed following peripheral administration of daLUXendin. Furthermore, as dual and triple agonists share similar structures (309,466,467), it will be possible to engineer daLUXendin variants that possess the properties of novel drugs e.g. glucagon receptor affinity in triple GLP1R/GIPR/GCGR agonists such as Retatrutide (136). This expanded repertoire of fluorescent labels will allow exploration of foundational mechanisms (e.g. cell targets, importance/influence of direct and indirect signalling) of

novel agents as they emerge and determine ways to optimise pharmacology for the next generation of therapeutic agents.

Chapter 6: daLUXendin in vivo

Introduction

Evidence for central effects of GIP and GLP1

Given that GLP1 and GIP are rapidly degraded by DPP4 (509), it has been argued that gut-derived incretins are unlikely to signal centrally, i.e. in the brain, and that indirect mechanisms lead to the effects of incretins on the brain. However, recent studies have demonstrated that peripherally administered analogues are able to access the brain, activate neurones implicated in weight homeostasis to drive weight loss through central mechanisms.

GIP

Firstly, in the case of GIP, circulating GIP levels are higher in individuals with obesity (510), affording greater likelihood of GIP accessing the brain before degradation. In mice, *Gipr* expression has been found in nuclei related to feeding, including the arcuate, paraventricular and dorsomedial hypothalamic nuclei (267,511,512). In humans, *Gipr* expression has been found in both hypothalamic neuronal and non-neuronal cells (third ventricle ependymal cells) (513). Furthermore, peripheral administration of long-acting GIPRA decreases food intake and body weight in diet-induced obesity (DIO) mice (253,512,514).

Suggesting that central GIPR signalling is key for GIPR agonism, acylated GIP and dual GIPR/GLP1R agonist had a blunted effect upon weight loss and food intake in CNS GIPR KO mice (514) and in specific GABA-ergic neurone GIPR KO mice (253,254). In contrast, GIPRA-mediated weight loss and reduction in food intake is preserved in *Glp1r*-deficient

mice (237,514), suggesting that GIPR agonism-mediated weight loss is achieved via GLP1R-independent pathways, likely involving GABA-ergic neurones.

GIPR antagonism has also been shown to reduce weight via central mechanisms. Combined GLP1R agonism/GIPR antagonism activates neurones (determined by c-Fos expression) involved in food intake (244). Analysis of snRNA-seq data found that GIPR antagonism upregulates gene expression in neurones within the dorsal vagal complex (DVC), a hind brain structure involved in energy regulation, in a similar manner to GLP1RA whereas GIPR agonism is negatively associated with DVC gene transcription (250). Neuronal knockout of either GLP1R or GIPR attenuates the effect of GIPR antagonism (250) or combined GLP1R agonism/GIPR antagonism (244) upon weight loss and food intake. Additionally, neuronal (244) or GABA-ergic neuronal (250) knockout of GIPR augments the effect of GLP1RA upon weight loss and food intake, compared to control mice. Taken together, these findings suggest that firstly, activity at both receptors is key for the central effects of GIPR antagonism and engages mechanisms distinct from GIPR agonism. Secondly these findings also suggest that loss of GIPR signalling may sensitise the neuronal networks to GLP1R activity and thirdly that weight loss may be driven by reducing food intake.

Whether GIPR-mediated changes in weight are a result of reduced food intake or increased energy expenditure remains debated. Kaneko et al administered a GIPR antagonistic antibody centrally and found that weight loss was observed in obese mice but not in lean mice without any change in energy expenditure (231). These findings were supported by further work formally measuring food intake, showing that peripheral or central administration of GIP reduces weight and food intake in a comparable manner (244,267,407). Furthermore, chemogenetic activation of GIPR+ neurones in the hypothalamus or hindbrain reduces food intake in mice (267,407).

However, some GIPR KO studies suggest that the weight loss is driven by changes in energy expenditure, with no observed change in food intake (251,350,440,442) and seemingly only protecting against weight gain from HFD and not standard chow (442). Similarly, ablation of GIP-secreting K cells resulted in reduced weight gain, reduced food intake and increased expenditure when transgenic mice were fed HFD but not when fed standard chow (214). To date, no human studies have assessed the effect of GIPR agonism or antagonism, or the known GIPR missense variants (232), upon energy expenditure. There is evidence that GIP signalling in the area postrema (AP) seems to attenuate the undesirable central effects of GLP1R agonism which may contribute to the increased efficacy of dual GLP1R/GIPR agonists. GIPR agonists potentiate the anorexigenic effects of GLP1RA whilst attenuating its nauseating and taste avoidance effects across several species (260,515,516). However, confirmatory evidence in humans is limited, with only one recent study demonstrating that rapid GLP1RA dose escalation induced fewer GI side effects when administered concomitantly with a long-acting GIPR agonist, when compared to placebo (517). However, this was performed in individuals without diabetes or obesity and did not administer a unimolecular agent with imbalanced or biased agonism, all of which are variables that may modulate the impact of GIPR agonism upon GLP1R agonism. Furthermore, the dose-dependent nausea and vomiting associated with GLP1RA use (518) was reported at a similar frequency in patients treated with tirzepatide or semaglutide in a head-to-head trial (243). Therefore, currently, the translational effects of GIPR agonism on GLP1-induced nausea require further investigation before they can fully be exploited for therapeutic advantage.

GLP1

For GLP1, it has been well characterised that GLP1 produced in the brain acts as neuropeptide which signals satiety in brainstem–hypothalamus pathways (519–521). Central administration of GLP1 reduces food intake and causes weight loss (288,521–523). Loss of function through central GLP1R antagonism or CNS-specific or global knock out models has been shown to cause hyperphagia and weight gain (522–524) but in other studies to have no impact upon food intake or weight (288,525,526).

When injected intraperitoneally, exendin-4 stimulated neuronal activity (determined by c-Fos expression) in the paraventricular nucleus of the hypothalamus (PVN) and the nucleus tractus solitarius (NTS) (527), regions which are known mediators of energy homeostasis (528). However, only central injection activated neurones in the arcuate nucleus (527), suggesting that targets of GLP1 produced in the brain may be different to GLP1 produced in the periphery.

A GLP1RA-GIPR antagonist peptide-antibody conjugate was able to activate c-Fos expression in the NTS as well as the dorsomedial hypothalamic nucleus (DMH), AP and several nuclei where *Glp1r*/*Gipr* is not known to be expressed, such as the parasubthalamic and central amydalar nuclei (244). This suggests that at least part of central GLP1RA or GIPR antagonism action involves indirect modulation of downstream pathways. It also highlights the differences in activity between ligands and the need to study individual ligands rather than draw conclusions about mechanism of action from seemingly similar molecules.

Further supporting the role of GLP1 in modulating food intake via direct central actions, *Glp1r* mRNA and GLP1R have been identified in areas close to the blood-brain or blood-cerebrospinal (CSF) barrier; hypothalamic nuclei such as the PVN, the NTS, and the AP (529–531) in mice. In humans, *Glp1r* expressing neurones have been localised to the

arcuate nucleus, and in the PVN and supraoptic nuclei (SON) where they overlap with *Gipr* expression (513).

However, it remains unclear if peripherally produced i.e. gut-derived GLP1 can be sensed by and directly signal to the brain, given its rapid degradation by DPP4 (509) and the impermeability of the blood-brain barrier to peptide hormone diffusion (532,533).

Unlike with GIP, there has been limited evidence that circulating GLP1 levels ever experience a sustained rise that would allow GLP1 the time to reach the brain and have sustained effects (as reviewed in (534–536)). It has been estimated that only 25% of GLP1 secreted by the intestines reaches the portal vein circulation (509). Furthermore, meal-induced GLP1 secretion only reached significantly raised levels in the portal circulation but not the vena cava (537). Many other studies have been performed with supraphysiological doses of GLP1 or analogues and recruited routes of access which may not be physiologically relevant for assessing whether gut-derived GLP1 can access the brain e.g. intracardiac or jugular vein injection (536,538).

Inhibiting the degradation of GLP1 with DPP4-inhibitors does not induce weight loss (539). Therefore, this may suggest that sustained higher concentrations of GLP1 are not required for central actions, or that the concentration of GLP1 is still insufficient to cross the blood-brain or blood-CSF barriers relative to exogenously administered GLP1RA, or that signalling is indirect via cells closer to the intestines.

It has been postulated that gut-derived GLP1 exerts its central effects via the afferent vagal nerve (540–542) or signalling from visceral afferent neurones (543). An intact vagal-brainstem-hypothalamic is required for peripherally administered GLP1 to reduce food intake and activate connected hypothalamic neurones (544). However, vagal *Glp1r* knockout did not attenuate liraglutide's effects on reducing food intake (525). This result is supported by previous studies showing that vagotomy had no effect upon peripherally

administered GLP1-mediated anorexia (545–548) suggesting that GLP1 (also) acts in a vagal-independent manner, potentially directly on the brain.

Disruption to the AP attenuates the anorectic effect of GLP1 infused into the hepatic portal vein but not intraperitoneal GLP1 infusion (537). This suggests that gut-derived GLP1 could act both via vagal nerve afferents in the portal system as well directly when in the circulation.

Also in favour of the action of gut-derived GLP1 acting directly on the brain is the finding that despite the median eminence (ME) and AP (and other circumventricular organs, with a reduced blood brain barrier) being rich in GLP1R (549), they receive very little input from GLP1-producing neurones of the brain (550).

Additionally, liraglutide administered to the jugular vein was able to access the ME within one minute (551), less than the 3-4 minutes taken for GLP1 to be degraded by DPP4 (509), suggesting that transient spikes in circulating post-prandial GLP1 levels could reach the brain. Furthermore, robust c-Fos expression in CVO *Glp1r*- and *Gipr*-expressing neurones was observed after peripheral administration of respective agonists (407,552), suggesting that central sensing of circulating GLP1 and GIP is occurring.

Finally, it is also pertinent to highlight that there may be differences between the effect of native incretins and their engineered agonists upon the brain. The GLP1R agonist exendin-4 was found to be more potent than GLP1 at reducing food intake after central administration in mice and was able to continue reducing food intake in the presence of an antagonist, despite the same antagonism abolishing GLP1 effects (523). This highlights the importance of studying the pharmacodynamics of novel agents themselves and not inferring likely modes of action or accessibility from GLP1-based experiments. This is even more pertinent when considering the discrete pharmacological differences that likely underpin the therapeutic efficacy of some ligands, for example signal bias and acylation.

For example, at the mouse GLP1R it has been demonstrated that ligands which result in abolishment of ß arrestin recruitment have superior anti-hyperglycaemia effects (553). Given that there remains debate about whether peripherally produced or administered incretins can access and exert effects on the brain, techniques to visualise and quantify the ability of peripherally administered incretin receptor agonists or antagonists accessing the brain are needed.

Peptide access to the brain

If gut-derived GLP1 and GIP are able to reach the brain before degradation, the exact location of uptake or signalling requires further study and is likely influenced by the protective mechanisms which guard the brain against access from undesired molecules. The blood-brain barrier (BBB) is a restrictive interface between the general circulation and the brain parenchyma that tightly regulates the diffusion of small molecules and uptake of larger molecules, such as peptide hormones and large molecule drugs, into the brain (532,533). The paracellular, passive diffusion of small molecules is limited to those which are lipophilic (LogP <5) and <500 Da (554). For larger molecules, access to the brain is transcellular via specific transporters or cognate receptors expressed on BBB endothelial cells, such as insulin (532,555). Pericytes, which form part of the BBB, are known to express receptors for many metabolic hormones (556,557) and transport of peptide hormones into brain parenchyma via these cognate receptors is slow and saturable (558). There is evidence which suggests that obesity can lead to impaired peptide hormone transport across the BBB. Studies of leptin have found defective transport across the BBB in a state of obesity (559,560) which, in conjunction with early saturation of cognate receptors (561,562), leads to leptin resistance.

Circulating molecules can also gain access to the brain by crossing the blood-CSF barrier (BCB). At the BCB, transfer of substances from circulating blood to the CSF is similar to transfer at the BBB, with transport of small molecules via diffusion through fenestrated capillaries, and active, transcellular transport of larger molecules (534,563). There are two specially adapted sites for this; the choroid plexus and the circumventricular organs (CVOs).

The epithelium of the choroid plexus has been found to express transporters and cognate receptors for several peptide hormones relevant to energy homeostasis, such as GLP1, insulin, leptin and prolactin (564–567). Leptin, a peptide hormone which modulates feeding and energy expenditure by binding to its cognate receptors in several brain regions (568,569), has been shown to cross the BCB via a transporter (570) before binding to leptin receptors on ependymal cells to interact with the brain parenchyma (571).

The CVOs are specialised areas of the brain, within the walls of the 3rd and 4th ventricles, without a functional BBB (572) which provide an additional site for BCB transfer of molecules from the general circulation. This occurs either under the regulation of ependymal cells called tanycytes (573,574) or via diffusion through fenestrated capillaries (575). Diffusion across the ME has been shown for molecules <40kDa including the gut-derived peptide hormone ghrelin (575). Not only are the CVOs important sites for potential transport of peptides across the BCB, but some are closely related to hypothalamic nuclei which control feeding and energy homeostasis. Such CVOs of interest are the ME and the "sensory CVOs"; the AP, organum vasculosum of the lamina terminalis (OVLT) and the subfornical organ (SFO). Figure 64 illustrates the location of the different CVOs involved in BCB transport and the potential cells involved.

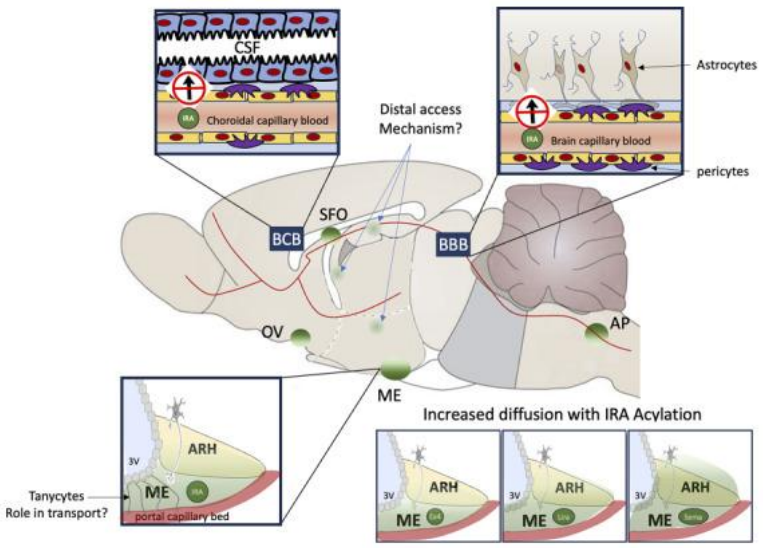

Figure 64: Sensory circumventricular organs involved in brain access for incretins. Reproduced from Buller and Blouet [26]. AP = area postrema, ARH = arcuate nucleus of the hypothalamus, BBB = blood brain barrier, BCB = blood-cerebrospinal fluid barrier, CSF = cerebrospinal fluid, IRA = incretin receptor agonist, ME = median eminence, OVLT = organum vasculosum of the lamina terminalis, SFO = subfornical organ.

The ME mediates the transport of molecules between the systemic circulation and the arcuate nucleus (ARH) (575–578). The ARH is a key centre for integrating peripheral signals relating to feeding (579,580) where circulating molecules interact with neurones of varying, sometimes opposing, function to modulate homeostatic metabolic responses (528,579–581). The ME has demonstrated plasticity in peptide access to the ARH in response to food intake or fasting, with increased diffusion of ghrelin in the fasted state (575,578). Ghrelin is a peptide hormone secreted from the stomach (582,583) and brain (582,584) and is a potent stimulator of food consumption (585,586) via the ARH as well as the NTS and PVN (587–590).

Most CVOs receive nerve terminals from the brain but the area postrema (AP), subfornical organ (SFO), and organum vasculosum of the lamina terminalis (OVLT) are the only CVOs which neuronal cell bodies (591). Subsequently, they are termed “sensory CVOs” and acts as relay centres for circulating peptides to modulate certain neuroendocrine, as well as cardiovascular and immune functions (592,593).

The AP is closely linked with the nucleus tractus solitarius (NTS). The AP/NTS region is located in the hindbrain and is a major site of afferent vagal and splanchnic neurones projection, relaying sensory information from the abdominal cavity (594–596). The AP/NTS region also partly mediates the effects of the satiety hormones amylin, cholecystokinin and bombesin (597–599).

Neurones from the SFO project into lateral hypothalamus and the ARH (600,601), which contain both orexigenic/anabolic neurones and anorexigenic/catabolic neurones (602,603).

Neurones from the OVLT project into the PVN (604,605), which suppresses food intake (606–609).

Therefore, when exploring sites of access for peptide hormones regulating food intake and energy homeostasis, the choroid plexus and CVOs associated with feeding and appetite nuclei would be prudent sites to start from.

GIP/GLP1 access to the brain

GIP

Our fluorescent sGIP probes label the choroid plexus and CVOs including the AP and ME (407) but to determine how GIP can cross the BCB barrier at these sites, it would need to be next explored if GIPR is expressed on cells responsible for transcytosis in the choroid plexus; ependymal cells such as tanycytes.

In terms of GIP access via the BBB, radio-labelled GIP was found to cross the BBB in a saturable manner but not in the presence of excess, unlabelled GIP, suggesting that any uptake is dependent on the GIPR (610). Further, GIPR is highly expressed in pericytes (611), vascular cells which modulate the permeability of the BBB (612), which could

mediate GIP transport across the BBB. However, sGIP did not show any labelling outside of the CVOs (407).

The only evidence of GIP production in the brain is limited to discrete areas (613). If the lack of widespread GIP production in the brain is confirmed in future studies, in the context of extensive central GIPR expression (267), it would support the idea of GIP uptake across the BBB or BCB.

GLP1

GLP1R is expressed in the choroid plexus (298,614) which is the primary site of CSF production (615), controlling intracranial pressure. Peripherally administered GLP1R agonists have been shown to reduced intracranial pressure in humans (311,616) and this has been demonstrated in rodents to be the result of a GLP1R-mediated reduction in CSF production (614).

Some studies have demonstrated that GLP1R agonists can pass the BBB (617–619) although other studies have not found this to be the case (620) and the exact mechanism is yet to be elucidated. Exendin-4 injected intravenously has been found to cross the blood brain barrier in a saturable manner (621). However, Exendin-4 has a similar distribution to the antagonistic Exendin-9 at the ARH and NTS when administered peripherally (298,548,620), suggesting that internalisation via GLP1R is not necessary to cross the BBB at these locations. Furthermore, the ability of different GLP1R agonists to cross the BBB has been shown to be vary, with acylation has been shown to prevent GLP1R agonists from crossing the BBB (622) but still allowing labelling of CVOs via the BCB (548).

To support the notion that GLP1 accesses brain sites via the BCB, intra-cardiac injection of ^{125}I-GLP1 into anaesthetised rats labelled the AP and SFO (538). Peripherally administered liraglutide labels the brain in the CVOs and binds to neurones in the ARH and other regions

of the hypothalamus (548). This was mediated by GLP1R as brain labelling was not present in *Glp1r*$^{-/-}$ mice (548). After intraperitoneal injection, exendin-4 is able to stimulate neuronal activity (determined by c-Fos expression) in the AP (527).

It has been proposed that GLP1R agonists gain access to the brain at the BCB via transcytosis through β2-tanycytes (573). Tanycytes are specialised ependymal cells found within the hypothalamus (623) which facilitate transport of substrates, including peptides, from the peripheral circulation to the cerebrospinal fluid (573,624). Additionally, tanycytes have been proposed to play a role in hypothalamic glucose sensing (625). While fluorescently labelled liraglutide labels tanycytes (551), sparse GLP1R immunoreactivity has been detected in these cells (626,627). However, it is worth noting that there are limited GLP1R antibodies which have shown sufficient sensitivity or specificity in brain (257,259,628).

Chapter aim

Several questions remain without detailed answers in the field of central incretin action. Of relevance to this work, whether GLP1 or GIP and their agonists can directly access the brain via the BBB or BCB and if so, in which areas and via what mechanisms (i.e. diffusion or transcytosis mediated by which cells).

Our fluorescent probes are well suited for interrogating such functionally relevant access mechanisms and target sites, given their receptor specificity and suitability for in vivo administration.

Therefore, this chapter details our in vivo work with daLUXendin probes, confirming the phenotypic effects when administered peripherally and the target sites labelled when administered peripherally and centrally.

Results

daLUXendin660 demonstrates efficacy and reduced mGLP1R:mGIPR selectivity in vivo

To determine if in the vitro pharmacology is representative of efficacy in vivo, we examined the effects of daLUXendin660 and tirzepatide on food intake and glycaemic control in mice. To maximally engage the GLP1R and GIPR, mice were administered 10nmol/kg tirzepatide or daLUXendin660 (412,414).

For food intake studies, mice were fasted prior to their dark phase and subcutaneously injected with either ligand before food was reintroduced and intake measured. Both daLUXendin660 and tirzepatide reduced food intake during the subsequent dark cycle and for 24h afterwards, when compared with vehicle-treated mice (Figure 65). The reduction in food intake at 12- and 24-hours post-injection was 40% greater with tirzepatide than compared with daLUXendin660 (Figure 65). This is likely related to diacid side chain of tirzepatide conferring a longer half-life via albumin binding which is expected to make a difference during 12-24h dosing (414).

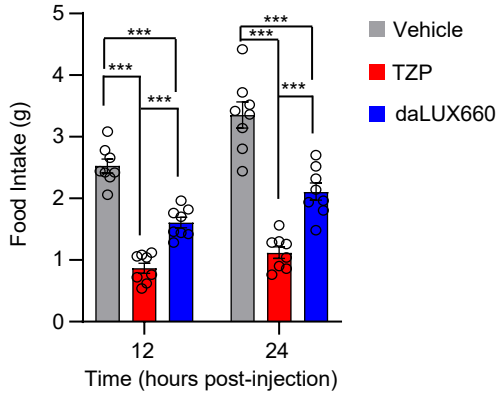

Figure 65: daLUXendin food intake study.
Graph showing cumulative food intake 12 hours and 24 hours post-injection (n = 8 per condition) (RM two-way ANOVA)

To determine the impact of the ligands upon glycaemic control, intraperitoneal glucose tolerance tests (IPGTT) were performed in WT/heterozygous and GLP1RKO mice. Loss of one *Glp1r* allele has been shown to have no impact upon glucose tolerance during IPGTT (289).

In pooled results from *Glp1r*$^{WT/WT}$ and *Glp1r*$^{WT/KO}$ mice (termed here as WT), both daLUXendin660 and tirzepatide significantly lowered glucose levels with similar area-under-the-curves (AUC) (Figure 66a). In *Glp1r*$^{KO/KO}$ mice, the glucose-lowering effects of the ligands was reduced but not abolished, reflecting the ongoing engagement of the mGIPR (Figure 66b).

Completely knocking out the GLP1R had a greater effect on tirzepatide's glucose-lowering effect than for daLUXendin (Figure 66a-c). This suggests that tirzepatide is more selective for mGLP1R than mGIPR, in keeping with previous literature (412), and that daLUXendin660 is more dependent on mGIPR than mGLP1R, in keeping with our in vitro work up. Furthermore, it is worth noting that in WT mice daLUXendin660 and tirzepatide lowered glucose equally, suggesting that the side chain and albumin binding becomes important at time courses >180 minutes at these doses.

By comparing the AUC of WT to *Glp1r*$^{KO/KO}$ we can observe the dependence of the effects of each ligand on mGLP1R vs mGIPR. Comparative ratios for mGLP1R:mGIPR selectivity are lower for daLUXendin660 than tirzepatide (Figure 66d). They confirm that tirzepatide is more selective of mGLP1R:mGIPR than daLUXendin660 which is in keeping with our in vitro pharmacological assessment of receptor selectivity (Chapter 5).

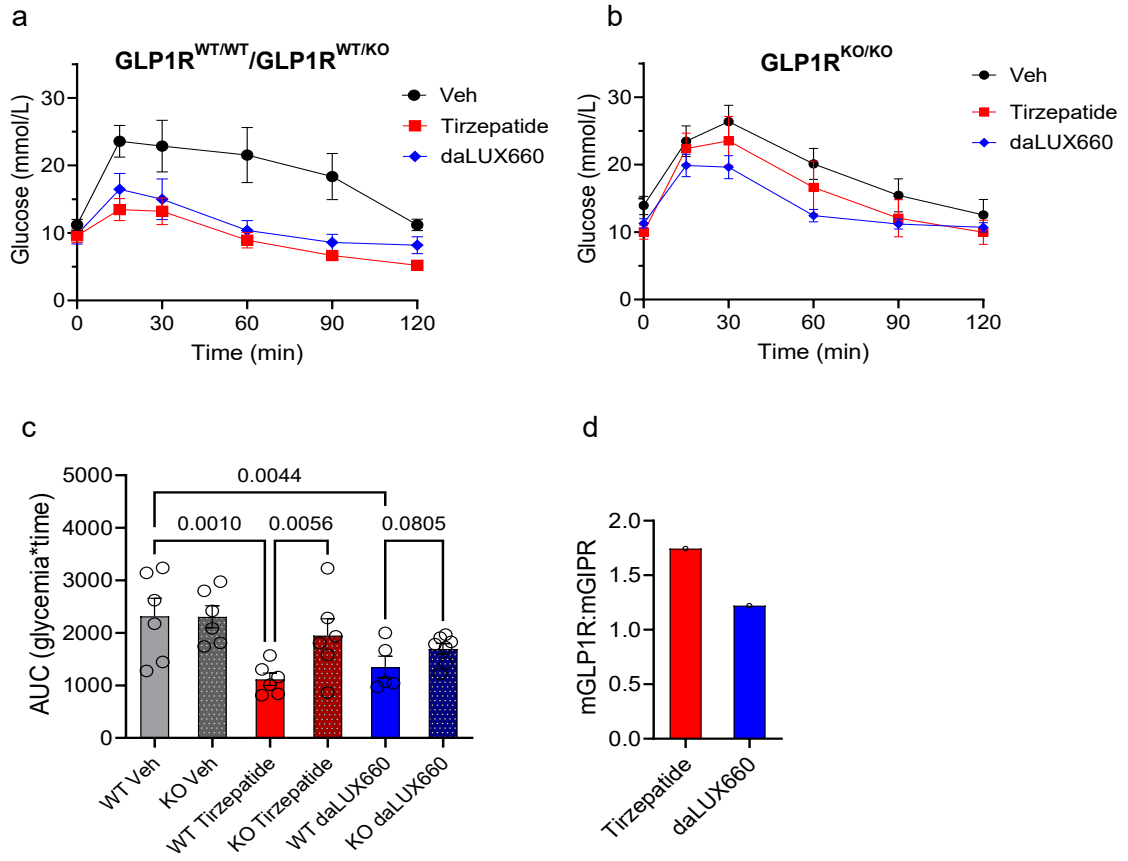

Figure 66: daLUXendin IPGTT studies
IPGTT results in pooled WT/heterozygous mice (a) or GLP1R$^{KO/KO}$ mice (b) after injection with vehicle, tirzepatide or daLUXendin660. AUC was calculated for WT vs KO for each ligand (c) then ratio of AUC for WT vs KO calculated for tirzepatide and daLUXendin660 (d).

Given that daLUXendin660 had similar glucose-lowering effects in *Glp1r*$^{WT/WT}$/*Glp1r*$^{WT/KO}$ and *Glp1r*$^{KO/KO}$ (Figure 66c), to confirm that heterozygosity was not impacting on IPGTT results in the WT group we compared IPGTT responses between *Glp1r*$^{WT/WT}$ and *Glp1r*$^{WT/KO}$. In heterozygous *Glp1r*$^{WT/KO}$ mice, treatment with tirzepatide or daLUXendin660 markedly lowered glucose compared with vehicle-treated mice but the reduction was similar to WT mice (Figure 67). Therefore, it is unlikely that grouping GLP1R$^{WT/KO}$ with GLP1R$^{WT/WT}$ has confounded the GLP1R$^{WT/WT}$ effect and the subsequent comparison to GLP1R$^{KO/KO}$ results. This is as expected from previously published work which found that heterozygous loss of GLP1R did not alter glucose tolerance (289).

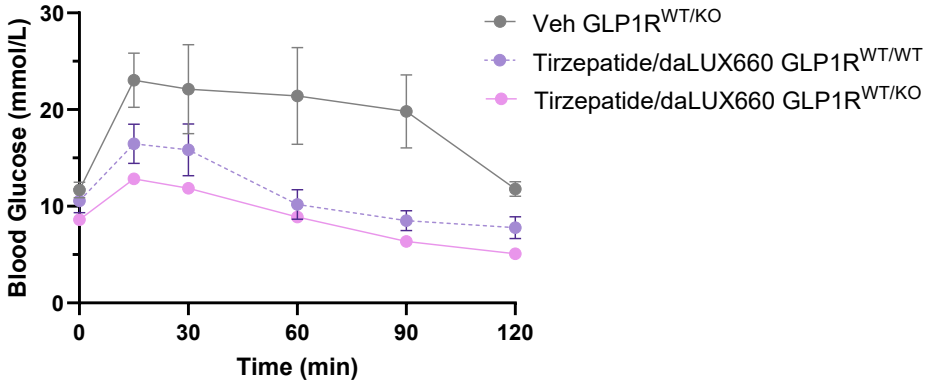

Figure 67: daLUXendin IPGTT responses in WT and heterozygous WT/GLP1RKO mice. $GLP1R^{WT/WT}$ vs $GLP1R^{WT/KO}$ mice treated with tirzepatide and daLUXendin660 compared to heterozygous mice treated with vehicle

daLUXendin660 labels islet *Glp1r*- and *Gipr*-positive cells in vivo

Current knowledge about cell substrates that dual agonists bind to when administered peripherally is lacking. To facilitate the exploration of dual agonist access to different tissues in vivo, we administered daLUXendin660 peripherally (intravenously) to *Glp1r* (*Glp1r*-Cre:tdRFP) and *Gipr* (GIPR-Cre:GFP) reporter mice. daLUXendin660 was able to label pancreatic islets in pancreatic sections obtained post-mortem (Figure 68, Figure 69). Upon quantification of daLUXendin660 fluorescence in cells positive for reporter fluorophores, labelling was present in *Gipr* and *Glp1r*-expressing cells. There was some labelling of cells negative for $Glp1r^{RFP}$ (Figure 70) which is in keeping with daLUXendin660 labelling alpha and delta cells which do not express (much) GLP1R. There was negligible labelling of cells negative for $Gipr^{GFP}$ (Figure 70) which is in keeping with GIPR being expressed on all the major endocrine cells in the pancreatic islet.

Some cells which were positive for the reporter fluorophore were not labelled with daLUXendin660. This could be due to differences in access when injected peripherally but given the bright membrane and cytosolic labelling of adjacent cells, this is not likely. It

could be highlighting the known discordance between gene expression and receptor expression of incretins (261), further highlighting the need for techniques that measure locate or identify protein expression rather than just gene expression.

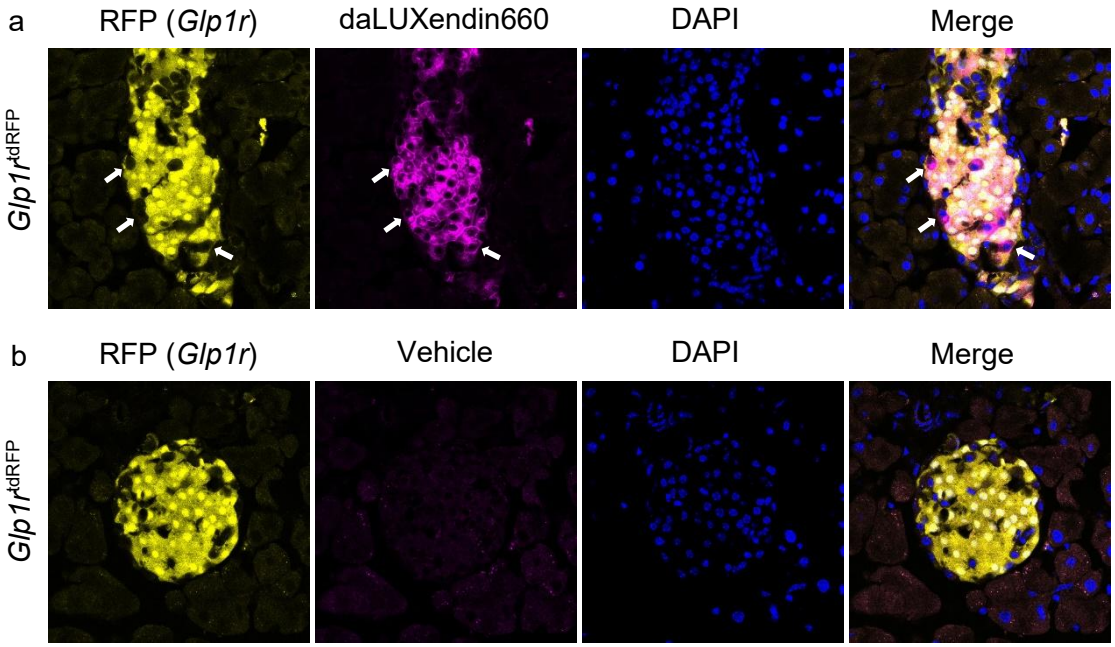

Figure 68: daLUXendin in Glp1rtdRFP mouse pancreas sections.
Representative images of islets from pancreas sections taken from Glp1r^{tdRFP} mice peripherally administered with daLUXendin660 (a) or vehicle (b). Arrows show daLUXendin labelling RFP negative cells, presumed to be GIPR-expressing α or δ cells.

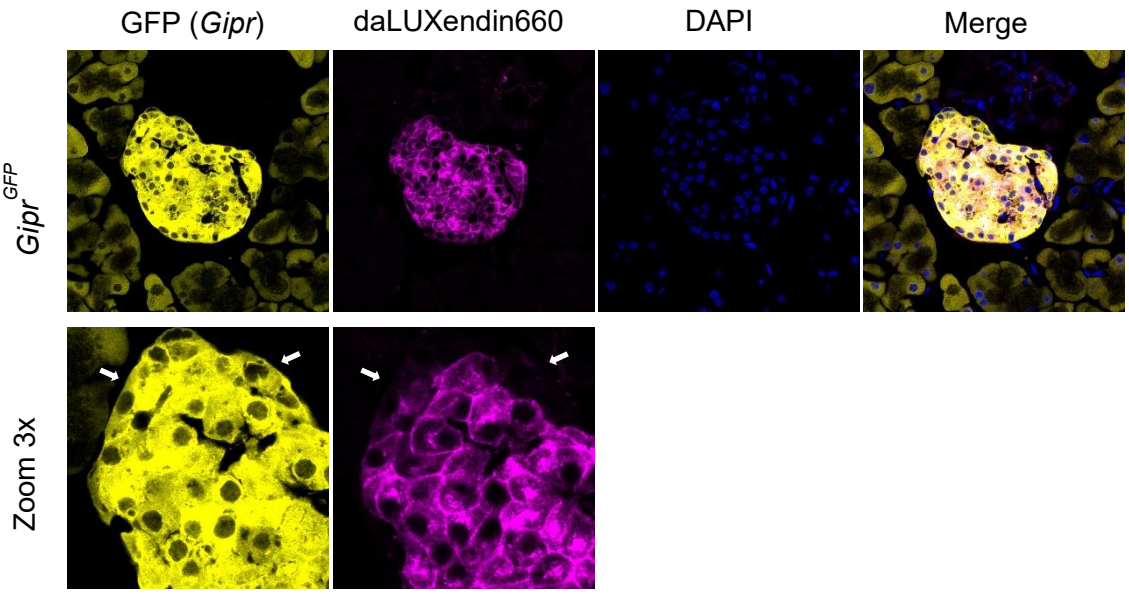

Figure 69: daLUXendin in GiprGFP mouse pancreas sections.
Representative images of islets from GIPR^{GFP} mice peripherally administered with daLUXendin660 in vivo. Arrows highlight GFP positive cells not labelled with daLUXendin660.

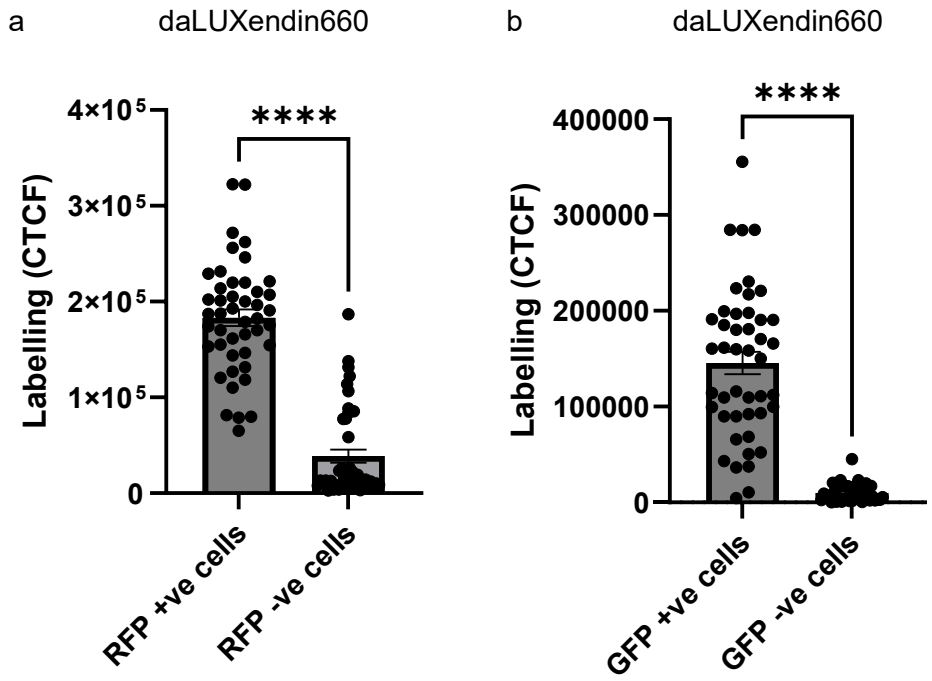

Figure 70: daLUXendin fluorescence in Glp1r/Gipr reporter mice.
CTCF values of daLUXendin660 in (a) RFP-positive cells vs RFP-negative cells in a Glp1r-Cre:tdRFP mouse and (b) GFP-positive and GFP-negative cells in a Gipr-Cre:GFP mouse showing significant difference p<0.0001, unpaired t-test (n=38-40 cells/condition from one Glp1r-Cre:tdRFP and Gipr-Cre:GFP mouse).

daLUXendin660 labels *Glp1r* and *Gipr* positive cells after peripheral administration and tanycytes after central administration

As discussed above, it is known that the central nervous system is a target of incretins (173), particularly circumventricular organs (CVOs) (298,407) - specialised areas without a blood-brain barrier (572). How peptides access and act at deeper structures is unclear. Therefore, we next assessed the ability of daLUXendin660 to visualise dual agonist access to the brain following peripheral and central administration.

Both peripherally administered daLUXendin660 and the acylated daLUXendin660+ were able to label several CVOs but there was no penetration into deeper structures (Figure 71). The GLP1R antagonist probe LUXendin645 similarly labelled CVOs after peripheral administration (Figure 71).

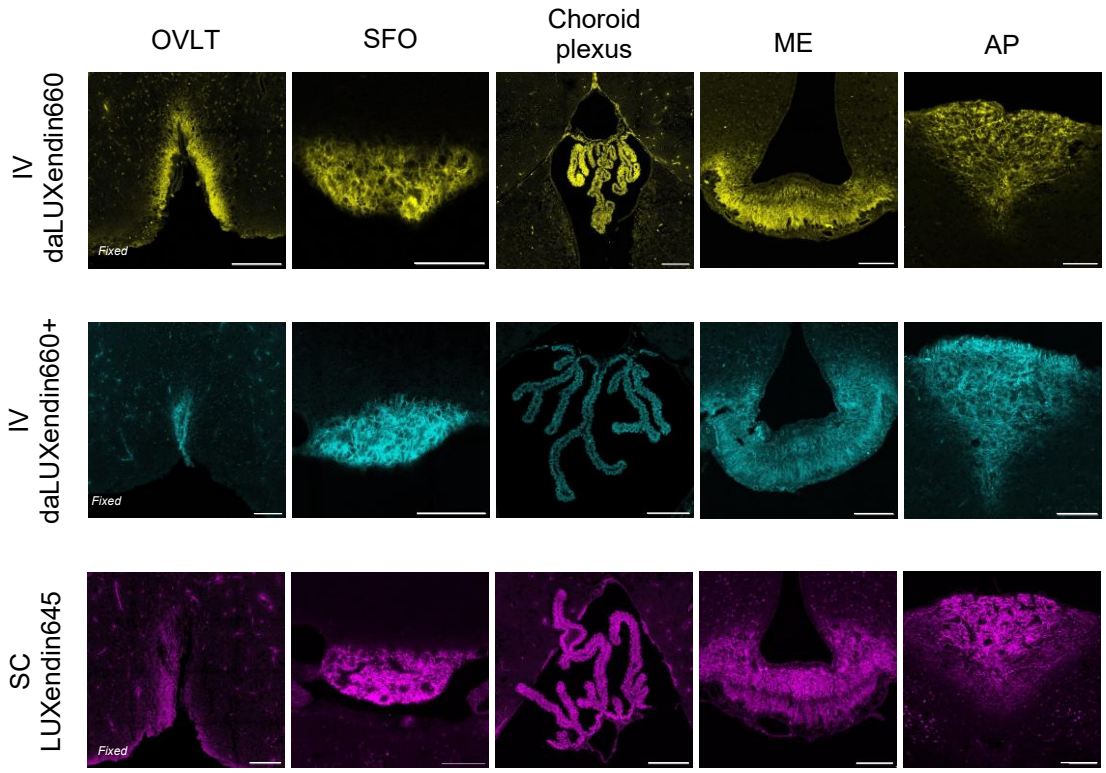

Figure 71: daLUXendin brain labelling after peripheral administration.
Intravenous administration of 100 nmol/kg daLUXendin660, 100 nmol/kg daLUXendin660+, and subcutaneous administration of 100 nmol/kg LUXendin645 (GLP1R antagonist) into mice led to staining in circumventricular organs of the brain and the choroid plexus. Shown are (from left to right): organum vasculosum of the lamina terminalis (OVLT), subfornical organ (SFO), choroid plexus, median eminence (ME) and area postrema (AP).

Next, we aimed to determine whether brain dual agonist binding was in neuronal and non-neuronal cell types expressing GLP1R or GIPR, or both. In reporter mice which harboured fluorescent markers for transcription of *Glp1r* (GLP1R-Cre:tdTomato) and *Gipr* (GIPR-Cre:GCaMP6), daLUXendin660 co-localised with *Glp1r*- and *Gipr*-positive neurones in several CVOs with strong labelling the AP of the dorsal vagal complex (DVC) (Figure 72, Figure 73). The lack of labelling in deeper structures of the brain is in keeping with peptidic ligands being blood brain barrier impermeable and reliant upon retrograde transport through the fenestrated vessels in the median eminence or elsewhere (575,578).

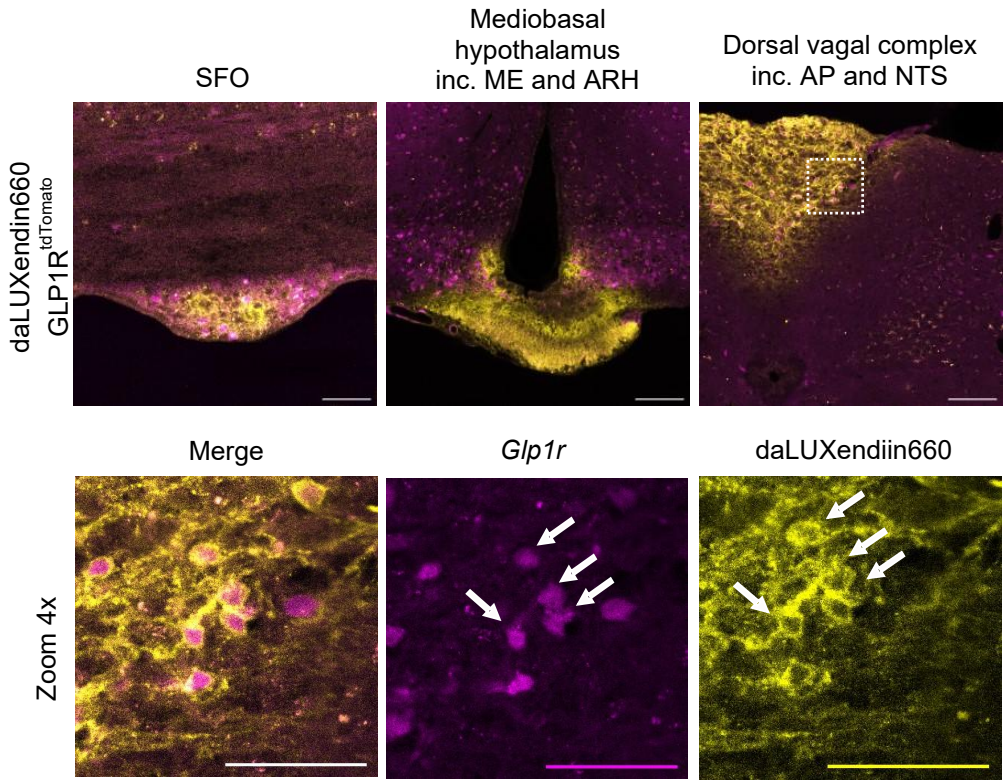

Figure 72: daLUXendin brain labelling in Glp1r reporter mice
Representative images of GLP1R-Cre:tdTomato mouse brain after intravenous administration of 100 nmol/kg daLUXendin660, showing daLUXendin660 labelling of Glp1r-expressing cells (indicated by white arrows in zoom panel). Scale bars: 100 µm.

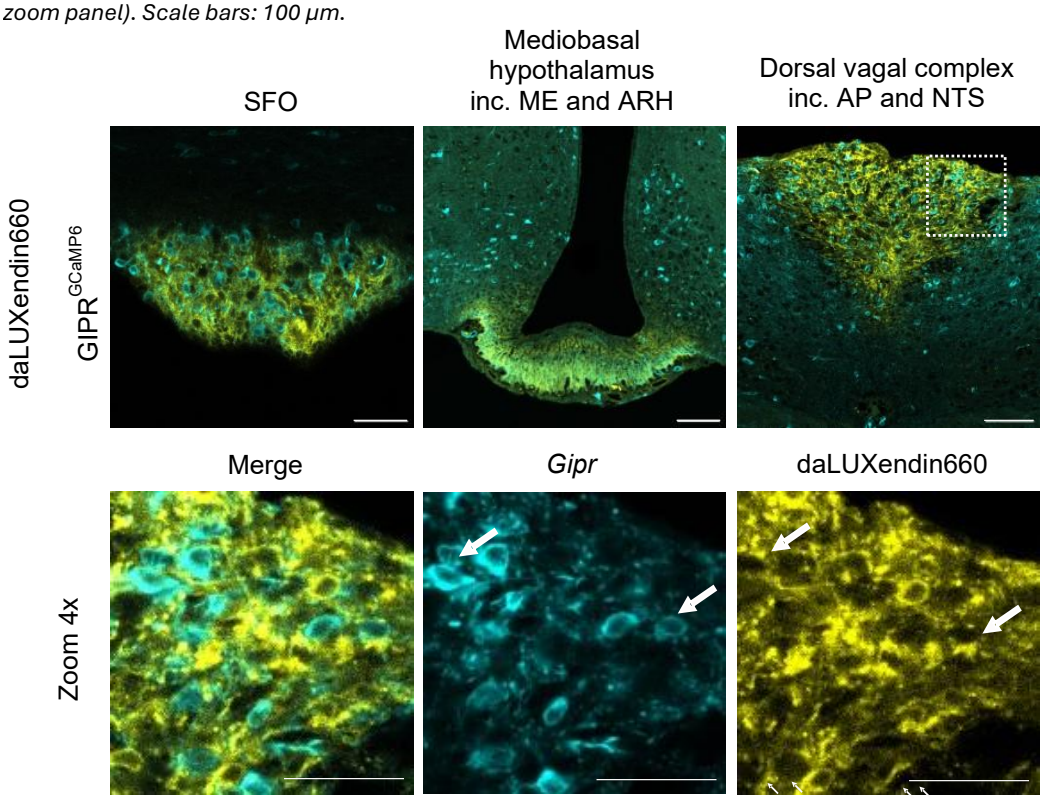

Figure 73: daLUXendin brain labelling in Gipr reporter mice.
Representative images of GLP1R-Cre:GCaMP6 mouse brain after intravenous administration of 100 nmol/kg daLUXendin660, showing daLUXendin660 labelling of Gipr-expressing cells (indicated by white arrows in zoom

To interrogate deeper binding sites accessible from the CSF, daLUXendin660 was administered via intracerebroventricular injection into the third ventricle of mice. Samples were co-stained for vimentin. Vimentin is an intermediate filament protein strongly expressed in ependymal cells (629), of which only tanycytes would be expected in the median eminence (630).

There was uptake of daLUXendin660 from the CSF into the brain parenchyma. daLUXendin660 labelled cells lining in the third ventricle, co-localising with tanycytes identified with vimentin immunostaining (Figure 74). The 3D render highlights the extent of co-localisation of daLUXendin660 with not just the apical body of the tanycytes but also along the length of the tanycytes' projection into the brain parenchyma.

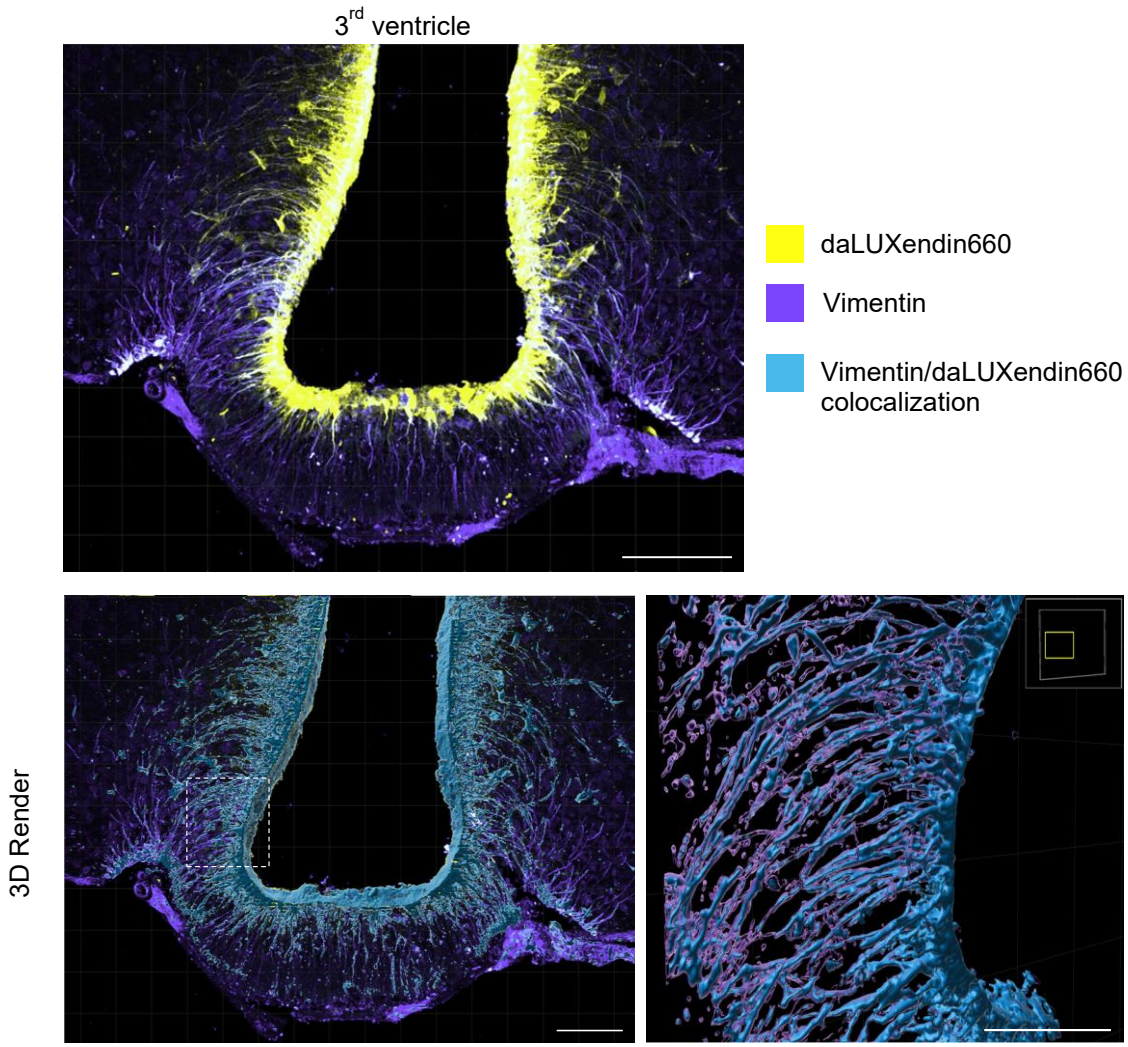

Figure 74: daLUXendin labelling after central administration and vimentin labelling.
Representative images of daLUXendin660 labelling of cells lining the 3rd ventricle with co-localisation with vimentin-positive cells. 3D rendering further demonstrates the extensive co-localisation. Scale bars 100µm.

To visualise GLP1R and GIPR accessible from the CSF, daLUXendin660 was also administered into the third ventricle of *Glp1r* and *Gipr* in reporter mice (GLP1R-Cre:tdTomato and GIPR-Cre:GCaMP6, respectively). daLUXendin co-localised with peri-ventricular cells expressing *Glp1r* (Figure 75), a modest number of cells expressing *Gipr* (Figure 76) as well as a small number of cells expressing both (Figure 77).

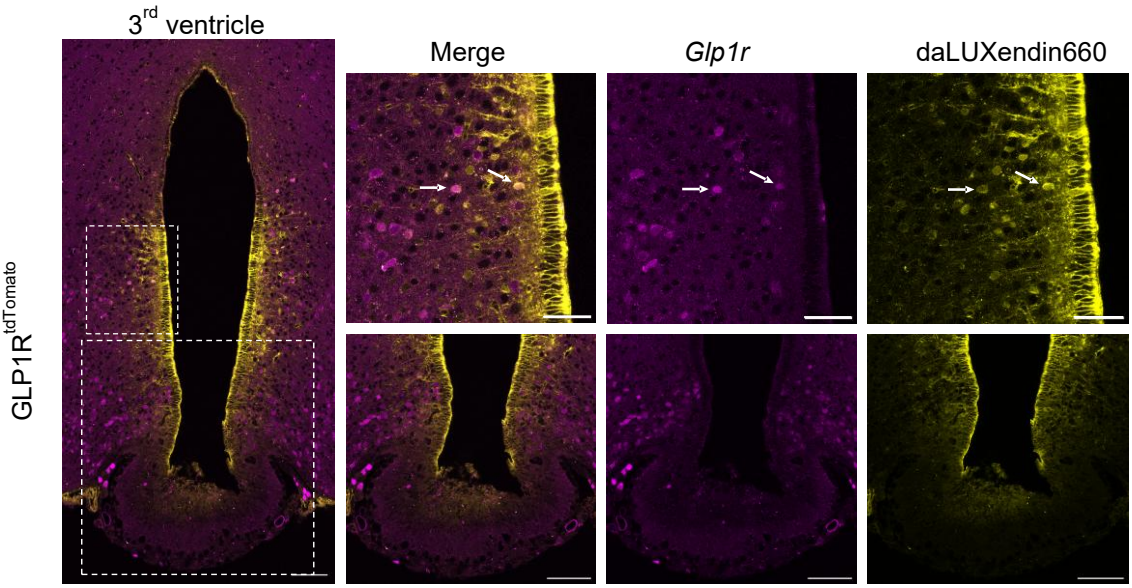

Figure 75: daLUXendin brain labelling after central administration in Glp1r reporter mice. Representative images of 3rd ventricle of GLP1R-Cre:tdTomato mouse following administration of daLUXendin660 into 3rd ventricle. Zoomed panels and white arrows highlight co-localisation of daLUXendin660 with Glp1r-expressing cells lining the 3rd ventricle. Scale bar 100µm.

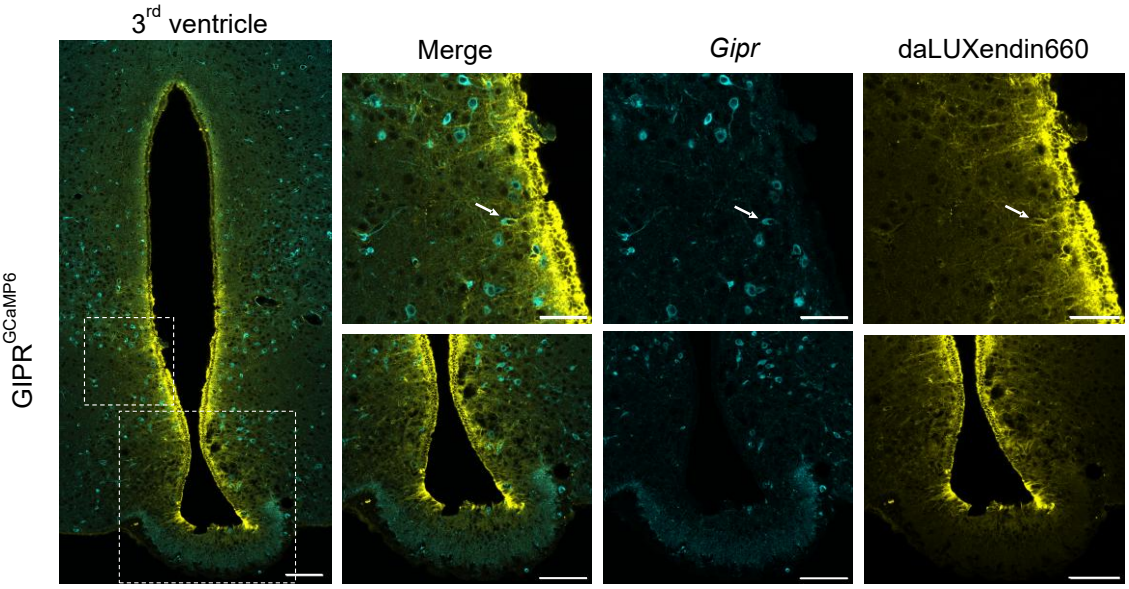

Figure 76: daLUXendin brain labelling after central administration in Gipr reporter mice. Representative images of 3rd ventricle of GIPR-Cre:GCaMP6 mouse following administration of daLUXendin660 into 3rd ventricle. Zoomed panels and white arrows highlight co-localisation of daLUXendin660 with Gipr-expressing cells lining the 3rd ventricle. Scale bars 100µm.

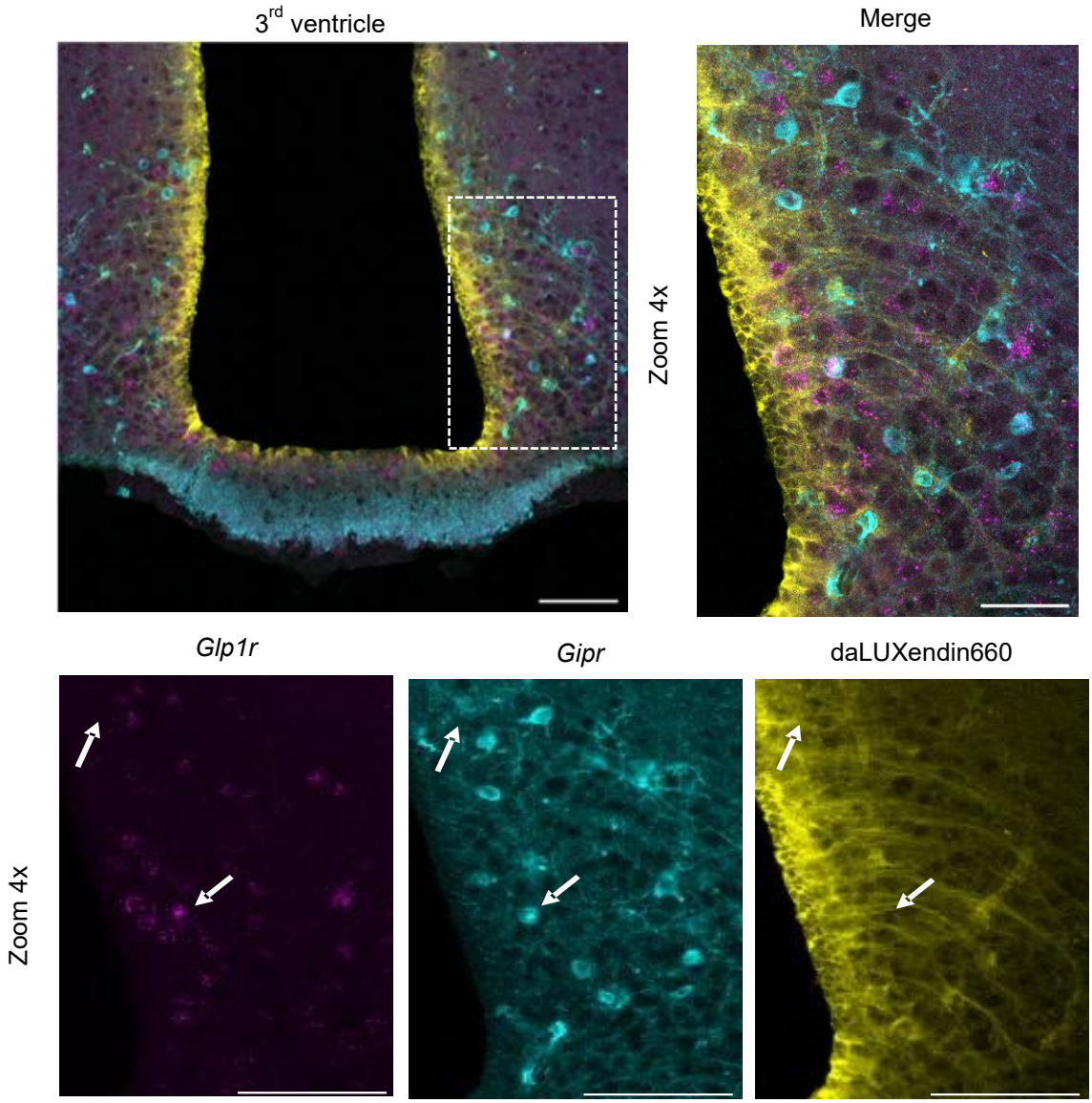

Figure 77: daLUXendin brain labelling after central administration in Gipr reporter mice with Glp1r RNAscope.
Representative images of 3rd ventricle of GIPR-Cre:GCaMP6 mouse following administration of daLUXendin660 into 3rd ventricle and RNAscope identification of Glp1r RNA. Scale bar 100µm.

Discussion

In this chapter, we have demonstrated that daLUXendins reduce food intake and improve glucose tolerance in mice, to a similar extent as tirzepatide. The lack of diacid side chain and therefore reduced albumin binding and shorter half-life is a plausible reason for the reduced efficacy of daLUXendin upon 12h- and 24h-food intake when compared with tirzepatide.

Tirzepatide's interaction with GLP1R and GIPR differs between species, with greater dependence on GIPR >GLP1R in humans but vice versa in mice (412). Confirming pharmacological assessment of daLUXendins, daLUXendin probes were more dependent on signalling via GIPR over GLP1R in the mouse setting. This is advantageous for daLUXendins as it means that in a mouse model, they act more like tirzepatide does at human receptors and subsequent functional studies with daLUXendins may be more translatable – with the caveat that surrounding systems may be different.

Peripherally injected daLUXendins were able to label pancreatic islets and CVOs including the ME, OVLT, SFO and AP. Similar to previous work with GLP1R (298) and GIPR (407) probes, daLUXendin labelling was limited to the CVOs and did not penetrate to deeper structures, specifically those protected by the BBB. Additionally, a GLP1RA agonist/GIPR antagonist peptide-antibody conjugate has a similar degree of penetration but was able to activate c-Fos expression in the NTS as well as the DMH, AP and several nuclei where *Glp1r*/*Gipr* is not known to be expressed (244). Therefore, our findings support the hypothesis that the superior efficacy of modulating GIPR alongside GLP1R agonism is related to the specific neuronal populations engaged with rather than the depth of brain accessed.

Studies of the central effects of single or dual agonists are often performed via central administration and interpretation is therefore limited by the sparse evidence of where and how peripherally administered dual agonists can access the brain. The daLUXendins are bridging this gap by determining the fate of peripherally administered dual agonists and identifying sites where specific knock out of GLP1R/GIPR might be useful for interrogation of dual agonism. For example, focusing on the AP/NTS to confirm snRNAseq work suggesting that the hypophagia associated with dual agonists is due to GIPR activation of a subpopulation of neurones in the AP/NTS region (260,407). Similar studies to delineate which neuronal populations are engaged by dual GLP1R/GIPR agonists or GLP1R agonist/GIPR antagonists would be insightful for the development of further molecules.

As described at the start of the chapter, GIPR agonism appears to exert its central effects in a GLP1R-independent manner via GABA-ergic neurones while GIPR antagonism is dependent upon the presence of both GLP1R and GIPR in non-GABA-ergic neurones. What remains to be seen is whether these agents are targeting neurones that express both receptors, or just one. The low number of dual *Glp1r/Gipr*-expressing cells and sparse co-localisation of ICV-administered daLUXendin660 to neurones expressing both *Glp1r* and *Gipr* suggest that the different components of dual agonists/antagonists may be binding to different neurones in the CVOs.

In the DVC, GIPR antagonism has appeared to mimic GLP1R agonism in relation to DVC neurone gene expression (250), with increases in gene expression from GLP1RA and GIPR antagonism in the same clusters of neurones and decreases in expression in response to GIPR agonism in other clusters of neurones (250). However, in the hypothalamus, gene expression was negatively correlated between GLP1RA and GIPR antagonism across most cell subpopulations (250). This suggests that GIPR antagonism effects upon neurones and augmenting GLP1R action is not uniform across neuronal populations.

Within the AP, *Glp1r* mRNA has been found in different cell populations to those expressing *Gipr* mRNA (244,511), but with the cells in close proximity to one another (244). Intraperitoneal GIP administration increases c-Fos activation within the AP, which was blocked when administered after pre-treatment with an antagonistic GIPR antibody (244). GLP1RA/GIPR antagonistic peptide-antibody conjugate also induced a high degree of c-Fos expression with subsequent treatment with GIP attenuating this expression compared with vehicle treatment (244). Taken together these results suggests that within the AP, the GLP1RA component and GIPR antagonist component of this conjugate act upon different neuronal subpopulations.

In the PVN and SON, spatial transcriptomics have found that with the neurones with the highest *Glp1r* expression also co-express *Gipr* (513). The same authors found that *Glp1r* is only expressed in neurones whereas *Gipr* is expressed in both neurones and non-neuronal cells, such as ependymal cells (513).

Therefore, it is likely that the targets of the components of the ligands modulating GLP1R vs components modulating GIPR differ between brain regions, but with modulation of GIPR playing a bigger role in non-neuronal cells. The daLUXendins could contribute to further exploration of this given their suitability for in vivo administration and for co-staining with other cell or protein markers, such as fluorescent reporter mice for specific neuronal subpopulations.

Although previous studies have demonstrated that incretins are able to access CVOs (253,407,548,627) and activate neurones (253,515,631,632), definitive evidence of the method of incretin transport across the BBB or BCB has yet to be produced. Tanycytes have been suggested to be responsible for GLP1R agonist uptake (551) but such transport has been yet to be elucidated for GIP. This work provides the first confirmation that tanycytes are involved in GIP and dual agonist transport into the brain. This could be

further confirmed by assessing daLUXendin labelling in tanycyte-specific GIPR +/- GLP1R knock out mice (551).

There is evidence that CVOs are able to modify their BCB properties in response to the nutritional status of the individual. In the fasted state, there is greater uptake of critical metabolic substrates such as glucose (623) and increased permeability to peptidic hormones, such as ghrelin (575,633) in certain CVOs lined with tanycytes. This plasticity of the BCB enables access of circulating metabolic signals to the hypothalamic nuclei controlling feeding behaviour, to be adapted to the nutritional state (623).

Specific to incretins, obesity and acute changes in blood glucose levels have been shown to modulate GLP1 access to the hypothalamus, mediated by tanycytes (634); the daLUXendins are well suited to determine if this is the case for dual agonists. By being able to visualise the areas accessible by daLUXendins vs single GLP1R/GIPR agonists in obese model mice, we may be able to determine whether modulation of the BCB or an ability to overcome changes in the BCB are responsible for dual agonist or GLP1RA/GIPR antagonist superior efficacy.

To summarise, in this chapter we have showcased the suitability of daLUXendins for in vivo work, the advantageous selectivity for mGIPR compared with tirzepatide and contributed to the crucial, ongoing work determining how and where incretins are able to access the brain.

Chapter 7: General discussion

Incretins in diabetes and obesity

The incretin hormones GLP1 and GIP play a significant role in the physiology of glucose homeostasis and the pathophysiology of type 2 diabetes and obesity.

The incretin effect delivers a vastly amplified response to oral glucose compared to the equivalent level of hyperglycaemia induced through intravenous glucose (438,635) and GIP is regarded as the main contributor to the incretin effect (439).

Despite this amplification, the risk of hypoglycaemia is low with incretin-based medication (636). This has been attributed to the glucose-dependent nature of GLP1 insulinotropic activity (637,638), sustained glucagon response to hypoglycaemia (reviewed in (636)) and rapid degradation of GLP1 and GIP by DPP4 (639).

The incretin effect is perturbed in people with type 2 diabetes (197) and obesity (219,432).

With GLP1 the defect in diabetes does not appear to be reduced secretion (198,199) but rather reduced responsiveness to GLP1 (200–204) or reduced GLP1R expression (204,640). However, in obesity, whether there are changes in GLP1 secretion remain debated (224–226) although overall response to GLP1 is reduced (641).

Similarly, GIP secretion has been found to be preserved in diabetes (197,202) but its insulinotropic effects are attenuated (206–208) likely due to GIPR downregulation (209–211,640) or defective post-receptor signalling (202,208). In obesity, GIP is hyper secreted (510).

Incretin based treatments

Incretin based therapies for the treatment of diabetes and obesity have been developed for the past several decades (642) and the global GLP1-based medication market size is currently estimated to be worth billions of dollars (643).

The GLP1R agonist liraglutide was the first medication to be licensed for obesity in the UK for over 20 years (28,108). Weight loss affords a reduction in insulin resistance and a delay in diabetes progression (644,645) with the degree of weight loss being a strong predictor of the degree of improved insulin sensitivity (646). However, it has also been shown that GLP1RAs improve insulin resistance and glycaemic control in a weight loss-independent manner (647–649).

GLP1R agonists have since shown promise in several other conditions such as idiopathic intracranial hypertension (311,616), alcohol use disorder (650), Alzheimer's and Parkinson's disease (651) and metabolic dysfunction-associated steatotic liver disease (MASLD) (652–654). Although proteomic data has supported the notion that GLP1RAs (semaglutide) have a beneficial effect of upon these conditions in humans as well (655), most of the data remains pre-clinical or is only supported by real-world observational data (650). Only in MASLD have studies progressed into clinical trials (656,657) using semaglutide, with interim results of the phase 3 trial reporting that semaglutide resolves steatohepatitis and reduces fibrosis, by 28.7% and 14.4% respectively, more than placebo (657). By comparison, resolution of steatohepatitis without worsening of fibrosis was achieved in approximately 20% more than placebo, in trial participants taking the only other licensed medication for liver fibrosis, resmetirom, with a 10% increase in fibrosis improvement compared to placebo (658).

Many patients do not achieve their target glucose and treatment escalation is frequently needed as type 2 diabetes progresses (104). Additionally, discontinuation rates are over 50% for GLP1RAs, with side effects being a main driver for discontinuation (659). Therefore, there is a

drive to develop novel agents with not only improved outcomes for glycaemic control and weight loss but also with an improved side effect profile.

However, there remain many unanswered questions about incretin physiology which could address these clinical issues. Whilst pharmacology of incretins and incretin-based medications is well understood, which cells and tissues are accessible and targeted by incretin-based medications is a current roadblock.

Our contribution to the literature

Generation of well-validated GIPR and dual GLP1R/GIPR fluorescent probes

As discussed in previous chapters, the ability to answer these questions using currently available techniques, such as reporter mice, self-label enzymes and antibodies is limited in terms of both availability of suitably validated reagents and the degree of insight that they can innately provide. Therefore, we generated fluorescent peptide probes; sGIPs, agonists for the GIPR, and daLUXendins, dual GLP1R/GIPR agonists.

Given that the therapeutic efficacy of some ligands is in part due to distinct pharmacological differences, such as signal bias and acylation (660), the need to use dual agonist reagents to investigate dual agonist biology is paramount. The daLUXendins are the first dual GLP1R/GIPR agonist probes to be rigorously validated and published in detail. As described previously, Alexa647-conjugated tirzepatide has been reported but pharmacological validation, such as binding affinity and potency was not included and therefore it should not be regarded as a specific reagent (256).

Validation of any new reagent is crucial to avoid generating inaccurate findings. Unfortunately, there have been several previously published GLP1R antibodies which have been subsequently found to be non-specific (172,257,259). One of the major strengths of our work is the presentation of both pharmacology and in vitro validation of our probes against suitable

controls. Any modification to a peptide ligand can alter key properties and make it a less suitable surrogate (324,338,339).

Pharmacological studies in over expression systems are important to ensure that such key properties, such as binding affinity or imbalanced agonism, of a novel ligand is suitably similar to the ligand it purports to substitute. In vitro validation seeks to reassure users that the ligands are effective and specific, with use of knock out models or co-localisation with other specific markers regarded as high standards for validation (257,259). Furthermore, assessment of reagents in islets is an important facet of validation as the function of islet cell types are reliant on intercellular communication and paracrine action (discussed below) and it has been shown that α and ß cells exist in heterogenous populations in terms of transcriptomics and function (661,662). Therefore, new reagents in this field should demonstrate effective labelling and activation of receptors in islets as well as cell lines.

For the daLUXendins, further validation would include assessing labelling in *Gipr*$^{-/-}$ mice +/- GLP1R antagonism and/or double *Glp1r*$^{-/-}$/*Gipr*$^{-/-}$ mice to confirm specificity.

daLUXendins are suited for exploring imbalanced agonism

Efforts to understand the impressive actions of tirzepatide's dual GLP1R/GIPR agonism compared to single GLP1R agonism have led to the discovery of imbalanced agonism. However, further understanding of how this imbalanced agonism leads to improved outcomes are limited as the imbalance differs between species (255). Although the difference in imbalance is unlikely to alter the cellular substrates that tirzepatide accesses or binds to, it does impede the ability to understand how the biased agonism alters cell or tissue responses.

The engineering of our daLUXendin probes has resulted in an advantageous imbalanced agonism at mouse GLP1R/GIPR. Tirzepatide favours GIPR in human islets and GLP1R in mouse islets (255). This difference is the likely reason behind tirzepatide's attenuated insulinotropic

effect in mice, rendering it equivocal or non-superior to the GLP1R agonist semaglutide (255,412). One previously published dual agonist probe, Alexa647-conjugated tirzepatide had minimal signal in *Glp1r*$^{-/-}$ islets, suggesting a similar favouring of GLP1R (256).

In mice, daLUXendins exhibited a reduced selectivity for GLP1R over GIPR (1:2 GIPR:GLP1R) when compared to tirzepatide (1:8 GIPR:GLP1R), shown both in vitro and in vivo. As a result, daLUXendin probes could be a useful tool for exploring dual agonism in mice, with a biased agonism that is more reflective of tirzepatide action in the human setting. It would also be possible to explore modifications to daLUXendin to drive even greater GIPR selectivity, repeating studies with *Gipr*$^{-/-}$ mice to confirm the selectivity of GIPR binding after modification. Furthermore, it would be helpful from a translational point of view to explore how the inclusion of a diacid side chain might influence receptor selectivity by repeating IPGTTs and cAMP potency studies with daLUXendin+ probes, compared with GIP, GLP1 and tirzepatide.

GLP1R expression is increased in *Gipr*$^{-/-}$ mice

Not only has our validation demonstrated that our probes are specific but has shed further light on the impact that GIPR exerts upon GLP1R. In the global *Gipr*$^{-/-}$ mouse islets, we found an increase in GLP1R labelling, suggesting an increase in GLP1R expression. This adds to the literature debating the mechanism behind why GIPR knockout or antagonism leads to an increased sensitivity to GLP1 (252,389,391). Plasticity of the incretin system has been demonstrated in work led by a colleague, who found that GLP1R is upregulated in ageing and preclinical models of HFD (401). Further studies exploring the effects of chronic GIPR agonism or antagonism upon GLP1R expression would also be informative to determine if that is the key to either of their efficacies or even the nexus of their overlapping efficacies.

daLUXendins label all cell types in the pancreatic islet

It is unclear if the enhanced glycaemic control from tirzepatide is islet-centric or driven by other mechanisms. Given the benefits of glucagon secretion enhancing insulin secretion via GLP1R or GCGR (471), it was thought that tirzepatide capitalises on this through α cell GIPR agonism. Therefore, is the significant improvement in glycaemic control of GIPR antagonism combined with GLP1R agonism (125) unrelated to α cell GIPR mediated glucagon release and suggestive of an extra-islet mechanism? To answer, this it is important to determine which cells tirzepatide binds to within the islet.

The daLUXendin probes co-labelled cells positive for insulin (to the greatest degree), glucagon and somatostatin. The degree of GLP1R and GIPR expression in each cell type coupled with the imbalanced agonism of the daLUXendin probes may suggest the mechanisms by which tirzepatide stimulates the release of all three hormones now that we have confirmed the cellular substrates.

Given that tirzepatide has a greater affinity for GIPR>GLP1R in humans (255), the insulinotropic action upon ß cells is likely to be mediated to a greater degree through GIPR with a smaller contribution from GLP1R activation. As GIPR is more abundant than GLP1R on α cells, glucagon secretion mediated by tirzepatide is also likely driven through GIPR activation.

Recent super-resolution imaging work from our lab did not detect the presence of GLP1R in δ cells (identified using a knock-out-validated antibody) (labelled with anti-somatostatin antibody) (401). However, although fluorescence-activated cell sorting (FACS) studies did not find GLP1R protein in somatostatin-positive cells, they did identify *Glp1r* transcripts (261) and δ cells have been found to release somatostatin in response to GLP1 (40,185,187,469,470). Additionally, δ cells have demonstrated plasticity and the ability to adopt a ß cell-like identity after ß cell ablation (663–665), so GLP1R could therefore be upregulated in these cells. Taken together, this may suggest that GLP1R expression occurs in δ cells but at levels below the sensitivity of currently available reagents or that they may only be detected in the dysregulated,

ß cell deficient settings of diabetes. Therefore, dual GLP1R/GIPR agonist action upon δ cells may occur via both receptors.

Given the highly interrelated activity between islet cell types and the likely mediation of this via GLP1R and GIPR (reviewed in (349)), it is likely that tirzepatide is modulating glycaemic control through both direct insulinotropic effects on ß cells in addition to paracrine actions. For example, insulin secretion is co-ordinated between ß cells via gap junctions (666) and glucagon released from α cells binds to both GLP1R and GCGR to stimulate insulin release (385,471,499,667) in a co-ordinated manner (553).

Furthermore, damage or disruption to one cell type is likely to affect the function of the other cell types (40,472,668,669). Determining the importance of GLP1R and GIPR in these relationships could establish whether tirzepatide or future novel agents can rescue this disruption and could explain their enhanced efficacy. sGIP and daLUXendin probes would be well suited to investigate facets of this line of enquiry if applied to α or δ cell specific *Glp1r* or *Gipr* knock out islets.

Dual agonism increases nanodomain formation

GPCRs form clusters, known as nanodomains, both at the cell surface and intracellularly which are important for signalling (269,275,493). By comparing nanodomain formation induced by single GLP1R antagonist (LUXendin), single GIPR agonist (sGIP) and daLUXendin probes we found that dual agonism increases the number of nanodomains compared to single GIPR agonism.

The number of receptors per nanodomain and the size of the nanodomains were similar across all three probes. Therefore, we postulate that the increase in nanodomain formation from dual agonism over single GIPR agonism is either due to triggering GLP1R clustering or inducing heterotypic clustering of GLP1R and GIPR. GLP1R-GIPR dimers have been postulated to be

generated by a GIPR Ab-GLP1R peptide conjugate and simultaneous activation of both receptors by one molecule is thought to be key to triggering ß arrestin recruitment (283). Additionally, cAMP nanodomain formation related to GLP1R has been linked to amplification of certain signalling pathways (505) and given that tirzepatide enhances GLP1R surface expression, this could suggest other potential intra-islet mechanisms for the increased efficacy of dual GLP1R/GIPR agonists on glycaemic control.

sGIP and daLUXendins access the brain via CVOs

Both sGIP and daLUXendin probes have provided further insight into the target substrates in the brain.

GIPR expression is necessary for the enhanced weight loss induced by dual GLP1R/GIPR agonism (514) and weight loss still occurs, albeit attenuated, in GLP1RKO mice when GIPR is blocked (244,659). This suggests a central role for modulating GIPR signalling in the brain and the importance of determining its function in energy homeostasis. Work has been undertaken with specific neuronal knock out models to delineate which neuronal populations are involved in GIPR-driven mechanisms of weight loss (407). However, to link the actions of peripherally administered single or dual agonists with central effects it needs to be confirmed that such agonists can access relevant parts of the brain.

sGIP (407) and daLUXendin administration in vivo has been found to label the circumventricular organs but were unable to label deeper structures. Recent work has also confirmed the importance of CVOs for incretin access to the brain and suggested that GLP1R and GIPR are expressed on different cell populations within the AP (244). This work, using a GIPRAb/GLP1RA antibody-peptide conjugate that blocked GIPR whilst agonising GLP1R, found that their conjugate accessed the CVOs and activated downstream neurones involved in appetite regulation (244). Therefore, it seems likely that the superior effects of dual agonists are not

related to the extent of brain penetration but pertain either to the amount of ligand that is able to access the brain, the different neuronal populations engaged or perhaps interaction between GLP1R and GIPR.

The question of how the ligands are permitted to cross the blood-brain or blood-CSF barrier remains unclear. To this aim, following central administration daLUXendin we demonstrated localisation not just to *Gipr* and *Glp1r* positive neurones, but also to tanycytes. Not only do tanycytes control the transport of molecules across the blood-CSF barrier (573,670), but they also control neuronal function by releasing both orexigenic and anorexigenic factors (reviewed in (671). Tanycytes have been shown to activate neurones in the arcuate nucleus (672), and indeed, tanycyte ablation in the arcuate nucleus and median eminence resulted in increased weight gain from HFD and less fat oxidation compared to WT controls (673). Access and activity of peripherally administered GLP1 is reliant upon tanycytes (634) so demonstrating dual GLP1R/GIPR agonist binding to tanycytes suggests further direction for interrogation. Is GIP agonism (or antagonism) action in the brain also reliant upon tanycyte mediation? Does tanycyte access and activation of neurones differ if they are bound by both GLP1 and GIP, compared to just one ligand? Recent reviews of GIPR agonism and antagonism have suggested that GIP plays an inhibitory role, via GABAergic neurones, in modulating GLP1 action in the brain which results in attenuation of the satiating effect of GLP1 but also decreasing aversive responses (126,173). Could a similar regulatory action of GIP be occurring in or via tanycytes?

Limitations of our work

While daLUXendins were able to retain labelling islets post-fixation, it was unfortunate that the sGIP probes were not able to. Being able to co-label cells stained for insulin, glucagon and somatostatin would have contributed to the literature regarding which cells within the pancreatic islet express GIPR. Currently, the data regarding this is mainly limited to RNA levels,

which may not be reflective of protein expression. Understanding this would give us greater insight into the impact of GIP upon islet paracrine activity and potentially provide further understanding of whether improved paracrine action is responsible for the impressive improvement in glycaemic control caused by dual GLP1R/GIPR agonists.

Although the daLUXendin probes demonstrated comparable binding affinity and cAMP generation to tirzepatide, it is important to note that they are different molecules. Detailed pharmacokinetic studies (particularly signal bias) would need to be completed to confirm that the daLUXendin probes are an equivalent proxy for tirzepatide. However, the addition of a side chain in the daLUXendin+ probes yielded similar pharmacology, receptor binding and brain labelling results as daLUXendins, suggesting that the lack of side chain did not cause a major disturbance. Therefore, it is reasonable to conclude that these probes are useful tools for pre-clinical investigation of dual agonism.

daLUXendin660 reduced food intake at 12h and 24h after post-dose but the degree of reduction was greater with tirzepatide. We postulate that this is related to the diacid side chain conferring a longer half-life so further assessment with daLUXendin+ probes, which harbour the side chain, would be helpful in determining if this is true. However, glucose tolerance was similar between daLUXendin660 and tirzepatide which may suggest that the longer half-life is more integral to central actions of tirzepatide than islet action. To confirm this hypothesis, studies could be repeated with daLUXendin+ probes, which have an intact diacid side chain and therefore longer half-life through albumin-binding.

We did not pursue work in human islets with the daLUXendin probes due to the significant autofluorescence, likely due to lipofuscin accumulation (82). Additionally, our lab (401) and others (480,481) have experienced significant heterogeneity in GLP1R/GIPR expression and stimulation in human islets. Therefore, we made the pragmatic decision to continue work using induced pluripotent stem cell derived islets which, in our experience, have proved a more consistent model of GLP1R/GIPR expression and identification (401).

Our sGIP and daLUXendin probes currently have a limited colour palette of Cy3, Cy5 and SiR-d12 fluorophores which may limit their use alongside other markers or reagents. These fluorophores were chosen because they have previously demonstrated a high-quality labelling in complex tissue (269,298,419) and do not have properties are unfavourable for labelling – such as the repulsion from Alexa647 (269,428). In the future, the range of probes could be grown to include a wider range of fluorophores and/or epitope tags to facilitate signal amplification. Furthermore, they are suitable for modification to include affinity for other receptors of interest and we have now generated a triple GLP1R/GIPR/GCGR agonist probe to study the targets and effects of triple agonists such as retatrutide.

The next steps for incretin research

GIPR – to agonise or antagonise?

As these probes are suitable for in vivo administration, they could be used to determine the answer to a key question in GIP pharmacology – if chronic agonism of GIPR leads to functional antagonism through downregulation of GIPR. By chronically dosing animals with sGIP, GIPR presence could be visualised at different time points to determine if downregulation occurs, alongside assessment of food intake and weight and comparison to mice administered unlabelled GIP. Similar work could be performed with daLUXendin probes, with staining of fixed islets for insulin, glucagon and somatostatin to ascertain if any downregulation occurs more predominantly in specific cell compartments.

Questions remain regarding how both GIPR agonism and antagonism, when paired with GLP1R agonism, can both be beneficial for weight loss. One theory is that GIPR activation inhibits GLP1R action in the CNS, both reducing GLP1 anorectic effects but also aversive responses (674). Whereas GIPR antagonism permits the full anorectic effects of GLP1 at the expense of higher degree of aversive responses (674).

It has been shown that GIP engages distinct anorexigenic pathways in different brain regions (407) and therefore suggested that the target substrates and signalling pathways of GIPR agonists and antagonists may also differ. To support this, weight loss and reduced food intake from GIPR agonism has been shown to act via GABA-ergic *Gipr* positive neurones (253) whereas GIPR antagonism, via a blocking antibody, has induced weight loss when GIPR is knocked out from GABA-ergic neurones (244,250). Furthermore, the weight loss and food-intake reducing effects of GIPR antagonism are dependent upon functional GLP1R (244,250).

The extent of brain penetration of both GIPR agonists (407) and antagonists (244) is similar and limited to the CVOs. Therefore, it seems that the key to determining their contradicting efficacies is to confirm the divergence in neuronal networks engaged by agonists and antagonists and to explore the GLP1R-dependency of GIPR antagonists (674).

Exploring the different neuronal pathways engaged by GIPR antagonists and antagonists could be achieved through comparing cFos activation of specific neuronal populations linked to food intake and weight loss (e.g. arcuate nucleus in the hypothalamic and the DVC in the hindbrain) after peripheral administration of GIPR agonist and antagonist in neurone specific knock out models. Alternatively, or additionally, the RiboTag technique could be used to interrogate the profile of actively transcribed mRNA of selected neurones (675). This technique involves crossing the RiboTag mouse model, which has a floxed hemagglutinin(HA)-tagged allele of a ribosomal protein, with a cell-type-specific Cre recombinase-expressing mouse (675). When the Cre recombinase is activated by expression of the associated cell-specific gene, the epitope-tagged ribosomal protein is expressed and after immunoprecipitation of the polysomes containing a antibodies against HA, mRNA transcripts from a specific cell type can be obtained (675). Determining and comparing the transcriptome of neurones activated by GIPR agonists and antagonists would allow further delineation of central mechanisms of action. The specificity of sGIP648 central labelling has been demonstrated by failure to activate cFos in the DVC in *Gipr*$^{-/-}$ mice (407). By using sGIP648 or a daLUXendin probe as an agonist, there would be

visual confirmation of which neurones are accessed and whether there may be compensatory changes in GIPR expression in knock out models.

GIPR in adipose tissue

Whether GIPR induces weight loss through peripheral action on adipose tissue remains debated. This is in part because identification of the cellular source of GIPR expression within white or brown adipose tissue has not been confirmed but also because the effect of GIP upon lipogenesis, independent of insulin, is unclear (reviewed in (380)).

One proposed mechanism for GIPR-induced weight loss is increased energy expenditure in white adipose tissue, via futile calcium cycling (284). The authors found that increased GIPR expression was associated with decreased fat mass in obese mice and a transient decreased in food intake which normalised after 5 days (284). However, these studies were performed in an overexpression model where GIPR was induced in adipocytes so conclusions cannot be drawn regarding whether these mechanisms occur with endogenously expressed GIPR.

For white adipose tissue (WAT), pre-clinical work in cell lines originating from adipocyte precursors found that *Gipr* mRNA expression increased in line with other markers of differentiation (such as *GLUT-4* and *leptin*), as differentiation was induced (676) suggesting that it is expressed natively. Selective knock-in of *Gipr* in adipocytes of $Gipr^{-/-}$ mice (441) and knockout in $Gipr^{-/-Ap2}$ mice (350) found that *Gipr* in adipocytes did not play a significant role in GIP mediated protection against diet induced obesity and attributed any weight loss to a reduction in lean mass. However, the expression of the *Ap2* promoter has been reported as promiscuous, with its expression permitting Cre activity in adipocyte precursors, endothelial cells and the brain (677). *Gipr*/GIPR levels were not comprehensively reported, meaning that *Gipr* knockout in other tissues could have contributed to the phenotype.

GIPR mRNA has been found in samples of subcutaneous (678) and visceral WAT, but receptors were downregulated and lower responsiveness to GIP in samples from people with obesity compared with lean subjects was reported (679). In post-menopausal women with obesity, *GIPR* mRNA was also found in WAT and at a reduced level in samples from women with obesity compared with women without obesity (680).

For BAT *Gipr* mRNA transcripts have been detected, and use of a promoter (*Myf5-Cre*) specific to BAT has enabled the development of a BAT-specific *Gipr* knockout model. $Gipr^{-/-BAT}$ mice demonstrated perturbed lipid metabolism but no protection against diet induced obesity unless in the setting of an acute cold challenge (681).

In both WAT and BAT, expression of GIPR protein has not been fully investigated. sGIP probes could be a useful tool for corroborating mRNA-based findings and further delineating which cell types within adipose tissue (if any) express GIPR, given that sGIP is suitable for co-labelling with markers for other cells or protein of interest.

Incorporating GCGR agonism

In recent years, incretin research has been partly driven by advances in incretin-based pharmaceuticals whose pharmacological evaluation and clinical results have subsequently suggestedinterrogable aspects to incretin biology. On the horizon are agents which incorporate GCGR receptor activity. Survodutide is a dual GLP1R/GCGR agonist being developed for obesity and metabolic dysfunction associated steatohepatitis and fibrosis (682). Recent phase 2 trials for its use in the treatment of obesity reported a total body weight loss for maximally dosed survodutide of 12.1% greater than placebo (683) and it is currently undergoing phase 3 trials for people with obesity with and without type 2 diabetes (684). Retatrutide is a triple GLP1R/GIPR/GCGR agonist showing promise as a novel agent for obesity with Phase 2 trials demonstrating an additional loss of 22.1% total body weight more than placebo (136).

Glucagon is known to reduce food intake and weight in both rodents (685,686) and humans (687–690) via stimulating vagus afferent fibres in the liver which communicate with feeding centres in the hypothalamus (691). Its central actions induce satiation rather than affecting satiety (692,693) or food aversion (694). Glucagon's effects upon satiation have been attributed to activation of vagal afferents in the liver (692,695).

Glucagon's role in inducing hyperglycaemia through heightened hepatic glucose output has, until now, limited its therapeutic role to rescuing hypoglycaemia. However, several preclinical studies found that co-agonism of GLP1R and GCGR ((696) and reviewed in (691)) and triple agonism of GLP1R/GIPR/GCGR (444) corrected diet-induced obesity, hepatic steatosis, hypercholesterolaemia and hyperglycaemia. Additionally, GCGR expression on ß cells has been demonstrated to be key to insulin secretion; in particular *Ggcr*$^{-/-ßcell}$ islets demonstrated loss of co-ordinated Ca^{2+} oscillations and impaired early GSIS (553). Furthermore, a balanced GLP1R/GIPR/GCGR triple agonist was superior to a dual GLP1R/GIPR agonist in normalising body weight in obese mice (697). This was postulated to be due to the thermogenic, lipolytic and anorexigenic effects of GCGR agonism, with GLP1R agonism constraining glucagon's hyperglycaemic action (444,696). Attenuated effects after knocking out each of the receptors confirmed the importance of each axis to the performance of the dual GLP1R/GIPR agonists (696) and triple GLP1R/GIPR/GCGR agonists (444). For triple agonists, it appears that while GLP1R and GIPR are essential for the improvement of glycaemic control and total body weight loss, GCGR agonism is required for fat mass reduction via increased energy expenditure (444). Additionally, combined GCGR and GLP1R agonism has shown impressive effects in improving hepatic steatosis and fibrosis (reviewed in (698)).

We have already generated a modified daLUXendin probe which incorporates GCGR agonism, to confirm where triple agonists are able to access after in vivo administration and explore cellular substrates in tissues postulated to be of importance to triple agonist effects. For example, GCGR is present in abundance in the brainstem, arcuate nucleus and DVC (699) but

not in the mesolimbic reward centres, such as the hippocampus, where it is thought that GLP1R agonism modulates reward pathways (700,701). Could the structure and any further imbalanced agonism of triple agonists alter the neuronal networks engaged, compared to single or dual agonists? GCGR is highly expressed in the liver (702,703) whereas GIPR (703–705) and GLP1R (703,705,706) have not been reported to be expressed there. (702,703) It would therefore be helpful to confirm if triple agonists access the liver which may suggest that the enhanced effect of GCGR agonism upon GLP1R/GIPR agonism lies in the liver, perhaps through activating vagal afferents to induce satiation. Liver specific knockout of GCGR would be necessary to confirm this.

Concluding remarks

In this thesis, two important sets of novel fluorescent probes have been presented. We have carried out pharmacological validation compared to native ligands and described how to label cells for both live imaging and imaging after fixation.

Overall, we have shown that these novel probes are specific and versatile, suitable for use with other labelling techniques and a range of microscopy modalities. We have added to the literature surrounding GIPR expression upon δ cells and the consequences of GIPR knock out on GLP1R expression. Additionally, we have provided the first insights into the effect of dual GLP1R/GIPR agonism upon nanodomain formation and access to the brain, suggesting that the beneficial effects of dual agonists may be reliant upon enhanced receptor clustering and that centrally mediated weight loss is due to the activation of different neuronal pathways rather than extent of drug access.

The understanding of incretin biology has been reliant upon complimentary work of many researchers developing and using a range of reagents. sGIP and daLUXendin probes have successfully contributed to the selection of tools available to interrogate incretin biology and to shine a light on further areas of study.

As we experience the next leap forward in incretin-based pharmaceuticals, our probes, and further iterations, will help illuminate incretin biology to find interrogable mechanisms and ultimately facilitate optimising treatments for people with diabetes, obesity and other chronic conditions.

Appendix 1

	GLP-1	GIP	Tirzepatide
hGLP1R EC50 best-fit	3.358E-09	0.00004436	5.67E-08
hGLP1R EC50 95% CI	2.507e-009 to 4.459e-009	N/A	3.740e-008 to 8.632e-008
mGLP1R EC50 best-fit	1.297E-09	0.00002552	2.944E-08
mGLP1R EC50 95% CI	9.533e-010 to 1.757e-009	N/A	2.030e-008 to 4.244e-008
hGIPR EC50 best-fit	1.072E-07	1.18E-10	6.414E-10
hGIPR EC50 95% CI	1.142e-008 to 2.579e-006	6.934e-011 to 1.993e-010	3.689e-010 to 1.091e-009
mGIPR EC50 best-fit	6.034E-08	5.564E-10	1.116E-07
mGIPR EC50 95% CI	N/A	3.663e-010 to 8.349e-010	6.451e-008 to 1.906e-007

	daLUXendin544	daLUXendin660
hGLP1R EC50 best-fit	2.552E-07	1.389E-08
hGLP1R EC50 95% CI	1.549e-007 to 4.372e-007	8.683e-009 to 2.167e-008
mGLP1R EC50 best-fit	6.941E-08	5.737E-09
mGLP1R EC50 95% CI	4.186e-008 to 1.144e-007	3.789e-009 to 8.602e-009
hGIPR EC50 best-fit	5.141E-09	2.66E-10
hGIPR EC50 95% CI	2.936e-009 to 8.892e-009	1.432e-010 to 4.861e-010
mGIPR EC50 best-fit	8.756E-08	4.402E-09
mGIPR EC50 95% CI	4.499e-008 to 1.677e-007	2.597e-009 to 7.249e-009

EC_{50} values for GLP1, GIP, Tirzepatide, daLUXendin544 and daLUXendin660 against human GLP1R (hGLP1R), mouse GLP1R (mGLP1R), human GIPR (hGIPR) and mouse GIPR (mGIPR).

	hGLP1R	hGIPR	mGLP1R	mGIPR
Tirzepatide fold-change GLP1/GIP	16.904	5.408	22.699	200.447
daLUXendin544 fold-change GLP1/GIP	76.033	43.351	53.58	157.398
daLUXendin660 fold-change GLP1/GIP	4.14	2.239	4.426	7.907

Ligand selectivity of tirzepatide), daLUX544 and daLUX660 for human GLP1R (hGLP1R), human GIPR (hGIPR), mouse GLP1R (mGLP1R) and mouse GIPR (mGIPR), calculated as fold-decrease in cAMP EC_{50} versus either GLP1 or GIP (n = 4 independent repeats).

References

1. International Diabetes Federation. IDF Diabetes Atlas 2025 [Internet]. 2025 [cited 2025 May 28]. Available from: https://diabetesatlas.org/resources/idf-diabetes-atlas-2025/
2. Department of Health and Social Care. Diabetes - Data - Fingertips [Internet]. 2025 [cited 2025 May 28]. Available from: https://fingertips.phe.org.uk/profile/diabetes-ft/data#page/1
3. NHS England. National Diabetes Audit - 2024-25 Quarterly Report [Internet]. 2025 [cited 2025 May 28]. Available from: https://digital.nhs.uk/data-and-information/publications/statistical/national-diabetes-audit
4. World Obesity Federation. Global Obesity Observatory [Internet]. 2025 [cited 2025 May 28]. Available from: https://data.worldobesity.org/
5. Department of Health and Social Care. Obesity Profile - Data - Fingertips [Internet]. 2024 [cited 2025 May 28]. Available from: https://fingertips.phe.org.uk/profile/national-child-measurement-programme/data#page/1/gid/1938133368/pat/159/par/K02000001/ati/15/are/E92000001/yrr/1/cid/4/tbm/1
6. NHS England Digital. Health survey for England - Adult overweight and obesity [Internet]. 2024 Sep [cited 2025 May 28]. Available from: https://digital.nhs.uk/data-and-information/publications/statistical/health-survey-for-england/2022-part-2/adult-overweight-and-obesity#overweight-obesity-and-health
7. NHS England, NHS Wales, Diabetes UK, Health Quality Improvement Partnership. National Diabetes Audit - Complications and Mortality Outcomes Dashboard [Internet]. 2024 [cited 2025 May 28]. Available from:

https://app.powerbi.com/view?r=eyJrIjoiM2FlZTQ4NzgtZTk3My00ODc1LTkxN2MtMDkxZTNkMzA0ZTU5IiwidCI6IjM3YzM1NGIyLTg1YjAtNDdmNS1iMjIyLTA3YjQ4ZDc3NGVlMyJ9

8. Must A, Spadano J, Coakley EH, Field AE, Colditz G, Dietz WH. The Disease Burden Associated With Overweight and Obesity. JAMA [Internet]. 1999 Oct 27 [cited 2025 May 28];282(16):1523–9. Available from: https://jamanetwork.com/journals/jama/fullarticle/192030

9. Pi-Sunyer FX. Medical hazards of obesity. Ann Intern Med [Internet]. 1993 Aug 15 [cited 2025 May 28];119(7 II):655–60. Available from: /doi/pdf/10.7326/0003-4819-119-7_Part_2-199310011-00006?download=true

10. Burton BT, Foster WR. Health Implications of Obesity: An NIH Consensus Development Conference. J Am Diet Assoc [Internet]. 1985 Sep 1 [cited 2025 May 28];85(9):1117–21. Available from: https://www.sciencedirect.com/science/article/pii/S0002822321037688

11. Mandic M, Safizadeh F, Schöttker B, Holleczek B, Hoffmeister M, Brenner H. Body mass index across adulthood, weight gain and cancer risk: a population-based cohort study. BMC Cancer [Internet]. 2025 Dec 1 [cited 2025 May 28];25(1):1–10. Available from: https://bmccancer.biomedcentral.com/articles/10.1186/s12885-025-13855-0

12. Obesity and Cancer Fact Sheet - NCI [Internet]. [cited 2025 May 28]. Available from: https://www.cancer.gov/about-cancer/causes-prevention/risk/obesity/obesity-fact-sheet

13. World Obesity Federation. World Obesity Atlas 2025 [Internet]. London; 2025 [cited 2025 May 28]. Available from: www.worldobesity.org

14. Zhou XD, Chen QF, Yang W, Zuluaga M, Targher G, Byrne CD, et al. Burden of disease attributable to high body mass index: an analysis of data from the Global Burden of Disease Study 2021. EClinicalMedicine [Internet]. 2024 Oct 1 [cited 2025 May 28];76:102848. Available from: https://pmc.ncbi.nlm.nih.gov/articles/PMC11462227/

15. Zhang H, Zhou XD, Shapiro MD, Lip GYH, Tilg H, Valenti L, et al. Global burden of metabolic diseases, 1990–2021. Metabolism [Internet]. 2024 Nov 1 [cited 2025 May 28];160. Available from: https://www.metabolismjournal.com/action/showFullText?pii=S0026049524002269

16. Hex N, MacDonald R, Pocock J, Uzdzinska B, Taylor M, Atkin M, et al. Estimation of the direct health and indirect societal costs of diabetes in the UK using a cost of illness model. Diabetic Medicine. 2024 Sep 1;

17. Okunogbe A, Nugent R, Spencer G, Powis J, Ralston J, Wilding J. Economic impacts of overweight and obesity: current and future estimates for 161 countries. BMJ Glob Health [Internet]. 2022 Sep 20 [cited 2025 May 28];7(9):e009773. Available from: https://pmc.ncbi.nlm.nih.gov/articles/PMC9494015/

18. Frontier economics. Estimating the full costs of obesity: A report for Novo Nordisk [Internet]. 2022 Jan [cited 2025 May 28]. Available from: https://www.frontier-economics.com/uk/en/news-and-insights/articles/article-i9130-the-annual-social-cost-of-obesity-in-the-uk/

19. Abdullah A, Peeters A, de Courten M, Stoelwinder J. The magnitude of association between overweight and obesity and the risk of diabetes: A meta-analysis of prospective cohort studies. Diabetes Res Clin Pract [Internet]. 2010 Sep 1 [cited 2025 May 29];89(3):309–19. Available from: https://www.diabetesresearchclinicalpractice.com/action/showFullText?pii=S0168822710001944

20. Kahn SE, Hull RL, Utzschneider KM. Mechanisms linking obesity to insulin resistance and type 2 diabetes. Nature [Internet]. 2006 Dec 14 [cited 2025 May 29];444(7121):840–6. Available from: https://www.nature.com/articles/nature05482

21. Grundy SM, Cleeman JI, Daniels SR, Donato KA, Eckel RH, Franklin BA, et al. Diagnosis and Management of the Metabolic Syndrome. Circulation [Internet]. 2005 Oct 25 [cited

2025 May 29];112(17):2735–52. Available from: /doi/pdf/10.1161/CIRCULATIONAHA.105.169404?download=true

22. Zimmet P, Magliano D, Matsuzawa Y, Alberti G, Shaw J. The Metabolic Syndrome: A Global Public Health Problem and A New Definition. J Atheroscler Thromb. 2005;12(6):295–300.
23. Swarup S, Ahmed I, Grigorova Y, Zeltser R. Metabolic Syndrome. StatPearls [Internet]. 2024 Mar 7 [cited 2025 May 29]; Available from: https://www.ncbi.nlm.nih.gov/books/NBK459248/
24. World Health Organisation. Diabetes fact sheet [Internet]. 2024 [cited 2025 Jun 6]. Available from: https://www.who.int/news-room/fact-sheets/detail/diabetes
25. World Health Organization. Diagnosis and Management of Type 2 Diabetes (HEARTS-D) [Internet]. Geneva; 2020 [cited 2025 Jun 6]. Available from: https://iris.who.int/bitstream/handle/10665/331710/WHO-UCN-NCD-20.1-eng.pdf
26. NICE. Diabetes - type 2 - Diagnosis in adults (CKS) [Internet]. 2025 [cited 2025 Jun 6]. Available from: https://cks.nice.org.uk/topics/diabetes-type-2/diagnosis/diagnosis-in-adults/
27. World Health Organisation. A healthy lifestyle - WHO recommendations [Internet]. 2012 [cited 2025 May 29]. Available from: https://www.who.int/europe/news-room/fact-sheets/item/a-healthy-lifestyle---who-recommendations
28. NICE. Overweight and obesity management [NICE NG246]. 2025 Jan 14 [cited 2025 May 29]; Available from: https://www.nice.org.uk/guidance/ng246
29. World Obesity Federation. Obesity Classification [Internet]. 2022 [cited 2025 May 29]. Available from: https://www.worldobesity.org/about/about-obesity/obesity-classification
30. Sharma AM, Kushner RF. A proposed clinical staging system for obesity. Int J Obes [Internet]. 2009 Mar 3 [cited 2025 May 29];33(3):289–95. Available from: https://www.nature.com/articles/ijo20092

31. Hu C, Chen Y, Yin X, Xu R, Yin C, Wang C, et al. Pancreatic endocrine and exocrine signaling and crosstalk in physiological and pathological status. Signal Transduction and Targeted Therapy 2025 10:1 [Internet]. 2025 Feb 14 [cited 2025 Jun 6];10(1):1–30. Available from: https://www.nature.com/articles/s41392-024-02098-3

32. Röder P V., Wu B, Liu Y, Han W. Pancreatic regulation of glucose homeostasis. Exp Mol Med [Internet]. 2016 Mar 11 [cited 2025 Jun 10];48(3):e219. Available from: https://pmc.ncbi.nlm.nih.gov/articles/PMC4892884/

33. Brissova M, Fowler MJ, Nicholson WE, Chu A, Hirshberg B, Harlan DM, et al. Assessment of human pancreatic islet architecture and composition by laser scanning confocal microscopy. Journal of Histochemistry and Cytochemistry [Internet]. 2005 Sep 1 [cited 2025 Jan 16];53(9):1087–97. Available from: https://journals.sagepub.com/doi/10.1369/jhc.5C6684.2005?url_ver=Z39.88-2003&rfr_id=ori%3Arid%3Acrossref.org&rfr_dat=cr_pub++0pubmed

34. Wierup N, Svensson H, Mulder H, Sundler F. The ghrelin cell: a novel developmentally regulated islet cell in the human pancreas. Regul Pept [Internet]. 2002 Jul 15 [cited 2025 Jun 10];107(1–3):63–9. Available from: https://www.sciencedirect.com/science/article/pii/S0167011502000678?via%3Dihub

35. Katsuura G, Asakawa A, Inui A. Roles of pancreatic polypeptide in regulation of food intake. Peptides (NY) [Internet]. 2002 Feb 1 [cited 2025 Jun 10];23(2):323–9. Available from: https://www.sciencedirect.com/science/article/pii/S0196978101006040?via%3Dihub

36. Weir GC, Bonner-Weir S. Pancreatic Somatostatin. Adv Exp Med Biol [Internet]. 1985 [cited 2025 Jun 7];188:403–23. Available from: https://link.springer.com/chapter/10.1007/978-1-4615-7886-4_22

37. Gromada J, Franklin I, Wollheim CB. α-Cells of the Endocrine Pancreas: 35 Years of Research but the Enigma Remains. Endocr Rev [Internet]. 2007 Feb 1 [cited 2025 Jun 7];28(1):84–116. Available from: https://dx.doi.org/10.1210/er.2006-0007

38. Weir GC, Bonner-Weir S. Islets of Langerhans: the puzzle of intraislet interactions and their relevance to diabetes. Journal of Clinical Investigation [Internet]. 1990 [cited 2025 Jun 7];85(4):983. Available from: https://pmc.ncbi.nlm.nih.gov/articles/PMC296525/

39. Samols E, Bonner-Weir S, Weir GC. 2 Intra-islet insulin—glucagon—somatostatin relationships. Clin Endocrinol Metab [Internet]. 1986 Feb 1 [cited 2025 Jun 7];15(1):33–58. Available from: https://www.sciencedirect.com/science/article/pii/S0300595X8680041X

40. Rorsman P, Huising MO. The somatostatin-secreting pancreatic δ-cell in health and disease. Nature Reviews Endocrinology 2018 14:7 [Internet]. 2018 May 17 [cited 2025 Apr 15];14(7):404–14. Available from: https://www.nature.com/articles/s41574-018-0020-6

41. Kim A, Miller K, Jo J, Kilimnik G, Wojcik P, Hara M. Islet architecture: A comparative study. Islets [Internet]. 2009 [cited 2025 Jan 16];1(2):129. Available from: https://pmc.ncbi.nlm.nih.gov/articles/PMC2894473/

42. Cabrera O, Berman DM, Kenyon NS, Ricordi C, Berggren PO, Caicedo A. The unique cytoarchitecture of human pancreatic islets has implications for islet cell function. Proc Natl Acad Sci U S A [Internet]. 2006 Feb 14 [cited 2025 Jan 16];103(7):2334. Available from: https://pmc.ncbi.nlm.nih.gov/articles/PMC1413730/

43. Kilimnik G, Jo J, Periwal V, Zielinski MC, Hara M. Quantification of islet size and architecture. Islets [Internet]. 2012 Mar [cited 2025 Jan 16];4(2):167. Available from: https://pmc.ncbi.nlm.nih.gov/articles/PMC3396703/

44. Ionescu-Tirgoviste C, Gagniuc PA, Gubceac E, Mardare L, Popescu I, Dima S, et al. A 3D map of the islet routes throughout the healthy human pancreas. Sci Rep [Internet]. 2015

Sep 29 [cited 2025 Jan 16];5:14634. Available from: https://pmc.ncbi.nlm.nih.gov/articles/PMC4586491/

45. Göke B. Islet cell function: α and β cells – partners towards normoglycaemia. Int J Clin Pract [Internet]. 2008 Mar [cited 2025 Jun 10];62(SUPPL. 159):2–7. Available from: /doi/pdf/10.1111/j.1742-1241.2007.01686.x

46. Epstein FH, Moller DE, Flier JS. Insulin Resistance — Mechanisms, Syndromes, and Implications. New England Journal of Medicine [Internet]. 1991 Sep 26 [cited 2025 Jun 6];325(13):938–48. Available from: https://www.nejm.org/doi/pdf/10.1056/NEJM199109263251307

47. Leung PS. Physiology of the pancreas. Adv Exp Med Biol [Internet]. 2010 [cited 2025 Jun 10];690:13–27. Available from: https://link.springer.com/chapter/10.1007/978-90-481-9060-7_2

48. Noguchi GM, Huising MO. Integrating the inputs that shape pancreatic islet hormone release. Nat Metab [Internet]. 2019 Dec 1 [cited 2025 Jan 16];1(12):1189. Available from: https://pmc.ncbi.nlm.nih.gov/articles/PMC7378277/

49. Rix I, Nexøe-Larsen C, Bergmann NC, Lund A, Knop FK. Glucagon Physiology. Can J Diabetes [Internet]. 2019 Jul 16 [cited 2025 Jun 10];34(3):187–8. Available from: https://www.ncbi.nlm.nih.gov/books/NBK279127/

50. Briant L, Salehi A, Vergari E, Zhang Q, Rorsman P. Glucagon secretion from pancreatic α-cells. Ups J Med Sci [Internet]. 2016 Apr 2 [cited 2025 Jun 10];121(2):113. Available from: https://pmc.ncbi.nlm.nih.gov/articles/PMC4900066/

51. Huising MO, van der Meulen T, Huang JL, Pourhosseinzadeh MS, Noguchi GM. The Difference δ-Cells Make in Glucose Control. Physiology [Internet]. 2018 Nov 1 [cited 2025 Jun 10];33(6):403. Available from: https://pmc.ncbi.nlm.nih.gov/articles/PMC6347098/

52. Samols E, Marri G, Marks V. PROMOTION OF INSULIN SECRETION BY GLUCAGON. The Lancet [Internet]. 1965 Aug 28 [cited 2025 Jun 10];286(7409):415–6. Available from: https://www.sciencedirect.com/science/article/pii/S0140673665907610

53. Samols E, Marri G, Marks V. Interrelationship of Glucagon, Insulin and Glucose: The Insulinogenic Effect of Glucagon. Diabetes [Internet]. 1966 Dec 1 [cited 2025 Jun 10];15(12):855–66. Available from: https://dx.doi.org/10.2337/diab.15.12.855

54. Patton GS, Dobbs R, Orci L, Vale W, Unger RH. Stimulation of pancreatic immunoreactive somatostatin (IRS) release by glucagon. Metabolism [Internet]. 1976 [cited 2025 Jun 10];25(11 sup. 1):1499. Available from: https://pubmed.ncbi.nlm.nih.gov/790097/

55. Unger RH, Orci L. Possible Roles of the Pancreatic D-cell in the Normal and Diabetic States. Diabetes [Internet]. 1977 Mar 1 [cited 2025 Jun 10];26(3):241–4. Available from: https://dx.doi.org/10.2337/diab.26.3.241

56. Samols E, Harrison J. Intraislet negative insulin-glucagon feedback. Metabolism [Internet]. 1976 [cited 2025 Jun 10];25(11 SUPPL.):1443–7. Available from: https://pubmed.ncbi.nlm.nih.gov/790090/

57. UNGER RH, EISENTRAUT AM, McCALL MS, MADISON LL. MEASUREMENTS OF ENDOGENOUS GLUCAGON IN PLASMA AND THE INFLUENCE OF BLOOD GLUCOSE CONCENTRATION UPON ITS SECRETION. Journal of Clinical Investigation [Internet]. 1962 [cited 2025 Jun 10];41(4):682. Available from: https://pmc.ncbi.nlm.nih.gov/articles/PMC290970/

58. Unger RH. Insulin-Glucagon Relationships in the Defense Against Hypoglycemia. Diabetes [Internet]. 1983 Jun 1 [cited 2025 Jun 10];32(6):575–83. Available from: https://dx.doi.org/10.2337/diab.32.6.575

59. Unger RH, Orci L. Glucagon and the A cell: physiology and pathophysiology (first two parts). N Engl J Med [Internet]. 1981 Jun 18 [cited 2025 Jun 10];304(25):1518–24. Available from: http://www.ncbi.nlm.nih.gov/pubmed/7015132

60. Hauge-Evans AC, King AJ, Carmignac D, Richardson CC, Robinson ICAF, Low MJ, et al. Somatostatin Secreted by Islet δ-Cells Fulfills Multiple Roles as a Paracrine Regulator of Islet Function. Diabetes [Internet]. 2009 Feb [cited 2025 Jun 10];58(2):403. Available from: https://pmc.ncbi.nlm.nih.gov/articles/PMC2628614/

61. Alberti KGMM, Juel Christensen N, Engkjær Christensen S, Prange Hansen A, Iversen J, Lundbæk K, et al. INHIBITION OF INSULIN SECRETION BY SOMATOSTATIN. The Lancet [Internet]. 1973 Dec 8 [cited 2025 Jun 10];302(7841):1299–301. Available from: https://www.sciencedirect.com/science/article/pii/S0140673673928730

62. Caicedo A. Paracrine and autocrine interactions in the human islet: More than meets the eye. Semin Cell Dev Biol [Internet]. 2013 Jan 1 [cited 2025 Oct 22];24(1):11–21. Available from: https://www.sciencedirect.com/science/article/pii/S1084952112001723?via%3Dihub

63. Wieland FC, van Blitterswijk CA, van Apeldoorn A, LaPointe VLS. The functional importance of the cellular and extracellular composition of the islets of Langerhans. J Immunol Regen Med [Internet]. 2021 Aug 1 [cited 2025 Oct 22];13:100048. Available from: https://www.sciencedirect.com/science/article/pii/S2468498821000111#bib106

64. Ferrannini E, Nannipieri M, Williams K, Gonzales C, Haffner SM, Stern MP. Mode of Onset of Type 2 Diabetes from Normal or Impaired Glucose Tolerance. Diabetes [Internet]. 2004 Jan 1 [cited 2025 Jun 7];53(1):160–5. Available from: https://dx.doi.org/10.2337/diabetes.53.1.160

65. Weyer C, Bogardus C, Mott DM, Pratley RE. The natural history of insulin secretory dysfunction and insulin resistance in the pathogenesis of type 2 diabetes mellitus. Journal of Clinical Investigation [Internet]. 1999 [cited 2025 Jun 7];104(6):787. Available from: https://pmc.ncbi.nlm.nih.gov/articles/PMC408438/

66. Tabák AG, Jokela M, Akbaraly TN, Brunner EJ, Kivimäki M, Witte DR. Trajectories of Glycemia, Insulin Sensitivity and Insulin Secretion Preceding the Diagnosis of Type 2

Diabetes: The Whitehall II Study. Lancet [Internet]. 2009 [cited 2025 Jun 7];373(9682):2215. Available from: https://pmc.ncbi.nlm.nih.gov/articles/PMC2726723/

67. Weir GC, Bonner-Weir S. Five Stages of Evolving Beta-Cell Dysfunction During Progression to Diabetes. Diabetes [Internet]. 2004 Dec 1 [cited 2025 Jun 7];53(suppl_3):S16–21. Available from: https://dx.doi.org/10.2337/diabetes.53.suppl_3.S16

68. Mulder H. Transcribing β-cell mitochondria in health and disease. Mol Metab [Internet]. 2017 Sep 1 [cited 2025 Jun 6];6(9):1040. Available from: https://pmc.ncbi.nlm.nih.gov/articles/PMC5605719/

69. Bonner-Weir S. Islet growth and development in the adult. J Mol Endocrinol [Internet]. 2000 Jun 1 [cited 2025 Jun 6];24(3):297–302. Available from: https://jme.bioscientifica.com/view/journals/jme/24/3/297.xml

70. Polonsky KS. Dynamics of insulin secretion in obesity and diabetes. Int J Obes [Internet]. 2000 Jul 24 [cited 2025 Jun 6];24(2):S29–31. Available from: https://www.nature.com/articles/0801273

71. Porte D. β-cells in type II diabetes mellitus. Diabetes [Internet]. 1991 Feb 1 [cited 2025 Jun 6];40(2):166–80. Available from: https://dx.doi.org/10.2337/diab.40.2.166

72. Kudva YC, Butler PC. Insulin Secretion in Type II Diabetes Mellitus. Clinical Research in Diabetes and Obesity [Internet]. 1997 [cited 2025 Jun 6];119–36. Available from: https://link.springer.com/chapter/10.1007/978-1-4757-3906-0_7

73. DeFronzo RA. The Triumvirate: β-Cell, Muscle, Liver: A Collusion Responsible for NIDDM. Diabetes [Internet]. 1988 Jun 1 [cited 2025 Jun 6];37(6):667–87. Available from: https://dx.doi.org/10.2337/diab.37.6.667

74. Dela F, Helge JW. Insulin resistance and mitochondrial function in skeletal muscle. Int J Biochem Cell Biol [Internet]. 2013 Jan 1 [cited 2025 Jun 6];45(1):11–5. Available from: https://www.sciencedirect.com/science/article/pii/S1357272512003305

75. Hesselink MKC, Schrauwen-Hinderling V, Schrauwen P. Skeletal muscle mitochondria as a target to prevent or treat type 2 diabetes mellitus. Nature Reviews Endocrinology 2016 12:11 [Internet]. 2016 Jul 22 [cited 2025 Jun 6];12(11):633–45. Available from: https://www.nature.com/articles/nrendo.2016.104

76. Zhyzhneuskaya S, Taylor R. Obesity and Type 2 Diabetes. Endocrinology (Switzerland). 2019;195–226.

77. Stumvoll M, Goldstein BJ, Van Haeften TW. Type 2 diabetes: principles of pathogenesis and therapy. The Lancet [Internet]. 2005 Apr 9 [cited 2025 Jun 11];365(9467):1333–46. Available from: https://www.sciencedirect.com/science/article/pii/S014067360561032X

78. Galicia-Garcia U, Benito-Vicente A, Jebari S, Larrea-Sebal A, Siddiqi H, Uribe KB, et al. Pathophysiology of Type 2 Diabetes Mellitus. Int J Mol Sci [Internet]. 2020 Sep 1 [cited 2025 Jun 11];21(17):6275. Available from: https://pmc.ncbi.nlm.nih.gov/articles/PMC7503727/

79. Dinneen S, Gerich J, Rizza R. Carbohydrate Metabolism in Non-Insulin-Dependent Diabetes Mellitus. New England Journal of Medicine [Internet]. 1992 Sep 3 [cited 2025 Jun 13];327(10):707–13. Available from: https://www.nejm.org/doi/pdf/10.1056/NEJM199209033271007

80. Ling C, Rönn T. Epigenetics in Human Obesity and Type 2 Diabetes. Cell Metab [Internet]. 2019 May 7 [cited 2025 Jun 23];29(5):1028. Available from: https://pmc.ncbi.nlm.nih.gov/articles/PMC6509280/

81. Taylor R. Pathogenesis of type 2 diabetes: Tracing the reverse route from cure to cause. Diabetologia [Internet]. 2008 Oct 26 [cited 2025 Jun 6];51(10):1781–9. Available from: https://link.springer.com/article/10.1007/s00125-008-1116-7

82. Cnop M, Hughes SJ, Igoillo-Esteve M, Hoppa MB, Sayyed F, Van De Laar L, et al. The long lifespan and low turnover of human islet beta cells estimated by mathematical modeling of lipofuscin accumulation. Diabetologia [Internet]. 2010 Feb 24 [cited 2025 Jan

20];53(2):321–30. Available from: https://link.springer.com/article/10.1007/s00125-009-1562-x

83. Zhang H, Zhang J, Pope CF, Crawford LA, Vasavada RC, Jagasia SM, et al. Gestational Diabetes Mellitus Resulting From Impaired β-Cell Compensation in the Absence of FoxM1, a Novel Downstream Effector of Placental Lactogen. Diabetes [Internet]. 2009 Jan [cited 2025 Jun 13];59(1):143. Available from: https://pmc.ncbi.nlm.nih.gov/articles/PMC2797915/

84. Ahrén B, Pacini G. Insufficient islet compensation to insulin resistance vs. reduced glucose effectiveness in glucose-intolerant mice. Am J Physiol Endocrinol Metab [Internet]. 2002 [cited 2025 Jun 13];283(4 46-4):738–44. Available from: /doi/pdf/10.1152/ajpendo.00199.2002

85. Okamoto H, Hribal ML, Lin H V., Bennett WR, Ward A, Accili D. Role of the forkhead protein FoxO1 in β cell compensation to insulin resistance. Journal of Clinical Investigation [Internet]. 2006 Mar 1 [cited 2025 Jun 13];116(3):775. Available from: https://pmc.ncbi.nlm.nih.gov/articles/PMC1370178/

86. Butler AE, Janson J, Bonner-Weir S, Ritzel R, Rizza RA, Butler PC. β-Cell Deficit and Increased β-Cell Apoptosis in Humans With Type 2 Diabetes. Diabetes [Internet]. 2003 Jan 1 [cited 2025 Jun 13];52(1):102–10. Available from: https://dx.doi.org/10.2337/diabetes.52.1.102

87. Fontés G, Zarrouki B, Hagman DK, Latour MG, Semache M, Roskens V, et al. Glucolipotoxicity age-dependently impairs beta cell function in rats despite a marked increase in beta cell mass. Diabetologia [Internet]. 2010 Nov [cited 2025 Jun 13];53(11):2369. Available from: https://pmc.ncbi.nlm.nih.gov/articles/PMC2947580/

88. Cerf ME. High fat programming of beta cell compensation, exhaustion, death and dysfunction. Pediatr Diabetes. 2015 Mar 1;16(2):71–8.

89. Halban PA, Polonsky KS, Bowden DW, Hawkins MA, Ling C, Mather KJ, et al. β-Cell Failure in Type 2 Diabetes: Postulated Mechanisms and Prospects for Prevention and Treatment. Diabetes Care [Internet]. 2014 [cited 2025 Jun 13];37(6):1751. Available from: https://pmc.ncbi.nlm.nih.gov/articles/PMC4179518/

90. Christensen AA, Gannon M. The Beta Cell in Type 2 Diabetes. Curr Diab Rep [Internet]. 2019 Sep 1 [cited 2025 Jun 13];19(9):1–8. Available from: https://link.springer.com/article/10.1007/s11892-019-1196-4

91. Pi-Sunyer FX. The Obesity Epidemic: Pathophysiology and Consequences of Obesity. Obes Res [Internet]. 2002 Dec 1 [cited 2025 May 28];10(S12):97S-104S. Available from: /doi/pdf/10.1038/oby.2002.202

92. Mraz M, Haluzik M. The role of adipose tissue immune cells in obesity and low-grade inflammation. Journal of Endocrinology [Internet]. 2014 Sep 1 [cited 2025 Jun 23];222(3):R113–27. Available from: https://joe.bioscientifica.com/view/journals/joe/222/3/R113.xml

93. Kinlen D, Cody D, O'Shea D. Complications of obesity. QJM: An International Journal of Medicine [Internet]. 2018 Jul 1 [cited 2025 Jun 23];111(7):437–43. Available from: https://dx.doi.org/10.1093/qjmed/hcx152

94. Hotamisligil GS. Inflammation, metaflammation and immunometabolic disorders. Nature 2017 542:7640 [Internet]. 2017 Feb 9 [cited 2025 Jun 23];542(7640):177–85. Available from: https://www.nature.com/articles/nature21363

95. Carolan E, Hogan AE, Corrigan M, Gaotswe G, O'Connell J, Foley N, et al. The Impact of Childhood Obesity on Inflammation, Innate Immune Cell Frequency, and Metabolic MicroRNA Expression. J Clin Endocrinol Metab [Internet]. 2014 Mar 1 [cited 2025 Jun 23];99(3):E474–8. Available from: https://dx.doi.org/10.1210/jc.2013-3529

96. Ley RE. Obesity and the human microbiome. Curr Opin Gastroenterol [Internet]. 2010 Jan [cited 2025 Jun 23];26(1):5–11. Available from: https://journals.lww.com/co-gastroenterology/fulltext/2010/01000/obesity_and_the_human_microbiome.3.aspx

97. Hu D, Zhao J, Zhang H, Wang G, Gu Z. Fecal Microbiota Transplantation for Weight and Glycemic Control of Obesity as Well as the Associated Metabolic Diseases: Meta-Analysis and Comprehensive Assessment. Life [Internet]. 2023 Jul 1 [cited 2025 Jun 23];13(7):1488. Available from: https://pmc.ncbi.nlm.nih.gov/articles/PMC10381135/

98. Tilg H, Kaser A. Gut microbiome, obesity, and metabolic dysfunction. J Clin Invest [Internet]. 2011 Jun 1 [cited 2025 Jun 23];121(6):2126. Available from: https://pmc.ncbi.nlm.nih.gov/articles/PMC3104783/

99. Friedman JE, Dohm GL, Leggett-Frazier N, Elton CW, Tapscott EB, Pories WP, et al. Restoration of insulin responsiveness in skeletal muscle of morbidly obese patients after weight loss. Effect on muscle glucose transport and glucose transporter GLUT4. Journal of Clinical Investigation [Internet]. 1992 [cited 2025 Jun 23];89(2):701. Available from: https://pmc.ncbi.nlm.nih.gov/articles/PMC442905/

100. Sattar N, Presslie C, Rutter MK, McGuire DK. Cardiovascular and Kidney Risks in Individuals With Type 2 Diabetes: Contemporary Understanding With Greater Emphasis on Excess Adiposity. Diabetes Care [Internet]. 2024 Mar 25 [cited 2025 Jun 17];47(4):531–43. Available from: https://dx.doi.org/10.2337/dci23-0041

101. Group TDC and CTR. The Effect of Intensive Treatment of Diabetes on the Development and Progression of Long-Term Complications in Insulin-Dependent Diabetes Mellitus. New England Journal of Medicine [Internet]. 1993 Sep 30 [cited 2025 Jun 17];329(14):977–86. Available from: https://www.nejm.org/doi/pdf/10.1056/NEJM199309303291401

102. King P, Peacock I, Donnelly R. The UK Prospective Diabetes Study (UKPDS): clinical and therapeutic implications for type 2 diabetes. 1999.

103. Currie CJ, Peters JR, Tynan A, Evans M, Heine RJ, Bracco OL, et al. Survival as a function of HbA1c in people with type 2 diabetes: a retrospective cohort study. The Lancet [Internet]. 2010 Feb 6 [cited 2025 Jun 10];375(9713):481–9. Available from: https://www.thelancet.com/action/showFullText?pii=S0140673609619693

104. Fonseca VA. Defining and Characterizing the Progression of Type 2 Diabetes. Diabetes Care [Internet]. 2009 [cited 2025 Jul 21];32(Suppl 2):S151. Available from: https://pmc.ncbi.nlm.nih.gov/articles/PMC2811457/

105. NICE. Type 2 diabetes in adults: management [NICE NG28] [Internet]. 2022 [cited 2025 Jun 17]. Available from: https://www.nice.org.uk/guidance/ng28/chapter/Recommendations#drug-treatment

106. British National Formulary. Type 2 diabetes - BNF [Internet]. 2025 [cited 2025 Jun 17]. Available from: https://bnf.nice.org.uk/treatment-summaries/type-2-diabetes/

107. NHS England. Interim commissioning guidance: implementation of the NICE technology appraisal TA1026 and the NICE funding variation for tirzepatide (Mounjaro®) for the management of obesity [Internet]. 2025 [cited 2025 Aug 26]. Available from: https://www.england.nhs.uk/publication/interim-commissioning-guidance-implementation-of-the-nice-technology-appraisal-ta1026-and-the-nice-funding-variation-for-tirzepatide-mounjaro-for-the-management-of-obesity/

108. British National Formulary. Obesity - BNF [Internet]. 2025 [cited 2025 Jun 17]. Available from: https://bnf.nice.org.uk/treatment-summaries/obesity/#drug-treatment

109. British National Formulary. Orlistat - BNF [Internet]. 2025 [cited 2025 Jun 23]. Available from: https://bnf.nice.org.uk/drugs/orlistat/

110. Bansal AB, Patel P, Khalili Y Al. Orlistat. xPharm: The Comprehensive Pharmacology Reference [Internet]. 2024 Feb 14 [cited 2025 Jun 23];1–3. Available from: https://www.ncbi.nlm.nih.gov/books/NBK542202/

111. Rucker D, Padwal R, Li SK, Curioni C, Lau DCW. Long term pharmacotherapy for obesity and overweight: updated meta-analysis. BMJ : British Medical Journal [Internet]. 2007 Dec 8 [cited 2025 Jun 23];335(7631):1194. Available from: https://pmc.ncbi.nlm.nih.gov/articles/PMC2128668/

112. Sibutramine: suspension of EU licences recommended - GOV.UK [Internet]. [cited 2025 Oct 1]. Available from: https://www.gov.uk/drug-safety-update/sibutramine-suspension-of-eu-licences-recommended

113. The European Medicines Agency recommends suspension of the marketing authorisation of Acomplia | European Medicines Agency (EMA) [Internet]. [cited 2025 Oct 1]. Available from: https://www.ema.europa.eu/en/news/european-medicines-agency-recommends-suspension-marketing-authorisation-acomplia

114. Pi-Sunyer X, Astrup A, Fujioka K, Greenway F, Halpern A, Krempf M, et al. A Randomized, Controlled Trial of 3.0 mg of Liraglutide in Weight Management. New England Journal of Medicine [Internet]. 2015 Jul 2 [cited 2025 Jun 23];373(1):11–22. Available from: https://www.nejm.org/doi/pdf/10.1056/NEJMoa1411892

115. Rubino DM, Greenway FL, Khalid U, O'Neil PM, Rosenstock J, Sørrig R, et al. Effect of Weekly Subcutaneous Semaglutide vs Daily Liraglutide on Body Weight in Adults With Overweight or Obesity Without Diabetes: The STEP 8 Randomized Clinical Trial. JAMA [Internet]. 2022 Jan 11 [cited 2025 Jun 23];327(2):138–50. Available from: https://jamanetwork.com/journals/jama/fullarticle/2787907

116. Jastreboff AM, Aronne LJ, Ahmad NN, Wharton S, Connery L, Alves B, et al. Tirzepatide Once Weekly for the Treatment of Obesity. New England Journal of Medicine. 2022;205–16.

117. Rodriguez PJ, Goodwin Cartwright BM, Gratzl S, Brar R, Baker C, Gluckman TJ, et al. Semaglutide vs Tirzepatide for Weight Loss in Adults With Overweight or Obesity. JAMA

Intern Med [Internet]. 2024 Sep 1 [cited 2025 Apr 10];184(9):1056–64. Available from: https://jamanetwork.com/journals/jamainternalmedicine/fullarticle/2821080

118. Nguyen NT, Kim E, Vu S, Phelan M. Ten-year Outcomes of a Prospective Randomized Trial of Laparoscopic Gastric Bypass Versus Laparoscopic Gastric Banding. Ann Surg [Internet]. 2018 Jul 1 [cited 2025 Jun 23];268(1):106. Available from: https://pmc.ncbi.nlm.nih.gov/articles/PMC5867269/

119. By-Band-Sleeve Collaborative Group. Roux-en-Y gastric bypass, adjustable gastric banding, or sleeve gastrectomy for severe obesity (By-Band-Sleeve): a multicentre, open label, three-group, randomised controlled trial. Lancet Diabetes Endocrinol [Internet]. 2025 Mar 31 [cited 2025 Jun 23];13(5):410–26. Available from: http://www.ncbi.nlm.nih.gov/pubmed/40179925

120. American Diabetes Association. New GLP-1 Therapies Enhance Quality of Weight Loss by Improving Muscle Preservation - Press release [Internet]. 85th Scientific Sessions of the American Diabetes Association. Chicago; 2025 Jun [cited 2025 Aug 22]. Available from: https://diabetes.org/newsroom/press-releases/new-glp-1-therapies-enhance-quality-weight-loss-improving-muscle-0

121. Pfizer. Pfizer Provides Update on Oral GLP-1 Receptor Agonist Danuglipron [Internet]. 2025 [cited 2025 Jun 23]. Available from: https://www.pfizer.com/news/press-release/press-release-detail/pfizer-provides-update-oral-glp-1-receptor-agonist

122. FirstWord Pharma. Novo Nordisk lifts full-year guidance as Wegovy sales soar [Internet]. 2023 [cited 2025 Jun 23]. Available from: https://firstwordpharma.com/story/5769412

123. Melson E, Ashraf U, Papamargaritis D, Davies MJ. What is the pipeline for future medications for obesity? Int J Obes [Internet]. 2024 Mar 1 [cited 2025 May 9];49(3):433–51. Available from: https://www.nature.com/articles/s41366-024-01473-y

124. Véniant MM, Lu SC, Atangan L, Komorowski R, Stanislaus S, Cheng Y, et al. A GIPR antagonist conjugated to GLP-1 analogues promotes weight loss with improved

metabolic parameters in preclinical and phase 1 settings. Nat Metab [Internet]. 2024 Feb 1 [cited 2025 Aug 25];6(2):290. Available from: https://pmc.ncbi.nlm.nih.gov/articles/PMC10896721/

125. Jastreboff AM, Ryan DH, Bays HE, Ebeling PR, Mackowski MG, Philipose N, et al. Once-Monthly Maridebart Cafraglutide for the Treatment of Obesity — A Phase 2 Trial. New England Journal of Medicine [Internet]. 2025 Jun 23 [cited 2025 Jun 25]; Available from: http://www.nejm.org/doi/10.1056/NEJMoa2504214

126. Douros JD, Mowery SA, Knerr PJ. The Premise of the Paradox: Examining the Evidence That Motivated GIPR Agonist and Antagonist Drug Development Programs. Journal of Clinical Medicine 2025, Vol 14, Page 3812 [Internet]. 2025 May 29 [cited 2025 Jul 11];14(11):3812. Available from: https://www.mdpi.com/2077-0383/14/11/3812/htm

127. Kawai T, Sun B, Yoshino H, Feng D, Suzuki Y, Fukazawa M, et al. Structural basis for GLP-1 receptor activation by LY3502970, an orally active nonpeptide agonist. Proc Natl Acad Sci U S A [Internet]. 2020 Nov 24 [cited 2025 Aug 25];117(47):29959–67. Available from: https://pmc.ncbi.nlm.nih.gov/articles/PMC7703558/

128. Lilly. Lilly's oral GLP-1, orforglipron, delivers weight loss of up to an average of 27.3 lbs in first of two pivotal Phase 3 trials in adults with obesity | Eli Lilly and Company [Internet]. 2025 [cited 2025 Aug 8]. Available from: https://investor.lilly.com/news-releases/news-release-details/lillys-oral-glp-1-orforglipron-delivers-weight-loss-average-273

129. Pratt E, Ma X, Liu R, Robins D, Coskun T, Sloop KW, et al. Orforglipron (LY3502970), a novel, oral non-peptide glucagon-like peptide-1 receptor agonist: A Phase 1b, multicentre, blinded, placebo-controlled, randomized, multiple-ascending-dose study in people with type 2 diabetes. Diabetes Obes Metab [Internet]. 2023 Sep 1 [cited 2025 Aug 25];25(9):2642–9. Available from: /doi/pdf/10.1111/dom.15150

130. Rosenstock J, Hsia S, Nevarez Ruiz L, Eyde S, Cox D, Wu WS, et al. Orforglipron, an Oral Small-Molecule GLP-1 Receptor Agonist, in Early Type 2 Diabetes. New England Journal

of Medicine [Internet]. 2025 Jun 21 [cited 2025 Aug 25]; Available from: https://www.nejm.org/doi/pdf/10.1056/NEJMoa2505669

131. Aronne LJ, Horn DB, le Roux CW, Ho W, Falcon BL, Gomez Valderas E, et al. Tirzepatide as Compared with Semaglutide for the Treatment of Obesity. New England Journal of Medicine [Internet]. 2025 Jul 3 [cited 2025 Aug 25];393(1):26–36. Available from: https://www.nejm.org/doi/pdf/10.1056/NEJMoa2416394

132. Nuhoho S, Gupta J, Hansen BB, Fletcher-Louis M, Dang-Tan T, Paine A. Orally Administered Semaglutide Versus GLP-1 RAs in Patients with Type 2 Diabetes Previously Receiving 1–2 Oral Antidiabetics: Systematic Review and Network Meta-Analysis. Diabetes Therapy [Internet]. 2019 Dec 1 [cited 2025 Aug 25];10(6):2183. Available from: https://pmc.ncbi.nlm.nih.gov/articles/PMC6848399/

133. ClinicalTrials.gov. Study Details - A Study of Retatrutide (LY3437943) in Participants With Obesity and Cardiovascular Disease [Internet]. 2025 [cited 2025 Aug 26]. Available from: https://clinicaltrials.gov/study/NCT05882045

134. Coskun T, Urva S, Roell WC, Qu H, Loghin C, Moyers JS, et al. LY3437943, a novel triple glucagon, GIP, and GLP-1 receptor agonist for glycemic control and weight loss: From discovery to clinical proof of concept. Cell Metab [Internet]. 2022 Sep 6 [cited 2025 Aug 26];34(9):1234-1247.e9. Available from: https://www.cell.com/action/showFullText?pii=S1550413122003126

135. Rosenstock J, Frias J, Jastreboff AM, Du Y, Lou J, Gurbuz S, et al. Retatrutide, a GIP, GLP-1 and glucagon receptor agonist, for people with type 2 diabetes: a randomised, double-blind, placebo and active-controlled, parallel-group, phase 2 trial conducted in the USA. The Lancet [Internet]. 2023 Aug 12 [cited 2025 Aug 25];402(10401):529–44. Available from: https://www.thelancet.com/action/showFullText?pii=S014067362301053X

136. Jastreboff AM, Kaplan LM, Frías JP, Wu Q, Du Y, Gurbuz S, et al. Triple–Hormone-Receptor Agonist Retatrutide for Obesity — A Phase 2 Trial. New England Journal of Medicine

[Internet]. 2023 Aug 10 [cited 2025 Apr 24];389(6):514–26. Available from: https://www.nejm.org/doi/pdf/10.1056/NEJMoa2301972

137. Clinical Trials.gov. A Research Study Investigating NNC0247-0829 for Weight Management in People With Overweight or Obesity (NCT04010786) - Study Details [Internet]. 2024 [cited 2025 Jun 23]. Available from: https://clinicaltrials.gov/study/NCT04010786

138. Clinical Trials.gov. Study to Assess Safety, Tolerability and Efficacy of SC Administered MBL949 in Obese Participants With or Without T2DM (NCT05199090) - Study Details [Internet]. 2024 [cited 2025 Jun 23]. Available from: https://clinicaltrials.gov/study/NCT05199090

139. Bio Space. Novartis Cuts 'Unique' Obesity Drug After Poor Phase II Results [Internet]. 2023 [cited 2025 Jun 23]. Available from: https://www.biospace.com/novartis-cuts-unique-obesity-drug-after-poor-phase-results

140. Clinical Trials.gov. A Study of LY3541105 in Healthy and Overweight Participants (NCT05380323) - Study Details [Internet]. 2024 [cited 2025 Jun 23]. Available from: https://clinicaltrials.gov/study/NCT05380323

141. Fierce Biotech. Eli Lilly lops Alzheimer's and obesity assets from pipeline [Internet]. 2025 [cited 2025 Jun 23]. Available from: https://www.fiercebiotech.com/biotech/eli-lilly-lops-alzheimers-and-obesity-assets-pipeline-q4-update

142. Nishizaki H, Matsuoka O, Kagawa T, Kobayashi A, Watanabe M, Moritoh Y. SCO-267, a GPR40 Full Agonist, Stimulates Islet and Gut Hormone Secretion and Improves Glycemic Control in Humans. Diabetes [Internet]. 2021 Oct 1 [cited 2025 Jun 23];70(10):2364. Available from: https://pmc.ncbi.nlm.nih.gov/articles/PMC8571351/

143. Ernest Henry Starling. The Croonian lectures on the chemical correlation of the functions of the body : delivered before the Royal College of Physicians of London - Wellcome

Collection [Internet]. 1905 [cited 2025 Jun 24]. Available from: https://wellcomecollection.org/works/rd4gsvmp/items?canvas=24

144. Bayliss WM, Starling EH. The mechanism of pancreatic secretion. J Physiol [Internet]. 1902 Sep 12 [cited 2025 Jun 24];28(5):325. Available from: https://pmc.ncbi.nlm.nih.gov/articles/PMC1540572/

145. Moore B, Edie ES, Abram JH. On the treatment of Diabetus mellitus by acid extract of Duodenal Mucous Membrane. Biochemical Journal [Internet]. 1906 Jan 1 [cited 2025 Jun 24];1(1):28. Available from: https://pmc.ncbi.nlm.nih.gov/articles/PMC1276119/

146. Rehfeld JF. The Origin and Understanding of the Incretin Concept. Front Endocrinol (Lausanne) [Internet]. 2018 Jul 16 [cited 2025 Jun 24];9(JUL):387. Available from: https://pmc.ncbi.nlm.nih.gov/articles/PMC6054964/

147. Seino Y, Fukushima M, Yabe D. GIP and GLP-1, the two incretin hormones: Similarities and differences. J Diabetes Investig [Internet]. 2010 Feb [cited 2020 Jul 26];1(1–2):8–23. Available from: https://onlinelibrary.wiley.com/doi/10.1111/j.2040-1124.2010.00022.x

148. Banting FG, Best CH. The internal secretion of the pancreas. J Lab Clin Med. 1922 Feb;7(5):251–66.

149. YALOW RS, BERSON SA. IMMUNOASSAY OF ENDOGENOUS PLASMA INSULIN IN MAN. Journal of Clinical Investigation [Internet]. 1960 [cited 2025 Jun 24];39(7):1157. Available from: https://pmc.ncbi.nlm.nih.gov/articles/PMC441860/

150. Elrick H, Stimmler L, Hlad CJ, Arai Y. Plasma Insulin Response To Oral and Intravenous Glucose Administration. J Clin Endocrinol Metab. 1964;24(December):1076–82.

151. Mcintyre N, Holdsworth CD, Turner DS. NEW INTERPRETATION OF ORAL GLUCOSE TOLERANCE. The Lancet [Internet]. 1964 Jul 4 [cited 2025 Jun 24];284(7349):20–1. Available from: https://www.sciencedirect.com/science/article/pii/S014067366490011X

152. Dupre J, Ross SA, Watson D, Brown JC. STIMULATION OF INSULIN SECRETION BY GASTRIC INHIBITORY POLYPEPTIDE IN MAN. J Clin Endocrinol Metab [Internet]. 1973 Nov

1 [cited 2022 Oct 15];37(5):826–8. Available from: https://academic.oup.com/jcem/article/37/5/826/2686318

153. Samols E, Tyler J, Megyesi C, Marks V. Immunochemical glucagon in human pancreas, gut, and plasma. Lancet [Internet]. 1966 Oct 1 [cited 2025 Jun 24];2(7466):727–9. Available from: https://www.thelancet.com/action/showFullText?pii=S0140673666929825

154. Unger RH, Ketterer H, Eisentraut AM. Distribution of immunoassayable glucagon in gastrointestinal tissues. Metabolism [Internet]. 1966 [cited 2025 Jun 24];15(10):865–7. Available from: https://pubmed.ncbi.nlm.nih.gov/5923522/

155. Bell GI, Sanchez-Pescador R, Laybourn PJ, Najarian RC. Exon duplication and divergence in the human preproglucagon gene. Nature [Internet]. 1983 [cited 2025 Jun 24];304(5924):368–71. Available from: https://www.nature.com/articles/304368a0

156. Bell GI, Santerre RF, Mullenbach GT. Hamster preproglucagon contains the sequence of glucagon and two related peptides [20]. Nature [Internet]. 1983 Apr 1 [cited 2025 Jun 24];302(5910):716–8. Available from: https://www.nature.com/articles/302716a0

157. Holst JJ, Ørskov C, Vagn Nielsen O, Schwartz TW. Truncated glucagon-like peptide I, an insulin-releasing hormone from the distal gut. FEBS Lett [Internet]. 1987 Jan 26 [cited 2025 May 8];211(2):169–74. Available from: /doi/pdf/10.1016/0014-5793%2887%2981430-8

158. Mojsov S, Weir GC, Habener JF. Insulinotropin: glucagon-like peptide I (7-37) co-encoded in the glucagon gene is a potent stimulator of insulin release in the perfused rat pancreas. Journal of Clinical Investigation [Internet]. 1987 [cited 2025 May 8];79(2):616. Available from: https://pmc.ncbi.nlm.nih.gov/articles/PMC424143/

159. Ørskov C, Holst JJ, Nielsen O V. Effect of Truncated Glucagon-Like Peptide-1 [Proglucagon-(78–107) amide] on Endocrine Secretion from Pig Pancreas, Antrum, and

Nonantral Stomach. Endocrinology [Internet]. 1988 Oct 1 [cited 2025 Jun 24];123(4):2009–13. Available from: https://dx.doi.org/10.1210/endo-123-4-2009

160. Creutzfeldt WOC, Kleine N, Willms B, Ørskov C, Holst JJ, Nauck MA. Glucagonostatic Actions and Reduction of Fasting Hyperglycemia by Exogenous Glucagon-Like Peptide I(7–36) amide in type I diabetic patients. Diabetes Care [Internet]. 1996 Jun 1 [cited 2025 Jun 24];19(6):580–6. Available from: https://dx.doi.org/10.2337/diacare.19.6.580

161. Drucker DJ. Glucagon-Like Peptide 2. J Clin Endocrinol Metab [Internet]. 2001 Apr 1 [cited 2025 Jun 24];86(4):1759–64. Available from: https://dx.doi.org/10.1210/jcem.86.4.7386

162. British National Formulary. Short bowel syndrome - BNF [Internet]. 2025 [cited 2025 Aug 21]. Available from: https://bnf.nice.org.uk/treatment-summaries/short-bowel-syndrome/

163. Zhu C, Li Y. An updated overview of glucagon-like peptide-2 analog trophic therapy for short bowel syndrome in adults. J Int Med Res [Internet]. 2022 Mar 1 [cited 2025 Aug 21];50(3):03000605221086145. Available from: https://pmc.ncbi.nlm.nih.gov/articles/PMC8966062/

164. Sabra HK, Remeih GS, Kereet IM, Hamad M, Ahmed YA, Jahangir K, et al. Efficacy and safety of glucagon-like peptide 2 in patients with short bowel syndrome: a systematic review and network meta-analysis. Journal of Gastrointestinal Surgery [Internet]. 2024 Jul 1 [cited 2025 Aug 21];28(7):1194–205. Available from: https://www.sciencedirect.com/science/article/pii/S1091255X24004128

165. Brown JC. Gastric inhibitory polypeptide. Monogr Endocrinol [Internet]. 1982 [cited 2025 Jun 24];24. Available from: https://pubmed.ncbi.nlm.nih.gov/6214707/

166. EISSELE R, GÖKE R, WILLEMER S, HARTHUS H -P, VERMEER H, ARNOLD R, et al. Glucagon-like peptide-1 cells in the gastrointestinal tract and pancreas of rat, pig and man. Eur J Clin Invest [Internet]. 1992 Apr 1 [cited 2025 Jun 24];22(4):283–91. Available from: /doi/pdf/10.1111/j.1365-2362.1992.tb01464.x

167. Kreymann B, Ghatei MA, Burnet P, Williams G, Kanse S, Diani AR, et al. Characterization of glucagon-like peptide-1-(7–36)amide in the hypothalamus. Brain Res [Internet]. 1989 Nov 20 [cited 2025 May 8];502(2):325–31. Available from: https://www.sciencedirect.com/science/article/abs/pii/0006899389906288?via%3Dihub

168. Diakogiannaki E, Gribble FM, Reimann F. Nutrient detection by incretin hormone secreting cells. Physiol Behav. 2012 Jun 6;106(3):387–93.

169. Kuhre RE, Wewer Albrechtsen NJ, Larsen O, Jepsen SL, Balk-Møller E, Andersen DB, et al. Bile acids are important direct and indirect regulators of the secretion of appetite- and metabolism-regulating hormones from the gut and pancreas. Mol Metab. 2018 May 1;11:84–95.

170. Kieffer TJ, Mc Intosh CHS, Pederson RA. Degradation of glucose-dependent insulinotropic polypeptide and truncated glucagon-like peptide 1 in vitro and in vivo by dipeptidyl peptidase IV. Endocrinology. 1995;136(8):3585–96.

171. Wei Y, Mojsov S. Tissue-specific expression of the human receptor for glucagon-like peptide-I: brain, heart and pancreatic forms have the same deduced amino acid sequences. FEBS Lett [Internet]. 1995 Jan 30 [cited 2025 May 8];358(3):219–24. Available from: https://pubmed.ncbi.nlm.nih.gov/7843404/

172. Baggio LL, Yusta B, Mulvihill EE, Cao X, Streutker CJ, Butany J, et al. GLP-1 Receptor Expression Within the Human Heart. Endocrinology [Internet]. 2018 Apr 1 [cited 2025 Jun 24];159(4):1570. Available from: https://pmc.ncbi.nlm.nih.gov/articles/PMC5939638/

173. McLean BA, Wong CK, Campbell JE, Hodson DJ, Trapp S, Drucker DJ. Revisiting the Complexity of GLP-1 Action from Sites of Synthesis to Receptor Activation. Endocr Rev [Internet]. 2020 Apr 1 [cited 2025 Apr 1];42(2):101. Available from: https://pmc.ncbi.nlm.nih.gov/articles/PMC7958144/

174. Nauck MA, Quast DR, Wefers J, Pfeiffer AFH. The evolving story of incretins (GIP and GLP-1) in metabolic and cardiovascular disease: A pathophysiological update. Diabetes Obes

Metab [Internet]. 2021 Sep 1 [cited 2025 Apr 9];23(S3):5–29. Available from: https://onlinelibrary.wiley.com/doi/full/10.1111/dom.14496

175. Baggio LL, Drucker DJ. Biology of Incretins: GLP-1 and GIP. Gastroenterology [Internet]. 2007 May [cited 2020 Jul 26];132(6):2131–57. Available from: https://linkinghub.elsevier.com/retrieve/pii/S001650850700580X

176. Marzook A, Tomas A, Jones B. The Interplay of Glucagon-Like Peptide-1 Receptor Trafficking and Signalling in Pancreatic Beta Cells. Front Endocrinol (Lausanne) [Internet]. 2021 May 10 [cited 2025 Oct 22];12:678055. Available from: https://pmc.ncbi.nlm.nih.gov/articles/PMC8143046/

177. Ding WG, Gromada J. Protein kinase A-dependent stimulation of exocytosis in mouse pancreatic β-cells by glucose-dependent insulinotropic polypeptide. Diabetes. 1997;46(4):615–21.

178. Gromada J, Bokvist K, Ding W guang G, Holst JJ, Nielsen JH, Rorsman P. Glucagon-like peptide 1(7-36) amide stimulates exocytosis in human pancreatic beta-cells by both proximal and distal regulatory steps in stimulus-secretion coupling. Diabetes [Internet]. 1998 [cited 2020 Aug 12];1(1):57–65. Available from: https://search.proquest.com/docview/216460161/fulltextPDF/F286489BAFFE438BPQ/1?accountid=49002

179. Kashima Y, Miki T, Shibasaki T, Ozaki N, Miyazaki M, Yano H, et al. Critical Role of cAMP-GEFII·Rim2 Complex in Incretin-potentiated Insulin Secretion. Journal of Biological Chemistry [Internet]. 2001 Dec 7 [cited 2025 Apr 9];276(49):46046–53. Available from: https://www.jbc.org/action/showFullText?pii=S0021925819374022

180. Ehses JA, Lee SST, Pederson RA, McIntosh CHS. A new pathway for glucose-dependent insulinotropic polypeptide (GIP) receptor signaling: Evidence for the involvement of phospholipase A2 in GIP-stimulated insulin secretion. Journal of Biological Chemistry

[Internet]. 2001 Jun 29 [cited 2025 Apr 9];276(26):23667–73. Available from: https://www.jbc.org/action/showFullText?pii=S0021925820783626

181. Kim SJ, Choi WS, Han JSM, Warnock G, Fedida D, McIntosh CHS. A Novel Mechanism for the Suppression of a Voltage-gated Potassium Channel by Glucose-dependent Insulinotropic Polypeptide: PROTEIN KINASE A-DEPENDENT ENDOCYTOSIS. Journal of Biological Chemistry. 2005 Aug 5;280(31):28692–700.

182. Nauck MA, Heimesaat MM, Behle K, Holst JJ, Nauck MS, Ritzel R, et al. Effects of Glucagon-Like Peptide 1 on Counterregulatory Hormone Responses, Cognitive Functions, and Insulin Secretion during Hyperinsulinemic, Stepped Hypoglycemic Clamp Experiments in Healthy Volunteers [Internet]. Vol. 87, J Clin Endocrinol Metab. 2002 [cited 2020 Aug 12]. Available from: https://academic.oup.com/jcem/article/87/3/1239/2847222

183. De Marinis YZ, Salehi A, Ward CE, Zhang Q, Abdulkader F, Bengtsson M, et al. GLP-1 Inhibits and Adrenaline Stimulates Glucagon Release by Differential Modulation of N- and L-Type Ca2+ Channel-Dependent Exocytosis. Cell Metab. 2010 Jun 9;11(6):543–53.

184. Ramracheya R, Chapman C, Chibalina M, Dou H, Miranda C, González A, et al. GLP-1 suppresses glucagon secretion in human pancreatic alpha-cells by inhibition of P/Q-type Ca2+ channels. Physiol Rep [Internet]. 2018 Sep 1 [cited 2025 Apr 16];6(17):e13852. Available from: https://onlinelibrary.wiley.com/doi/full/10.14814/phy2.13852

185. Fehmann HC, Habener JF. Functional receptors for the insulinotropic hormone glucagon-like peptide-I(7–37) on a somatostatin secreting cell line. FEBS Lett [Internet]. 1991 Feb 25 [cited 2025 Apr 10];279(2):335–40. Available from: https://onlinelibrary.wiley.com/doi/full/10.1016/0014-5793%2891%2980182-3

186. Gros L, Thorens B, Bataille D, Kervran A. Glucagon-like peptide-1-(7-36) amide, oxyntomodulin, and glucagon interact with a common receptor in a somatostatin-

secreting cell line. Endocrinology [Internet]. 1993 Aug 1 [cited 2025 Apr 15];133(2):631–8. Available from: https://dx.doi.org/10.1210/endo.133.2.8102095

187. Heller RS, Aponte GW. Intra-islet regulation of hormone secretion by glucagon-like peptide-1- (7-36) amide. Am J Physiol Gastrointest Liver Physiol. 1995;269(6 32-6).

188. DiGruccio MR, Mawla AM, Donaldson CJ, Noguchi GM, Vaughan J, Cowing-Zitron C, et al. Comprehensive alpha, beta and delta cell transcriptomes reveal that ghrelin selectively activates delta cells and promotes somatostatin release from pancreatic islets. Mol Metab [Internet]. 2016 Jul 1 [cited 2025 Jan 28];5(7):449. Available from: https://pmc.ncbi.nlm.nih.gov/articles/PMC4921781/

189. Balboa D, Barsby T, Lithovius V, Saarimäki-Vire J, Omar-Hmeadi M, Dyachok O, et al. Functional, metabolic and transcriptional maturation of human pancreatic islets derived from stem cells. Nature Biotechnology 2022 40:7 [Internet]. 2022 Mar 3 [cited 2024 Aug 6];40(7):1042–55. Available from: https://www.nature.com/articles/s41587-022-01219-z

190. Mawla A, Huising M. Huising Lab Dataset: Integrated Human scRNA-Seq Studies [Internet]. [cited 2025 Apr 16]. Available from: https://huisinglab.com/diabetes_2019/index.html

191. Adriaenssens AE, Svendsen B, Lam BYH, Yeo GSH, Holst JJ, Reimann F, et al. Transcriptomic profiling of pancreatic alpha, beta and delta cell populations identifies delta cells as a principal target for ghrelin in mouse islets. Diabetologia [Internet]. 2016 Oct 1 [cited 2022 Oct 17];59(10):2156. Available from: /pmc/articles/PMC5016554/

192. Segerstolpe Å, Palasantza A, Eliasson P, Andersson EM, Andréasson AC, Sun X, et al. Single-Cell Transcriptome Profiling of Human Pancreatic Islets in Health and Type 2 Diabetes. Cell Metab [Internet]. 2016 Oct 11 [cited 2025 Apr 10];24(4):593. Available from: https://pmc.ncbi.nlm.nih.gov/articles/PMC5069352/

193. Li Y, Hansotia T, Yusta B, Ris F, Halban PA, Drueker DJ. Glucagon-like Peptide-1 Receptor Signaling Modulates β Cell Apoptosis. Journal of Biological Chemistry [Internet]. 2003 Jan

3 [cited 2025 Jun 30];278(1):471–8. Available from: https://www.sciencedirect.com/science/article/pii/S0021925819312943#FN150

194. Cornu M, Yang JY, Jaccard E, Poussin C, Widmann C, Thorens B. Glucagon-Like Peptide-1 Protects β-Cells Against Apoptosis by Increasing the Activity of an Igf-2/Igf-1 Receptor Autocrine Loop. Diabetes [Internet]. 2009 Aug [cited 2025 Jun 30];58(8):1816. Available from: https://pmc.ncbi.nlm.nih.gov/articles/PMC2712796/

195. Tru¨mper A, Tru¨mper T, Tru¨mper K, Trusheim H, Arnold R, Go¨ke B, et al. Glucose-Dependent Insulinotropic Polypeptide Is a Growth Factor for β (INS-1) Cells by Pleiotropic Signaling. Molecular Endocrinology [Internet]. 2001 Sep 1 [cited 2025 Jun 25];15(9):1559–70. Available from: https://dx.doi.org/10.1210/mend.15.9.0688

196. Campbell JE, Ussher JR, Mulvihill EE, Kolic J, Baggio LL, Cao X, et al. TCF1 links GIPR signaling to the control of beta cell function and survival. Nature Medicine 2015 22:1 [Internet]. 2015 Dec 7 [cited 2022 Oct 15];22(1):84–90. Available from: https://www.nature.com/articles/nm.3997

197. Nauck M, Stöckmann F, Ebert R, Creutzfeldt W. Reduced incretin effect in Type 2 (non-insulin-dependent) diabetes. Diabetologia [Internet]. 1986 Jan [cited 2020 Sep 26];29(1):46–52. Available from: https://pubmed.ncbi.nlm.nih.gov/3514343/

198. Nauck MA, Vardarli I, Deacon CF, Holst JJ, Meier JJ. Secretion of glucagon-like peptide-1 (GLP-1) in type 2 diabetes: What is up, what is down? Diabetologia [Internet]. 2011 Jan 25 [cited 2025 Jun 25];54(1):10–8. Available from: https://link.springer.com/article/10.1007/s00125-010-1896-4

199. Meier JJ, Nauck MA. Is secretion of glucagon-like peptide-1 reduced in type 2 diabetes mellitus? Nat Clin Pract Endocrinol Metab [Internet]. 2008 Nov 26 [cited 2025 Jun 25];4(11):606–7. Available from: https://www.nature.com/articles/ncpendmet0946

200. Thorens B, Waeber G. Glucagon-Like Peptide-I and the Control of Insulin Secretion in the Normal State and in NIDDM. Diabetes [Internet]. 1993 Sep 1 [cited 2025 Jun 25];42(9):1219–25. Available from: https://dx.doi.org/10.2337/diab.42.9.1219

201. Kjems LL, Holst JJ, Vølund A, Madsbad S. The Influence of GLP-1 on Glucose-Stimulated Insulin SecretionEffects on β-Cell Sensitivity in Type 2 and Nondiabetic Subjects. Diabetes [Internet]. 2003 Feb 1 [cited 2025 Jun 25];52(2):380–6. Available from: https://dx.doi.org/10.2337/diabetes.52.2.380

202. Holst JJ, Knop FK, Vilsbøll T, Krarup T, Madsbad S. Loss of Incretin Effect Is a Specific, Important, and Early Characteristic of Type 2 Diabetes. Diabetes Care [Internet]. 2011 May [cited 2025 Jun 25];34(Suppl 2):S251. Available from: https://pmc.ncbi.nlm.nih.gov/articles/PMC3632188/

203. Calanna S, Christensen M, Holst JJ, Laferrère B, Gluud LL, Vilsbøll T, et al. Secretion of glucagon-like peptide-1 in patients with type 2 diabetes mellitus: systematic review and meta-analyses of clinical studies. Diabetologia [Internet]. 2013 May [cited 2025 Jun 25];56(5):965. Available from: https://pmc.ncbi.nlm.nih.gov/articles/PMC3687347/

204. Hodson DJ, Mitchell RK, Bellomo EA, Sun G, Vinet L, Meda P, et al. Lipotoxicity disrupts incretin-regulated human β cell connectivity. J Clin Invest [Internet]. 2013 [cited 2020 Jul 26];123(10):4182–94. Available from: http://www.jci.org

205. Xu G, Kaneto H, Laybutt DR, Duvivier-Kali VF, Trivedi N, Suzuma K, et al. Downregulation of GLP-1 and GIP Receptor Expression by HyperglycemiaPossible Contribution to Impaired Incretin Effects in Diabetes. Diabetes [Internet]. 2007 Jun 1 [cited 2025 Jun 25];56(6):1551–8. Available from: https://dx.doi.org/10.2337/db06-1033

206. Krarup T, Saurbrey N, Moody AJ, Kühl C, Madsbad S. Effect of porcine gastric inhibitory polypeptide on beta-cell function in type I and type II diabetes mellitus. Metabolism [Internet]. 1987 [cited 2025 Apr 8];36(7):677–82. Available from: https://pubmed.ncbi.nlm.nih.gov/3298936/

207. Højberg P V, Vilsbøll T, Rabøl R, Knop FK, Bache M, Krarup T, et al. Four weeks of near-normalisation of blood glucose improves the insulin response to glucagon-like peptide-1 and glucose-dependent insulinotropic polypeptide in patients with type 2 diabetes. Diabetologia. 2008;52:199–207.

208. Vilsbøll T, Krarup T, Madsbad S, Holst J. Defective amplification of the late phase insulin response to glucose by GIP in obese Type II diabetic patients. Diabetologia [Internet]. 2002 [cited 2022 Oct 15];45(8):1111–9. Available from: https://pubmed.ncbi.nlm.nih.gov/12189441/

209. Piteau S, Olver A, Kim SJ, Winter K, Pospisilik JA, Lynn F, et al. Reversal of islet GIP receptor down-regulation and resistance to GIP by reducing hyperglycemia in the Zucker rat. Biochem Biophys Res Commun [Internet]. 2007 Nov 3 [cited 2025 Jun 25];362(4):1007–12. Available from: https://www.sciencedirect.com/science/article/pii/S0006291X07018220?via%3Dihub

210. Gupta D, Peshavaria M, Monga N, Jetton TL, Leahy JL. Physiologic and Pharmacologic Modulation of Glucose-Dependent Insulinotropic Polypeptide (GIP) Receptor Expression in β-Cells by Peroxisome Proliferator–Activated Receptor (PPAR)-γ Signaling: Possible Mechanism for the GIP Resistance in Type 2 Diabetes. Diabetes [Internet]. 2010 Jun [cited 2025 Jun 25];59(6):1445. Available from: https://pmc.ncbi.nlm.nih.gov/articles/PMC2874705/

211. Zhou J, Livak MFA, Bernier M, Muller DC, Carlson OD, Elahi D, et al. Ubiquitination is involved in glucose-mediated downregulation of GIP receptors in islets. Am J Physiol Endocrinol Metab [Internet]. 2007 Aug [cited 2020 Sep 27];293(2):E538. Available from: /pmc/articles/PMC2640485/?report=abstract

212. Pamir N, Lynn FC, Buchan AMJ, Ehses J, Hinke SA, Pospisilik JA, et al. Glucose-dependent insulinotropic polypeptide receptor null mice exhibit compensatory changes in the enteroinsular axis. Am J Physiol Endocrinol Metab [Internet]. 2003 May 1 [cited

2025 Jan 20];284(5 47-5). Available from: https://journals.physiology.org/doi/10.1152/ajpendo.00270.2002

213. Nasteska D, Harada N, Suzuki K, Yamane S, Hamasaki A, Joo E, et al. Chronic Reduction of GIP Secretion Alleviates Obesity and Insulin Resistance Under High-Fat Diet Conditions. Diabetes [Internet]. 2014 Jul 1 [cited 2025 Jan 23];63(7):2332–43. Available from: https://dx.doi.org/10.2337/db13-1563

214. Althage MC, Ford EL, Wang S, Tso P, Polonsky KS, Wice BM. Targeted Ablation of Glucose-dependent Insulinotropic Polypeptide-producing Cells in Transgenic Mice Reduces Obesity and Insulin Resistance Induced by a High Fat Diet. J Biol Chem [Internet]. 2008 Jun 27 [cited 2025 Jan 23];283(26):18365. Available from: https://pmc.ncbi.nlm.nih.gov/articles/PMC2440595/

215. Killion EA, Lu SC, Fort M, Yamada Y, Véniant MM, Lloyd DJ. Glucose-Dependent Insulinotropic Polypeptide Receptor Therapies for the Treatment of Obesity, Do Agonists = Antagonists? Endocr Rev [Internet]. 2020 Feb 1 [cited 2025 Jun 25];41(1):1–21. Available from: https://dx.doi.org/10.1210/endrev/bnz002

216. VilsbØll T, Toft-Nielsen MB, Krarup T, Madsbad S, Dinesen B, Holst JJ. Evaluation of beta-cell secretory capacity using glucagon-like peptide 1. Diabetes Care [Internet]. 2000 Jun 1 [cited 2025 Jun 25];23(6):807–12. Available from: https://dx.doi.org/10.2337/diacare.23.6.807

217. Nauck MA, Heimesaat MM, Orskov C, Holst JJ, Ebert R, Creutzfeldt W. Preserved incretin activity of glucagon-like peptide 1 [7-36 amide] but not of synthetic human gastric inhibitory polypeptide in patients with type-2 diabetes mellitus. Journal of Clinical Investigation [Internet]. 1993 [cited 2022 Oct 15];91(1):301. Available from: /pmc/articles/PMC330027/?report=abstract

218. Elahi D, McAloon-Dyke M, Fukagawa NK, Meneilly GS, Sclater AL, Minaker KL, et al. The insulinotropic actions of glucose-dependent insulinotropic polypeptide (GIP) and

glucagon-like peptide-1 (7–37) in normal and diabetic subjects. Regul Pept [Internet]. 1994 Apr 14 [cited 2025 Jun 25];51(1):63–74. Available from: https://www.sciencedirect.com/science/article/pii/0167011594901368?via%3Dihub

219. Muscelli E, Mari A, Casolaro A, Camastra S, Seghieri G, Gastaldelli A, et al. Separate Impact of Obesity and Glucose Tolerance on the Incretin Effect in Normal Subjects and Type 2 Diabetic Patients. Diabetes [Internet]. 2008 May 1 [cited 2025 Jun 25];57(5):1340–8. Available from: https://dx.doi.org/10.2337/db07-1315

220. Aulinger BA, Vahl TP, Prigeon RL, D'Alessio DA, Elder DA. The incretin effect in obese adolescents with and without type 2 diabetes: impaired or intact? Am J Physiol Endocrinol Metab [Internet]. 2016 May 1 [cited 2025 Jun 25];310(9):E774. Available from: https://pmc.ncbi.nlm.nih.gov/articles/PMC4867309/

221. Knop FK, Aaboe K, Vilsbøll T, Vølund A, Holst JJ, Krarup T, et al. Impaired incretin effect and fasting hyperglucagonaemia characterizing type 2 diabetic subjects are early signs of dysmetabolism in obesity. Diabetes Obes Metab [Internet]. 2012 Jun 1 [cited 2025 Jun 25];14(6):500–10. Available from: /doi/pdf/10.1111/j.1463-1326.2011.01549.x

222. Galderisi A, Tricò D, Pierpont B, Shabanova V, Samuels S, Man CD, et al. A Reduced Incretin Effect Mediated by the rs7903146 Variant in the TCF7L2 Gene Is an Early Marker of β-Cell Dysfunction in Obese Youth. Diabetes Care [Internet]. 2020 Oct 1 [cited 2025 Jun 25];43(10):2553. Available from: https://pmc.ncbi.nlm.nih.gov/articles/PMC7510033/

223. Galderisi A, Tricò D, Lat J, Samuels S, Weiss R, Van Name M, et al. Incretin effect determines glucose trajectory and insulin sensitivity in youths with obesity. JCI Insight [Internet]. 2023 [cited 2025 Jun 25];8(22):e165709. Available from: https://pmc.ncbi.nlm.nih.gov/articles/PMC10721315/

224. Ranganath LR, Beety JM, Morgan LM, Wright JW, Howland R, Marks V. Attenuated GLP-1 secretion in obesity: cause or consequence? Gut [Internet]. 1996 Jun 1 [cited 2025 Jun 25];38(6):916–9. Available from: https://gut.bmj.com/content/38/6/916

225. Hira T, Pinyo J, Hara H. What Is GLP-1 Really Doing in Obesity? Trends in Endocrinology and Metabolism [Internet]. 2020 Feb 1 [cited 2025 Jun 25];31(2):71–80. Available from: https://www.cell.com/action/showFullText?pii=S1043276019301870

226. Vilsbøll T, Krarup T, Sonne J, Madsbad S, Vølund A, Juul AG, et al. Incretin Secretion in Relation to Meal Size and Body Weight in Healthy Subjects and People with Type 1 and Type 2 Diabetes Mellitus. J Clin Endocrinol Metab [Internet]. 2003 Jun 1 [cited 2025 Jun 25];88(6):2706–13. Available from: https://dx.doi.org/10.1210/jc.2002-021873

227. Miyawaki K, Yamada Y, Ban N, Ihara Y, Tsukiyama K, Zhou H, et al. Inhibition of gastric inhibitory polypeptide signaling prevents obesity. Nat Med [Internet]. 2002 Jun 17 [cited 2025 Jun 25];8(7):738–42. Available from: https://www.nature.com/articles/nm727

228. McClean PL, Irwin N, Cassidy RS, Holst JJ, Gault VA, Flatt PR. GIP receptor antagonism reverses obesity, insulin resistance, and associated metabolic disturbances induced in mice by prolonged consumption of high-fat diet. Am J Physiol Endocrinol Metab [Internet]. 2007 Dec [cited 2025 Jan 23];293(6):1746–55. Available from: https://journals.physiology.org/doi/10.1152/ajpendo.00460.2007

229. McClean PL, Irwin N, Cassidy RS, Holst JJ, Gault VA, Flatt PR. GIP receptor antagonism reverses obesity, insulin resistance, and associated metabolic disturbances induced in mice by prolonged consumption of high-fat diet. Am J Physiol Endocrinol Metab [Internet]. 2007 Dec [cited 2025 Jun 25];293(6):1746–55. Available from: /doi/pdf/10.1152/ajpendo.00460.2007

230. Irwin N, McClean PL, O'Harte FPM, Gault VA, Harriott P, Flatt PR. Early administration of the glucose-dependent insulinotropic polypeptide receptor antagonist (Pro3)GIP prevents the development of diabetes and related metabolic abnormalities associated

with genetically inherited obesity in ob/ob mice. Diabetologia [Internet]. 2007 Jul 8 [cited 2025 Jun 25];50(7):1532–40. Available from: https://link.springer.com/article/10.1007/s00125-007-0692-2

231. Kaneko K, Fu Y, Lin HY, Cordonier EL, Mo Q, Gao Y, et al. Gut-derived GIP activates central Rap1 to impair neural leptin sensitivity during overnutrition. J Clin Invest [Internet]. 2019 Sep 3 [cited 2025 Apr 10];129(9):3786–91. Available from: https://doi.org/10.1172/JCI126107.

232. Turcot V, Lu Y, Highland HM, Schurmann C, Justice AE, Fine RS, et al. Protein-altering variants associated with body mass index implicate pathways that control energy intake and expenditure underpinning obesity. Nat Genet [Internet]. 2017 Jan 1 [cited 2025 Aug 4];50(1):26. Available from: https://pmc.ncbi.nlm.nih.gov/articles/PMC5945951/

233. Akbari P, Gilani A, Sosina O, Kosmicki JA, Khrimian L, Fang YY, et al. Sequencing of 640,000 exomes identifies GPR75 variants associated with protection from obesity. Science (1979) [Internet]. 2021 Jul 2 [cited 2025 Aug 4];373(6550). Available from: /doi/pdf/10.1126/science.abf8683

234. Kizilkaya HS, Sørensen K V., Madsen JS, Lindquist P, Douros JD, Bork-Jensen J, et al. Characterization of genetic variants of GIPR reveals a contribution of β-arrestin to metabolic phenotypes. Nature Metabolism 2024 6:7 [Internet]. 2024 Jun 13 [cited 2024 Aug 15];6(7):1268–81. Available from: https://www.nature.com/articles/s42255-024-01061-4

235. Speliotes EK, Willer CJ, Berndt SI, Monda KL, Thorleifsson G, Jackson AU, et al. Association analyses of 249,796 individuals reveal eighteen new loci associated with body mass index. Nat Genet [Internet]. 2010 Nov 1 [cited 2025 Aug 25];42(11):937. Available from: https://pmc.ncbi.nlm.nih.gov/articles/PMC3014648/

236. Saxena R, Hivert MF, Langenberg C, Tanaka T, Pankow JS, Vollenweider P, et al. Genetic variation in GIPR influences the glucose and insulin responses to an oral glucose

challenge. Nat Genet [Internet]. 2010 Feb [cited 2025 Aug 4];42(2):142. Available from: https://pmc.ncbi.nlm.nih.gov/articles/PMC2922003/

237. Mroz PA, Finan B, Gelfanov V, Yang B, Tschöp MH, DiMarchi RD, et al. Optimized GIP analogs promote body weight lowering in mice through GIPR agonism not antagonism. Mol Metab. 2019 Feb 1;20:51–62.

238. Nørregaard PK, Deryabina MA, Tofteng Shelton P, Fog JU, Daugaard JR, Eriksson PO, et al. A novel GIP analogue, ZP4165, enhances glucagon-like peptide-1-induced body weight loss and improves glycaemic control in rodents. Diabetes Obes Metab [Internet]. 2018 Jan 1 [cited 2020 Aug 14];20(1):60–8. Available from: https://pubmed.ncbi.nlm.nih.gov/28598027/

239. Finan B, Ma T, Ottaway N, Müller TD, Habegger KM, Heppner KM, et al. Unimolecular dual incretins maximize metabolic benefits in rodents, monkeys, and humans. Sci Transl Med [Internet]. 2013 Oct 30 [cited 2025 Mar 28];5(209). Available from: https://www.science.org/doi/10.1126/scitranslmed.3007218

240. Lamont BJ, Drucker DJ. Differential Antidiabetic Efficacy of Incretin Agonists Versus DPP-4 Inhibition in High Fat–Fed Mice. Diabetes [Internet]. 2008 Jan 1 [cited 2025 Apr 10];57(1):190–8. Available from: https://dx.doi.org/10.2337/db07-1202

241. Killion EA, Chen M, Falsey JR, Sivits G, Hager T, Atangan L, et al. Chronic glucose-dependent insulinotropic polypeptide receptor (GIPR) agonism desensitizes adipocyte GIPR activity mimicking functional GIPR antagonism. Nature Communications 2020 11:1 [Internet]. 2020 Oct 5 [cited 2022 Oct 31];11(1):1–17. Available from: https://www.nature.com/articles/s41467-020-18751-8

242. Davies I, Adriaenssens AE, Scott WR, Carling D, Murphy KG, Minnion JS, et al. Chronic GIPR agonism results in pancreatic islet GIPR functional desensitisation. Mol Metab [Internet]. 2025 Feb 1 [cited 2025 Aug 25];92:102094. Available from: https://www.sciencedirect.com/science/article/pii/S2212877825000018#bib7

243. Frías JP, Davies MJ, Rosenstock J, Pérez Manghi FC, Fernández Landó L, Bergman BK, et al. Tirzepatide versus Semaglutide Once Weekly in Patients with Type 2 Diabetes. New England Journal of Medicine [Internet]. 2021 Aug 5 [cited 2024 Jun 7];385(6):503–15. Available from: https://www.nejm.org/doi/full/10.1056/NEJMoa2107519

244. Liu CM, Killion EA, Hammoud R, Lu SC, Komorowski R, Liu T, et al. GIPR-Ab/GLP-1 peptide–antibody conjugate requires brain GIPR and GLP-1R for additive weight loss in obese mice. Nature Metabolism 2025 [Internet]. 2025 Apr 29 [cited 2025 May 2];1–16. Available from: https://www.nature.com/articles/s42255-025-01295-w

245. Rajagopal S, Shenoy SK. GPCR Desensitization: Acute and Prolonged Phases. Cell Signal [Internet]. 2017 Jan 1 [cited 2025 Jun 25];41:9. Available from: https://pmc.ncbi.nlm.nih.gov/articles/PMC5533627/

246. Mohammad S, Patel RT, Bruno J, Panhwar MS, Wen J, McGraw TE. A Naturally Occurring GIP Receptor Variant Undergoes Enhanced Agonist-Induced Desensitization, Which Impairs GIP Control of Adipose Insulin Sensitivity. Mol Cell Biol [Internet]. 2014 Oct [cited 2022 Oct 15];34(19):3618. Available from: /pmc/articles/PMC4187723/

247. Yip RGC, Boylan MO, Kieffer TJ, Wolfe MM. Functional GIP Receptors Are Present on Adipocytes. Endocrinology [Internet]. 1998 Sep 1 [cited 2025 Aug 22];139(9):4004–7. Available from: https://dx.doi.org/10.1210/endo.139.9.6288

248. Rudovich N, Kaiser S, Engeli S, Osterhoff M, Gögebakan Ö, Bluher M, et al. GIP receptor mRNA expression in different fat tissue depots in postmenopausal non-diabetic women. Regul Pept [Internet]. 2007 Aug 16 [cited 2025 Aug 22];142(3):138–45. Available from: https://www.sciencedirect.com/science/article/abs/pii/S0167011507000535?via%3Dihub

249. Ceperuelo-Mallafré V, Duran X, Pachón G, Roche K, Garrido-Sánchez L, Vilarrasa N, et al. Disruption of GIP/GIPR Axis in Human Adipose Tissue Is Linked to Obesity and Insulin

Resistance. J Clin Endocrinol Metab [Internet]. 2014 May 1 [cited 2025 Aug 22];99(5):E908–19. Available from: https://dx.doi.org/10.1210/jc.2013-3350

250. Gutgesell RM, Khalil A, Liskiewicz A, Maity-Kumar G, Novikoff A, Grandl G, et al. GIPR agonism and antagonism decrease body weight and food intake via different mechanisms in male mice. Nat Metab [Internet]. 2025 Jun 1 [cited 2025 Jul 20]; Available from: https://www.researchgate.net/publication/391282940_GIPR_agonism_and_antagonism_decrease_body_weight_and_food_intake_via_different_mechanisms_in_male_mice

251. Boer GA, Keenan SN, Miotto PM, Holst JJ, Watt MJ. GIP receptor deletion in mice confers resistance to high-fat diet-induced obesity via alterations in energy expenditure and adipose tissue lipid metabolism. Am J Physiol Heart Circ Physiol [Internet]. 2021 [cited 2025 May 2];320(4):E835–45. Available from: https://journals.physiology.org/doi/pdf/10.1152/ajpendo.00646.2020

252. Killion EA, Wang J, Yie J, Shi SDH, Bates D, Min X, et al. Anti-obesity effects of GIPR antagonists alone and in combination with GLP-1R agonists in preclinical models. Sci Transl Med [Internet]. 2018 Dec 19 [cited 2025 Mar 14];10(472):3392. Available from: https://www.science.org

253. Liskiewicz A, Khalil A, Liskiewicz D, Novikoff A, Grandl G, Maity-Kumar G, et al. Glucose-dependent insulinotropic polypeptide regulates body weight and food intake via GABAergic neurons in mice. Nature Metabolism 2023 5:12 [Internet]. 2023 Nov 9 [cited 2025 Mar 14];5(12):2075–85. Available from: https://www.nature.com/articles/s42255-023-00931-7

254. Wean J, Kowalsky AH, Laker R, Will S, Drucker DJ, Rhodes CJ, et al. Specific loss of GIPR signaling in GABAergic neurons enhances GLP-1R agonist-induced body weight loss. Mol Metab [Internet]. 2025 May 1 [cited 2025 Jun 25];95:102074. Available from: https://www.sciencedirect.com/science/article/pii/S2212877824002059

255. Willard FS, Douros JD, Gabe MB, Showalter AD, Wainscott DB, Suter TM, et al. Tirzepatide is an imbalanced and biased dual GIP and GLP-1 receptor agonist. JCI Insight [Internet]. 2020 Sep 3 [cited 2020 Nov 21];5(17). Available from: https://pubmed.ncbi.nlm.nih.gov/32730231/

256. Sun B, Willard FS, Feng D, Alsina-Fernandez J, Chen Q, Vieth M, et al. Structural determinants of dual incretin receptor agonism by tirzepatide. Proc Natl Acad Sci U S A [Internet]. 2022 Mar 29 [cited 2024 Aug 19];119(13):e2116506119. Available from: https://www.pnas.org/doi/abs/10.1073/pnas.2116506119

257. Pyke C, Knudsen LB. The Glucagon-Like Peptide-1 Receptor—or Not? Endocrinology [Internet]. 2013 Jan 1 [cited 2025 Jun 30];154(1):4–8. Available from: https://dx.doi.org/10.1210/en.2012-2124

258. Drucker DJ. Incretin action in the pancreas: Potential promise, possible perils, and pathological pitfalls. Diabetes [Internet]. 2013 Oct [cited 2025 Mar 16];62(10):3316–23. Available from: https://pmc.ncbi.nlm.nih.gov/articles/PMC3781450/

259. Ast J, Broichhagen J, Hodson DJ. Reagents and models for detecting endogenous GLP1R and GIPR. EBioMedicine [Internet]. 2021 Dec 1 [cited 2022 Oct 17];74. Available from: /pmc/articles/PMC8669301/

260. Borner T, Geisler CE, Fortin SM, Cosgrove R, Alsina-Fernandez J, Dogra M, et al. GIP Receptor Agonism Attenuates GLP-1 Receptor Agonist–Induced Nausea and Emesis in Preclinical Models. Diabetes [Internet]. 2021 Nov 1 [cited 2025 May 8];70(11):2545. Available from: https://pmc.ncbi.nlm.nih.gov/articles/PMC8564411/

261. Gray SM, Xin Y, Ross EC, Chazotte BM, Capozzi ME, El K, et al. Discordance between GLP-1R gene and protein expression in mouse pancreatic islet cells. J Biol Chem [Internet]. 2020 Aug 8 [cited 2022 Oct 17];295(33):11529. Available from: /pmc/articles/PMC7450118/

262. Liu Y, Beyer A, Aebersold R. On the Dependency of Cellular Protein Levels on mRNA Abundance. Cell [Internet]. 2016 Apr 21 [cited 2025 Oct 22];165(3):535–50. Available from: https://www.cell.com/action/showFullText?pii=S0092867416302707

263. Li JJ, Bickel PJ, Biggin MD. System wide analyses have underestimated protein abundances and the importance of transcription in mammals. PeerJ [Internet]. 2014 [cited 2025 Oct 22];2014(1):1–26. Available from: https://pmc.ncbi.nlm.nih.gov/articles/PMC3940484/

264. El K, Douros JD, Willard FS, Novikoff A, Sargsyan A, Perez-Tilve D, et al. The incretin co-agonist tirzepatide requires GIPR for hormone secretion from human islets. Nat Metab [Internet]. 2023 Jun 1 [cited 2025 Mar 20];5(6):945. Available from: https://pmc.ncbi.nlm.nih.gov/articles/PMC10290954/

265. Andersen DB, Grunddal K V., Pedersen J, Kuhre RE, Lund ML, Holst JJ, et al. Using a Reporter Mouse to Map Known and Novel Sites of GLP-1 Receptor Expression in Peripheral Tissues of Male Mice. Endocrinology [Internet]. 2021 Mar 1 [cited 2025 Mar 14];162(3):1–19. Available from: https://dx.doi.org/10.1210/endocr/bqaa246

266. Richards P, Parker HE, Adriaenssens AE, Hodgson JM, Cork SC, Trapp S, et al. Identification and characterisation of glucagon-like peptide-1 receptor expressing cells using a new transgenic mouse model. Diabetes [Internet]. 2014 Apr [cited 2024 Jul 31];63(4):1224. Available from: /pmc/articles/PMC4092212/

267. Adriaenssens AE, Biggs EK, Darwish T, Tadross J, Sukthankar T, Girish M, et al. Glucose-Dependent Insulinotropic Polypeptide Receptor-Expressing Cells in the Hypothalamus Regulate Food Intake. Cell Metab [Internet]. 2019 Nov 11 [cited 2022 Oct 15];30(5):987. Available from: /pmc/articles/PMC6838660/

268. Jing C, Cornish VW. Chemical Tags for Labeling Proteins Inside Living Cells. Acc Chem Res [Internet]. 2011 Sep 9 [cited 2024 Aug 8];44(9):784. Available from: /pmc/articles/PMC3232020/

269. Ast J, Nasteska D, Fine NHF, Nieves DJ, Koszegi Z, Lanoiselée Y, et al. Revealing the tissue-level complexity of endogenous glucagon-like peptide-1 receptor expression and signaling. Nat Commun [Internet]. 2023 Dec 1 [cited 2024 Jun 7];14(1). Available from: /pmc/articles/PMC9849236/

270. Jing C, Cornish VW. Chemical Tags for Labeling Proteins Inside Living Cells. Acc Chem Res. 2011 Sep 9;44(9):784.

271. Cole NB. Site-Specific Protein Labeling with SNAP-Tags. Current protocols in protein science / editorial board, John E Coligan . [et al] [Internet]. 2013 Aug 1 [cited 2024 Sep 3];73:30.1.1. Available from: /pmc/articles/PMC3920298/

272. Watkins RW, Lavis LD, Kung VM, Los G V., Raines RT. Fluorogenic affinity label for the facile, rapid imaging of proteins in live cells. Org Biomol Chem [Internet]. 2009 [cited 2025 Jun 30];7(19):3969. Available from: https://pmc.ncbi.nlm.nih.gov/articles/PMC2800956/

273. Los G V., Encell LP, McDougall MG, Hartzell DD, Karassina N, Zimprich C, et al. HaloTag: A novel protein labeling technology for cell imaging and protein analysis. ACS Chem Biol [Internet]. 2008 Jun 20 [cited 2025 Jun 30];3(6):373–82. Available from: https://pubs.acs.org/doi/abs/10.1021/cb800025k

274. Gautier A, Juillerat A, Heinis C, Corrêa IR, Kindermann M, Beaufils F, et al. An Engineered Protein Tag for Multiprotein Labeling in Living Cells. Chem Biol. 2008 Feb 22;15(2):128–36.

275. Buenaventura T, Bitsi S, Laughlin WE, Burgoyne T, Lyu Z, Oqua AI, et al. Agonist-induced membrane nanodomain clustering drives GLP-1 receptor responses in pancreatic beta cells. PLoS Biol [Internet]. 2019 Aug 20 [cited 2025 Apr 4];17(8):e3000097. Available from: https://pmc.ncbi.nlm.nih.gov/articles/PMC6716783/

276. Podewin T, Ast J, Broichhagen J, Fine NHF, Nasteska D, Leippe P, et al. Conditional and Reversible Activation of Class A and B G Protein-Coupled Receptors Using Tethered

Pharmacology. ACS Cent Sci [Internet]. 2018 Feb 28 [cited 2024 Sep 3];4(2):166–79. Available from: /pmc/articles/PMC5832994/

277. Roed SN, No AC, Wismann P, Iversen H, Bräuner-Osborne H, Knudsen SM, et al. Functional Consequences of Glucagon-like Peptide-1 Receptor Cross-talk and Trafficking. J Biol Chem [Internet]. 2014 Jan 9 [cited 2025 Jun 30];290(2):1233. Available from: https://pmc.ncbi.nlm.nih.gov/articles/PMC4294488/

278. Roßmann K, Birke R, Levitz J, Jones B, Broichhagen J. Red and far-red cleavable fluorescent dyes for self-labelling enzyme protein tagging and interrogation of GPCR co-internalization. RSC Chem Biol [Internet]. 2024 Nov 18 [cited 2025 Jun 30];6(1):11. Available from: https://pmc.ncbi.nlm.nih.gov/articles/PMC11599839/

279. Birke R, Ast J, Roosen DA, Lee J, Roßmann K, Huhn C, et al. Sulfonated red and far-red rhodamines to visualize SNAP- and Halo-tagged cell surface proteins. Org Biomol Chem [Internet]. 2022 Aug 3 [cited 2025 Jan 28];20(30):5967–80. Available from: https://pubs.rsc.org/en/content/articlehtml/2022/ob/d1ob02216d

280. Poc P, Gutzeit VA, Ast J, Lee J, Jones BJ, D'Este E, et al. Interrogating surface *versus* intracellular transmembrane receptor populations using cell-impermeable SNAP-tag substrates. Chem Sci [Internet]. 2020 [cited 2024 Aug 14];11(30):7871–83. Available from: https://xlink.rsc.org/?DOI=D0SC02794D

281. Davies I, Manchanda Y, Sloop KW, Bloom SR, Tan TMM, Tomas A, et al. The physiological impact of an N-terminal Halo-tag on glucose-dependent insulinotropic polypeptide receptor function in mice. Diabetes Obes Metab [Internet]. 2025 Apr 1 [cited 2025 Jul 9];27(4):2294. Available from: https://pmc.ncbi.nlm.nih.gov/articles/PMC11885072/

282. Poc P, Gutzeit VA, Ast J, Lee J, Jones BJ, D'este E, et al. Interrogating surface versus intracellular transmembrane receptor populations using cell-impermeable SNAP-tag substrates †. 2020;

283. Lu SC, Chen M, Atangan L, Killion EA, Komorowski R, Cheng Y, et al. GIPR antagonist antibodies conjugated to GLP-1 peptide are bispecific molecules that decrease weight in obese mice and monkeys. Cell Rep Med [Internet]. 2021 May 5 [cited 2022 Oct 15];2(5):100263. Available from: /pmc/articles/PMC8149376/

284. Yu X, Chen S, Funcke JB, Straub LG, Pirro V, Emont MP, et al. The GIP receptor activates futile calcium cycling in white adipose tissue to increase energy expenditure and drive weight loss in mice. Cell Metab [Internet]. 2024 Dec 4 [cited 2025 Jan 15];37(1):187-204.e7. Available from: http://www.ncbi.nlm.nih.gov/pubmed/39642881

285. Manchanda Y, Bitsi S, Chen S, Broichhagen J, Bernardino De La Serna J, Jones B, et al. Enhanced Endosomal Signaling and Desensitization of GLP-1R vs GIPR in Pancreatic Beta Cells. Endocrinology [Internet]. 2023 Mar 13 [cited 2025 Jan 28];164(5):1–15. Available from: https://dx.doi.org/10.1210/endocr/bqad028

286. Fukuda M. The Role of GIP Receptor in the CNS for the Pathogenesis of Obesity. Diabetes [Internet]. 2021 Sep 1 [cited 2025 May 2];70(9):1929. Available from: https://pmc.ncbi.nlm.nih.gov/articles/PMC8576424/

287. El K, Campbell JE. The role of GIP in α-cells and glucagon secretion. Peptides (NY) [Internet]. 2020;125:170213. Available from: https://doi.org/10.1016/j.peptides.2019.170213

288. Scrocchi LA, Brown TJ, MacLusky N, Brubaker PL, Auerbach AB, Joyner AL, et al. Glucose intolerance but normal satiety in mice with a null mutation in the glucagon-like peptide 1 receptor gene. Nat Med [Internet]. 1996 Nov [cited 2025 May 6];2(11):1254–8. Available from: https://www.nature.com/articles/nm1196-1254

289. Smith EP, An Z, Wagner C, Lewis AG, Cohen EB, Li B, et al. The role of β-cell GLP-1 signaling in glucose regulation and response to diabetes drugs. Cell Metab [Internet]. 2014 Jun 3 [cited 2025 Mar 27];19(6):1050. Available from: https://pmc.ncbi.nlm.nih.gov/articles/PMC4109713/

290. Joo E, Harada N, Yamane S, Fukushima T, Taura D, Iwasaki K, et al. Inhibition of Gastric Inhibitory Polypeptide Receptor Signaling in Adipose Tissue Reduces Insulin Resistance and Hepatic Steatosis in High-Fat Diet–Fed Mice. Diabetes [Internet]. 2017 Apr 1 [cited 2025 Jun 30];66(4):868–79. Available from: https://dx.doi.org/10.2337/db16-0758

291. Hansotia T, Baggio LL, Delmeire D, Hinke SA, Yamada Y, Tsukiyama K, et al. Double Incretin Receptor Knockout (DIRKO) Mice Reveal an Essential Role for the Enteroinsular Axis in Transducing the Glucoregulatory Actions of DPP-IV Inhibitors. Diabetes [Internet]. 2004 May 1 [cited 2025 Jun 30];53(5):1326–35. Available from: https://dx.doi.org/10.2337/diabetes.53.5.1326

292. Graham FL, Smiley J, Russell WC, Nairn R. Characteristics of a human cell line transformed by DNA from human adenovirus type 5. Journal of General Virology. 1977 Jul 1;36(1):59–72.

293. Miyazaki S, Tashiro F, Tsuchiya T, Sasaki K, Miyazaki J ichi. Establishment of a long-term stable β-cell line and its application to analyze the effect of Gcg expression on insulin secretion. Sci Rep [Internet]. 2021 Dec 1 [cited 2022 Oct 15];11(1):477. Available from: /pmc/articles/PMC7804151/

294. Blanchi B, Taurand M, Colace C, Thomaidou S, Audeoud C, Fantuzzi F, et al. EndoC-βH5 cells are storable and ready-to-use human pancreatic beta cells with physiological insulin secretion. Mol Metab. 2023 Oct 1;76:101772.

295. Adriaenssens AE, Biggs EK, Darwish T, Tadross J, Sukthankar T, Girish M, et al. Glucose-Dependent Insulinotropic Polypeptide Receptor-Expressing Cells in the Hypothalamus Regulate Food Intake. Cell Metab. 2019 Nov 11;30(5):987.

296. Campbell JE, Ussher JR, Mulvihill EE, Kolic J, Baggio LL, Cao X, et al. TCF1 links GIPR signaling to the control of beta cell function and survival. Nat Med. 2016 Jan 1;22(1):84–90.

297. Wicksteed B, Brissova M, Yan W, Opland DM, Plank JL, Reinert RB, et al. Conditional Gene Targeting in Mouse Pancreatic β-Cells: Analysis of Ectopic Cre Transgene Expression in the Brain. Diabetes. 2010 Dec;59(12):3090.

298. Ast J, Arvaniti A, Fine NHF, Nasteska D, Ashford FB, Stamataki Z, et al. Super-resolution microscopy compatible fluorescent probes reveal endogenous glucagon-like peptide-1 receptor distribution and dynamics. Nat Commun [Internet]. 2020 Dec 1 [cited 2020 Sep 26];11(1). Available from: /pmc/articles/PMC6981144/?report=abstract

299. Ast J, Arvaniti A, Fine NHF, Nasteska D, Ashford FB, Stamataki Z, et al. Super-resolution microscopy compatible fluorescent probes reveal endogenous glucagon-like peptide-1 receptor distribution and dynamics. Nat Commun. 2020 Dec 1;11(1).

300. Ast J, Nasteska D, Fine NHF, Nieves DJ, Koszegi Z, Lanoiselée Y, et al. Revealing the tissue-level complexity of endogenous glucagon-like peptide-1 receptor expression and signaling. Nat Commun. 2023 Dec 1;14(1).

301. Richards P, Parker HE, Adriaenssens AE, Hodgson JM, Cork SC, Trapp S, et al. Identification and characterisation of glucagon-like peptide-1 receptor expressing cells using a new transgenic mouse model. Diabetes. 2014 Apr;63(4):1224.

302. Luche H, Weber O, Rao TN, Blum C, Fehling HJ. Faithful activation of an extra-bright red fluorescent protein in “knock-in” Cre-reporter mice ideally suited for lineage tracing studies. Eur J Immunol. 2007 Jan;37(1):43–53.

303. Zariwala HA, Borghuis BG, Hoogland TM, Madisen L, Tian L, de Zeeuw CI, et al. A Cre-Dependent GCaMP3 Reporter Mouse for Neuronal Imaging In Vivo. The Journal of Neuroscience [Internet]. 2012 Feb 2 [cited 2024 Aug 28];32(9):3131. Available from: /pmc/articles/PMC3315707/

304. Rezania A, Bruin JE, Arora P, Rubin A, Batushansky I, Asadi A, et al. Reversal of diabetes with insulin-producing cells derived in vitro from human pluripotent stem cells. Nature

Biotechnology 2014 32:11 [Internet]. 2014 Sep 11 [cited 2024 Aug 6];32(11):1121–33. Available from: https://www.nature.com/articles/nbt.3033

305. Ast J, Arvaniti A, Fine N, Nasteska D, Ashford F, Stamataki Z, et al. LUXendins reveal endogenous glucagon-like peptide-1 receptor distribution and dynamics. 2019;

306. Nguyen KP, O'Neal TJ, Bolonduro OA, White E, Kravitz A V. Feeding Experimentation Device (FED): A flexible open-source device for measuring feeding behavior. J Neurosci Methods [Internet]. 2016 Jul 15 [cited 2025 Aug 15];267:108. Available from: https://pmc.ncbi.nlm.nih.gov/articles/PMC4884551/

307. Ester M, Kriegel HP, Sander J, Xu X. A density-based algorithm for discovering clusters in large spatial databases with noise. In: Simoudis E et al., editor. KDD'96: Proc 2nd Int Conf Knowledge Discovery and Data Mining. AAAI Press; 1996. p. 226–31.

308. Dunn KW, Kamocka MM, McDonald JH. A practical guide to evaluating colocalization in biological microscopy. Am J Physiol Cell Physiol [Internet]. 2011 Apr [cited 2025 Aug 15];300(4):C723. Available from: https://pmc.ncbi.nlm.nih.gov/articles/PMC3074624/

309. Gutgesell RM, Nogueiras R, Tschöp MH, Müller TD, Gutgesell RM, Müller · T D, et al. Dual and Triple Incretin-Based Co-agonists: Novel Therapeutics for Obesity and Diabetes. Diabetes Therapy [Internet]. 2024 May 1 [cited 2025 Apr 9];15(5):1069. Available from: https://pmc.ncbi.nlm.nih.gov/articles/PMC11043266/

310. Davis RL. Mechanism of Action and Target Identification: A Matter of Timing in Drug Discovery. iScience [Internet]. 2020 Sep 25 [cited 2025 Jul 9];23(9):101487. Available from: https://pmc.ncbi.nlm.nih.gov/articles/PMC7479624/

311. Mitchell JL, Lyons HS, Walker JK, Yiangou A, Grech O, Alimajstorovic Z, et al. The effect of GLP-1RA exenatide on idiopathic intracranial hypertension: a randomized clinical trial. Brain [Internet]. 2023 May 1 [cited 2025 May 12];146(5):1821. Available from: https://pmc.ncbi.nlm.nih.gov/articles/PMC10151178/

312. Loomba R, Hartman ML, Lawitz EJ, Vuppalanchi R, Boursier J, Bugianesi E, et al. Tirzepatide for Metabolic Dysfunction–Associated Steatohepatitis with Liver Fibrosis. New England Journal of Medicine [Internet]. 2024 Jul 25 [cited 2025 Jul 10];391(4):299–310. Available from: /doi/pdf/10.1056/NEJMoa2401943?download=true

313. Sanyal AJ, Bedossa P, Fraessdorf M, Neff GW, Lawitz E, Bugianesi E, et al. A Phase 2 Randomized Trial of Survodutide in MASH and Fibrosis. New England Journal of Medicine [Internet]. 2024 Jul 25 [cited 2025 Jul 10];391(4):311–9. Available from: /doi/pdf/10.1056/NEJMoa2401755?download=true

314. Kosiborod MN, Petrie MC, Borlaug BA, Butler J, Davies MJ, Hovingh GK, et al. Semaglutide in Patients with Obesity-Related Heart Failure and Type 2 Diabetes. New England Journal of Medicine [Internet]. 2024 Apr 18 [cited 2025 Jul 10];390(15):1394–407. Available from: https://www.nejm.org/doi/pdf/10.1056/NEJMoa2313917

315. Herman RJ, Schmidt HD. Targeting GLP-1 receptors to reduce nicotine use disorder: Preclinical and clinical evidence. Physiol Behav [Internet]. 2024 Jul 1 [cited 2025 Jul 10];281:114565. Available from: https://www.sciencedirect.com/science/article/abs/pii/S0031938424001100

316. Wang W, Volkow ND, Berger NA, Davis PB, Kaelber DC, Xu R. Association of semaglutide with reduced incidence and relapse of cannabis use disorder in real-world populations: a retrospective cohort study. Mol Psychiatry [Internet]. 2024 Aug 1 [cited 2025 Jul 10];29(8):2587–98. Available from: https://www.nature.com/articles/s41380-024-02498-5

317. Human GIPR Antibody MAB8210: R&D Systems [Internet]. [cited 2025 Jul 9]. Available from: https://www.rndsystems.com/products/human-gipr-antibody-591853_mab8210#product-details

318. Yu X, Chen S, Funcke JB, Straub LG, Pirro V, Emont MP, et al. The GIP receptor activates futile calcium cycling in white adipose tissue to increase energy expenditure and drive

weight loss in mice. Cell Metab [Internet]. 2025 Jan 7 [cited 2025 Jul 9];37(1):187-204.e7. Available from: https://www.cell.com/action/showFullText?pii=S1550413124004492

319. Moody AJ, Thim L, Valverde I. The isolation and sequencing of human gastric inhibitory peptide (GIP). FEBS Lett. 1984 Jul 9;172(2):142–8.

320. Fukuda M. The Role of GIP Receptor in the CNS for the Pathogenesis of Obesity. Diabetes [Internet]. 2021 Sep 1 [cited 2025 Jul 9];70(9):1929. Available from: https://pmc.ncbi.nlm.nih.gov/articles/PMC8576424/

321. El K, Campbell JE. The role of GIP in α-cells and glucagon secretion. Peptides (NY) [Internet]. 2019 Mar 1 [cited 2025 Jul 9];125:170213. Available from: https://pmc.ncbi.nlm.nih.gov/articles/PMC7580028/

322. Preston AN, Farr JD, O'Neill BK, Thompson KK, Tsirka SE, Laughlin ST. Visualizing the brain's astrocytes with diverse chemical scaffolds. ACS Chem Biol [Internet]. 2018 Jun 15 [cited 2025 Aug 12];13(6):1493. Available from: https://pmc.ncbi.nlm.nih.gov/articles/PMC6287642/

323. Cunningham CW, Mukhopadhyay A, Lushington GH, Blagg BSJ, Prisinzano TE, Krise JP. Uptake, Distribution and Diffusivity of Reactive Fluorophores in Cells: Implications Toward Target Identification. Mol Pharm [Internet]. 2010 Aug 2 [cited 2025 Aug 12];7(4):1301. Available from: https://pmc.ncbi.nlm.nih.gov/articles/PMC2916926/

324. Hinke SA, Manhart S, Speck M, Pederson RA, Demuth HU, McIntosh CHS. In depth analysis of the N-terminal bioactive domain of gastric inhibitory polypeptide. Life Sci [Internet]. 2004 Aug 27 [cited 2024 Aug 19];75(15):1857–70. Available from: https://pubmed.ncbi.nlm.nih.gov/15302229/

325. Baker JG, Middleton R, Adams L, May LT, Briddon SJ, Kellam B, et al. Influence of fluorophore and linker composition on the pharmacology of fluorescent adenosine A 1 receptor ligands: Themed section: Imaging in pharmacology research paper. Br J Pharmacol. 2010 Feb;159(4):772–86.

326. Vernall AJ, Stoddart LA, Briddon SJ, Ng HW, Laughton CA, Doughty SW, et al. Conversion of a non-selective adenosine receptor antagonist into A3-selective high affinity fluorescent probes using peptide-based linkers. Org Biomol Chem [Internet]. 2013 Aug 7 [cited 2025 Jul 4];11(34):5673–82. Available from: https://pubs.rsc.org/en/content/articlehtml/2013/ob/c3ob41221k

327. Stoddart LA, Kilpatrick LE, Briddon SJ, Hill SJ. Probing the pharmacology of G protein-coupled receptors with fluorescent ligands. Neuropharmacology [Internet]. 2015 Nov 1 [cited 2025 Jul 4];98:48–57. Available from: https://www.sciencedirect.com/science/article/pii/S0028390815001628#bib7

328. Finan B, Müller TD, Clemmensen C, Perez-Tilve D, DiMarchi RD, Tschöp MH. Reappraisal of GIP Pharmacology for Metabolic Diseases. Trends Mol Med [Internet]. 2016 May 1 [cited 2025 Jul 4];22(5):359–76. Available from: https://www.sciencedirect.com/science/article/pii/S1471491416000575

329. Wang L, Wang N, Zhang W, Cheng X, Yan Z, Shao G, et al. Therapeutic peptides: current applications and future directions. Signal Transduction and Targeted Therapy 2022 7:1 [Internet]. 2022 Feb 14 [cited 2025 Jul 4];7(1):1–27. Available from: https://www.nature.com/articles/s41392-022-00904-4

330. Yang B, Gelfanov VM, El K, Chen A, Rohlfs R, DuBois B, et al. Discovery of a potent GIPR peptide antagonist that is effective in rodent and human systems. Mol Metab [Internet]. 2022 Dec 1 [cited 2025 Jul 4];66:101638. Available from: https://pmc.ncbi.nlm.nih.gov/articles/PMC9719863/

331. Hinke SA, Manhart S, Pamir N, Demuth HU, W. Gelling R, Pederson RA, et al. Identification of a bioactive domain in the amino-terminus of glucose-dependent insulinotropic polypeptide (GIP). Biochimica et Biophysica Acta (BBA) - Protein Structure and Molecular Enzymology. 2001 May 5;1547(1):143–55.

332. Gelling RW, Wheeler MB, Xue J, Gyomorey S, Nian C, Pederson RA, et al. Localization of the Domains Involved in Ligand Binding and Activation of the Glucose-Dependent Insulinotropic Polypeptide Receptor. Endocrinology. 1997 Jun 1;138(6):2640–3.

333. Morrow GW, Kieffer TJ, McIntosh CHS, MacGillivray RTA, Brown JC, St. Pierre S, et al. The insulinotropic region of gastric inhibitory polypeptide; fragment analysis suggests the bioactive site lies between residues 19 and 30. Can J Physiol Pharmacol. 1996 Jan 1;74(1):65–72.

334. Sun B, Willard FS, Feng D, Alsina-Fernandez J, Chen Q, Vieth M, et al. Structural determinants of dual incretin receptor agonism by tirzepatide. Proc Natl Acad Sci U S A. 2022 Mar 29;119(13):e2116506119.

335. Parthier C, Kleinschmidt M, Neumann P, Rudolph R, Manhart S, Schlenzig D, et al. Crystal structure of the incretin-bound extracellular domain of a G protein-coupled receptor. Proc Natl Acad Sci U S A. 2007 Aug 8;104(35):13942.

336. Gault VA, Parker JC, Harriott P, Flatt PR, O'Harte FPM. Evidence that the major degradation product of glucose-dependent insulinotropic polypeptide, GIP(3-42), is a GIP receptor antagonist in vivo. Journal of Endocrinology. 2002 Nov 1;175(2):525–33.

337. Hinke SA, Manhart S, Speck M, Pederson RA, Demuth HU, McIntosh CHS. In depth analysis of the N-terminal bioactive domain of gastric inhibitory polypeptide. Life Sci. 2004 Aug 27;75(15):1857–70.

338. Hinke SA, Manhart S, Pamir N, Demuth HU, W. Gelling R, Pederson RA, et al. Identification of a bioactive domain in the amino-terminus of glucose-dependent insulinotropic polypeptide (GIP). Biochimica et Biophysica Acta (BBA) - Protein Structure and Molecular Enzymology. 2001 May 5;1547(1):143–55.

339. Gault VA, Harriott P, Flatt PR, O'harte FPM. Cyclic AMP Production and Insulin Releasing Activity of Synthetic Fragment Peptides of Glucose-Dependent Insulinotropic

Polypeptide. Biosci Rep [Internet]. 2002 Dec 1 [cited 2024 Aug 19];22(6). Available from: http://portlandpress.com/bioscirep/article-pdf/22/5-6/523/470548/bsr0220523.pdf

340. Brown JC, Dahl M, Kwauk S, McIntosh CHS, Otte SC, Pederson RA. Actions of GIP. Peptides (NY). 1981 Jan 1;2(SUPPL. 2):241–5.

341. Harikumar KG, Hosohata K, Pinon DI, Miller LJ. Use of Probes with Fluorescence Indicator Distributed throughout the Pharmacophore to Examine the Peptide Agonist-binding Environment of the Family B G Protein-coupled Secretin Receptor. Journal of Biological Chemistry [Internet]. 2006 Feb 3 [cited 2025 Jul 4];281(5):2543–50. Available from: https://www.sciencedirect.com/science/article/pii/S0021925820706745

342. Arttamangkul S, Alvarez-Maubecin V, Thomas G, Williams JT, Grandy DK. Binding and internalization of fluorescent opioid peptide conjugates in living cells. Mol Pharmacol [Internet]. 2000 Dec 1 [cited 2025 Jul 4];58(6):1570–80. Available from: https://molpharm.aspetjournals.org/action/showFullText?pii=S0026895X24127320

343. Chen X, Zaro JL, Shen WC. Fusion Protein Linkers: Property, Design and Functionality. Adv Drug Deliv Rev. 2013 Oct 10;65(10):1357.

344. McIntosh CHS, Wheeler MB, Gelling RW, Brown JC, Pederson RA. GIP receptors and signal-transduction mechanisms. Acta Physiol Scand. 1996;157(3):361–5.

345. Willard FS, Douros JD, Gabe MB, Showalter AD, Wainscott DB, Suter TM, et al. Tirzepatide is an imbalanced and biased dual GIP and GLP-1 receptor agonist. JCI Insight. 2020 Sep 3;5(17).

346. Müller TD, Adriaenssens A, Ahrén B, Blüher M, Birkenfeld AL, Campbell JE, et al. Glucose-dependent insulinotropic polypeptide (GIP). Mol Metab [Internet]. 2025 May 1 [cited 2025 Aug 13];95:102118. Available from: https://pmc.ncbi.nlm.nih.gov/articles/PMC11931254/

347. Stewart MP, Langer R, Jensen KF. Intracellular Delivery by Membrane Disruption: Mechanisms, Strategies, and Concepts. Chem Rev [Internet]. 2018 Aug 22 [cited 2025 Jul 3];118(16):7409. Available from: https://pmc.ncbi.nlm.nih.gov/articles/PMC6763210/

348. Kawaguchi Y, Futaki S. Finding ways into the cytosol: Peptide-mediated approaches for delivering proteins into cells. Curr Opin Chem Biol [Internet]. 2024 Aug 1 [cited 2025 Jul 3];81:102482. Available from: https://www.sciencedirect.com/science/article/pii/S1367593124000589

349. Shilleh AH, Viloria K, Broichhagen J, Campbell JE, Hodson DJ. GLP1R and GIPR expression and signaling in pancreatic alpha cells, beta cells and delta cells. Peptides (NY). 2024 May 1;175:171179.

350. Miyawaki K, Yamada Y, Ban N, Ihara Y, Tsukiyama K, Zhou H, et al. Inhibition of gastric inhibitory polypeptide signaling prevents obesity. Nature Medicine 2002 8:7 [Internet]. 2002 Jun 17 [cited 2025 Jan 20];8(7):738–42. Available from: https://www.nature.com/articles/nm727

351. Dai C, Brissova M, Hang Y, Thompson C, Poffenberger G, Shostak A, et al. Islet-enriched gene expression and glucose-induced insulin secretion in human and mouse islets. Diabetologia [Internet]. 2011 Mar [cited 2025 Jul 11];55(3):707. Available from: https://pmc.ncbi.nlm.nih.gov/articles/PMC3268985/

352. Kitzmann JP, Pepper AR, Gala-Lopez B, Pawlick R, Kin T, O'Gorman D, et al. Human islet viability and function is maintained during high density shipment in silicone rubber membrane vessels. Transplant Proc [Internet]. 2014 [cited 2025 Jul 11];46(6):1989. Available from: https://pmc.ncbi.nlm.nih.gov/articles/PMC4169700/

353. Negi S, Jetha A, Aikin R, Hasilo C, Sladek R, Paraskevas S. Analysis of Beta-Cell Gene Expression Reveals Inflammatory Signaling and Evidence of Dedifferentiation following Human Islet Isolation and Culture. PLoS One [Internet]. 2012 Jan 27 [cited 2025 Jul

11];7(1):e30415. Available from: https://journals.plos.org/plosone/article?id=10.1371/journal.pone.0030415

354. Kaddis JS, Hanson MS, Cravens J, Qian D, Olack B, Antler M, et al. Standardized transportation of human islets: An islet cell resource center study of more than 2,000 shipments. Cell Transplant [Internet]. 2013 [cited 2025 Jul 16];22(7):1101–11. Available from: https://scholar.google.com/scholar_url?url=https://journals.sagepub.com/doi/pdf/10.3727/096368912X653219&hl=en&sa=T&oi=ucasa&ct=ufr&ei=wrB3aM-yOpOIieoP0rSEwQg&scisig=AAZF9b_Y5rP2Wq7XKAj0Snrpz8EA

355. Yang NJ, Hinner MJ. Getting Across the Cell Membrane: An Overview for Small Molecules, Peptides, and Proteins. Methods Mol Biol [Internet]. 2015 [cited 2025 Jul 16];1266:29. Available from: https://pmc.ncbi.nlm.nih.gov/articles/PMC4891184/

356. Holmdahl R, Malissen B. The need for littermate controls. Eur J Immunol [Internet]. 2012 Jan 1 [cited 2025 Jan 15];42(1):45–7. Available from: https://onlinelibrary.wiley.com/doi/full/10.1002/eji.201142048

357. Erhardt V, Hartig E, Lorenzo K, Megathlin HR, Tarchini B, Hosur V. Systematic optimization and prediction of cre recombinase for precise genome editing in mice. Genome Biol [Internet]. 2025 Dec 1 [cited 2025 Jul 15];26(1):1–28. Available from: https://genomebiology.biomedcentral.com/articles/10.1186/s13059-025-03560-3

358. Schmidt-Supprian M, Rajewsky K. Vagaries of conditional gene targeting. Nat Immunol [Internet]. 2007 Jul [cited 2025 Jul 15];8(7):665–8. Available from: https://www.nature.com/articles/ni0707-665

359. Loonstra A, Vooijs M, Beverloo HB, Allak B Al, Van Drunen E, Kanaar R, et al. Growth inhibition and DNA damage induced by Cre recombinase in mammalian cells. Proc Natl Acad Sci U S A [Internet]. 2001 Jul 31 [cited 2025 Jul 15];98(16):9209–14. Available from: /doi/pdf/10.1073/pnas.161269798?download=true

360. Bohin N, Carlson EA, Samuelson LC. Genome Toxicity and Impaired Stem Cell Function after Conditional Activation of CreERT2 in the Intestine. Stem Cell Reports [Internet]. 2018 Dec 11 [cited 2025 Jul 15];11(6):1337. Available from: https://pmc.ncbi.nlm.nih.gov/articles/PMC6294112/

361. Harno E, Cottrell EC, White A. Metabolic Pitfalls of CNS Cre-Based Technology. Cell Metab [Internet]. 2013 Jul 2 [cited 2025 Jul 15];18(1):21–8. Available from: https://www.sciencedirect.com/science/article/pii/S155041311300209X#bib15

362. Lee JY, Ristow M, Lin X, White MF, Magnuson MA, Hennighausen L. RIP-Cre Revisited, Evidence for Impairments of Pancreatic β-Cell Function. Journal of Biological Chemistry [Internet]. 2006 Feb 3 [cited 2025 Jul 15];281(5):2649–53. Available from: https://www.sciencedirect.com/science/article/pii/S0021925820706861

363. Teitelman G, Kedees M. Mouse Insulin Cells Expressing an Inducible RIPCre Transgene Are Functionally Impaired. J Biol Chem [Internet]. 2014 Feb 6 [cited 2025 Jul 15];290(6):3647. Available from: https://pmc.ncbi.nlm.nih.gov/articles/PMC4319030/

364. Magnuson MA, Burlison JS. Caveats and considerations for performing pancreas-specific gene manipulations in the mouse. Diabetes Obes Metab [Internet]. 2007 [cited 2025 Jul 15];9(SUPPL. 2):5–13. Available from: /doi/pdf/10.1111/j.1463-1326.2007.00771.x

365. Johnson JD. A practical guide to genetic engineering of pancreatic β-cells in vivo: Getting a grip on RIP and MIP. Islets [Internet]. 2014 Jul 1 [cited 2025 Jul 15];6(3):e944439. Available from: https://pmc.ncbi.nlm.nih.gov/articles/PMC4376052/

366. Toseland CP. Fluorescent labeling and modification of proteins. J Chem Biol [Internet]. 2013 Jul [cited 2025 Jan 21];6(3):85. Available from: https://pmc.ncbi.nlm.nih.gov/articles/PMC3691395/

367. Hedegaard SF, Derbas MS, Lind TK, Kasimova MR, Christensen MV, Michaelsen MH, et al. Fluorophore labeling of a cell-penetrating peptide significantly alters the mode and

degree of biomembrane interaction. Sci Rep [Internet]. 2018 Dec 1 [cited 2025 Jan 21];8(1):6327. Available from: https://pmc.ncbi.nlm.nih.gov/articles/PMC5910404/

368. Birch D, Christensen MV, Staerk D, Franzyk H, Nielsen HM. Fluorophore labeling of a cell-penetrating peptide induces differential effects on its cellular distribution and affects cell viability. Biochimica et Biophysica Acta (BBA) - Biomembranes. 2017 Dec 1;1859(12):2483–94.

369. Gallwitz B, Witt M, Morys-Wortmann C, Fölsch UR, Schmidt WE. GLP-1GIP chimeric peptides define the structural requirements for specific ligand-receptor interaction of GLP-1. Regul Pept [Internet]. 1996 May 7 [cited 2025 Aug 12];63(1):17–22. Available from: https://www.sciencedirect.com/science/article/pii/0167011596000195

370. Donocoff RS, Teteloshvili N, Chung H, Shoulson R, Creusot RJ. Optimization of tamoxifen-induced Cre activity and its effect on immune cell populations. Sci Rep [Internet]. 2020 Dec 1 [cited 2025 Jul 15];10(1):1–12. Available from: https://www.nature.com/articles/s41598-020-72179-0

371. Valny M, Honsa P, Kirdajova D, Kamenik Z, Anderova M. Tamoxifen in the Mouse Brain: Implications for Fate-Mapping Studies Using the Tamoxifen-Inducible Cre-loxP System. Front Cell Neurosci [Internet]. 2016 Oct 20 [cited 2025 Jul 15];10(OCT2016):243. Available from: https://pmc.ncbi.nlm.nih.gov/articles/PMC5071318/

372. Leong TYM, Leong ASY. How does antigen retrieval work? Adv Anat Pathol. 2007 Mar;14(2):129–31.

373. Lippincott-Schwartz J, Manley S. Putting super-resolution fluorescence microscopy to work. Nat Methods [Internet]. 2009 [cited 2025 Jan 21];6(1):21. Available from: https://pmc.ncbi.nlm.nih.gov/articles/PMC3658619/

374. Schnell U, Dijk F, Sjollema KA, Giepmans BNG. Immunolabeling artifacts and the need for live-cell imaging. Nature Methods 2012 9:2 [Internet]. 2012 Jan 30 [cited 2025 Jan 21];9(2):152–8. Available from: https://www.nature.com/articles/nmeth.1855

375. Joosen L, Hink MA, Gadella TWJ, Goedhart J. Effect of fixation procedures on the fluorescence lifetimes of Aequorea victoria derived fluorescent proteins. J Microsc [Internet]. 2014 Dec 1 [cited 2025 Jan 21];256(3):166–76. Available from: https://onlinelibrary.wiley.com/doi/full/10.1111/jmi.12168

376. Böhme I, Beck-Sickinger AG. Illuminating the life of GPCRs. Cell Communication and Signaling [Internet]. 2009 Jul 14 [cited 2025 Jan 21];7(1):1–22. Available from: https://biosignaling.biomedcentral.com/articles/10.1186/1478-811X-7-16

377. Irgen-Gioro S, Yoshida S, Walling V, Chong S. Fixation can change the appearance of phase separation in living cells. Elife. 2022 Nov 1;11.

378. Teng IT, Bu X, Chung I. Conjugation of Fab' Fragments with Fluorescent Dyes for Single-Molecule Tracking On Live Cells. Bio Protoc [Internet]. 2019 Sep 20 [cited 2025 Aug 12];9(18):e3375. Available from: https://pmc.ncbi.nlm.nih.gov/articles/PMC7853996/

379. Campbell JE, Müller TD, Finan B, DiMarchi RD, Tschöp MH, D'Alessio DA. GIPR/GLP-1R dual agonist therapies for diabetes and weight loss—chemistry, physiology, and clinical applications. Cell Metab. 2023 Sep 5;35(9):1519–29.

380. Campbell JE. Targeting the GIPR for obesity: To agonize or antagonize? Potential mechanisms. Mol Metab [Internet]. 2020 Apr 1 [cited 2025 Jan 23];46:101139. Available from: https://pmc.ncbi.nlm.nih.gov/articles/PMC8085569/

381. Gault VA, Harriott P, Flatt PR, O'harte FPM. Cyclic AMP Production and Insulin Releasing Activity of Synthetic Fragment Peptides of Glucose-Dependent Insulinotropic Polypeptide. Biosci Rep. 22(6).

382. Waller DG, Sampson AP. Principles of pharmacology and mechanisms of drug action. Medical Pharmacology and Therapeutics. 2018 Jan 1;3–31.

383. Wei T, Cui X, Jiang Y, Wang K, Wang D, Li F, et al. Glucagon Acting at the GLP-1 Receptor Contributes to β-Cell Regeneration Induced by Glucagon Receptor Antagonism in

Diabetic Mice. Diabetes [Internet]. 2023 May 1 [cited 2025 Aug 12];72(5):599. Available from: https://pmc.ncbi.nlm.nih.gov/articles/PMC10130488/

384. Cabrera O, Ficorilli J, Shaw J, Echeverri F, Schwede F, Chepurny OG, et al. Intra-islet glucagon confers β-cell glucose competence for first-phase insulin secretion and favors GLP-1R stimulation by exogenous glucagon. J Biol Chem [Internet]. 2021 Feb 1 [cited 2025 Aug 12];298(2):101484. Available from: https://pmc.ncbi.nlm.nih.gov/articles/PMC8789663/

385. Svendsen B, Larsen O, Gabe MBN, Christiansen CB, Rosenkilde MM, Drucker DJ, et al. Insulin Secretion Depends on Intra-islet Glucagon Signaling. Cell Rep [Internet]. 2018 Oct 30 [cited 2025 Apr 24];25(5):1127-1134.e2. Available from: https://www.sciencedirect.com/science/article/pii/S2211124718315948

386. Jorgensen R, Martini L, Schwartz TW, Elling CE. Characterization of Glucagon-Like Peptide-1 Receptor β-Arrestin 2 Interaction: A High-Affinity Receptor Phenotype. Molecular Endocrinology [Internet]. 2005 Mar 1 [cited 2025 Aug 12];19(3):812–23. Available from: https://dx.doi.org/10.1210/me.2004-0312

387. Gadgaard S, van der Velden WJC, Schiellerup SP, Hunt JE, Gabe MBN, Windeløv JA, et al. Novel agonist and antagonist radioligands for the GLP-2 receptor. Useful tools for studies of basic GLP-2 receptor pharmacology. Br J Pharmacol. 2022 May 1;179(9):1998–2015.

388. Gabe MBN, Gasbjerg LS, Gadgaard S, Lindquist P, Holst JJ, Rosenkilde MM. N-terminal alterations turn the gut hormone GLP-2 into an antagonist with gradual loss of GLP-2 receptor selectivity towards more GLP-1 receptor interaction. Br J Pharmacol. 2022 Sep 1;179(18):4473–85.

389. Miyawaki K, Yamada Y, Yano H, Niwa H, Ban N, Ihara Y, et al. Glucose intolerance caused by a defect in the entero-insular axis: A study in gastric inhibitory polypeptide receptor knockout mice. Proc Natl Acad Sci U S A [Internet]. 1999 Dec 21 [cited 2025 Jan 23];96(26):14843. Available from: https://pmc.ncbi.nlm.nih.gov/articles/PMC24735/

390. Killion EA, Wang J, Yie J, Shi SDH, Bates D, Min X, et al. Anti-obesity effects of GIPR antagonists alone and in combination with GLP-1R agonists in preclinical models. Sci Transl Med [Internet]. 2018 Dec 19 [cited 2025 Jan 21];10(472). Available from: https://www.science.org/doi/10.1126/scitranslmed.aat3392

391. Svendsen B, Capozzi ME, Nui J, Hannou SA, Finan B, Naylor J, et al. Pharmacological antagonism of the incretin system protects against diet-induced obesity. Mol Metab [Internet]. 2019 Feb 1 [cited 2025 Jan 21];32:44. Available from: https://pmc.ncbi.nlm.nih.gov/articles/PMC6939028/

392. Wang Y zhe, Yang D hua, Wang M wei. Signaling profiles in HEK 293T cells co-expressing GLP-1 and GIP receptors. Acta Pharmacol Sin [Internet]. 2021 Jun 1 [cited 2025 Jul 16];43(6):1453. Available from: https://pmc.ncbi.nlm.nih.gov/articles/PMC9159978/

393. Bensellam M, Jonas JC, Laybutt DR. Mechanisms of β-cell dedifferentiation in diabetes: recent findings and future research directions. Journal of Endocrinology [Internet]. 2018 Feb 1 [cited 2025 Jul 15];236(2):R109–43. Available from: https://joe.bioscientifica.com/view/journals/joe/236/2/JOE-17-0516.xml

394. Weir GC, Aguayo-Mazzucato C, Bonner-Weir S. β-cell dedifferentiation in diabetes is important, but what is it? Islets [Internet]. 2013 [cited 2025 Aug 12];5(5):233. Available from: https://pmc.ncbi.nlm.nih.gov/articles/PMC4010577/

395. Song J, Ni Q, Sun J, Xie J, Liu J, Ning G, et al. Aging Impairs Adaptive Unfolded Protein Response and Drives Beta Cell Dedifferentiation in Humans. J Clin Endocrinol Metab [Internet]. 2022 Dec 1 [cited 2025 Aug 12];107(12):3231. Available from: https://pmc.ncbi.nlm.nih.gov/articles/PMC9693768/

396. Sun T, Han X. Death versus dedifferentiation: The molecular bases of beta cell mass reduction in type 2 diabetes. Semin Cell Dev Biol [Internet]. 2020 Jul 1 [cited 2025 Aug 12];103:76–82. Available from: https://www.sciencedirect.com/science/article/pii/S1084952119302046?via%3Dihub

397. Talchai C, Xuan S, Lin H V., Sussel L, Accili D. Pancreatic β-Cell Dedifferentiation As Mechanism Of Diabetic β-Cell Failure. Cell [Internet]. 2012 Sep 14 [cited 2025 Aug 12];150(6):1223. Available from: https://pmc.ncbi.nlm.nih.gov/articles/PMC3445031/

398. Khin PP, Lee JH, Jun HS. A Brief Review of the Mechanisms of β-Cell Dedifferentiation in Type 2 Diabetes. Nutrients [Internet]. 2021 May 1 [cited 2025 Aug 12];13(5):1593. Available from: https://pmc.ncbi.nlm.nih.gov/articles/PMC8151793/

399. Müller TD, Finan B, Bloom SR, D'Alessio D, Drucker DJ, Flatt PR, et al. Glucagon-like peptide 1 (GLP-1). Mol Metab [Internet]. 2019 Dec 1 [cited 2025 Aug 12];30:72. Available from: https://pmc.ncbi.nlm.nih.gov/articles/PMC6812410/

400. Li Y, Cao X, Li LX, Brubaker PL, Edlund H, Drucker DJ. β-Cell Pdx1 Expression Is Essential for the Glucoregulatory, Proliferative, and Cytoprotective Actions of Glucagon-Like Peptide-1. Diabetes [Internet]. 2005 Feb 1 [cited 2025 Apr 9];54(2):482–91. Available from: https://dx.doi.org/10.2337/diabetes.54.2.482

401. Tong JCL, Frazer-Morris C, Shilleh AH, Viloria K, de Bray A, Nair AM, et al. Localized GLP1 receptor pre-internalization directs pancreatic alpha cell to beta cell communication. Cell Metab [Internet]. 2025 Jul 14 [cited 2025 Jul 18]; Available from: https://linkinghub.elsevier.com/retrieve/pii/S1550413125003043

402. Nie L, Wu G, Zhang W. Correlation of mRNA Expression and Protein Abundance Affected by Multiple Sequence Features Related to Translational Efficiency in Desulfovibrio vulgaris: A Quantitative Analysis. Genetics [Internet]. 2006 [cited 2025 Jul 15];174(4):2229. Available from: https://pmc.ncbi.nlm.nih.gov/articles/PMC1698625/

403. Kharchenko P V., Silberstein L, Scadden DT. Bayesian approach to single-cell differential expression analysis. Nature Methods 2014 11:7 [Internet]. 2014 May 18 [cited 2025 Aug 12];11(7):740–2. Available from: https://www.nature.com/articles/nmeth.2967

404. Qiu P. Embracing the dropouts in single-cell RNA-seq analysis. Nat Commun [Internet]. 2020 Dec 1 [cited 2025 Aug 12];11(1):1–9. Available from: https://www.nature.com/articles/s41467-020-14976-9

405. Jovanovic M, Rooney MS, Mertins P, Przybylski D, Chevrier N, Satija R, et al. Dynamic profiling of the protein life cycle in response to pathogens. Science (1979) [Internet]. 2015 Mar 6 [cited 2025 Jul 15];347(6226). Available from: https://pubmed.ncbi.nlm.nih.gov/25745177/

406. Adriaenssens A, Broichhagen J, De Bray A, Ast J, Hasib A, Jones B, et al. Hypothalamic and brainstem glucose-dependent insulinotropic polypeptide receptor neurons employ distinct mechanisms to affect feeding. 2023;

407. Adriaenssens A, Broichhagen J, De Bray A, Ast J, Hasib A, Jones B, et al. Hypothalamic and brainstem glucose-dependent insulinotropic polypeptide receptor neurons employ distinct mechanisms to affect feeding. JCI Insight [Internet]. 2023 May 22 [cited 2024 Mar 11]; Available from: https://doi.org/10.1172/jci.insight.164921DS1

408. Campbell JE, Müller TD, Finan B, DiMarchi RD, Tschöp MH, D'Alessio DA. GIPR/GLP-1R dual agonist therapies for diabetes and weight loss– Chemistry, Physiology and Clinical application. Cell Metab [Internet]. 2023 Sep 5 [cited 2025 Mar 20];35(9):1519. Available from: https://pmc.ncbi.nlm.nih.gov/articles/PMC10528201/

409. Premont RT. Keys to the Kingdom: GPCR phosphorylation patterns direct β-arrestin. EMBO Rep [Internet]. 2020 Sep 3 [cited 2025 Jul 31];21(9):e51249. Available from: https://pmc.ncbi.nlm.nih.gov/articles/PMC7507377/

410. Gurevich V V., Gurevich E V. GPCR Signaling Regulation: The Role of GRKs and Arrestins. Front Pharmacol [Internet]. 2019 [cited 2025 Jul 31];10(FEB):125. Available from: https://pmc.ncbi.nlm.nih.gov/articles/PMC6389790/

411. Yuliantie E, Darbalaei S, Dai A, Zhao P, Yang D, Sexton PM, et al. Pharmacological characterization of mono-, dual- and tri-peptidic agonists at GIP and GLP-1 receptors. Biochem Pharmacol. 2020 Jul 1;177.

412. El K, Douros JD, Willard FS, Novikoff A, Sargsyan A, Perez-Tilve D, et al. The incretin co-agonist tirzepatide requires GIPR for hormone secretion from human islets. Nature Metabolism 2023 5:6 [Internet]. 2023 Jun 5 [cited 2025 Feb 7];5(6):945–54. Available from: https://www.nature.com/articles/s42255-023-00811-0

413. Yu X, Chen S, Funcke JB, Straub LG, Pirro V, Emont MP, et al. The GIP receptor activates futile calcium cycling in white adipose tissue to increase energy expenditure and drive weight loss in mice. Cell Metab [Internet]. 2024 Dec 4 [cited 2025 Mar 14];37(1):187-204.e7. Available from: http://www.ncbi.nlm.nih.gov/pubmed/39642881

414. Coskun T, Sloop KW, Loghin C, Alsina-Fernandez J, Urva S, Bokvist KB, et al. LY3298176, a novel dual GIP and GLP-1 receptor agonist for the treatment of type 2 diabetes mellitus: From discovery to clinical proof of concept. Mol Metab [Internet]. 2018 Dec 1 [cited 2025 Mar 20];18:3. Available from: https://pmc.ncbi.nlm.nih.gov/articles/PMC6308032/

415. Wang L. Designing a Dual GLP-1R/GIPR Agonist from Tirzepatide: Comparing Residues Between Tirzepatide, GLP-1, and GIP. Drug Des Devel Ther [Internet]. 2022 [cited 2025 Mar 27];16:1547. Available from: https://pmc.ncbi.nlm.nih.gov/articles/PMC9149770/

416. Bokvist BK, Coskun T, Cummins RC, Alsina-Fernandez J. United States Patent No. US 9,474,780 B2 [Internet]. Vol. 10, Cu. United States; 2016 [cited 2025 Mar 20]. Available from: https://patentimages.storage.googleapis.com/e4/20/b1/04165a87d59f23/US9474780.pdf

417. Thorens B, Hodson DJ. Building the Glucagon-Like Peptide-1 Receptor Brick by Brick: Revisiting a 1993 Diabetes Classic by Thorens et al. Diabetes [Internet]. 2024 Jul 1 [cited 2025 Jul 31];73(7):1027. Available from: https://pmc.ncbi.nlm.nih.gov/articles/PMC11189827/

418. Arttamangkul S, Alvarez-Maubecin V, Thomas G, Williams JT, Grandy DK. Binding and Internalization of Fluorescent Opioid Peptide Conjugates in Living Cells. Mol Pharmacol [Internet]. 2000 Dec 1 [cited 2025 Jan 21];58(6):1570–80. Available from: http://molpharm.aspetjournals.org/article/S0026895X24127320/fulltext

419. Ast J, Novak AN, Podewin T, Fine NHF, Jones B, Tomas A, et al. Expanded LUXendin Color Palette for GLP1R Detection and Visualization in Vitro and in Vivo. JACS Au [Internet]. 2022 Apr 25 [cited 2025 Feb 5];2(4):1007–17. Available from: https://pubs.acs.org/doi/full/10.1021/jacsau.2c00130

420. Zhao F, Zhou Q, Cong Z, Hang K, Zou X, Zhang C, et al. Structural insights into multiplexed pharmacological actions of tirzepatide and peptide 20 at the GIP, GLP-1 or glucagon receptors. Nature Communications 2022 13:1 [Internet]. 2022 Feb 25 [cited 2025 Mar 20];13(1):1–16. Available from: https://www.nature.com/articles/s41467-022-28683-0

421. Jun LS, Showalter AD, Ali N, Dai F, Ma W, Coskun T, et al. A Novel Humanized GLP-1 Receptor Model Enables Both Affinity Purification and Cre-LoxP Deletion of the Receptor. PLoS One [Internet]. 2014 Apr 2 [cited 2025 Oct 22];9(4):e93746. Available from: https://pmc.ncbi.nlm.nih.gov/articles/PMC3973576/

422. Gasbjerg LS, Rasmussen RS, Dragan A, Lindquist P, Melchiorsen JU, Stepniewski TM, et al. Altered desensitization and internalization patterns of rodent versus human glucose-dependent insulinotropic polypeptide (GIP) receptors. An important drug discovery challenge. Br J Pharmacol [Internet]. 2025 Jul 1 [cited 2025 Oct 22];182(14):3353–70. Available from: /doi/pdf/10.1111/bph.16478

423. Miyazaki JI, Araki K, Yamato E, Ikegami H, Asano T, Shibasaki Y, et al. Establishment of a Pancreatic β Cell Line That Retains Glucose-Inducible Insulin Secretion: Special Reference to Expression of Glucose Transporter Isoforms. Endocrinology [Internet]. 1990 Jul 1 [cited 2025 Mar 5];127(1):126–32. Available from: https://dx.doi.org/10.1210/endo-127-1-126

424. Kang ZF, Deng Y, Zhou Y, Fan RR, Chan JCN, Laybutt DR, et al. Pharmacological reduction of NEFA restores the efficacy of incretin-based therapies through GLP-1 receptor signalling in the beta cell in mouse models of diabetes. Diabetologia [Internet]. 2013 Feb 28 [cited 2025 Mar 5];56(2):423–33. Available from: https://link.springer.com/article/10.1007/s00125-012-2776-x

425. Blanchi B, Taurand M, Colace C, Thomaidou S, Audeoud C, Fantuzzi F, et al. EndoC-βH5 cells are storable and ready-to-use human pancreatic beta cells with physiological insulin secretion. Mol Metab [Internet]. 2023 Oct 1 [cited 2025 Feb 13];76:101772. Available from: https://pmc.ncbi.nlm.nih.gov/articles/PMC10407753/

426. Ast J, Arvaniti A, Fine N, Nasteska D, Ashford F, Stamataki Z, et al. LUXendins reveal endogenous glucagon-like peptide-1 receptor distribution and dynamics. 2019 [cited 2020 Sep 26]; Available from: https://doi.org/10.1101/557132

427. Galsgaard KD, Vergara J, Jepsen SL, Bazzichi A, Kissow H, Smits MM, et al. Single incretin receptor knockout mice do not compensate by increasing glucose-stimulated secretion of the remaining incretin hormone. Am J Physiol Endocrinol Metab [Internet]. 2025 Mar 1 [cited 2025 Mar 28];328(3):E435–46. Available from: http://www.ncbi.nlm.nih.gov/pubmed/39933706

428. Stockinger F, Poc P, Möhwald A, Karch S, Häfner S, Alzheimer C, et al. Multicolor, Cell-Impermeable, and High Affinity BACE1 Inhibitor Probes Enable Superior Endogenous Staining and Imaging of Single Molecules. J Med Chem [Internet]. 2024 Jun 27 [cited 2025 Mar 16];67(12):10152–67. Available from: https://pubs.acs.org/doi/full/10.1021/acs.jmedchem.4c00339

429. Tornehave D, Kristensen P, Rømer J, Knudsen LB, Heller RS. Expression of the GLP-1 receptor in mouse, rat, and human pancreas. Journal of Histochemistry and Cytochemistry [Internet]. 2008 Sep [cited 2020 Sep 26];56(9):841–51. Available from: /pmc/articles/PMC2516959/?report=abstract

430. Creutzfeldt W, Nauck M. Gut hormones and diabetes mellitus. Diabetes Metab Rev [Internet]. 1992 Jul 1 [cited 2025 Apr 8];8(2):149–77. Available from: https://onlinelibrary.wiley.com/doi/full/10.1002/dmr.5610080206

431. Vilsbøll T, Knop FK, Krarup T, Johansen A, Madsbad S, Larsen S, et al. The Pathophysiology of Diabetes Involves a Defective Amplification of the Late-Phase Insulin Response to Glucose by Glucose-Dependent Insulinotropic Polypeptide—Regardless of Etiology and Phenotype. J Clin Endocrinol Metab [Internet]. 2003 Oct 1 [cited 2025 Apr 8];88(10):4897–903. Available from: https://dx.doi.org/10.1210/jc.2003-030738

432. Knop FK, Aaboe K, Vilsbøll T, Vølund A, Holst JJ, Krarup T, et al. Impaired incretin effect and fasting hyperglucagonaemia characterizing type 2 diabetic subjects are early signs of dysmetabolism in obesity. Diabetes Obes Metab [Internet]. 2012 Jun 1 [cited 2025 Apr 8];14(6):500–10. Available from: https://onlinelibrary.wiley.com/doi/full/10.1111/j.1463-1326.2011.01549.x

433. Vilsbøll T, Krarup T, Deacon CF, Madsbad S, Holst JJ. Reduced Postprandial Concentrations of Intact Biologically Active Glucagon-Like Peptide 1 in Type 2 Diabetic Patients. Diabetes [Internet]. 2001 Mar 1 [cited 2025 Apr 8];50(3):609–13. Available from: https://dx.doi.org/10.2337/diabetes.50.3.609

434. Toft-Nielsen MB, Damholt MB, Madsbad S, Hilsted LM, Hughes TE, Michelsen BK, et al. Determinants of the Impaired Secretion of Glucagon-Like Peptide-1 in Type 2 Diabetic Patients. J Clin Endocrinol Metab [Internet]. 2001 Aug 1 [cited 2025 Apr 8];86(8):3717–23. Available from: https://dx.doi.org/10.1210/jcem.86.8.7750

435. Nauck MA, Kleine N, Ørskov C, Holst JJ, Willms B, Creutzfeldt W. Normalization of fasting hyperglycaemia by exogenous glucagon-like peptide 1 (7-36 amide) in Type 2 (non-insulin-dependent) diabetic patients. Diabetologia [Internet]. 1993 [cited 2025 Apr 9];36(8):741–4. Available from: https://link.springer.com/article/10.1007/BF00401145

436. Flint A, Raben A, Astrup A, Holst JJ. Glucagon-like peptide 1 promotes satiety and suppresses energy intake in humans. J Clin Invest [Internet]. 1998 Feb 1 [cited 2025 Apr 9];101(3):515–20. Available from: https://pubmed.ncbi.nlm.nih.gov/9449682/

437. Gasbjerg LS, Helsted MM, Hartmann B, Jensen MH, Gabe MBN, Sparre-Ulrich AH, et al. Separate and Combined Glucometabolic Effects of Endogenous Glucose-Dependent Insulinotropic Polypeptide and Glucagon-like Peptide 1 in Healthy Individuals. Diabetes [Internet]. 2019 May 1 [cited 2025 Apr 8];68(5):906–17. Available from: https://dx.doi.org/10.2337/db18-1123

438. Nauck MA, Meier JJ. The incretin effect in healthy individuals and those with type 2 diabetes: Physiology, pathophysiology, and response to therapeutic interventions. Lancet Diabetes Endocrinol [Internet]. 2016 Jun 1 [cited 2020 Aug 14];4(6):525–36. Available from: http://www.thelancet.com/article/S2213858715004829/fulltext

439. Nauck MA, Bartels E, Ørskov C, Ebert R, Creutzfeldt W. Additive insulinotropic effects of exogenous synthetic human gastric inhibitory polypeptide and glucagon-like peptide-1-(7-36) amide infused at near-physiological insulinotropic hormone and glucose concentrations. J Clin Endocrinol Metab [Internet]. 1993 [cited 2022 Oct 15];76(4):912–7. Available from: https://pubmed.ncbi.nlm.nih.gov/8473405/

440. Bates HE, Campbell JE, Ussher JR, Baggio LL, Maida A, Seino Y, et al. Gipr Is Essential for Adrenocortical Steroidogenesis; However, Corticosterone Deficiency Does Not Mediate the Favorable Metabolic Phenotype of Gipr−/− Mice. Diabetes [Internet]. 2012 Jan 1 [cited 2025 Apr 10];61(1):40–8. Available from: https://dx.doi.org/10.2337/db11-1060

441. Ugleholdt R, Pedersen J, Bassi MR, Füchtbauer EM, Jørgensen SM, Kissow HL, et al. Transgenic Rescue of Adipocyte Glucose-dependent Insulinotropic Polypeptide Receptor Expression Restores High Fat Diet-induced Body Weight Gain. Journal of Biological Chemistry. 2011 Dec 30;286(52):44632–45.

442. Hansotia T, Maida A, Flock G, Yamada Y, Tsukiyama K, Seino Y, et al. Extrapancreatic incretin receptors modulate glucose homeostasis, body weight, and energy expenditure. J Clin Invest [Internet]. 2007 Jan 4 [cited 2022 Oct 13];117(1):143–52. Available from: https://pubmed.ncbi.nlm.nih.gov/17187081/

443. Kim SJ, Nian C, Karunakaran S, Clee SM, Isales CM, McIntosh CHS. GIP-Overexpressing mice demonstrate reduced diet-induced obesity and steatosis, and improved glucose homeostasis. PLoS One [Internet]. 2012 Jul 3 [cited 2020 Aug 14];7(7):40156. Available from: /pmc/articles/PMC3388996/?report=abstract

444. Finan B, Yang B, Ottaway N, Smiley DL, Ma T, Clemmensen C, et al. A rationally designed monomeric peptide triagonist corrects obesity and diabetes in rodents. Nature Medicine 2014 21:1 [Internet]. 2014 Dec 8 [cited 2025 Apr 10];21(1):27–36. Available from: https://www.nature.com/articles/nm.3761

445. Mori Y, Matsui T, Hirano T, Yamagishi SI. GIP as a Potential Therapeutic Target for Atherosclerotic Cardiovascular Disease–A Systematic Review. Int J Mol Sci [Internet]. 2020 Feb 2 [cited 2025 Aug 18];21(4):1509. Available from: https://pmc.ncbi.nlm.nih.gov/articles/PMC7073149/

446. Helsted MM, Schaltz NL, Gasbjerg LS, Christensen MB, Vilsbøll T, Knop FK. Safety of native glucose-dependent insulinotropic polypeptide in humans. Peptides (NY) [Internet]. 2024 Jul 1 [cited 2025 Aug 18];177:171214. Available from: https://www.sciencedirect.com/science/article/pii/S0196978124000676

447. Højberg P V., Vilsbøll T, Rabøl R, Knop FK, Bache M, Krarup T, et al. Four weeks of near-normalisation of blood glucose improves the insulin response to glucagon-like peptide-1 and glucose-dependent insulinotropic polypeptide in patients with type 2 diabetes. Diabetologia [Internet]. 2009 Feb 27 [cited 2025 Apr 8];52(2):199–207. Available from: https://link.springer.com/article/10.1007/s00125-008-1195-5

448. Sarramegna V, Talmont F, Demange P, Milon A. Heterologous expression of G-protein-coupled receptors: Comparison of expression systems from the standpoint of large-scale production and purification. Cellular and Molecular Life Sciences [Internet]. 2003 Aug 1 [cited 2025 Aug 18];60(8):1529–46. Available from: https://link.springer.com/article/10.1007/s00018-003-3168-7

449. Baron M, Veres A, Wolock SL, Faust AL, Gaujoux R, Vetere A, et al. A Single-Cell Transcriptomic Map of the Human and Mouse Pancreas Reveals Inter- and Intra-cell Population Structure. Cell Syst [Internet]. 2016 Oct 26 [cited 2025 Apr 15];3(4):346. Available from: https://pmc.ncbi.nlm.nih.gov/articles/PMC5228327/

450. Lawlor N, George J, Bolisetty M, Kursawe R, Sun L, Sivakamasundari V, et al. Single-cell transcriptomes identify human islet cell signatures and reveal cell-type-specific expression changes in type 2 diabetes. Genome Res [Internet]. 2017 Feb 1 [cited 2025 Apr 15];27(2):208–22. Available from: https://pmc.ncbi.nlm.nih.gov/articles/PMC5287227/

451. Muraro MJ, Dharmadhikari G, Grün D, Groen N, Dielen T, Jansen E, et al. A Single-Cell Transcriptome Atlas of the Human Pancreas. Cell Syst [Internet]. 2016 Oct 26 [cited 2025 Apr 15];3(4):385. Available from: https://pmc.ncbi.nlm.nih.gov/articles/PMC5092539/

452. Xin Y, Kim J, Okamoto H, Ni M, Wei Y, Adler C, et al. RNA Sequencing of Single Human Islet Cells Reveals Type 2 Diabetes Genes. Cell Metab [Internet]. 2016 Oct 11 [cited 2025 Apr 15];24(4):608–15. Available from: https://www.cell.com/action/showFullText?pii=S155041311630434X

453. Heller RS, Kieffer TJ, Habener JF. Insulinotropic Glucagon-Like Peptide I Receptor Expression in Glucagon-Producing α-Cells of the Rat Endocrine Pancreas. Diabetes [Internet]. 1997 May 1 [cited 2025 Apr 9];46(5):785–91. Available from: https://dx.doi.org/10.2337/diab.46.5.785

454. Moens K, Heimberg H, Flamez D, Huypens P, Quartier E, Ling Z, et al. Expression and functional activity of glucagon, glucagon-like peptide I, and glucose-dependent insulinotropic peptide receptors in rat pancreatic islet cells. Diabetes [Internet]. 1996 [cited 2020 Sep 26];45(2):257–61. Available from: https://pubmed.ncbi.nlm.nih.gov/8549871/

455. Mawla AM, Huising MO. Navigating the depths and avoiding the shallows of pancreatic islet cell transcriptomes. Diabetes [Internet]. 2019 Jul 1 [cited 2021 Jan 3];68(7):1380–93. Available from: https://doi.org/10.2337/dbi18-0019

456. Saponaro C, Gmyr V, Thévenet J, Moerman E, Delalleau N, Pasquetti G, et al. The GLP1R Agonist Liraglutide Reduces Hyperglucagonemia Induced by the SGLT2 Inhibitor Dapagliflozin via Somatostatin Release. Cell Rep [Internet]. 2019 Aug 6 [cited 2025 Apr 10];28(6):1447-1454.e4. Available from: https://www.cell.com/action/showFullText?pii=S221112471930899X

457. Ramracheya R, Chapman C, Chibalina M, Dou H, Miranda C, González A, et al. GLP-1 suppresses glucagon secretion in human pancreatic alpha-cells by inhibition of P/Q-type Ca2+ channels. Physiol Rep [Internet]. 2018 Sep 1 [cited 2025 Apr 10];6(17):e13852. Available from: https://onlinelibrary.wiley.com/doi/full/10.14814/phy2.13852

458. Gandasi NR, Gao R, Kothegala L, Pearce A, Santos C, Acreman S, et al. GLP-1 metabolite GLP-1(9–36) is a systemic inhibitor of mouse and human pancreatic islet glucagon secretion. Diabetologia [Internet]. 2024 Mar 1 [cited 2025 Apr 10];67(3):528–46. Available from: https://link.springer.com/article/10.1007/s00125-023-06060-w

459. Schmid R, Schusdziarra V, Auelehner R, Weigert N, Classen M. Zeitschrift für Gastroenterologie. 1990 [cited 2025 Apr 24]. p. 280–4 Comparison of GLP-1 (7-36amide) and GIP on release of somatostatin-like immunoreactivity and insulin from the isolated rat pancreas - PubMed. Available from: https://pubmed.ncbi.nlm.nih.gov/2238756/

460. Yoshimoto Y, Fukuyama Y, Horio Y, Inanobe A, Gotoh M, Kurachi Y. Somatostatin induces hyperpolarization in pancreatic islet α cells by activating a G protein-gated K+ channel. FEBS Lett [Internet]. 1999 Feb 12 [cited 2025 Apr 15];444(2–3):265–9. Available from: https://onlinelibrary.wiley.com/doi/full/10.1016/S0014-5793%2899%2900076-9

461. Gromada J, Høy M, Buschard K, Salehi A, Rorsman P. Somatostatin inhibits exocytosis in rat pancreatic α-cells by Gi2-dependent activation of calcineurin and depriming of secretory granules. J Physiol [Internet]. 2001 Sep 1 [cited 2025 Apr 15];535(Pt 2):519. Available from: https://pmc.ncbi.nlm.nih.gov/articles/PMC2278803/

462. Gromada J, Rorsman P. New insights into the regulation of glucagon secretion by glucagon-like peptide-1. Hormone and Metabolic Research [Internet]. 2004 Nov [cited 2025 Apr 15];36(11–12):822–9. Available from: http://www.thieme-connect.de/products/ejournals/html/10.1055/s-2004-826169

463. Waser B, Blank A, Karamitopoulou E, Perren A, Reubi JC. Glucagon-like-peptide-1 receptor expression in normal and diseased human thyroid and pancreas. Modern Pathology. 2015 Mar 1;28(3):391–402.

464. Schaum N, Karkanias J, Neff NF, May AP, Quake SR, Wyss-Coray T, et al. Single-cell transcriptomics of 20 mouse organs creates a Tabula Muris: The Tabula Muris Consortium. Nature [Internet]. 2018 Oct 18 [cited 2025 Aug 18];562(7727):367. Available from: https://pmc.ncbi.nlm.nih.gov/articles/PMC6642641/

465. Campbell JE, Müller TD, Finan B, DiMarchi RD, Tschöp MH, D'Alessio DA. GIPR/GLP-1R dual agonist therapies for diabetes and weight loss—chemistry, physiology, and clinical applications. Cell Metab. 2023 Sep 5;35(9):1519–29.

466. Finan B, Yang B, Ottaway N, Smiley DL, Ma T, Clemmensen C, et al. A rationally designed monomeric peptide triagonist corrects obesity and diabetes in rodents. Nat Med [Internet]. 2015 Jan 1 [cited 2025 Apr 24];21(1):27–36. Available from: https://www.nature.com/articles/nm.3761

467. Li W, Zhou Q, Cong Z, Yuan Q, Li W, Zhao F, et al. Structural insights into the triple agonism at GLP-1R, GIPR and GCGR manifested by retatrutide. Cell Discovery [Internet]. 2024 Dec 1 [cited 2025 Apr 24];10(1):1–4. Available from: https://www.nature.com/articles/s41421-024-00700-0

468. Cejvan K, Coy DH, Efendic S. Intra-islet somatostatin regulates glucagon release via type 2 somatostatin receptors in rats. Diabetes [Internet]. 2003 May 1 [cited 2025 Apr 15];52(5):1176–81. Available from: https://pubmed.ncbi.nlm.nih.gov/12716749/

469. Ørgaard A, Holst JJ. The role of somatostatin in GLP-1-induced inhibition of glucagon secretion in mice. Diabetologia [Internet]. 2017 Sep 1 [cited 2020 Aug 14];60(9):1731–9. Available from: /pmc/articles/PMC5552842/?report=abstract

470. De Heer J, Rasmussen C, Coy DH, Holst JJ. Glucagon-like peptide-1, but not glucose-dependent insulinotropic peptide, inhibits glucagon secretion via somatostatin (receptor subtype 2) in the perfused rat pancreas. Diabetologia [Internet]. 2008 Dec [cited 2020 Aug 14];51(12):2263–70. Available from: https://pubmed.ncbi.nlm.nih.gov/18795252/

471. Capozzi ME, Wait JB, Koech J, Gordon AN, Coch RW, Svendsen B, et al. Glucagon lowers glycemia when β cells are active. JCI Insight [Internet]. 2019 Aug 22 [cited 2025 Apr 24];4(16). Available from: https://pubmed.ncbi.nlm.nih.gov/31335319/

472. El K, Gray SM, Capozzi ME, Knuth ER, Jin E, Svendsen B, et al. GIP mediates the incretin effect and glucose tolerance by dual actions on α cells and β cells. Sci Adv [Internet]. 2021 Mar 12 [cited 2025 Apr 10];7(11):eabf1948. Available from: https://pmc.ncbi.nlm.nih.gov/articles/PMC7954443/

473. Ettinger A, Wittmann T. Fluorescence Live Cell Imaging. Methods Cell Biol [Internet]. 2014 [cited 2025 Apr 2];123:77. Available from: https://pmc.ncbi.nlm.nih.gov/articles/PMC4198327/

474. Sundarakrishnan A, Herrero Acero E, Coburn J, Chwalek K, Partlow B, Kaplan DL. Phenol red-silk tyrosine cross-linked hydrogels. Acta Biomater. 2016 Sep 15;42:102–13.

475. Billinton N, Knight AW. Seeing the Wood through the Trees: A Review of Techniques for Distinguishing Green Fluorescent Protein from Endogenous Autofluorescence. Anal Biochem. 2001 Apr 15;291(2):175–97.

476. TrueBlack® Lipofuscin Autofluorescence Quencher - Biotium [Internet]. [cited 2025 Apr 2]. Available from: https://biotium.com/product/trueblack-lipofuscin-autofluorescence-quencher/

477. Noonberg SB, Weiss TL, Garovoy MR, Hunt CA. Characterization and Minimization of Cellular Autofluorescence in the Study of Oligonucleotide Uptake Using Confocal Microscopy. Antisense Res Dev. 1992;2(4):303–13.

478. del Castillo P, Molero ML, Ferrer JM, Stockert JC. Autofluorescence and induced fluorescence in Epon embedded tissue sections. Histochemistry. 1986 Sep;85(5):439–40.

479. Tokumasu F, Dvorak J. Development and application of quantum dots for immunocytochemistry of human erythrocytes. J Microsc. 2003 Sep 1;211(3):256–61.

480. Gharib SA, Vemireddy R, Castillo JJ, Fountaine BS, Bammler TK, MacDonald JW, et al. Cystic fibrosis-related diabetes is associated with reduced islet protein expression of GLP-1 receptor and perturbation of cell-specific transcriptional programs. Sci Rep [Internet]. 2024 Dec 1 [cited 2025 Jul 18];14(1):1–14. Available from: https://www.nature.com/articles/s41598-024-76722-1

481. Kayton NS, Poffenberger G, Henske J, Dai C, Thompson C, Aramandla R, et al. Human islet preparations distributed for research exhibit a variety of insulin-secretory profiles. Am J Physiol Endocrinol Metab [Internet]. 2015 [cited 2025 Jan 20];308(7):E592. Available from: https://pmc.ncbi.nlm.nih.gov/articles/PMC4385877/

482. Lyon J, Manning Fox JE, Spigelman AF, Kim R, Smith N, O'Gorman D, et al. Research-Focused Isolation of Human Islets From Donors With and Without Diabetes at the

Alberta Diabetes Institute IsletCore. Endocrinology [Internet]. 2016 Feb 1 [cited 2025 Jan 20];157(2):560–9. Available from: https://dx.doi.org/10.1210/en.2015-1562

483. Langlois A, Pinget M, Kessler L, Bouzakri K. Islet Transplantation: Current Limitations and Challenges for Successful Outcomes. Cells [Internet]. 2024 Nov 1 [cited 2025 Apr 16];13(21):1783. Available from: https://pmc.ncbi.nlm.nih.gov/articles/PMC11544954/

484. Qi M, McFadden B, Valiente L, Omori K, Bilbao S, Juan J, et al. Human pancreatic islets isolated from donors with elevated hba1c levels: Islet yield and graft efficacy. Cell Transplant [Internet]. 2015 Sep 14 [cited 2025 Apr 16];24(9):1879–86. Available from: https://journals.sagepub.com/doi/10.3727/096368914X683548?url_ver=Z39.88-2003&rfr_id=ori%3Arid%3Acrossref.org&rfr_dat=cr_pub++0pubmed

485. Wang S, Du Y, Zhang B, Meng G, Liu Z, Liew SY, et al. Transplantation of chemically induced pluripotent stem-cell-derived islets under abdominal anterior rectus sheath in a type 1 diabetes patient. Cell [Internet]. 2024 Oct 31 [cited 2025 Apr 16];187(22):6152-6164.e18. Available from: http://www.ncbi.nlm.nih.gov/pubmed/39326417

486. Fujikura J, Anazawa T, Toyoda T, Ito R, Kimura Y, Yabe D. Toward a cure for diabetes: iPSC and ESC-derived islet cell transplantation trials. J Diabetes Investig [Internet]. 2025 Mar 1 [cited 2025 Apr 16];16(3):384–8. Available from: https://onlinelibrary.wiley.com/doi/full/10.1111/jdi.14366

487. Maestas MM, Bui MH, Millman JR. Recent progress in modeling and treating diabetes using stem cell-derived islets. Stem Cells Transl Med [Internet]. 2024 Oct 10 [cited 2025 Apr 16];13(10):949–58. Available from: https://dx.doi.org/10.1093/stcltm/szae059

488. Maxwell KG, Millman JR. Applications of iPSC-derived beta cells from patients with diabetes. Cell Rep Med [Internet]. 2021 Apr 20 [cited 2025 Apr 16];2(4):100238. Available from: https://pmc.ncbi.nlm.nih.gov/articles/PMC8080107/

489. Vilardaga JP, Bünemann M, Krasell C, Castro M, Lohse MJ. Measurement of the millisecond activation switch of G protein–coupled receptors in living cells. Nature

Biotechnology 2003 21:7 [Internet]. 2003 Jun 15 [cited 2025 Apr 4];21(7):807–12. Available from: https://www.nature.com/articles/nbt838

490. Calebiro D, Sungkaworn T. Single-Molecule Imaging of GPCR Interactions. Trends Pharmacol Sci [Internet]. 2018 Feb 1 [cited 2025 Apr 4];39(2):109–22. Available from: https://www.cell.com/action/showFullText?pii=S0165614717302055

491. Ma Y, Hinde E, Gaus K. Nanodomains in biological membranes. Essays Biochem [Internet]. 2015 Feb 15 [cited 2025 Apr 4];57:93–107. Available from: /essaysbiochem/article/doi/10.1042/bse0570093/78443/Nanodomains-in-biological-membranes

492. Ikonen E. Roles of lipid rafts in membrane transport. Curr Opin Cell Biol. 2001 Aug 1;13(4):470–7.

493. Sungkaworn T, Jobin ML, Burnecki K, Weron A, Lohse MJ, Calebiro D. Single-molecule imaging reveals receptor–G protein interactions at cell surface hot spots. Nature 2017 550:7677 [Internet]. 2017 Oct 18 [cited 2025 Apr 4];550(7677):543–7. Available from: https://www.nature.com/articles/nature24264

494. Kudalkar EM, Davis TN, Asbury CL. Single-Molecule Total Internal Reflection Fluorescence Microscopy. Cold Spring Harb Protoc [Internet]. 2016 May 1 [cited 2025 Apr 25];2016(5):pdb.top077800. Available from: https://pmc.ncbi.nlm.nih.gov/articles/PMC5577000/

495. Zalejski J, Sun J, Sharma A. Unravelling the Mystery inside Cells by Using Single-Molecule Fluorescence Imaging. J Imaging [Internet]. 2023 Sep 1 [cited 2025 Apr 25];9(9):192. Available from: https://pmc.ncbi.nlm.nih.gov/articles/PMC10532472/

496. Jeong S, Widengren J, Lee JC. Fluorescent Probes for STED Optical Nanoscopy. Nanomaterials [Internet]. 2021 Jan 1 [cited 2025 Apr 25];12(1):21. Available from: https://pmc.ncbi.nlm.nih.gov/articles/PMC8746377/

497. Roßmann K, Akkaya KC, Poc P, Charbonnier C, Eichhorst J, Gonschior H, et al. N-Methyl deuterated rhodamines for protein labelling in sensitive fluorescence microscopy. Chem Sci [Internet]. 2022 Jun 28 [cited 2025 Apr 4];13(29):8605. Available from: https://pmc.ncbi.nlm.nih.gov/articles/PMC9337740/

498. Rosenstock J, Wysham C, Frías JP, Kaneko S, Lee CJ, Fernández Landó L, et al. Efficacy and safety of a novel dual GIP and GLP-1 receptor agonist tirzepatide in patients with type 2 diabetes (SURPASS-1): a double-blind, randomised, phase 3 trial. The Lancet. 2021;398(10295):143–55.

499. Zhang Y, Han C, Zhu W, Yang G, Peng X, Mehta S, et al. Glucagon potentiates insulin secretion via β-cell GCGR at physiological concentrations of glucose. Cells [Internet]. 2021 Sep 1 [cited 2025 Jul 21];10(9):2495. Available from: https://pmc.ncbi.nlm.nih.gov/articles/PMC8471175/

500. Gasbjerg LS, Helsted MM, Hartmann B, Jensen MH, Gabe MBN, Sparre-Ulrich AH, et al. Separate and Combined Glucometabolic Effects of Endogenous Glucose-Dependent Insulinotropic Polypeptide and Glucagon-like Peptide 1 in Healthy Individuals. Diabetes [Internet]. 2019 May 1 [cited 2025 Apr 23];68(5):906–17. Available from: https://dx.doi.org/10.2337/db18-1123

501. Gray SM, Goonatilleke E, Emrick MA, Becker JO, Hoofnagle AN, Stefanovski D, et al. High Doses of Exogenous Glucagon Stimulate Insulin Secretion and Reduce Insulin Clearance in Healthy Humans. Diabetes [Internet]. 2024 Feb 20 [cited 2025 Apr 24];73(3):412–25. Available from: https://dx.doi.org/10.2337/db23-0201

502. Biocytogen. Gene Humanized Models: Human GIPR mice [Internet]. 2025 [cited 2025 Aug 19]. Available from: https://biocytogen.com/gene-humanized-models/b-hgipr-mice

503. Shanghai Model Organisms. Models - U0GEMMs - hGIPR [Internet]. 2025 [cited 2025 Aug 19]. Available from: https://en.modelorg.com/portal/article/index.html?id=210322&post_type=3

504. Gao W, Liu L, Huh E, Gbahou F, Cecon E, Oshima M, et al. Human GLP1R variants affecting GLP1R cell surface expression are associated with impaired glucose control and increased adiposity. Nature Metabolism 2023 5:10 [Internet]. 2023 Sep 14 [cited 2025 Aug 20];5(10):1673–84. Available from: https://www.nature.com/articles/s42255-023-00889-6

505. Anton SE, Kayser C, Maiellaro I, Nemec K, Möller J, Koschinski A, et al. Receptor-associated independent cAMP nanodomains mediate spatiotemporal specificity of GPCR signaling. Cell. 2022 Mar 31;185(7):1130-1142.e11.

506. Novikoff A, O'Brien SL, Bernecker M, Grandl G, Kleinert M, Knerr PJ, et al. Spatiotemporal GLP-1 and GIP receptor signaling and trafficking/recycling dynamics induced by selected receptor mono- and dual-agonists. Mol Metab [Internet]. 2021 Jul 1 [cited 2025 Aug 19];49:101181. Available from: https://www.sciencedirect.com/science/article/pii/S2212877821000211

507. Bock A, Annibale P, Konrad C, Hannawacker A, Anton SE, Maiellaro I, et al. Optical mapping of cAMP signaling at the nanometer scale. Cell [Internet]. 2020 Sep 17 [cited 2025 Apr 23];182(6):1519. Available from: https://pmc.ncbi.nlm.nih.gov/articles/PMC7984459/

508. Gaigalas AK, Li L, Henderson O, Vogt R, Barr J, Marti G, et al. The Development of Fluorescence Intensity Standards. J Res Natl Inst Stand Technol [Internet]. 2001 [cited 2025 Aug 19];106(2):381. Available from: https://pmc.ncbi.nlm.nih.gov/articles/PMC4862808/

509. Kieffer TJ, Mc Intosh CHS, Pederson RA. Degradation of glucose-dependent insulinotropic polypeptide and truncated glucagon-like peptide 1 in vitro and in vivo by dipeptidyl peptidase IV. Endocrinology [Internet]. 1995 [cited 2022 Oct 17];136(8):3585–96. Available from: https://pubmed.ncbi.nlm.nih.gov/7628397/

510. Creutzfeldt W, Ebert R, Willms B, Frerichs H, Brown JC. Gastric inhibitory polypeptide (GIP) and insulin in obesity: Increased response to stimulation and defective feedback control of serum levels. Diabetologia [Internet]. 1978 Jan [cited 2025 May 2];14(1):15–24. Available from: https://link.springer.com/article/10.1007/BF00429703

511. Ludwig MQ, Cheng W, Gordian D, Lee J, Paulsen SJ, Hansen SN, et al. A genetic map of the mouse dorsal vagal complex and its role in obesity. Nat Metab [Internet]. 2021 Apr 1 [cited 2025 Aug 5];3(4):530. Available from: https://pmc.ncbi.nlm.nih.gov/articles/PMC12009600/

512. Akindehin S, Liskiewicz A, Liskiewicz D, Bernecker M, Garcia-Caceres C, Drucker DJ, et al. Loss of GIPR in LEPR cells impairs glucose control by GIP and GIP:GLP-1 co-agonism without affecting body weight and food intake in mice. Mol Metab [Internet]. 2024 May 1 [cited 2025 Aug 4];83:101915. Available from: https://pmc.ncbi.nlm.nih.gov/articles/PMC10973979/

513. Tadross JA, Steuernagel L, Dowsett GKC, Kentistou KA, Lundh S, Porniece M, et al. A comprehensive spatio-cellular map of the human hypothalamus. Nature [Internet]. 2025 Mar 20 [cited 2025 Aug 5];639(8055):708. Available from: https://pmc.ncbi.nlm.nih.gov/articles/PMC11922758/

514. Zhang Q, Delessa CT, Augustin R, Bakhti M, Colldén G, Drucker DJ, et al. The glucose-dependent insulinotropic polypeptide (GIP) regulates body weight and food intake via CNS-GIPR signaling. Cell Metab [Internet]. 2021 Apr 6 [cited 2025 May 2];33(4):833. Available from: https://pmc.ncbi.nlm.nih.gov/articles/PMC8035082/

515. Zhang C, Vincelette LK, Reimann F, Liberles SD. A brainstem circuit for nausea suppression. Cell Rep [Internet]. 2022 Jun 14 [cited 2025 May 8];39(11):110953. Available from: https://pmc.ncbi.nlm.nih.gov/articles/PMC9260880/

516. Costa A, Ai M, Nunn N, Culotta I, Hunter J, Boudjadja MB, et al. Anorectic and aversive effects of GLP-1 receptor agonism are mediated by brainstem cholecystokinin neurons,

and modulated by GIP receptor activation. Mol Metab [Internet]. 2022 Jan 1 [cited 2025 Aug 9];55:101407. Available from: https://www.sciencedirect.com/science/article/pii/S2212877821002659

517. Knop FK, Urva S, Rettiganti M, Benson CT, Roell WC, Mather KJ, et al. A long-acting glucose-dependent insulinotropic polypeptide receptor agonist improves the gastrointestinal tolerability of glucagon-like peptide-1 receptor agonist therapy. Diabetes Obes Metab [Internet]. 2024 Nov 1 [cited 2025 Aug 4];26(11):5474–8. Available from: /doi/pdf/10.1111/dom.15875

518. Bettge K, Kahle M, Abd El Aziz MS, Meier JJ, Nauck MA. Occurrence of nausea, vomiting and diarrhoea reported as adverse events in clinical trials studying glucagon-like peptide-1 receptor agonists: A systematic analysis of published clinical trials. Diabetes Obes Metab [Internet]. 2017 Mar 1 [cited 2025 Aug 5];19(3):336–47. Available from: /doi/pdf/10.1111/dom.12824

519. Vrang N, Larsen PJ. Preproglucagon derived peptides GLP-1, GLP-2 and oxyntomodulin in the CNS: Role of peripherally secreted and centrally produced peptides. Prog Neurobiol [Internet]. 2010 Nov 1 [cited 2025 May 8];92(3):442–62. Available from: https://www.sciencedirect.com/science/article/pii/S0301008210001346?via%3Dihub

520. Tang-Christensen M, Larsen PJ, Göke R, Fink-Jensen A, Jessop DS, Møller M, et al. Central administration of GLP-1-(7-36) amide inhibits food and water intake in rats. https://doi.org/101152/ajpregu19962714R848 [Internet]. 1996 [cited 2025 May 8];271(4 40-4). Available from: /doi/pdf/10.1152/ajpregu.1996.271.4.R848

521. Turton MD, O'Shea D, Gunn I, Beak SA, Edwards CMB, Meeran K, et al. A role for glucagon-like peptide-1 in the central regulation of feeding. Nature [Internet]. 1996 Jan 4 [cited 2025 May 8];379(6560):69–72. Available from: https://www.nature.com/articles/379069a0

522. Meeran K, O'Shea D, Edwards CMB, Turton MD, Heath MM, Gunn I, et al. Repeated Intracerebroventricular Administration of Glucagon-Like Peptide-1-(7–36) Amide or Exendin-(9–39) Alters Body Weight in the Rat*This work was supported by the United Kingdom Medical Research Council. Endocrinology [Internet]. 1999 Jan 1 [cited 2025 May 6];140(1):244–50. Available from: https://dx.doi.org/10.1210/endo.140.1.6421

523. Barrera JG, D'Alessio DA, Drucker DJ, Woods SC, Seeley RJ. Differences in the Central Anorectic Effects of Glucagon-Like Peptide-1 and Exendin-4 in Rats. Diabetes [Internet]. 2009 Dec [cited 2025 May 6];58(12):2820. Available from: https://pmc.ncbi.nlm.nih.gov/articles/PMC2780868/

524. Barrera JG, Jones KR, Herman JP, D'Alessio DA, Woods SC, Seeley RJ. Hyperphagia and Increased Fat Accumulation in Two Models of Chronic CNS Glucagon-Like Peptide-1 Loss of Function. The Journal of Neuroscience [Internet]. 2011 Mar 9 [cited 2025 May 6];31(10):3904. Available from: https://pmc.ncbi.nlm.nih.gov/articles/PMC3700400/

525. Sisley S, Gutierrez-Aguilar R, Scott M, D'Alessio DA, Sandoval DA, Seeley RJ. Neuronal GLP1R mediates liraglutide's anorectic but not glucose-lowering effect. J Clin Invest [Internet]. 2014 Jun 2 [cited 2025 May 6];124(6):2456. Available from: https://pmc.ncbi.nlm.nih.gov/articles/PMC4038572/

526. Ayala JE, Bracy DP, James FD, Burmeister MA, Wasserman DH, Drucker DJ. Glucagon-Like Peptide-1 Receptor Knockout Mice Are Protected from High-Fat Diet-Induced Insulin Resistance. Endocrinology [Internet]. 2010 [cited 2025 May 6];151(10):4678. Available from: https://pmc.ncbi.nlm.nih.gov/articles/PMC2946144/

527. Baggio LL, Huang Q, Brown TJ, Drucker DJ. Oxyntomodulin and glucagon-like peptide-1 differentially regulate murine food intake and energy expenditure. Gastroenterology [Internet]. 2004 Aug 1 [cited 2025 May 8];127(2):546–58. Available from: https://www.gastrojournal.org/action/showFullText?pii=S0016508504007735

528. Gao Q, Horvath TL. Neuronal control of energy homeostasis. FEBS Lett [Internet]. 2007 Jan 9 [cited 2025 May 6];582(1):132. Available from: https://pmc.ncbi.nlm.nih.gov/articles/PMC4113225/

529. Merchenthaler I, Lane M, Shughrue P. Distribution of pre-pro-glucagon and glucagon-like peptide-1 receptor messenger RNAs in the rat central nervous system. Journal of Comparative Neurology. 1999 Jan 11;403(2):261–80.

530. Göke R, Larsen PJ, Mikkelsen JD, Sheikh SP. Distribution of GLP-1 Binding Sites in the Rat Brain: Evidence that Exendin-4 is a Ligand of Brain GLP-1 Binding Sites. European Journal of Neuroscience. 1995;7(11):2294–300.

531. Steuernagel L, Lam BYH, Klemm P, Dowsett GKC, Bauder CA, Tadross JA, et al. HypoMap—a unified single-cell gene expression atlas of the murine hypothalamus. Nature Metabolism 2022 4:10 [Internet]. 2022 Oct 20 [cited 2025 Aug 5];4(10):1402–19. Available from: https://www.nature.com/articles/s42255-022-00657-y

532. Villabona-Rueda A, Erice C, Pardo CA, Stins MF. The Evolving Concept of the Blood Brain Barrier (BBB): From a Single Static Barrier to a Heterogeneous and Dynamic Relay Center. Front Cell Neurosci [Internet]. 2019 Sep 20 [cited 2025 May 1];13:405. Available from: https://pmc.ncbi.nlm.nih.gov/articles/PMC6763697/

533. Banks WA, Kastin AJ. Peptide transport systems for opiates across the blood-brain barrier. Am J Physiol Endocrinol Metab [Internet]. 1990 [cited 2025 May 1];259(1 22-1). Available from: /doi/pdf/10.1152/ajpendo.1990.259.1.E1?download=true

534. Buller S, Blouet C. Brain access of incretins and incretin receptor agonists to their central targets relevant for appetite suppression and weight loss. Am J Physiol Endocrinol Metab [Internet]. 2024 Apr 1 [cited 2025 Apr 29];326(4):E472–80. Available from: https://pmc.ncbi.nlm.nih.gov/articles/PMC11193531/#sec2

535. Dailey MJ, Moran TH. Glucagon-like peptide 1 and appetite. Trends Endocrinol Metab [Internet]. 2013 Feb [cited 2025 Aug 5];24(2):85. Available from: https://pmc.ncbi.nlm.nih.gov/articles/PMC3594872/

536. Trapp S, Cork SC. PPG neurons of the lower brain stem and their role in brain GLP-1 receptor activation. Am J Physiol Regul Integr Comp Physiol [Internet]. 2015 [cited 2025 Aug 5];309(8):R795. Available from: https://pmc.ncbi.nlm.nih.gov/articles/PMC4666945/

537. Punjabi M, Arnold M, Rüttimann E, Graber M, Geary N, Pacheco-López G, et al. Circulating Glucagon-like Peptide-1 (GLP-1) Inhibits Eating in Male Rats by Acting in the Hindbrain and Without Inducing Avoidance. Endocrinology [Internet]. 2014 May 1 [cited 2025 May 6];155(5):1690–9. Available from: https://dx.doi.org/10.1210/en.2013-1447

538. Ørskov C, Poulsen SS, Møller M, Holst JJ. Glucagon-Like Peptide I Receptors in the Subfornical Organ and the Area Postrema Are Accessible to Circulating Glucagon-Like Peptide I. Diabetes [Internet]. 1996 Jun 1 [cited 2025 May 8];45(6):832–5. Available from: https://dx.doi.org/10.2337/diab.45.6.832

539. Niswender K, Pi-Sunyer X, Buse J, Jensen KH, Toft AD, Russell-Jones D, et al. Weight change with liraglutide and comparator therapies: An analysis of seven phase 3 trials from the liraglutide diabetes development programme. Diabetes Obes Metab [Internet]. 2013 Jan 1 [cited 2025 May 6];15(1):42–54. Available from: /doi/pdf/10.1111/j.1463-1326.2012.01673.x

540. Kanoski SE, Fortin SM, Arnold M, Grill HJ, Hayes MR. Peripheral and Central GLP-1 Receptor Populations Mediate the Anorectic Effects of Peripherally Administered GLP-1 Receptor Agonists, Liraglutide and Exendin-4. Endocrinology [Internet]. 2011 Aug [cited 2025 May 6];152(8):3103. Available from: https://pmc.ncbi.nlm.nih.gov/articles/PMC3138234/

541. Hunt J V., Washington MC, Sayegh AI. Exenatide and feeding: Possible peripheral neuronal pathways. Peptides (NY) [Internet]. 2012 Feb 1 [cited 2025 May 6];33(2):285–90.

Available from: https://www.sciencedirect.com/science/article/abs/pii/S0196978111005201?via%3Dihub

542. Hayes MR, Kanoski SE, de Jonghe BC, Leichner TM, Alhadeff AL, Fortin SM, et al. The common hepatic branch of the vagus is not required to mediate the glycemic and food intake suppressive effects of glucagon-like-peptide-1. Am J Physiol Regul Integr Comp Physiol [Internet]. 2011 Nov [cited 2025 May 6];301(5):R1479. Available from: https://pmc.ncbi.nlm.nih.gov/articles/PMC3213943/

543. Vahl TP, Tauchi M, Durler TS, Elfers EE, Fernandes TM, Bitner RD, et al. Glucagon-Like Peptide-1 (GLP-1) Receptors Expressed on Nerve Terminals in the Portal Vein Mediate the Effects of Endogenous GLP-1 on Glucose Tolerance in Rats. Endocrinology [Internet]. 2007 Oct 1 [cited 2025 May 6];148(10):4965–73. Available from: https://dx.doi.org/10.1210/en.2006-0153

544. Abbott CR, Monteiro M, Small CJ, Sajedi A, Smith KL, Parkinson JRC, et al. The inhibitory effects of peripheral administration of peptide YY3–36 and glucagon-like peptide-1 on food intake are attenuated by ablation of the vagal–brainstem–hypothalamic pathway. Brain Res [Internet]. 2005 May 17 [cited 2025 May 6];1044(1):127–31. Available from: https://www.sciencedirect.com/science/article/pii/S0006899305004002?via%3Dihub

545. Zhang J, Ritter RC. Circulating GLP-1 and CCK-8 reduce food intake by capsaicin-insensitive, nonvagal mechanisms. Am J Physiol Regul Integr Comp Physiol [Internet]. 2011 Jan [cited 2025 May 6];302(2):R264. Available from: https://pmc.ncbi.nlm.nih.gov/articles/PMC3349390/

546. Kanoski SE, Rupprecht LE, Fortin SM, De Jonghe BC, Hayes MR. The role of nausea in food intake and body weight suppression by peripheral GLP-1 receptor agonists, exendin-4 and liraglutide. Neuropharmacology [Internet]. 2011 Apr [cited 2025 May 6];62(0):1916. Available from: https://pmc.ncbi.nlm.nih.gov/articles/PMC4183930/

547. Rüttimann EB, Arnold M, Hillebrand JJ, Geary N, Langhans W. Intrameal Hepatic Portal and Intraperitoneal Infusions of Glucagon-Like Peptide-1 Reduce Spontaneous Meal Size in the Rat via Different Mechanisms. Endocrinology [Internet]. 2008 [cited 2025 May 6];150(3):1174. Available from: https://pmc.ncbi.nlm.nih.gov/articles/PMC2654737/

548. Secher A, Jelsing J, Baquero AF, Hecksher-Sørensen J, Cowley MA, Dalbøge LS, et al. The arcuate nucleus mediates GLP-1 receptor agonist liraglutide-dependent weight loss. J Clin Invest [Internet]. 2014 Oct 1 [cited 2025 May 8];124(10):4473. Available from: https://pmc.ncbi.nlm.nih.gov/articles/PMC4215190/

549. Farkas E, Szilvásy-Szabó A, Ruska Y, Sinkó R, Rasch MG, Egebjerg T, et al. Distribution and ultrastructural localization of the glucagon-like peptide-1 receptor (GLP-1R) in the rat brain. Brain Struct Funct [Internet]. 2020 Jan 1 [cited 2025 May 6];226(1):225. Available from: https://pmc.ncbi.nlm.nih.gov/articles/PMC7817608/

550. Llewellyn-Smith IJ, Reimann F, Gribble FM, Trapp S. PREPROGLUCAGON NEURONS PROJECT WIDELY TO AUTONOMIC CONTROL AREAS IN THE MOUSE BRAIN. Neuroscience [Internet]. 2011 Apr 28 [cited 2025 May 6];180:111. Available from: https://pmc.ncbi.nlm.nih.gov/articles/PMC4298012/

551. Imbernon M, Saponaro C, Helms HCC, Duquenne M, Fernandois D, Deligia E, et al. Tanycytes Control Hypothalamic Liraglutide Uptake and its Anti-Obesity Actions. Cell Metab [Internet]. 2022 Jul 5 [cited 2025 Apr 28];34(7):1054. Available from: https://pmc.ncbi.nlm.nih.gov/articles/PMC7613793/

552. Adams JM, Pei H, Sandoval DA, Seeley RJ, Chang RB, Liberles SD, et al. Liraglutide modulates appetite and body weight through glucagon-like peptide 1 receptor-expressing glutamatergic neurons. Diabetes [Internet]. 2018 Aug 1 [cited 2025 May 8];67(8):1538–48. Available from: https://pmc.ncbi.nlm.nih.gov/articles/PMC6054439/

553. Suba K, Patel Y, Martin-Alonso A, Hansen B, Xu X, Roberts A, et al. Intra-islet glucagon signalling regulates beta-cell connectivity, first-phase insulin secretion and glucose

homoeostasis. Mol Metab [Internet]. 2024 Jul 1 [cited 2025 Aug 1];85:101947. Available from: https://www.sciencedirect.com/science/article/pii/S2212877824000784?via%3Dihub

554. Lipinski CA, Lombardo F, Dominy BW, Feeney PJ. Experimental and computational approaches to estimate solubility and permeability in drug discovery and development settings. Adv Drug Deliv Rev [Internet]. 2001 Mar 1 [cited 2025 May 1];46(1–3):3–26. Available from: https://www.sciencedirect.com/science/article/abs/pii/S0169409X00001290?via%3Dihub

555. Preston JE, Joan Abbott N, Begley DJ. Transcytosis of Macromolecules at the Blood–Brain Barrier. Adv Pharmacol [Internet]. 2014 Jan 1 [cited 2025 Aug 7];71:147–63. Available from: https://www.sciencedirect.com/science/article/abs/pii/S1054358914000027?via%3Dihub

556. Hariharan A, Weir N, Robertson C, He L, Betsholtz C, Longden TA. The Ion Channel and GPCR Toolkit of Brain Capillary Pericytes. Front Cell Neurosci. 2020 Dec 18;14:601324.

557. Ren SY, Xia Y, Yu B, Lei QJ, Hou PF, Guo S, et al. Growth hormone promotes myelin repair after chronic hypoxia via triggering pericyte-dependent angiogenesis. Neuron [Internet]. 2024 Jul 3 [cited 2025 May 1];112(13):2177-2196.e6. Available from: https://www.sciencedirect.com/science/article/pii/S0896627324002332

558. Banks WA, Kastin AJ, Huang W, Jaspan JB, Maness LM. Leptin enters the brain by a saturable system independent of insulin. Peptides (NY) [Internet]. 1996 Jan 1 [cited 2025 May 1];17(2):305–11. Available from: https://www.sciencedirect.com/science/article/abs/pii/0196978196000253?via%3Dihub

559. Banks WA, DiPalma CR, Farrell CL. Impaired transport of leptin across the blood-brain barrier in obesity☆. Peptides (NY) [Internet]. 1999 Nov 1 [cited 2025 May 1];20(11):1341–

5. Available from: https://www.sciencedirect.com/science/article/pii/S0196978199001394?via%3Dihub

560. Halaas JL, Boozer C, Blair-West J, Fidahusein N, Denton DA, Friedman JM. Physiological response to long-term peripheral and central leptin infusion in lean and obese mice. Proc Natl Acad Sci U S A [Internet]. 1997 Aug 5 [cited 2025 May 1];94(16):8878–83. Available from: https://www.scopus.com/record/display.uri?eid=2-s2.0-0030737953&origin=inward&txGid=d60f14a472c48659b1009d82b8ca7fc1

561. Banks WA, Farr SA, Morley JE. The effects of high fat diets on the blood–brain barrier transport of leptin: Failure or adaptation? Physiol Behav [Internet]. 2006 Jun 30 [cited 2025 May 1];88(3):244–8. Available from: https://www.sciencedirect.com/science/article/pii/S0031938406002423?via%3Dihub

562. Burguera B, Couce ME. Leptin access into the brain: A saturated transport mechanism in obesity. Physiol Behav [Internet]. 2001 Nov 12 [cited 2025 May 1];74(4–5):717–20. Available from: https://www.sciencedirect.com/science/article/pii/S0031938401006151?via%3Dihub#BIB15

563. Duvernoy HM, Risold PY. The circumventricular organs: An atlas of comparative anatomy and vascularization. Brain Res Rev [Internet]. 2007 Nov 1 [cited 2025 May 1];56(1):119–47. Available from: https://www.sciencedirect.com/science/article/pii/S0165017307001075?via%3Dihub

564. Skipor J, Thiery JC. The choroid plexus - cerebrospinal fluid system: Undervaluated pathway of neuroendocrine signaling into the brain. Acta Neurobiol Exp (Wars) [Internet]. 2008 Sep 30 [cited 2025 May 1];68(3):414–28. Available from: https://ane.pl/index.php/ane/article/view/1708

565. Zlokovic B V., Jovanovic S, Miao W, Samara S, Verma S, Farrell CL. Differential Regulation of Leptin Transport by the Choroid Plexus and Blood-Brain Barrier and High Affinity

Transport Systems for Entry into Hypothalamus and Across the Blood-Cerebrospinal Fluid Barrier. Endocrinology [Internet]. 2000 Apr 1 [cited 2025 May 12];141(4):1434–41. Available from: https://dx.doi.org/10.1210/endo.141.4.7435

566. Chodobski A, Szmydynger-Chodobska J. Choroid plexus: Target for polypeptides and site of their synthesis. Microsc Res Tech. 2001 Jan 1;52(1):65–82.

567. Jensen MN, Israelsen IME, Wardman JH, Jensen DB, Andersen DB, Toft-Bertelsen TL, et al. Glucagon-like peptide-1 receptor modulates cerebrospinal fluid secretion and intracranial pressure in rats. Fluids Barriers CNS [Internet]. 2025 Dec 1 [cited 2025 Aug 1];22(1):41. Available from: https://pmc.ncbi.nlm.nih.gov/articles/PMC12020230/

568. Burguera B, Couce ME, Long J, Lamsam J, Laakso K, Jensen MD, et al. The long form of the leptin receptor (OB-Rh) is widely expressed in the human brain. Neuroendocrinology [Internet]. 2000 [cited 2025 May 1];71(3):187–95. Available from: https://pubmed.ncbi.nlm.nih.gov/10729790/

569. Grill HJ, Kaplan JM. The Neuroanatomical Axis for Control of Energy Balance. Front Neuroendocrinol [Internet]. 2002 Jan 1 [cited 2025 May 1];23(1):2–40. Available from: https://www.sciencedirect.com/science/article/pii/S0091302201902249

570. Bjørbæk C, Elmquist JK, Michl P, Ahima RS, van Bueren A, McCall AL, et al. Expression of Leptin Receptor Isoforms in Rat Brain Microvessels. Endocrinology [Internet]. 1998 Aug 1 [cited 2025 May 1];139(8):3485–91. Available from: https://dx.doi.org/10.1210/endo.139.8.6154

571. Maness LM, Kastin AJ, Farrell CL, Banks WA. Fate of Leptin after Intracerebroventricular Injection into the Mouse Brain. Endocrinology [Internet]. 1998 Nov 1 [cited 2025 May 1];139(11):4556–62. Available from: https://dx.doi.org/10.1210/endo.139.11.6319

572. Kaur C, Ling EA. The circumventricular organs. Histol Histopathol [Internet]. 2017 [cited 2025 Apr 2];32(9):879–92. Available from: https://pubmed.ncbi.nlm.nih.gov/28177105/

573. Langlet F, Mullier A, Bouret SG, Prevot V, Dehouck B. Tanycyte-Like Cells Form a Blood–Cerebrospinal Fluid Barrier in the Circumventricular Organs of the Mouse Brain. J Comp Neurol [Internet]. 2013 Oct 15 [cited 2025 Apr 29];521(15):3389. Available from: https://pmc.ncbi.nlm.nih.gov/articles/PMC3973970/

574. Balland E, Dam J, Langlet F, Caron E, Steculorum S, Messina A, et al. Hypothalamic tanycytes are an ERK-gated conduit for leptin into the brain. Cell Metab [Internet]. 2014 Feb 4 [cited 2025 Aug 8];19(2):293–301. Available from: https://www.cell.com/action/showFullText?pii=S1550413114000047

575. Schaeffer M, Langlet F, Lafont C, Molino F, Hodson DJ, Roux T, et al. Rapid sensing of circulating ghrelin by hypothalamic appetite-modifying neurons. Proc Natl Acad Sci U S A [Internet]. 2013 Jan 22 [cited 2025 Apr 2];110(4):1512–7. Available from: https://pmc.ncbi.nlm.nih.gov/articles/PMC3557016/

576. Rodríguez EM, Blázquez JL, Guerra M. The design of barriers in the hypothalamus allows the median eminence and the arcuate nucleus to enjoy private milieus: The former opens to the portal blood and the latter to the cerebrospinal fluid. Peptides (NY) [Internet]. 2010 Apr 1 [cited 2025 May 8];31(4):757–76. Available from: https://www.sciencedirect.com/science/article/pii/S0196978110000239?via%3Dihub

577. Mullier A, Bouret SG, Prevot V, Dehouck B. Differential distribution of tight junction proteins suggests a role for tanycytes in blood-hypothalamus barrier regulation in the adult mouse brain. J Comp Neurol [Internet]. 2010 Apr 1 [cited 2025 Apr 29];518(7):943. Available from: https://pmc.ncbi.nlm.nih.gov/articles/PMC2892518/

578. Romanò N, Lafont C, Campos P, Guillou A, Fiordelisio T, Hodson DJ, et al. Median eminence blood flow influences food intake by regulating ghrelin access to the metabolic brain. JCI Insight [Internet]. 2023 Feb 8 [cited 2025 Apr 2];8(3). Available from: https://doi.org/10.1172/jci.

579. Morton GJ, Meek TH, Schwartz MW. Neurobiology of food intake in health and disease. Nat Rev Neurosci [Internet]. 2014 [cited 2025 Aug 7];15(6):367. Available from: https://pmc.ncbi.nlm.nih.gov/articles/PMC4076116/

580. Myers MG, Olson DP. Central nervous system control of metabolism. Nature 2012 491:7424 [Internet]. 2012 Nov 14 [cited 2025 May 8];491(7424):357–63. Available from: https://www.nature.com/articles/nature11705

581. Morton GJ, Cummings DE, Baskin DG, Barsh GS, Schwartz MW. Central nervous system control of food intake and body weight. Nature [Internet]. 2006 Sep 21 [cited 2025 Aug 7];443(7109):289–95. Available from: https://www.nature.com/articles/nature05026

582. Kojima M, Hosoda H, Date Y, Nakazato M, Matsuo H, Kangawa K. Ghrelin is a growth-hormone-releasing acylated peptide from stomach. Nature [Internet]. 1999 Dec 9 [cited 2025 Aug 8];402(6762):656–60. Available from: https://www.nature.com/articles/45230

583. Dornonville De La Cour C, Björkqvist M, Sandvik AK, Bakke I, Zhao CM, Chen D, et al. A-like cells in the rat stomach contain ghrelin and do not operate under gastrin control. Regul Pept [Internet]. 2001 Jun 15 [cited 2025 Aug 8];99(2–3):141–50. Available from: https://www.sciencedirect.com/science/article/pii/S0167011501002439

584. Lu S, Guan JL, Wang QP, Uehara K, Yamada S, Goto N, et al. Immunocytochemical observation of ghrelin-containing neurons in the rat arcuate nucleus. Neurosci Lett [Internet]. 2002 Mar 22 [cited 2025 Aug 8];321(3):157–60. Available from: https://www.sciencedirect.com/science/article/pii/S0304394001025447

585. Cummings DE, Purnell JQ, Frayo RS, Schmidova K, Wisse BE, Weigle DS. A Preprandial Rise in Plasma Ghrelin Levels Suggests a Role in Meal Initiation in Humans. Diabetes [Internet]. 2001 Aug 1 [cited 2025 Aug 8];50(8):1714–9. Available from: http://diabetesjournals.org/diabetes/article-pdf/50/8/1714/368886/1714.pdf

586. Wren AM, Small CJ, Abbott CR, Dhillo WS, Seal LJ, Cohen MA, et al. Ghrelin Causes Hyperphagia and Obesity in Rats. Diabetes [Internet]. 2001 Nov 1 [cited 2025 Aug

8];50(11):2540–7. Available from: http://diabetesjournals.org/diabetes/article-pdf/50/11/2540/339793/db1101002540.pdf

587. Olszewski PK, Grace MK, Billington CJ, Levine AS. Hypothalamic paraventricular injections of ghrelin: effect on feeding and c-Fos immunoreactivity. Peptides (NY) [Internet]. 2003 Jun 1 [cited 2025 Aug 8];24(6):919–23. Available from: https://www.sciencedirect.com/science/article/pii/S0196978103001591#BIB18

588. Lawrence CB, Snape AC, Baudoin FMH, Luckman SM. Acute Central Ghrelin and GH Secretagogues Induce Feeding and Activate Brain Appetite Centers. Endocrinology [Internet]. 2002 Jan 1 [cited 2025 Aug 8];143(1):155–62. Available from: https://dx.doi.org/10.1210/endo.143.1.8561

589. Hewson AK, Dickson SL. Systemic administration of ghrelin induces Fos and Egr-1 proteins in the hypothalamic arcuate nucleus of fasted and fed rats. J Neuroendocrinol [Internet]. 2000 Nov 1 [cited 2025 Aug 8];12(11):1047–9. Available from: /doi/pdf/10.1046/j.1365-2826.2000.00584.x

590. Nakazato M, Murakami N, Date Y, Kojima M, Matsuo H, Kangawa K, et al. A role for ghrelin in the central regulation of feeding. Nature [Internet]. 2001 Jan 11 [cited 2025 Aug 8];409(6817):194–8. Available from: https://www.nature.com/articles/35051587

591. Hindmarch CCT, Ferguson A V. Physiological roles for the subfornical organ: a dynamic transcriptome shaped by autonomic state. J Physiol [Internet]. 2015 Mar 15 [cited 2025 May 9];594(6):1581. Available from: https://pmc.ncbi.nlm.nih.gov/articles/PMC4799992/

592. Fry M, Ferguson A V. The sensory circumventricular organs: Brain targets for circulating signals controlling ingestive behavior. Physiol Behav [Internet]. 2007 Jul 24 [cited 2025 May 9];91(4):413–23. Available from: https://www.sciencedirect.com/science/article/pii/S0031938407001308?via%3Dihub

593. Cottrell GT, Ferguson A V. Sensory circumventricular organs: central roles in integrated autonomic regulation. Regul Pept [Internet]. 2004 Jan 15 [cited 2025 May 9];117(1):11–

23. Available from: https://www.sciencedirect.com/science/article/pii/S0167011503002222?via%3Dihub

594. Hyde TM, Miselis RR. Effects of area postrema/caudal medial nucleus of solitary tract lesions on food intake and body weight. Am J Physiol Regul Integr Comp Physiol [Internet]. 1983 [cited 2025 May 8];13(4). Available from: /doi/pdf/10.1152/ajpregu.1983.244.4.R577

595. Norgren R, Smith GP. Central distribution of subdiaphragmatic vagal branches in the rat. Journal of Comparative Neurology [Internet]. 1988 Jul 8 [cited 2025 May 8];273(2):207–23. Available from: /doi/pdf/10.1002/cne.902730206

596. BRODAL A, ROSSI GF. Spinal Afferents to the Trigeminal Sensory Nuclei and the Nucleus of the Solitary Tract. Confin Neurol [Internet]. 1956 Jun 1 [cited 2025 May 8];16(6):321–32. Available from: https://dx.doi.org/10.1159/000105318

597. Ladenheim EE, Ritter RC. Caudal hindbrain participation in the suppression of feeding by central and peripheral bombesin. Am J Physiol Regul Integr Comp Physiol [Internet]. 1993 [cited 2025 May 8];264(6 33-6). Available from: /doi/pdf/10.1152/ajpregu.1993.264.6.R1229?download=true

598. Edwards GL, Ladenheim EE, Ritter RC. Dorsomedial hindbrain participation in cholecystokinin-induced satiety. Am J Physiol Regul Integr Comp Physiol [Internet]. 1986 [cited 2025 May 8];251(5 (20/5)). Available from: /doi/pdf/10.1152/ajpregu.1986.251.5.R971?download=true

599. Lutz TA, Senn M, Althaus J, Del Prete E, Ehrensperger F, Scharrer E. Lesion of the Area Postrema/Nucleus of the Solitary Tract (AP/NTS) Attenuates the Anorectic Effects of Amylin and Calcitonin Gene-Related Peptide (CGRP) in Rats. Peptides (NY) [Internet]. 1998 Feb 1 [cited 2025 May 8];19(2):309–17. Available from: https://www.sciencedirect.com/science/article/pii/S0196978197002921?via%3Dihub#aep-bibliography-id31

600. Gruber K, McRae-Degueurce A, Wilkin LD, Mitchell LD, Johnson AK. Forebrain and brainstem afferents to the arcuate nucleus in the rat: Potential pathways for the modulation of hypophyseal secretions. Neurosci Lett [Internet]. 1987 Mar 20 [cited 2025 May 9];75(1):1–5. Available from: https://www.sciencedirect.com/science/article/pii/0304394087900656?via%3Dihub

601. Tanaka J, Seto K. Lateral hypothalamic area and paraventricular nucleus connections with subfornical organ neurons: an electrophysiological study in the rat. Neurosci Res [Internet]. 1988 Oct 1 [cited 2025 May 9];6(1):45–52. Available from: https://www.sciencedirect.com/science/article/pii/0168010288900053?via%3Dihub

602. Farzi A, Lau J, Ip CK, Qi Y, Shi YC, Zhang L, et al. Arcuate nucleus and lateral hypothalamic CART neurons in the mouse brain exert opposing effects on energy expenditure. Elife [Internet]. 2018 Aug 21 [cited 2025 May 12];7:e36494. Available from: https://pmc.ncbi.nlm.nih.gov/articles/PMC6103747/

603. Joly-Amado A, Cansell C, Denis RGP, Delbes AS, Castel J, Martinez S, et al. The hypothalamic arcuate nucleus and the control of peripheral substrates. Best Pract Res Clin Endocrinol Metab [Internet]. 2014 Oct 1 [cited 2025 May 12];28(5):725–37. Available from: https://www.sciencedirect.com/science/article/pii/S1521690X14000505

604. Lind RW. Angiotensin and the lamina terminalis: Illustrations of a complex Unity. Clin Exp Hypertens [Internet]. 1988 [cited 2025 May 9];A10(S1):79–105. Available from: /doi/pdf/10.3109/10641968809075965?download=true

605. Armstrong WE, Tian M, Wong H. Electron microscopic analysis of synaptic inputs from the median preoptic nucleus and adjacent regions to the supraoptic nucleus in the rat. Journal of Comparative Neurology [Internet]. 1996 Sep 16 [cited 2025 May 9];373(2):228–39. Available from: https://www.scopus.com/record/display.uri?eid=2-s2.0-0029763444&origin=inward&txGid=ede8b6f00f866326669a81529813969f

606. Sims JS, Lorden JF. Effect of paraventricular nucleus lesions on body weight, food intake and insulin levels. Behavioural Brain Research [Internet]. 1986 Dec 1 [cited 2025 May 12];22(3):265–81. Available from: https://www.sciencedirect.com/science/article/pii/0166432886900719?via%3Dihub

607. Shor-Posner G, Azar AP, Insinga S, Leibowitz SF. Deficits in the control of food intake after hypothalamic paraventricular nucleus lesions. Physiol Behav [Internet]. 1985 Dec 1 [cited 2025 May 12];35(6):883–90. Available from: https://www.sciencedirect.com/science/article/pii/0031938485902550?via%3Dihub

608. Betley JN, Cao ZFH, Ritola KD, Sternson SM. XParallel, redundant circuit organization for homeostatic control of feeding behavior. Cell [Internet]. 2013 Dec 5 [cited 2025 May 12];155(6):1337–50. Available from: https://www.cell.com/action/showFullText?pii=S0092867413014141

609. Liu J, Conde K, Zhang P, Lilascharoen V, Xu Z, Lim BK, et al. Enhanced AMPA Receptor Trafficking Mediates the Anorexigenic Effect of Endogenous Glucagon-like Peptide-1 in the Paraventricular Hypothalamus. Neuron [Internet]. 2017 Nov 15 [cited 2025 May 12];96(4):897-909.e5. Available from: https://www.cell.com/action/showFullText?pii=S089662731730911X

610. Kaplan AM, Vigna SR. Gastric inhibitory polypeptide (GIP) binding sites in rat brain. Peptides (NY) [Internet]. 1994 Jan 1 [cited 2025 May 8];15(2):297–302. Available from: https://www.sciencedirect.com/science/article/pii/0196978194900167?via%3Dihub

611. Smith C, Patterson-Cross R, Woodward O, Lewis J, Chiarugi D, Merkle F, et al. A comparative transcriptomic analysis of Glucagon-like peptide-1 receptor- and Glucose-dependent insulinotropic polypeptide receptor-expressing cells in the hypothalamus. Appetite [Internet]. 2022 Jul 1 [cited 2025 May 8];174:106022. Available from: https://pmc.ncbi.nlm.nih.gov/articles/PMC7614381/

612. Armulik A, Genové G, Mäe M, Nisancioglu MH, Wallgard E, Niaudet C, et al. Pericytes regulate the blood-brain barrier. Nature [Internet]. 2010 Nov 25 [cited 2025 May 8];468(7323):557–61. Available from: https://pubmed.ncbi.nlm.nih.gov/20944627/

613. Nyberg J, Anderson MF, Meister B, Alborn AM, Ström AK, Brederlau A, et al. Glucose-Dependent Insulinotropic Polypeptide Is Expressed in Adult Hippocampus and Induces Progenitor Cell Proliferation. The Journal of Neuroscience [Internet]. 2005 Feb 16 [cited 2025 May 8];25(7):1816. Available from: https://pmc.ncbi.nlm.nih.gov/articles/PMC6725940/

614. Botfield HF, Uldall MS, Westgate CSJ, Mitchell JL, Hagen SM, Gonzalez AM, et al. A glucagon-like peptide-1 receptor agonist reduces intracranial pressure in a rat model of hydrocephalus. Sci Transl Med [Internet]. 2017 Aug 23 [cited 2025 May 12];9(404). Available from: /doi/pdf/10.1126/scitranslmed.aan0972

615. MacAulay N, Keep RF, Zeuthen T. Cerebrospinal fluid production by the choroid plexus: a century of barrier research revisited. Fluids and Barriers of the CNS 2022 19:1 [Internet]. 2022 Mar 22 [cited 2025 May 12];19(1):1–18. Available from: https://fluidsbarrierscns.biomedcentral.com/articles/10.1186/s12987-022-00323-1

616. Krajnc N, Itariu B, Macher S, Marik W, Harreiter J, Michl M, et al. Treatment with GLP-1 receptor agonists is associated with significant weight loss and favorable headache outcomes in idiopathic intracranial hypertension. Journal of Headache and Pain [Internet]. 2023 Dec 1 [cited 2025 May 12];24(1):1–12. Available from: https://thejournalofheadacheandpain.biomedcentral.com/articles/10.1186/s10194-023-01631-z

617. Hunter K, Hölscher C. Drugs developed to treat diabetes, liraglutide and lixisenatide, cross the blood brain barrier and enhance neurogenesis. BMC Neurosci [Internet]. 2012 Mar 23 [cited 2025 May 6];13(1):33. Available from: https://pmc.ncbi.nlm.nih.gov/articles/PMC3352246/

618. Kastin AJ, Akerstrom V, Pan W. Interactions of glucagon-like peptide-1 (GLP-1) with the blood-brain barrier. Journal of Molecular Neuroscience [Internet]. 2002 [cited 2025 May 8];18(1–2):7–14. Available from: https://link.springer.com/article/10.1385/JMN:18:1-2:07

619. Mcclean PL, Parthsarathy V, Faivre E, Holscher C. The Diabetes Drug Liraglutide Prevents Degenerative Processes in a Mouse Model of Alzheimer's Disease. The Journal of Neuroscience [Internet]. 2011 Apr 27 [cited 2025 May 8];31(17):6587. Available from: https://pmc.ncbi.nlm.nih.gov/articles/PMC6622662/

620. Skovbjerg G, Roostalu U, Salinas CG, Skytte JL, Perens J, Clemmensen C, et al. Uncovering CNS access of lipidated exendin-4 analogues by quantitative whole-brain 3D light sheet imaging. Neuropharmacology [Internet]. 2023 Nov 1 [cited 2025 May 8];238:109637. Available from: https://www.sciencedirect.com/science/article/pii/S0028390823002277?via%3Dihub

621. Kastin AJ, Akerstrom V. Entry of exendin-4 into brain is rapid but may be limited at high doses. Int J Obes [Internet]. 2003 Mar 1 [cited 2025 May 8];27(3):313–8. Available from: https://www.nature.com/articles/0802206

622. Salameh TS, Rhea EM, Talbot K, Banks WA. Brain uptake pharmacokinetics of incretin receptor agonists showing promise as Alzheimer's and Parkinson's disease therapeutics. Biochem Pharmacol [Internet]. 2020 Oct 1 [cited 2025 May 19];180:114187. Available from: https://pmc.ncbi.nlm.nih.gov/articles/PMC7606641/

623. Prevot V, Dehouck B, Sharif A, Ciofi P, Giacobini P, Clasadonte J. The Versatile Tanycyte: A Hypothalamic Integrator of Reproduction and Energy Metabolism. Endocr Rev [Internet]. 2018 Jun 1 [cited 2025 Apr 28];39(3):333–68. Available from: https://dx.doi.org/10.1210/er.2017-00235

624. Rodríguez EM, Blázquez JL, Pastor FE, Peláez B, Peña P, Peruzzo B, et al. Hypothalamic Tanycytes: A Key Component of Brain–Endocrine Interaction. Int Rev Cytol [Internet].

2005 Jan 1 [cited 2025 May 16];247:89–164. Available from: https://www.sciencedirect.com/science/article/pii/S0074769605470035

625. Elizondo-Vega R, Cortes-Campos C, Barahona MJ, Oyarce KA, Carril CA, García-Robles MA. The role of tanycytes in hypothalamic glucosensing. J Cell Mol Med [Internet]. 2015 Jul 1 [cited 2025 Apr 2];19(7):1471. Available from: https://pmc.ncbi.nlm.nih.gov/articles/PMC4511346/

626. Farkas E, Szilvásy-Szabó A, Ruska Y, Sinkó R, Rasch MG, Egebjerg T, et al. Distribution and ultrastructural localization of the glucagon-like peptide-1 receptor (GLP-1R) in the rat brain. Brain Struct Funct [Internet]. 2020 Jan 1 [cited 2025 May 8];226(1):225. Available from: https://pmc.ncbi.nlm.nih.gov/articles/PMC7817608/

627. Gabery S, Salinas CG, Paulsen SJ, Ahnfelt-Rønne J, Alanentalo T, Baquero AF, et al. Semaglutide lowers body weight in rodents via distributed neural pathways. JCI Insight [Internet]. 2020 Mar 26 [cited 2025 May 8];5(6):e133429. Available from: https://pmc.ncbi.nlm.nih.gov/articles/PMC7213778/

628. Jensen CB, Pyke C, Rasch MG, Dahl AB, Knudsen LB, Secher A. Characterization of the Glucagonlike Peptide-1 Receptor in Male Mouse Brain Using a Novel Antibody and In Situ Hybridization. Endocrinology [Internet]. 2018 Feb 1 [cited 2025 Aug 8];159(2):665–75. Available from: https://dx.doi.org/10.1210/en.2017-00812

629. Yamada T, Kawamata T, Walker DG, McGeer PL. Vimentin immunoreactivity in normal and pathological human brain tissue. Acta Neuropathol [Internet]. 1992 Jul [cited 2025 May 14];84(2):157–62. Available from: https://link.springer.com/article/10.1007/BF00311389

630. Prevot V, Nogueiras R, Schwaninger M. Tanycytes in the infundibular nucleus and median eminence and their role in the blood–brain barrier. Handb Clin Neurol [Internet]. 2021 Jan 1 [cited 2025 Apr 29];180:253–73. Available from: https://www.sciencedirect.com/science/article/pii/B9780128201077000161

631. Maxwell V, Shulkes A, Brown JC, Solomon TE, Walsh JH, Grossman MI. Effect of gastric inhibitory polypeptide on pentagastrin-stimulated acid secretion in man. Dig Dis Sci. 1980 Feb;25(2):113–6.

632. Samms RJ, Cosgrove R, Snider BM, Furber EC, Droz BA, Briere DA, et al. GIPR Agonism Inhibits PYY-Induced Nausea-Like Behavior. Diabetes [Internet]. 2022 Jul 1 [cited 2025 May 16];71(7):1410–23. Available from: https://dx.doi.org/10.2337/db21-0848

633. Leyris JP, Roux T, Trinquet E, Verdié P, Fehrentz JA, Oueslati N, et al. Homogeneous time-resolved fluorescence-based assay to screen for ligands targeting the growth hormone secretagogue receptor type 1a. Anal Biochem [Internet]. 2011 Jan 15 [cited 2025 Apr 28];408(2):253–62. Available from: https://www.sciencedirect.com/science/article/pii/S0003269710006159

634. Bakker W, Imbernon M, Salinas CG, Moro Chao DH, Hassouna R, Morel C, et al. Acute changes in systemic glycemia gate access and action of GLP-1R agonist on brain structures controlling energy homeostasis. Cell Rep [Internet]. 2022 Nov 22 [cited 2025 May 19];41(8):111698. Available from: https://pmc.ncbi.nlm.nih.gov/articles/PMC9715912/

635. Kreymann B, Ghatei MA, Williams G, Bloom SR. GLUCAGON-LIKE PEPTIDE-1 7-36: A PHYSIOLOGICAL INCRETIN IN MAN. The Lancet [Internet]. 1987 Dec 5 [cited 2025 Jul 16];330(8571):1300–4. Available from: https://www.thelancet.com/action/showFullText?pii=S0140673687911949

636. Farngren J, Ahrén B. Incretin-based medications (GLP-1 receptor agonists, DPP-4 inhibitors) as a means to avoid hypoglycaemic episodes. Metabolism [Internet]. 2019 Oct 1 [cited 2025 Aug 27];99:25–31. Available from: https://www.metabolismjournal.com/action/showFullText?pii=S0026049519301337

637. Nauck MA, Homberger E, Siegel EG, Allen RC, Eaton RP, Ebert R, et al. Incretin Effects of Increasing Glucose Loads in Man Calculated from Venous Insulin and C-Peptide

Responses. J Clin Endocrinol Metab [Internet]. 1986 Aug 1 [cited 2025 Jul 16];63(2):492–8. Available from: https://dx.doi.org/10.1210/jcem-63-2-492

638. Bagger JI, Knop FK, Lund A, Vestergaard H, Holst JJ, Vilsbøll T. Impaired Regulation of the Incretin Effect in Patients with Type 2 Diabetes. J Clin Endocrinol Metab [Internet]. 2011 Mar 1 [cited 2025 Jul 16];96(3):737–45. Available from: https://dx.doi.org/10.1210/jc.2010-2435

639. Deacon CF, Johnsen AH, Holst JJ. Degradation of glucagon-like peptide-1 by human plasma in vitro yields an N-terminally truncated peptide that is a major endogenous metabolite in vivo. J Clin Endocrinol Metab [Internet]. 1995 Mar [cited 2024 Oct 21];80(3):952–7. Available from: https://pubmed.ncbi.nlm.nih.gov/7883856/

640. Xu G, Kaneto H, Laybutt DR, Duvivier-Kali VF, Trivedi N, Suzuma K, et al. Downregulation of GLP-1 and GIP receptor expression by hyperglycemia: Possible contribution to impaired incretin effects in diabetes. Diabetes [Internet]. 2007 [cited 2020 Aug 12];56(6):1551–8. Available from: http://diabetes.diabetesjournals.org

641. Nauck MA, Meier JJ. Incretin hormones: Their role in health and disease. Diabetes Obes Metab [Internet]. 2018 Feb 1 [cited 2020 Aug 12];20:5–21. Available from: http://doi.wiley.com/10.1111/dom.13129

642. Holst JJ. From the incretin concept and the discovery of GLP-1 to today's diabetes therapy. Front Endocrinol (Lausanne) [Internet]. 2019 Apr 26 [cited 2025 Jun 24];10(APR):453933. Available from: www.frontiersin.org

643. Grand View Research. GLP-1 Agonists Weight Loss Drugs Market Size Report, 2030 [Internet]. 2025 [cited 2025 Jun 23]. Available from: https://www.grandviewresearch.com/industry-analysis/glp-1-agonists-weight-loss-drugs-market-report

644. De Mello VDF, Lindström J, Eriksson J, Ilanne-Parikka P, Keinänen-Kiukaanniemi S, Sundvall J, et al. Insulin secretion and its determinants in the progression of impaired

glucose tolerance to type 2 diabetes in impaired glucose-tolerant individuals: The Finnish diabetes prevention study. Diabetes Care [Internet]. 2012 Feb [cited 2025 Aug 27];35(2):211–7. Available from: https://pmc.ncbi.nlm.nih.gov/articles/PMC3263888/

645. Group DPPR. REDUCTION IN THE INCIDENCE OF TYPE 2 DIABETES WITH LIFESTYLE INTERVENTION OR METFORMIN. N Engl J Med [Internet]. 2002 Feb 7 [cited 2025 Aug 27];346(6):393. Available from: https://pmc.ncbi.nlm.nih.gov/articles/PMC1370926/

646. Fonseca VA, Capehorn MS, Garg SK, Gimeno EJ, Hansen OH, Holst AG, et al. Reductions in Insulin Resistance are Mediated Primarily via Weight Loss in Subjects With Type 2 Diabetes on Semaglutide. J Clin Endocrinol Metab [Internet]. 2019 Sep 1 [cited 2025 Aug 27];104(9):4078–86. Available from: https://dx.doi.org/10.1210/jc.2018-02685

647. Mashayekhi M, Nian H, Mayfield D, Devin JK, Gamboa JL, Yu C, et al. Weight Loss–Independent Effect of Liraglutide on Insulin Sensitivity in Individuals With Obesity and Prediabetes. Diabetes [Internet]. 2024 Jan 1 [cited 2025 Aug 27];73(1):38–50. Available from: https://dx.doi.org/10.2337/db23-0356

648. Jinnouchi H, Sugiyama S, Yoshida A, Hieshima K, Kurinami N, Suzuki T, et al. Liraglutide, a Glucagon-Like Peptide-1 Analog, Increased Insulin Sensitivity Assessed by Hyperinsulinemic-Euglycemic Clamp Examination in Patients with Uncontrolled Type 2 Diabetes Mellitus. J Diabetes Res [Internet]. 2015 [cited 2025 Aug 27];2015:706416. Available from: https://pmc.ncbi.nlm.nih.gov/articles/PMC4398938/

649. Fadini GP, Simioni N, Frison V, Dal Pos M, Bettio M, Rocchini P, et al. Independent glucose and weight-reducing effects of Liraglutide in a real-world population of type 2 diabetic outpatients. Acta Diabetol [Internet]. 2013 Dec 11 [cited 2025 Aug 27];50(6):943–9. Available from: https://link.springer.com/article/10.1007/s00592-013-0489-3

650. Wang W, Volkow ND, Berger NA, Davis PB, Kaelber DC, Xu R. Associations of semaglutide with incidence and recurrence of alcohol use disorder in real-world population. Nat

Commun [Internet]. 2024 Dec 1 [cited 2025 Aug 27];15(1):4548. Available from: https://pmc.ncbi.nlm.nih.gov/articles/PMC11133479/

651. Nowell J, Blunt E, Edison P. Incretin and insulin signaling as novel therapeutic targets for Alzheimer's and Parkinson's disease. Mol Psychiatry [Internet]. 2023 Jan 1 [cited 2025 Jul 9];28(1):217–29. Available from: https://www.nature.com/articles/s41380-022-01792-4

652. Havranek B, Loh R, Torre B, Redfield R, Halegoua-DeMarzio D. Glucagon-like peptide-1 receptor agonists improve metabolic dysfunction-associated steatotic liver disease outcomes. Sci Rep [Internet]. 2025 Dec 1 [cited 2025 Jul 17];15(1):1–11. Available from: https://www.nature.com/articles/s41598-025-89408-z

653. Kanwal F, Kramer JR, Li L, Yang YX, Cao Y, Yu X, et al. GLP-1 Receptor Agonists and Risk for Cirrhosis and Related Complications in Patients With Metabolic Dysfunction-Associated Steatotic Liver Disease. JAMA Intern Med [Internet]. 2024 Nov 4 [cited 2025 Jul 17];184(11):1314. Available from: https://pmc.ncbi.nlm.nih.gov/articles/PMC11406452/

654. Abushamat LA, Shah PA, Eckel RH, Harrison SA, Barb D. The Emerging Role of Glucagon-Like Peptide-1 Receptor Agonists for the Treatment of Metabolic Dysfunction-Associated Steatohepatitis. Clinical Gastroenterology and Hepatology [Internet]. 2024 Aug 1 [cited 2025 Jul 17];22(8):1565–74. Available from: https://www.cghjournal.org/action/showFullText?pii=S1542356524001605

655. Maretty L, Gill D, Simonsen L, Soh K, Zagkos L, Galanakis M, et al. Proteomic changes upon treatment with semaglutide in individuals with obesity. Nature Medicine 2025 31:1 [Internet]. 2025 Jan 3 [cited 2025 Aug 27];31(1):267–77. Available from: https://www.nature.com/articles/s41591-024-03355-2

656. Newsome PN, Buchholtz K, Cusi K, Linder M, Okanoue T, Ratziu V, et al. A Placebo-Controlled Trial of Subcutaneous Semaglutide in Nonalcoholic Steatohepatitis. New England Journal of Medicine [Internet]. 2021 Mar 25 [cited 2025 Aug 27];384(12):1113–24. Available from: https://www.nejm.org/doi/pdf/10.1056/NEJMoa2028395

657. Sanyal AJ, Newsome PN, Kliers I, Østergaard LH, Long MT, Kjær MS, et al. Phase 3 Trial of Semaglutide in Metabolic Dysfunction–Associated Steatohepatitis. New England Journal of Medicine [Internet]. 2025 Jun 5 [cited 2025 Aug 27];392(21):2089–99. Available from: https://www.nejm.org/doi/pdf/10.1056/NEJMoa2413258

658. Harrison SA, Bedossa P, Guy CD, Schattenberg JM, Loomba R, Taub R, et al. A Phase 3, Randomized, Controlled Trial of Resmetirom in NASH with Liver Fibrosis. New England Journal of Medicine [Internet]. 2024 Feb 8 [cited 2025 Aug 27];390(6):497–509. Available from: https://www.nejm.org/doi/pdf/10.1056/NEJMoa2309000

659. Rodriguez PJ, Zhang V, Gratzl S, Do D, Cartwright BG, Baker C, et al. Discontinuation and Reinitiation of Dual-Labeled GLP-1 Receptor Agonists Among US Adults With Overweight or Obesity. JAMA Netw Open [Internet]. 2025 Jan 2 [cited 2025 Jun 23];8(1):e2457349–e2457349. Available from: https://jamanetwork.com/journals/jamanetworkopen/fullarticle/2829779

660. Jones B. The therapeutic potential of GLP-1 receptor biased agonism. Br J Pharmacol [Internet]. 2021 Feb 1 [cited 2025 Jul 21];179(4):492. Available from: https://pmc.ncbi.nlm.nih.gov/articles/PMC8820210/

661. Dai XQ, Camunas-Soler J, Briant LJB, dos Santos T, Spigelman AF, Walker EM, et al. Heterogenous impairment of α-cell function in type 2 diabetes is linked to cell maturation state. Cell Metab [Internet]. 2022 Feb 1 [cited 2025 Jul 21];34(2):256. Available from: https://pmc.ncbi.nlm.nih.gov/articles/PMC8852281/

662. Benninger RKP, Hodson DJ. New Understanding of β-Cell Heterogeneity and In Situ Islet Function. Diabetes [Internet]. 2018 Apr 1 [cited 2025 Jul 21];67(4):537. Available from: https://pmc.ncbi.nlm.nih.gov/articles/PMC5860861/

663. Chera S, Baronnier D, Ghila L, Cigliola V, Jensen JN, Gu G, et al. Diabetes Recovery By Age-Dependent Conversion of Pancreatic δ-Cells Into Insulin Producers. Nature

[Internet]. 2014 Oct 23 [cited 2025 Aug 27];514(7523):503. Available from: https://pmc.ncbi.nlm.nih.gov/articles/PMC4209186/

664. Druelle N, Vieira A, Shabro A, Courtney M, Mondin M, Rekima S, et al. Ectopic expression of Pax4 in pancreatic δ cells results in β-like cell neogenesis. J Cell Biol [Internet]. 2017 [cited 2025 Aug 27];216(12):4299. Available from: https://pmc.ncbi.nlm.nih.gov/articles/PMC5716283/

665. Carril Pardo CA, Massoz L, Dupont MA, Bergemann D, Bourdouxhe J, Lavergne A, et al. A δ-cell subpopulation with a pro-β-cell identity contributes to efficient age-independent recovery in a zebrafish model of diabetes. Elife [Internet]. 2022 Jan 1 [cited 2025 Aug 27];11:e67576. Available from: https://pmc.ncbi.nlm.nih.gov/articles/PMC8820734/

666. Benninger RKP, Piston DW. Cellular Communication and Heterogeneity in Pancreatic Islet Insulin Secretion Dynamics. Trends Endocrinol Metab [Internet]. 2014 [cited 2025 Jan 16];25(8):399. Available from: https://pmc.ncbi.nlm.nih.gov/articles/PMC4112137/

667. Mentis N, Vardarli I, Köthe LD, Holst JJ, Deacon CF, Theodorakis M, et al. GIP does not potentiate the antidiabetic effects of GLP-1 in hyperglycemic patients with type 2 diabetes. Diabetes [Internet]. 2011 Apr [cited 2020 Nov 15];60(4):1270–6. Available from: /pmc/articles/PMC3064100/?report=abstract

668. Rayner Rodriguez-Diaz A, Damaris Molano R, Weitz JR, Pileggi A, Caicedo A, Berggren PO, et al. Clinical and Translational Report Paracrine Interactions within the Pancreatic Islet Determine the Glycemic Set Point Cell Metabolism Clinical and Translational Report Paracrine Interactions within the Pancreatic Islet Determine the Glycemic Set Point. Cell Metab [Internet]. 2018 [cited 2020 Aug 13];27:549-558.e4. Available from: https://doi.org/10.1016/j.cmet.2018.01.015

669. Huising MO. Paracrine regulation of insulin secretion. Diabetologia [Internet]. 2020 Oct 1 [cited 2025 Jul 21];63(10):2057–63. Available from: https://link.springer.com/article/10.1007/s00125-020-05213-5

670. Rodríguez EM, Blázquez JL, Pastor FE, Peláez B, Peña P, Peruzzo B, et al. Hypothalamic Tanycytes: A Key Component of Brain–Endocrine Interaction. Int Rev Cytol [Internet]. 2005 Jan 1 [cited 2025 May 16];247:89–164. Available from: https://www.sciencedirect.com/science/article/abs/pii/S0074769605470035?via%3Dihub

671. Bolborea M, Langlet F. What is the physiological role of hypothalamic tanycytes in metabolism? Am J Physiol Regul Integr Comp Physiol [Internet]. 2021 Jun 1 [cited 2025 Aug 27];320(6). Available from: /doi/pdf/10.1152/ajpregu.00296.2020

672. Bolborea M, Pollatzek E, Benford H, Sotelo-Hitschfeld T, Dale N. Hypothalamic tanycytes generate acute hyperphagia through activation of the arcuate neuronal network. Proc Natl Acad Sci U S A [Internet]. 2020 Jun 23 [cited 2025 Aug 27];117(25):14473–81. Available from: /doi/pdf/10.1073/pnas.1919887117?download=true

673. Yoo S, Cha D, Kim S, Jiang L, Cooke P, Adebesin M, et al. Tanycyte ablation in the arcuate nucleus and median eminence increases obesity susceptibility by increasing body fat content in male mice. Glia [Internet]. 2020 Oct 1 [cited 2025 Aug 27];68(10):1987. Available from: https://pmc.ncbi.nlm.nih.gov/articles/PMC7423758/

674. Campbell JE, Drucker DJ. Therapeutic Targeting of the GIP Receptor—Revisiting the Controversies. Diabetes [Internet]. 2025 Jul 21 [cited 2025 Jul 25];74(8):1320–5. Available from: https://dx.doi.org/10.2337/db25-0393

675. Sanz E, Yang L, Su T, Morris DR, McKnight GS, Amieux PS. Cell-type-specific isolation of ribosome-associated mRNA from complex tissues. Proc Natl Acad Sci U S A [Internet]. 2009 Aug 18 [cited 2025 Aug 26];106(33):13939. Available from: https://pmc.ncbi.nlm.nih.gov/articles/PMC2728999/

676. Timper K, Grisouard J, Radimerski T, Dembinski K, Peterli R, Häring A, et al. Glucose-Dependent Insulinotropic Polypeptide (GIP) Induces Calcitonin Gene-Related Peptide (CGRP)-I and Procalcitonin (Pro-CT) Production in Human Adipocytes. J Clin Endocrinol

Metab [Internet]. 2011 Feb 1 [cited 2025 Jul 21];96(2):E297–303. Available from: https://dx.doi.org/10.1210/jc.2010-1324

677. Jeffery E, Berry R, Church CD, Yu S, Shook BA, Horsley V, et al. Characterization of Cre recombinase models for the study of adipose tissue. Adipocyte [Internet]. 2014 [cited 2025 Jul 21];3(3):206–11. Available from: https://www.tandfonline.com/doi/pdf/10.4161/adip.29674

678. Tharp WG, Gupta D, Sideleva O, Deacon CF, Holst JJ, Elahi D, et al. Effects of Pioglitazone on Glucose-Dependent Insulinotropic Polypeptide–Mediated Insulin Secretion and Adipocyte Receptor Expression in Patients With Type 2 Diabetes. Diabetes [Internet]. 2020 Feb 1 [cited 2025 Aug 27];69(2):146–57. Available from: https://dx.doi.org/10.2337/db18-1163

679. Ceperuelo-Mallafré V, Duran X, Pachón G, Roche K, Garrido-Sánchez L, Vilarrasa N, et al. Disruption of GIP/GIPR Axis in Human Adipose Tissue Is Linked to Obesity and Insulin Resistance. J Clin Endocrinol Metab [Internet]. 2014 May 1 [cited 2025 Jul 21];99(5):E908–19. Available from: https://dx.doi.org/10.1210/jc.2013-3350

680. Rudovich N, Kaiser S, Engeli S, Osterhoff M, Gögebakan Ö, Bluher M, et al. GIP receptor mRNA expression in different fat tissue depots in postmenopausal non-diabetic women. Regul Pept [Internet]. 2007 Aug 16 [cited 2025 Jul 21];142(3):138–45. Available from: https://www.sciencedirect.com/science/article/pii/S0167011507000535

681. Beaudry JL, Kaur KD, Varin EM, Baggio LL, Cao X, Mulvihill EE, et al. Physiological roles of the GIP receptor in murine brown adipose tissue. Mol Metab [Internet]. 2019 Oct 1 [cited 2025 Jul 21];28:14–25. Available from: https://www.sciencedirect.com/science/article/pii/S2212877819306179

682. Sanyal AJ, Bedossa P, Fraessdorf M, Neff GW, Lawitz E, Bugianesi E, et al. A Phase 2 Randomized Trial of Survodutide in MASH and Fibrosis. New England Journal of Medicine

[Internet]. 2024 Jul 25 [cited 2025 Aug 26];391(4):311–9. Available from: /doi/pdf/10.1056/NEJMoa2401755?download=true

683. le Roux CW, Steen O, Lucas KJ, Startseva E, Unseld A, Hennige AM. Glucagon and GLP-1 receptor dual agonist survodutide for obesity: a randomised, double-blind, placebo-controlled, dose-finding phase 2 trial. Lancet Diabetes Endocrinol [Internet]. 2024 Mar 1 [cited 2025 Aug 26];12(3):162–73. Available from: https://www.thelancet.com/action/showFullText?pii=S221385872300356X

684. Wharton S, le Roux CW, Kosiborod MN, Platz E, Brueckmann M, Jastreboff AM, et al. Survodutide for treatment of obesity: rationale and design of two randomized phase 3 clinical trials (SYNCHRONIZETM-1 and -2). Obesity (Silver Spring) [Internet]. 2024 Jan 1 [cited 2025 Aug 26];33(1):67. Available from: https://pmc.ncbi.nlm.nih.gov/articles/PMC11664303/

685. Billington CJ, Briggs JE, Link JG, Levine AS. Glucagon in physiological concentrations stimulates brown fat thermogenesis in vivo. Am J Physiol Regul Integr Comp Physiol [Internet]. 1991 [cited 2025 Jul 20];261(2 30-2). Available from: /doi/pdf/10.1152/ajpregu.1991.261.2.R501

686. de Castro JM, Paullin SK, DeLugas GM. Insulin and glucagon as determinants of body weight set point and microregulation in rats. J Comp Physiol Psychol. 1978 Jun;92(3):571–9.

687. Geary N, Kissileff HR, Pi-Sunyer FX, Hinton V. Individual, but not simultaneous, glucagon and cholecystokinin infusions inhibit feeding in men. https://doi.org/101152/ajpregu19922626R975 [Internet]. 1992 [cited 2025 Jul 20];262(6 31-6). Available from: https://journals.physiology.org/doi/10.1152/ajpregu.1992.262.6.R975

688. Penick SB, Hinkle LE, Paulsen EG. Depression of Food Intake Induced in Healthy Subjects by Glucagon. New England Journal of Medicine [Internet]. 1961 May 4 [cited 2025 Jul

20];264(18):893–7. Available from: /doi/pdf/10.1056/NEJM196105042641801?download=true

689. SCHULMAN JL, CARLETON JL, WHITNEY G, WHITEHORN JC. Effect of glucagon on food intake and body weight in man. J Appl Physiol [Internet]. 1957 Nov 1 [cited 2025 Jul 20];11(3):419–21. Available from: /doi/pdf/10.1152/jappl.1957.11.3.419

690. Stunkard AJ, Van Itallie TB, Reis BB. The Mechanism of Satiety:Effect of Glucagon on Gastric Hunger Contractions in Man. (21776). Proceedings of the Society for Experimental Biology and Medicine [Internet]. 1955 [cited 2025 Jul 20];89(2):258–61. Available from: /doi/pdf/10.3181/00379727-89-21776?download=true

691. Müller TD, Finan B, Clemmensen C, Di Marchi RD, Tschöp MH. The new biology and pharmacology of glucagon. Physiol Rev [Internet]. 2017 Apr 1 [cited 2025 Jul 20];97(2):721–66. Available from: /doi/pdf/10.1152/physrev.00025.2016

692. Geary N, Le Sauter J, Noh U. Glucagon acts in the liver to control spontaneous meal size in rats. Am J Physiol Regul Integr Comp Physiol [Internet]. 1993 [cited 2025 Jul 20];264(1 33-1). Available from: https://pubmed.ncbi.nlm.nih.gov/8430871/

693. Le Sauter J, Noh U, Geary N. Hepatic portal infusion of glucagon antibodies increases spontaneous meal size in rats. Am J Physiol Regul Integr Comp Physiol [Internet]. 1991 [cited 2025 Jul 20];261(1 30-1). Available from: https://journals.physiology.org/doi/epdf/10.1152/ajpregu.1991.261.1.R162

694. Geary N, Smith GP. Pancreatic glucagon and postprandial satiety in the rat. Physiol Behav [Internet]. 1982 Feb 1 [cited 2025 Jul 21];28(2):313–22. Available from: https://www.sciencedirect.com/science/article/pii/0031938482900816?via%3Dihub

695. Weatherford SC, Ritter S. Lesion of vagal afferent terminals impairs glucagon-induced suppression of food intake. Physiol Behav [Internet]. 1988 Jan 1 [cited 2025 Aug 27];43(5):645–50. Available from: https://www.sciencedirect.com/science/article/pii/003193848890220X?via%3Dihub

696. Day JW, Ottaway N, Patterson JT, Gelfanov V, Smiley D, Gidda J, et al. A new glucagon and GLP-1 co-agonist eliminates obesity in rodents. Nat Chem Biol [Internet]. 2009 Jul 13 [cited 2025 Aug 27];5(10):749–57. Available from: https://www.nature.com/articles/nchembio.209

697. Knerr PJ, Mowery SA, Douros JD, Premdjee B, Hjøllund KR, He Y, et al. Next generation GLP-1/GIP/glucagon triple agonists normalize body weight in obese mice. Mol Metab [Internet]. 2022 Sep 1 [cited 2025 Jul 20];63:101533. Available from: https://pmc.ncbi.nlm.nih.gov/articles/PMC9305623/

698. Newsome PN, Ambery P. Incretins (GLP-1 receptor agonists and dual/triple agonists) and the liver. J Hepatol [Internet]. 2023 Dec 1 [cited 2025 Jul 21];79(6):1557–65. Available from: https://www.journal-of-hepatology.eu/action/showFullText?pii=S0168827823050468

699. Abraham MA, Lam TKT. Glucagon action in the brain. Diabetologia [Internet]. 2016 Jul 1 [cited 2025 Jul 21];59(7):1367–71. Available from: https://link.springer.com/article/10.1007/s00125-016-3950-3

700. Marquez-Meneses JD, Olaya-Bonilla SA, Barrera-Carreño S, Tibaduiza-Arévalo LC, Forero-Cárdenas S, Carrillo-Vaca L, et al. GLP-1 Analogues in the Neurobiology of Addiction: Translational Insights and Therapeutic Perspectives. Int J Mol Sci [Internet]. 2025 Jun 1 [cited 2025 Jul 21];26(11):5338. Available from: https://pmc.ncbi.nlm.nih.gov/articles/PMC12155186/

701. Gupta T, Kaur M, Shekhawat D, Aggarwal R, Nanda N, Sahni D. Investigating the Glucagon-like Peptide-1 and Its Receptor in Human Brain: Distribution of Expression, Functional Implications, Age-related Changes and Species Specific Characteristics. Basic Clin Neurosci [Internet]. 2023 May 1 [cited 2025 Jul 21];14(3):341. Available from: https://pmc.ncbi.nlm.nih.gov/articles/PMC10700809/

702. The Human Protein Atlas. Tissue expression of GCGR [Internet]. 2025 [cited 2025 Aug 27]. Available from: https://www.proteinatlas.org/ENSG00000215644-GCGR/tissue#rna_expression

703. Liver Cell Atlas. Human All liver cells [Internet]. 2025 [cited 2025 Aug 27]. Available from: https://www.livercellatlas.org/umap-humanAll.php

704. The Human Protein Atlas. Tissue expression of GIPR [Internet]. 2025 [cited 2025 Aug 27]. Available from: https://www.proteinatlas.org/ENSG00000010310-GIPR/tissue#expression_summary

705. da Silva Lima N, Cabaleiro A, Novoa E, Riobello C, Knerr PJ, He Y, et al. GLP-1 and GIP agonism has no direct actions in human hepatocytes or hepatic stellate cells. Cell Mol Life Sci [Internet]. 2024 Dec 1 [cited 2025 Aug 27];81(1):468. Available from: https://pmc.ncbi.nlm.nih.gov/articles/PMC11604888/

706. The Human Protein Atlas. Tissue expression of GLP1R [Internet]. 2025 [cited 2025 Aug 27]. Available from: https://www.proteinatlas.org/ENSG00000112164-GLP1R/tissue#rna_expression

707. Tarhan L, Bistline J, Chang J, Galloway B, Hanna E, Weitz E. Single Cell Portal: an interactive home for single-cell genomics data. bioRxiv [Internet]. 2023 Jul 17 [cited 2025 Aug 18];2023.07.13.548886. Available from: https://pmc.ncbi.nlm.nih.gov/articles/PMC10370058/